

APPENDIX D: CONCEPTUAL MODEL FOR THE DFW ATTAINMENT DEMONSTRATION SIP REVISION FOR THE 1997 EIGHT-HOUR OZONE STANDARD

EXECUTIVE SUMMARY

Ozone formation conceptual models characterize ozone trends, precursors, formation, and transport in a particular geographic area, to explain the dynamics of ozone formation in that area. This information is compiled and developed into a comprehensive picture of not only where and when ozone forms, but also how and why ozone forms in a geographic area. Conceptual models are required by the U.S. Environmental Protection Agency (U.S. EPA) to accompany photochemical modeling performed for State Implementation Plans (SIP) (U.S. EPA, 2007). This appendix updates the ozone conceptual model for the Dallas-Fort Worth (DFW) nonattainment area.

Conceptual models can be used as tools for selecting representative modeling episodes and for qualitatively evaluating and assessing photochemical modeling results. They are intended to guide modeling efforts conducted in compliance with SIP requirements by presenting the state of the science in terms of current understanding of factors that influence ozone formation and transport.

This conceptual model begins with a discussion of the fundamentals of ozone formation photochemistry, followed by more detailed treatment of the characteristics that make the ozone situation in the DFW area unique. This is followed by results of detailed investigations of trends and patterns in ozone and local precursor concentrations. Identifying and assessing trends in ozone and its precursors provide an initial appraisal of the current ozone situation in the DFW area, the magnitude of progress made to date, and the scale of future challenges.

Ozone design values, the statistics used to compare observed ambient ozone levels to the NAAQS, have decreased in the DFW area over the past seventeen years. The eight-hour ozone design value in 2009 was 86 ppb (recorded at both Eagle Mountain Lake (C75) and Keller (C17) monitors), only two ppb away from the 1997 eight-hour ozone NAAQS and a 18 percent decrease from the 1991 design value of 105 ppb (recorded at Keller (C17)). The one-hour ozone design value in 2009 was 115 ppb (recorded at Denton Airport South (C56) monitor), well below the vacated one-hour ozone NAAQS of 124 ppb, and an 18 percent decrease from the 1991 design value of 140 ppb (recorded at Keller (C17) monitor). Examination of design values at individual monitors corroborates these decreases, with over half at levels below the eight-hour standard by 2008 and all below the vacated one-hour standard by 2007. Decreases in exceedance days are also apparent. Despite an increase in the number of monitors located throughout the DFW area the number of eight-hour and one-hour ozone exceedance days fell 54 percent and 100 percent respectively. In addition, the ozone season was also determined to be less severe in recent years.

NO_x trends from 1991 to 2009 also exhibited decreases, with a 43 percent decrease in maximum NO_x and a 65 percent decrease in average daily peak NO_x. VOC trends decreased from 1999 to 2009, with a 33 percent decrease in 90th percentile VOC and a 29 percent decrease in median VOC at Dallas Hinton St. (C401/C60/AH161). Ft. Worth Northwest (C13/AH32), the other continuous VOC monitor in the DFW area, showed an 18 percent decrease in 90th percentile VOC and a 15 percent decrease in median VOC from 2003 to 2009. Most strikingly, 2009 experienced not only some of the lowest ozone design values in seventeen years, but also some of the lowest NO_x and VOC values.

Section 3 continues with analyses of local factors contributing to ozone formation, accumulation, transport, and fate in the DFW area, including a comprehensive examination of the impact of emissions from the Barnett Shale area. An investigation of geographic patterns in ozone reveals that, while ozone concentrations in the DFW area have been decreasing, the same geographic areas tend to experience the highest ozone concentrations year after year, with the highest levels of ozone typically occurring in the northwestern part of the region at the Keller (C17) and Eagle Mountain Lake (C75) monitors. Peak NO_x concentrations have also been declining across the region. Despite the reductions in severity, regions that observe the highest and lowest concentrations remain roughly the same, with the urban core of Dallas County, at Dallas Hinton St. (C401/C60/AH161), and Tarrant County, at Ft. Worth Northwest (C13/AH32), experiencing the highest NO_x concentrations.

The time of day and location of ozone peaks were found to differ on high and low ozone days. Ozone reaches a peak earlier in the day, around 13:00 LST, on high ozone days, beginning in areas around Midlothian OFW (C52/A137) and then Rockwall Heath (C69), Dallas North No.2 (C63), and Dallas Hinton St. (C401/C60/AH161). Ozone peaks latest in areas on the outer edges of the DFW area, around 17:00 LST at Parker County (C76), indicating that ozone is first formed in the core of DFW, where NO_x concentrations are highest, then transported to the outer edges of the nonattainment area.

Investigation of VOC and NO_x limitations reveal a variable pattern across the DFW area, indicating that different photochemical processes likely dominate in different regions. Urban monitors, such as Dallas Hinton St. (C401/C60/AH161), were found to be VOC limited, while others to the northwest of the DFW area were transitional between VOC limited and NO_x limited, such as Ft. Worth Northwest (C13/AH32). Monitors on the periphery tended to measure NO_x-limiting conditions, such as Denton Airport South (C56).

Although emissions from Barnett Shale were observed at monitors in the DFW area, extensive analyses of available data from monitors possibly impacted by emissions from the Barnett Shale region failed to confirm its influence on ozone. Analysis of upper level and surface wind trajectories indicated that emissions from drilling activity are rarely encountered east of the Barnett Shale region. Only one out of 19 ozone exceedance days in 2009 exhibited winds from the direction of the Barnett Shale.

Local geography, topography and meteorology of the DFW area all contribute to ozone dynamics. The physical environment is described by a relatively flat topography, lack of nearby marine influences, and lack of mountains that might constrain air masses. Surface winds are predominately from the south and southeast, with the majority from the southeast on high ozone days. Wind speeds also tend to be slower on days that experience high ozone concentrations. This corroborates the geographical analysis that shows peak ozone occurring in the northwest parts of the DFW area.

Finally, Section 4 explores meteorological factors contributing to transport of background ozone into the DFW area. All of these investigations point to the same general conclusion: decreasing trends in measured ozone concentrations are largely a result of real, quantifiable reductions in precursor emissions, and are not due to unusual meteorological conditions. The need to quantify background ozone, or ozone transported from outside the DFW area, in addition to quantifying local ozone production, is essential given that a large metropolitan area, such as Dallas-Fort Worth, regularly generates enough local ozone to exceed the standard when starting from a high background. Analysis revealed no discernible trend in background ozone, which will simplify interpretation of influences from background and local components of ambient ozone, as well as computation of benefits of local control strategies.

Studies of regional background eight-hour ozone in the DFW area show that regional background eight-hour ozone is higher on days with high ozone. Typically, on days with no exceedances, background ozone is roughly 40 ppb, as estimated by the EPA. Evaluation of ozone transported from both the north and south showed regional background ozone was higher when the ozone concentration for that day exceeded 75 ppb. These analyses show that regional background eight-hour ozone often exceeds 50 ppb and is especially pronounced during ozone season in the DFW area.

Investigation of HYSPLIT back trajectories identified likely transport of ozone into north Texas on days following elevated ozone episodes in eastern U.S. states. Back trajectories also showed that on high ozone days slower winds from the east and southeast are most frequent, while on low ozone days winds were much faster and from the south. These background and transport analyses show that efforts focused solely on controlling local emissions may be insufficient to bring the DFW area into ozone attainment given that, on many days, background estimates are well over half the eight-hour ozone NAAQS of 85 ppb.

Combining results from these various analyses gives a general picture of how high ozone is formed in the DFW area. High ozone is typically formed in the DFW area on days with slower wind speeds out of the east and southeast. These prevailing winds also lead to higher background ozone levels entering into the DFW area. High background ozone concentrations are then amplified as an air mass moves over the urban core of Dallas and Tarrant Counties, which both contain large amounts of NO_x emissions. Those emissions are then transported across the DFW area to the northwest, where the highest eight-hour ozone concentrations are observed. Analyses revealed that controlling VOC in more urban areas and NO_x in more rural areas would lead to the most effective controls for ozone in the DFW area. Due to the prevailing winds, VOC emissions from Barnett Shale rarely affect ozone concentrations in the DFW area.

TABLE OF CONTENTS

Executive Summary	i
Table of Contents	iv
List of Tables	vi
List of Figures	viii
1 Ozone Fundamentals	1
1.1 Basic Ozone Formation Photochemistry and Meteorology	1
1.2 Ozone in the Dallas-Fort Worth Area	5
2 Air Quality Trends in the Dallas-Fort Worth Area	8
2.1 Ozone Trends	8
2.2 Nitrogen Oxide Trends	19
2.3 Volatile Organic Compounds Trends	25
2.3.1 VOC Trends at Auto-GC Monitors	27
2.3.2 VOC trends from Canisters	30
2.4 Summary of Trends in Ozone and Ozone Precursors	33
3 Recent Findings in Local Ozone Dynamics in the Dallas-Fort Worth Area	35
3.1 Local Variation in Ozone	35
3.2 Spatial Variation in Nitrogen Oxides	38
3.3 Recent Findings on VOC and NO _x Limitations	42
3.3.1 VOC:NO _x Ratios	42
3.4 MAPPER	46
3.4.1 Ambient Highly Reactive Volatile Organic Compounds (HRVOC)	50
3.4.2 Comparison of Exceedances on Weekdays and Weekends	70
3.5 Relationship of Barnett Shale to Ozone in the DFW Area	76
3.5.1 Factor Analysis of Ambient Volatile Organic Compounds in the Fort Worth Area	77
3.5.2 Analysis of Trajectories at the Eagle Mountain Lake (C75) Monitor	86
3.5.3 Cluster Analysis of Winds on Elevated Ozone Days Using HYSPLIT	88
3.5.4 Frequency of Surface Winds on Elevated Ozone Days	90
3.5.5 Examination of VOC Canister Data at Denton Airport South (C56/A163/X157)	92
3.5.6 Case Study of Barnett Shale Emission on July 1, 2009	94
3.6 Meteorological Characterization and Trends	105

3.7	Summary of Recent Findings in Local Ozone Dynamics.....	112
4	Recent Findings in Background Ozone and Ozone Transport into the Dallas-Forth Worth Area.....	113
4.1	Background Ozone.....	114
4.1.1	Regional Background Ozone in the Dallas-Fort Worth Area and Other Eastern Texas Cities	115
4.1.2	Estimating Regional Background Ozone	119
4.1.3	Background Ozone on High Ozone Days Versus Low Ozone Days	125
4.1.4	Estimating Background Ozone by Month.....	127
4.1.5	Estimating Background Ozone Using Trajectories.....	129
4.2	Transport Wind Trajectories.....	131
4.3	Summary of Recent Findings in Background Ozone Transport.....	134
5	References.....	136

LIST OF TABLES

Table D-1: Eight-Hour Ozone Design Values by Monitor in the DFW Area	11
Table D-2: One-Hour Ozone Design Values by Monitor in the DFW Area.....	11
Table D-3: Annual Fourth Highest Eight-Hour Ozone Values and Design Values.....	14
Table D-4: Number of Days with an Eight-Hour Ozone Exceedance.....	17
Table D-5: Number of Days with a One-Hour Ozone Exceedance	17
Table D-6: Decreases in 90 th Percentile NO _x Concentrations.....	23
Table D-7: Description of Auto-GC and Canister Monitors in the DFW Area	26
Table D-8: TNMHC Yearly Median Linear Regression.....	30
Table D-9: Regression Results for Annual Geometric Mean TNMHC at CATMN Monitors	32
Table D-10: 2009 Mean NO _x Concentrations in the DFW Area	39
Table D-11: Summary of 2009 VOC:NO _x Ratios	46
Table D-12: Extent of Reaction by Site and Year.....	47
Table D-13: Regression Results for Annual Geometric Mean Ethene.....	52
Table D-14: Summary of HRVOC Linear Regression Fits.....	56
Table D-15: Summary Statistics for HRVOC at Two Auto-GC Monitors	60
Table D-16: Regression Results for Annual Geometric Mean Ethene and Propene at Two CATMN Monitors.....	66
Table D-17: Regression Results for Annual Geometric Mean 1,3-Butadiene, Trans-2-Butene, and Cis-2-Butene.....	67
Table D-18: Regression Results for Annual Geometric Mean 1-Butene at CATMN Monitors....	69
Table D-19: Ozone Exceedance Days by Day of Week, 2005-2009	72
Table D-20: Candidate PMF Analysis Scenarios.....	79
Table D-21: Frequency of Upper Level Trajectory Endpoints by County on High Ozone Days..	88
Table D-22: Source Directions of Trajectory Clusters Arriving at Eagle Mountain Lake (C75) on High Ozone Days.....	89
Table D-23: Frequencies of Surface Back Trajectory Endpoints by County on High Ozone Days	91
Table D-24: One-Hour Ozone Averages Recorded at Eagle Mountain Lake (C75) July 1, 2009	96
Table D-25: Cross-Correlations (R ²) for VOC Compounds Sampled at Ft. Worth Northwest (C13/AH302) Monitor July 1, 2009.....	99
Table D-26: Results of Regression of Isopentane on N-Butane at Ft. Worth Northwest (C13/AH302) on July 1, 2009	103
Table D-27: Results of Regression of Propane on Benzene at Ft. Worth Northwest (C13/AH302) on July 1, 2009	104
Table D-28: Summary of Wind Characteristics on High and Low Ozone Days.....	111
Table D-29: Background Ozone Concentrations During TexAQS II in 2006 (Hardesty et al., 2007)	116

Table D-30: Range of Monthly 90 th Percentile Daily Peak One-Hour Ozone Concentrations (ppb) for Subject Wind Directions	118
Table D-31: Perimeter Monitors Selected for Background Analysis	120
Table D-32: Summary Statistics for Background Ozone at Kaufman (C71/A304/X071)	121
Table D-33: Summary Statistics for Background Ozone at Eagle Mountain Lake (C75)	121
Table D-34: Summary Statistics for Background Ozone at Pilot Point (C1032)	122
Table D-35: Summary Statistics for Background Ozone at Italy (C1044/A323).....	122
Table D-36: Selected Summary Statistics for Three Background Monitors in the DFW Area (ppb)	125
Table D-37: Estimated Background and Local Contributions to One-Hour Ozone Concentrations by Wind Direction.....	130

LIST OF FIGURES

Figure D-1: Chemical Reactions that Form Ozone	2
Figure D-2: Typical Diurnal Ozone Cycle	3
Figure D-3: Example of Ozone Scavenging Downwind of a NO _x Source	3
Figure D-4: Example of Dynamics of Atmospheric Mixing Height.....	4
Figure D-5: Effect of Mixing Height on Parcel Concentration	4
Figure D-6: Eight-Hour Ozone Exceedance Days in DFW and Other Areas of Texas	6
Figure D-7: Daily Peak Eight-Hour Ozone Values in the DFW Area.....	9
Figure D-8: Ozone Design Values for the DFW Area	10
Figure D-9: Eight-Hour Ozone Design Value Statistics in the DFW Area	13
Figure D-10: One-Hour Ozone Design Value Statistics in the DFW Area.....	14
Figure D-11: Number of Monitors and Ozone Exceedance Days in the DFW Area.....	15
Figure D-12: Number of Eight-Hour Ozone Exceedance Days by Monitor	16
Figure D-13: Number of One-Hour Ozone Exceedance Days by Monitor.....	16
Figure D-14: Eight-Hour Ozone Exceedance Days by Month and Year in the DFW Area.....	19
Figure D-15: Daily Peak Hourly NO _x in the DFW Area.....	21
Figure D-16: Annual Mean Daily Peak NO _x	22
Figure D-17: 90 th Percentile Daily Peak NO _x Concentrations in the DFW Area	23
Figure D-18: Mean NO _x and Annual Percentage Change.....	24
Figure D-19: Locations of Auto-GC Monitors and Canisters in the DFW Area.....	26
Figure D-20: Daily Peak TNMHC Concentrations in the DFW Area	28
Figure D-21: 90 th Percentile and Median TNMHC in the DFW Area.....	29
Figure D-22: Quarterly Geometric Mean TNMHC at CATMN Monitors.....	31
Figure D-23: Annual Geometric Mean TNMHC at CATMN Monitors.....	32
Figure D-24: Eight-Hour Ozone Design Values for 2002, 2005, and 2009	36
Figure D-25: Time of Day of Peak Hourly Ozone	38
Figure D-26: Mean NO _x Concentrations in the DFW Area for 2002, 2005, and 2009	41
Figure D-27: Annual Geometric Mean of Auto-GC VOC:NO _x Ratio	43
Figure D-28: Hourly Geometric Mean of Auto-GC VOC:NO _x Ratios	44
Figure D-29: Geometric Mean VOC:NO _x Ratios from Canister Data	45
Figure D-30: AGC and CATMN VOC:NO _x Ratios, 2009.....	46
Figure D-31: MAPPER Estimated Extent of Reaction by Monitor	48
Figure D-32: 2009 Extent of Reaction at Each Monitor in the DFW Area	49
Figure D-33: Daily Maximum Ethene at Dallas Hinton St. (C401/C60/AH161) Monitor.....	51
Figure D-34: Daily Maximum Ethene at Ft. Worth Northwest (C13/AH32) Monitor.....	51
Figure D-35: Annual Geometric Mean Ethene at Dallas Hinton St. (C401/C60/AH161) and Ft. Worth Northwest (C13/AH32)	52
Figure D-36: Propene at Dallas Hinton St (C401/C60/AH161) Monitor	54

Figure D-37: Propene at Ft. Worth Northwest (C13/AH32) Monitor	54
Figure D-38: 90 th Percentile 1,3-Butadiene at Dallas Hinton St. (C401/C60/AH161) Monitor and Ft. Worth Northwest (C13/AH32) Monitor	55
Figure D-39: Box Plots of Ethene and Propene at Two Auto-GC Monitors	58
Figure D-40: Box Plots of 1,3-Butadiene and Trans-2-Butene at Two Auto-GC Monitors.....	59
Figure D-41: Box Plots of Cis-2-Butene and 1-Butene at Two Auto-GC Monitors.....	60
Figure D-42: Quarterly Geometric Mean Ethene at CATMN Monitors	63
Figure D-43: Quarterly Geometric Mean Propene at CATMN Monitors	63
Figure D-44: Annual Geometric Mean Ethene at Two CATMN Monitors.....	65
Figure D-45: Annual Geometric Mean Propene at Two CATMN Monitors	66
Figure D-46: Quarterly Geometric Mean 1,3-Butadiene at CATMN Monitors.....	67
Figure D-47: Quarterly Geometric Mean 1-Butene at CATMN Monitors	68
Figure D-48: Annual Geometric Mean 1-Butene at CATMN Monitors.....	69
Figure D-49: Frequency of Eight-Hour Exceedances by Day of Week (1999-2009)	71
Figure D-50: Frequency of Eight-Hour Ozone Exceedance Days by Year and Day of Week.....	72
Figure D-51: Frequency of Eight-Hour Ozone Exceedance Days on Weekdays (2005-2009)	73
Figure D-52: Frequency of Eight-Hour Ozone Exceedance Days on Weekends (2005-2009)....	74
Figure D-53: VOC:NO _x Ratio Annual Geometric Mean (5:00-10:00 LST) Dallas Hinton St. (C401/C60/AH161)	75
Figure D-54: Annual Geometric Mean VOC:NO _x Ratio at Ft. Worth Northwest (C13/AH302)	76
Figure D-55: Scatter Chart of Benzene Concentration as a Function of Ethane Concentration.	78
Figure D-56: Excerpt from a Source Speciation Chart	80
Figure D-57: Complete Reference Speciation Profiles Chart.....	81
Figure D-58: Observed Source Speciation for Ft. Worth Northwest (C13/AH302).....	82
Figure D-59: Emission Rose of Observed Source Species for Ft. Worth Northwest (C13/AH302)	83
Figure D-60: Comparison of Speciation Profiles for Different Scenarios	84
Figure D-61: Species Contributions by Source Type	85
Figure D-62: Oil and Gas Wells and Proximity to the Eagle Mountain Lake (C75) Monitor.....	86
Figure D-63: Seven HYSPLIT Cluster Means Centered at Eagle Mountain Lake (C75)	89
Figure D-64: Surface Back Trajectory Endpoints on High Ozone Days.....	91
Figure D-65: VOC at Denton Airport South (C56/A163/X157).....	93
Figure D-66: Back Trajectory at Eagle Mountain Lake (C75) Monitor for One-Hour Ozone on 1 July 2009.....	94
Figure D-67: Back Trajectory at Eagle Mountain for Lake (C75) Monitor for Eight-Hour Ozone on 1 July 2009	95
Figure D-68: Wind Directions at Eagle Mountain Lake (C75) Monitor Showing Wind Shift from West to East on July 1, 2009.....	96
Figure D-69: One-Hour Ozone at Eagle Mountain Lake on July 1, 2009	97

Figure D-70: One-Hour Ozone and Wind Direction at Eagle Mountain Lake (C75) on July 1, 2009	98
Figure D-71: Scatter Plot Matrix for July 1, 2009 at the Ft. Worth Northwest (C13/AH302) Monitor	99
Figure D-72: Correlations Between Toluene and Benzene at Ft. Worth Northwest (C13/AH302) on July 1, 2009, With (Left) and Without (Right) Outlier	101
Figure D-73: Diurnal Profile of Benzene and Toluene at Ft. Worth Northwest (C13/AH302) on July 1, 2009	102
Figure D-74: Scatter Plot of N-Butane Versus Isopentane at Ft. Worth Northwest (C13/AH302) on July 1, 2009	103
Figure D-75: Scatter Plot of Propane Versus Benzene at Ft. Worth Northwest (C13/AH302). ..	104
Figure D-76: Climatological Temperature Profile at the Ft. Worth Northwest (C13/AH302) Monitor	105
Figure D-77: Daily Maximum Temperature and Insolation at the Ft. Worth Northwest (C13/AH302) Monitor	106
Figure D-78: Daily Peak Ozone and Maximum Temperature at the Ft. Worth Northwest (C13/AH302) Monitor	107
Figure D-79: Daily Peak Ozone and Maximum Insolation at the Ft. Worth Northwest (C13/AH302) Monitor	108
Figure D-80: Wind Climatology in the DFW Area	109
Figure D-81: Wind Speeds by Wind Direction on High Ozone Days	110
Figure D-82: Wind Speeds by Wind Direction on Low Ozone Days	111
Figure D-83: Observed Background Ozone Concentrations in Eastern Texas	116
Figure D-84: Dallas Ozone from 1998 Through 2007 (black line), Partitioned by Estimated Background Contribution (blue) and Estimated Local Contribution (red) (Tobin and Nielsen-Gammon, 2010)	117
Figure D-85: Monthly Average Background Ozone (in units of ppm) Estimated for the DFW Area (Nielsen-Gammon et al. (2005a))	117
Figure D-86: Annual Variation in Regional Background Ozone Estimated for 1998 Through 2003 at Eastern Texas Cities (Nielsen-Gammon (2005a))	118
Figure D-87: Regional Background Ozone Monitors and Wind Direction Windows	120
Figure D-88: Regional Background Ozone at Kaufman (C71/A304/X071)	123
Figure D-89: Regional Background Ozone at Eagle Mountain Lake (C75)	124
Figure D-90: Regional Background Ozone at Pilot Point (C1032)	124
Figure D-91: Regional Background Ozone on High vs. Low Ozone Days at Kaufman (C71/A304/X071)	126
Figure D-92: Regional Background Ozone on High vs. Low Ozone Days at Pilot Point (C1032)	127
Figure D-93: Monthly Regional Background Ozone at Kaufman (C71/A304/X071) in 2009 ...	128
Figure D-94: Monthly Regional Background Ozone at Italy (C1044/A323) in 2009	128

Figure D-95: Example AQPlot Image Showing Forward Wind Trajectories (August 10, 2004) in Northeast Texas.....129

Figure D-96: Example AQplot Image Showing Constant Easterly Flow (August 13, 2004) in Northeast Texas.....130

Figure D-97: High Ozone Versus Low Ozone Back Trajectory Density132

Figure D-98: Comparison of Two Trajectories, One More and One Less Sinuous133

1 OZONE FUNDAMENTALS

Ozone formation conceptual models characterize ozone trends, precursors, formation, and transport in a particular geographic area, to explain the dynamics of ozone formation in that area. This information is compiled and developed into a comprehensive picture of not only where and when ozone forms, but also how and why ozone forms in a geographic area. Conceptual models are required by the U.S. Environmental Protection Agency (U.S. EPA) to accompany photochemical modeling performed for State Implementation Plans (SIP) (U.S. EPA, 2007). This appendix updates the ozone conceptual model for the Dallas-Fort Worth (DFW) nonattainment area.

Conceptual models can be used as tools for selecting representative modeling episodes and for qualitatively evaluating and assessing photochemical modeling results. They are intended to guide modeling efforts conducted in compliance with SIP requirements by presenting the state of the science in terms of current understanding of factors that influence ozone formation and transport. This conceptual model begins with a discussion of the fundamentals of ozone formation photochemistry, followed by a more detailed treatment of the characteristics that make the ozone situation in the DFW area unique. This is followed in Chapter 2 by presentation of results of detailed investigations of trends and patterns in ozone and local precursor concentrations. Chapter 3 continues with analyses of local factors contributing to ozone formation, accumulation, transport, and fate in the DFW area, including a comprehensive examination of the impact of emissions from the Barnett Shale area. Finally, Chapter 4 explores meteorological factors contributing to transport of background ozone into the DFW area. All of these investigations point to the same general conclusion: decreasing trends in measured ozone concentrations are largely a result of real, quantifiable reductions in precursor emissions, and are not due to unusual meteorological conditions.

1.1 Basic Ozone Formation Photochemistry and Meteorology

Tropospheric, or ground level, ozone pollution is a public health concern in many metropolitan areas throughout the United States (National Academy of Sciences, 1991; Bell, 2004, U.S. EPA, 2006, Currie, 2007). Other studies have linked ozone to damage to vegetation (Heck, 1984; Westenbarger and Frisvold, 1994; U.S. EPA 2010) and other materials (U.S. EPA, 2006). Large urban areas are prone to generating elevated levels of ozone in the ambient air because of a confluence of contributing factors: the presence of millions of people and a vast multitude of sources of ozone precursor emissions that support and serve that population, and meteorological conditions favorable to the formation of ozone from those emissions.

Ozone production is generally associated with relatively clear skies, light winds, abundant sunshine, and temperatures above 80 to 85 degrees Fahrenheit. Typically, these meteorological conditions are associated with high-pressure areas that migrate across the U.S. during the spring and summer (Nobis, 1998). Regional background ozone varies strongly by season, with peaks in spring and late summer, and a local minimum during mid-summer. The mid-summer minimum is probably caused by the dominance of high pressure in the southeast U.S., which results flow from the Gulf of Mexico over eastern Texas, and hence low background concentrations (Estes, 2010).

Ozone is a molecule of three oxygen atoms, expressed chemically as O₃. Ozone is created from oxygen, NO_x and VOC in the presence of sunlight. When discussing atmospheric chemistry, NO_x refers to the nitric oxide (NO) and nitrogen dioxide (NO₂). The catalytic cycle of ozone formation and destruction is displayed in Figure D-1: *Chemical Reactions that Form Ozone*. This diagram shows that in the presence of ultraviolet energy from sunlight, denoted by the term

“ $h\nu$,” NO_2 reacts with oxygen to form ozone and NO . In the absence of sunlight or under high NO_x concentrations, the process reverses and is known as ozone titration, or “scavenging.”

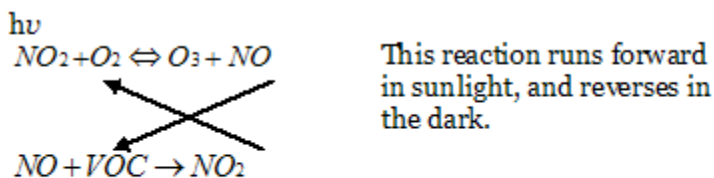


Figure D-1: Chemical Reactions that Form Ozone

The first reaction usually operates forward in sunlight and reverses in the dark. Note, however, that even in sunlight, it may reverse immediately downwind of a very large NO_x source.

The accumulation of ozone slows as the concentration of the reactants decreases: NO_x or VOC . If the reactant in short supply is NO_x , the area is said to be “ NO_x limited” because no further ozone is accumulated even though excess VOC might remain. Similarly, when the ozone accumulation slows due to a lack of VOC , the area is termed “ VOC limited.” Some areas may be NO_x or VOC limited at different times of the day, depending on wind direction and the concentrations of NO_x and VOC , in the ambient air and transported from upwind emission sources. Winds from one direction may transport emissions from a NO_x source to the area, while winds from a different direction may transport VOC emissions to the area. Therefore, consideration of changes in wind patterns, along with types and locations of emission sources, is essential in formulating effective policies to control ozone formation and accumulation.

Because precursor compounds, NO_x and VOC , also exist under natural conditions, ozone is created and destroyed on a natural cycle according to atmospheric conditions and chemical concentrations, even in the absence of additional anthropogenic precursor sources. This natural ozone formation is known as “natural background” ozone and is the starting point for measuring the contribution of ozone and precursors attributable to human activity. Within an urban area, not all ozone formation is necessarily caused by emissions produced locally because anthropogenic precursors, along with ozone formed by them, are often transported over long distances. Background ozone is discussed further below, and in detail in Chapter 4 of this Conceptual Model.

Figure D-2: *Typical Diurnal Ozone Cycle* shows that ozone formation occurs in a daily, or diurnal, cycle, starting from low levels before sunrise, increasing during the morning and into the afternoon, then declining to low (background) levels again after nightfall. Each morning, emissions of NO_x and VOC begin to mix with precursors remaining from the previous day. As the sun heats the atmosphere, providing energy in the form of light, this mixture begins to form ozone. As the energy of the sun dissipates in the evening, the process slows and finally halts overnight.

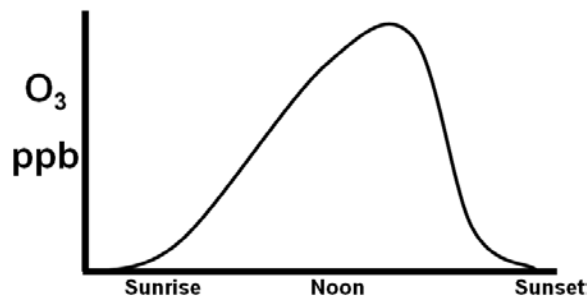


Figure D-2: Typical Diurnal Ozone Cycle

At locations downwind of a major NO_x source, such as depicted in Figure D-3: *Example of Ozone Scavenging Downwind of a NO_x Source*, there may be initial scavenging of ozone due to high levels of NO_x , near the source. However, with additional time and sunlight, the NO_x is gradually converted to additional ozone, resulting in even higher ozone concentrations farther downwind from the source (U.S. EPA, 2006). In the figure, note the initial spike in NO_x emissions (blue line) near mile zero and the corresponding drop in ozone (dark red line) soon after. Even though NO_x has dropped precipitously by about mile eight, ozone soon rebounds from its nadir and begins accumulating.

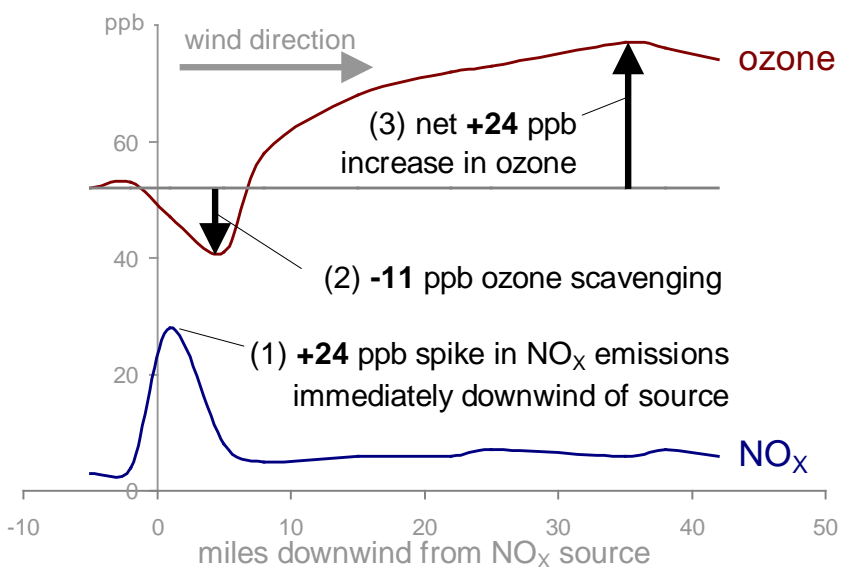


Figure D-3: Example of Ozone Scavenging Downwind of a NO_x Source

(1) An initial injection of NO_x emissions from a NO_x source quickly (2) reduces ambient ozone through scavenging. This reduction is later offset by (3) greater ozone production further downwind.

Meteorological conditions, such as wind direction and speed, temperature, mixing height, solar radiation and other factors, affect the rates at which ozone formation and scavenging reactions occur. The types, as well as the concentration, of precursors present, affect net reactivity of precursor compounds found in a plume of emissions. Concentration is determined by the quantity of emissions and volume of well-mixed air, which in turn is determined by the speed of

winds and the mixing height. Mixing height, determined by temperature and other factors, forms an atmospheric “ceiling” on the available volume of air in which mixing can occur. Figure D-4: *Example of Dynamics of Atmospheric Mixing Height* demonstrates this process. During daylight hours, sunlight heats the ground, which in turn heats surface air. Warm surface air rises and cools until it reaches the mixing height, where the relatively cooler air sinks downward. The cycle repeats until sundown.

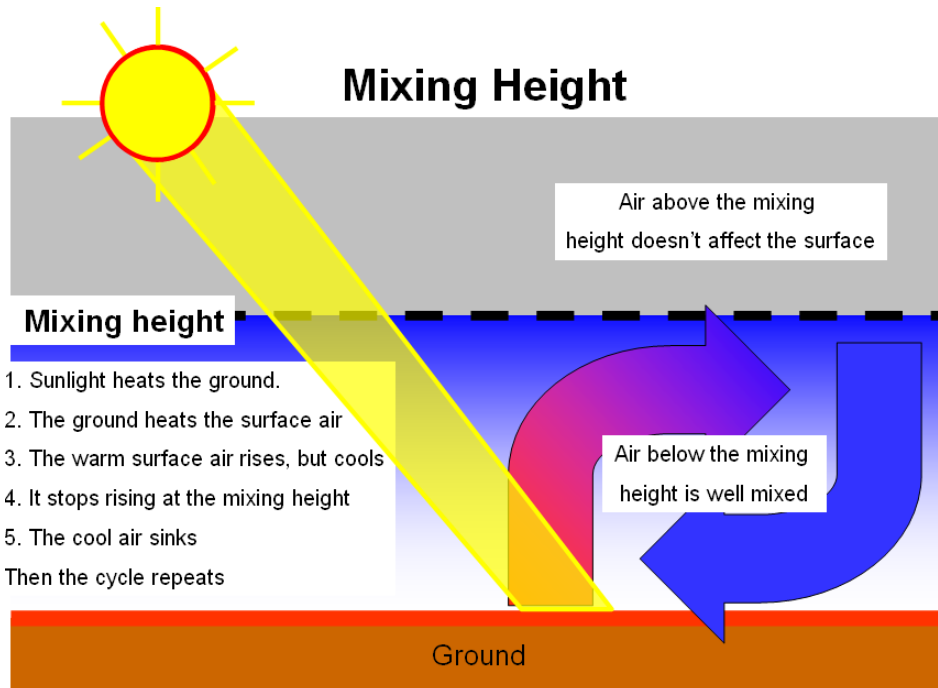


Figure D-4: Example of Dynamics of Atmospheric Mixing Height

For a fixed mass of precursor emissions, a lower mixing height results in a smaller volume of air than does a higher mixing height (Figure D-5: *Effect of Mixing Height on Parcel Concentration*). This gives a more concentrated, and thus more reactive, air parcel. A higher mixing height dilutes the precursors into a larger volume, thus resulting in a less reactive parcel.

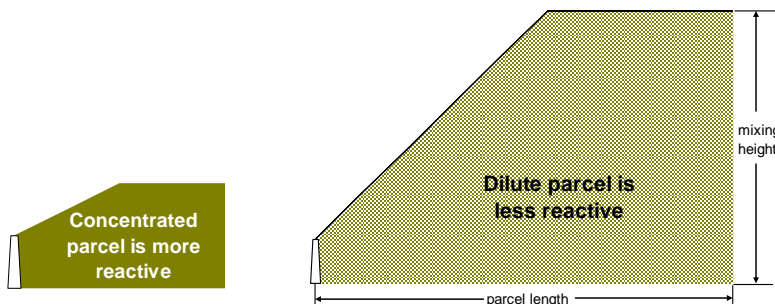


Figure D-5: Effect of Mixing Height on Parcel Concentration

1.2 Ozone in the Dallas-Fort Worth Area

Ozone formation in the DFW area, as in most areas, depends largely on interaction of three factors: local emissions of ozone precursors, ozone-conducive meteorology, and existing or transported background ozone and precursors. The Dallas-Fort Worth-Arlington area is the fourth largest metropolitan area in the U.S., home to nearly 6.5 million residents as of 2009 (U.S. Census Bureau, 2010). These residents own and use motor vehicles, recreational vehicles, lawn and garden equipment, and other emission sources in their daily activities. They work, shop, and recreate at a multitude of commercial, industrial, educational, and recreational sites that contribute emissions from all manner of equipment.

Substantial amounts of precursor compounds, chiefly nitrogen oxides (NO_x) and volatile organic compounds (VOC), are emitted by three major source categories: mobile sources, point sources and area sources. Mobile sources include cars, trucks, ships, planes, locomotives, and construction equipment. Point sources include most industrial equipment such as cement kilns, boilers, process heaters, gas, diesel, and dual-fuel fired stationary engines, stationary gas turbines, duct burners used in turbine exhaust ducts, lime, brick and ceramic kilns, metallurgical heat treat and reheat furnaces, lead smelting, reverberatory and blast furnaces, incinerators, glass, fiberglass and mineral wool processing facilities, natural gas-fired heaters dryers and ovens, and electricity generation facilities. The DFW area hosts all of the above equipment.

Other stationary sources of emissions that lack an identifiable exhaust aperture are grouped into area sources. These facilities include gas stations, dry cleaners, facilities such as commercial shopping centers or schools with compressors for heating and cooling, fertilizer application, personal care products and many more. Natural or biogenic sources, mainly trees, emit ozone precursors such as isoprene and pinene, which are known to react particularly quickly with NO_x to form ozone (Rapid Science Synthesis Team, 2006). Finally, precursor compounds, along with ozone, are often transported into urban areas from external locations.

Background ozone concentrations in north central Texas average about 50 ppb; however, this estimate is one of many and depends to a great extent on the definition being used, averaging time, time of year, and other factors. Natural background ozone, or the background ozone that would prevail in the absence of anthropogenic influences, tends to be lower than regional background ozone, or ozone transported into the region from elsewhere.

Higher background ozone concentrations in the DFW area are usually observed when winds originate from the south and southeast, while lower concentrations are observed when winds originate from the north and west. Background and transport appear at this time to play a secondary, though not inconsequential, role in DFW ozone photochemistry, at least when compared to local sources. However, these sources may contribute a greater fraction of the total in the future as local emissions reductions are implemented. Background ozone will be explored in detail in Chapter

In the absence of accidental releases or spills, whether high concentrations of pollutants form on a given day is controlled mostly by meteorological processes, which may transport the pollutants and either dilute pollutant emissions or allow them to accumulate. Meteorology also affects other key processes, such as chemical reaction rates (Banta, et al., 2005). High ozone concentrations are observed most frequently in the DFW area on days lacking strong synoptic, or large-scale, pressure gradients. When synoptic (large-scale) weather systems move through the region, ozone and precursor emissions tend to be diluted and carried out of the city, rather than concentrated in still, stagnating air, to be heated, reacted and turned into ozone. Days

dominated by strong synoptic weather systems tend to experience low ozone levels (Banta, et al., 2005).

Absent dominant synoptic weather systems, smaller-scale local wind patterns govern ozone formation. As precursor emissions are advected across the region, they mix with other local emissions, as well as compounds transported into the region, to generate elevated concentrations of ozone. On days with light winds, precursors generated in the morning, along with those remaining from the previous day, accumulate, and then react during the warmest and sunniest portion of the day. Ozone rich air masses typically begin to form in the center and south of the city. Later in the afternoon, southeasterly breezes can advect, or horizontally transport, the pool of high ozone over the city toward the west and northwest.

During the ozone season, and especially in late summer, the DFW area experiences relatively light winds and persistent hot, humid, and sunny conditions. Late summer peak ozone concentrations in the DFW area also tend to be higher than most other areas. Exceedances of the National Ambient Air Quality Standards (NAAQS) for eight-hour ozone tend to occur in the DFW area from March through October (Figure D-6: *Eight-Hour Ozone Exceedance Days in DFW and Other Areas of Texas*). An exceedance day is any day when an exceedance of the eight-hour ozone NAAQS is measured in an area. Note that the DFW area experiences more exceedance days throughout the year than most other area of Texas. DFW tends to record two peaks in the frequency of exceedance days, one in late spring, and another in late summer.

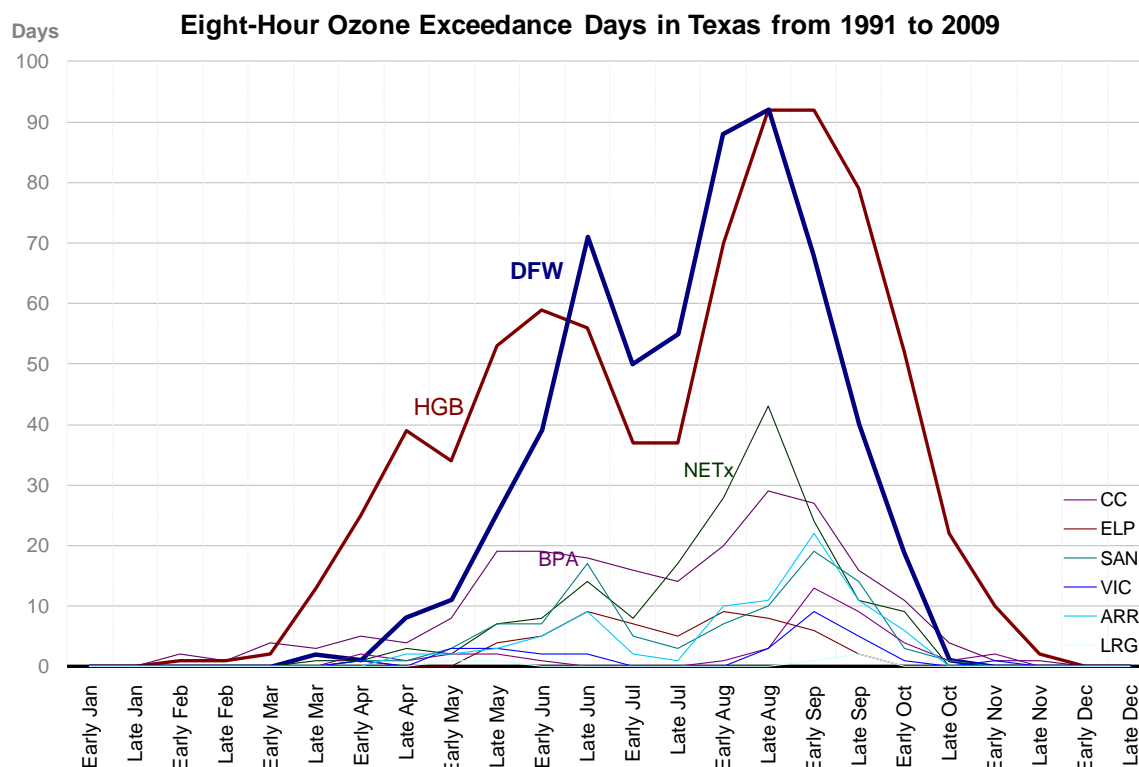


Figure D-6: Eight-Hour Ozone Exceedance Days in DFW and Other Areas of Texas
AUS = Austin; BPA = Beaumont-Port Arthur; CC = Corpus Christi; DFW = Dallas-Fort Worth; ELP = El Paso; HGB = Houston-Galveston-Brazoria; LRV = Lower Rio Grande Valley; SAN = San Antonio; TLM = Tyler-Longview-Marshall

While the details of ozone formation, accumulation, transport, and fate are highly technical and require complex algorithms to compute, a conceptual model provides insight into the unique characteristics of ozone processes in a region on a more simplified scale. The insights gained from a conceptual model provide guidance on modeling distinctive phenomena. This conceptual model draws on established scientific understanding of photochemical, physical, and meteorological processes, as well as recent findings on local ozone and precursor patterns, background ozone, and meteorology specific to the DFW area.

2 AIR QUALITY TRENDS IN THE DALLAS-FORT WORTH AREA

Trends in ozone and its precursors demonstrate not only the substantial progress the DFW area has made in improving air quality, but also the magnitude of the future challenge in attaining the National Ambient Air Quality Standard (NAAQS) for ozone. Trends are also useful as a first look at how ozone is related to its precursors. Ozone is a secondary pollutant, formed through a photochemical reaction of NO_x and sunlight. VOC can amplify ozone production, causing accumulation in the atmosphere. Decreases in NO_x and VOC demonstrate the effectiveness of policies to reduce emissions; however, due to its dependence on meteorological variables, ozone may not always exhibit trends identical to its precursors. Separating variations in meteorological factors from trends in ozone and its precursors can highlight whether ozone reductions are caused by decreases in precursor emissions or by to year-to-year variability in local meteorology (Sullivan, et al, 2009, Camalier, et al, 2007). This chapter discusses trends, both temporal and spatial, in ozone and its precursors.

2.1 Ozone Trends

A “design value” is a statistic used to compare an area’s concentrations of a particular pollutant to the pollutant’s NAAQS. Design values are commonly used to characterize ambient ozone concentrations because they summarize the severity of a local ozone problem into a single number. The criteria for attainment of the ozone NAAQS have changed over the past 12 years. Until its revocation on April 30, 2004, the ozone NAAQS was based on one-hour average concentrations of 0.12 parts per million (ppm), averaged over one hour (U.S. EPA, 2004). An exceedance occurred when the fourth highest one-hour ozone concentration in a three-year period equaled or exceeded 0.125 ppm. The eight-hour NAAQS for ozone was adopted in 1997, but not implemented until 2004, and was set at 0.08 ppm averaged over 8 hours. A monitor exceeds the eight-hour standard when its design value, a three-year average of the fourth highest eight-hour ozone concentration for each year, equals or exceeds 0.08 ppm. The design value of record for an area is the highest design value recorded at any monitor in the area.

This section examines the frequency at which the NAAQS (both one-hour and eight-hour) for ozone are exceeded, with the understanding that the eight-hour standard of 0.08 ppm is currently being used for control strategy development and that the one-hour standard is no longer in effect, but it is still a useful benchmark for understanding ozone behavior in the DFW area. While the Federal NAAQS is expressed in units of parts per million, this chapter will use the familiar convention of expressing concentrations in parts per billion (ppb). Following EPA truncation procedures, the eight-hour ozone NAAQS is often expressed as 85 ppb.

Daily peak eight-hour ozone concentrations for the years 1991 to 2009 in the DFW area are shown in Figure D-7: *Daily Peak Eight-Hour Ozone Values in the DFW Area*. The majority of days show ozone peaks below 85 ppb, but the highest days, which set the design values, are of particular interest. Annual maximum values and 90th percentile values have decreased over time; however, the median values appear to show no change or a very slight increase. Notable in the figure is the decrease in the number of daily peaks exceeding the 85 ppb NAAQS. It is also possible to identify the bi-modal character of the annual ozone cycle in several years. On an annual basis, ozone tends to peak first in spring and then again later in the summer (Nobis, 1998).

Ozone
(ppb)
200

Daily Peak Eight-Hour Ozone in the DFW Area

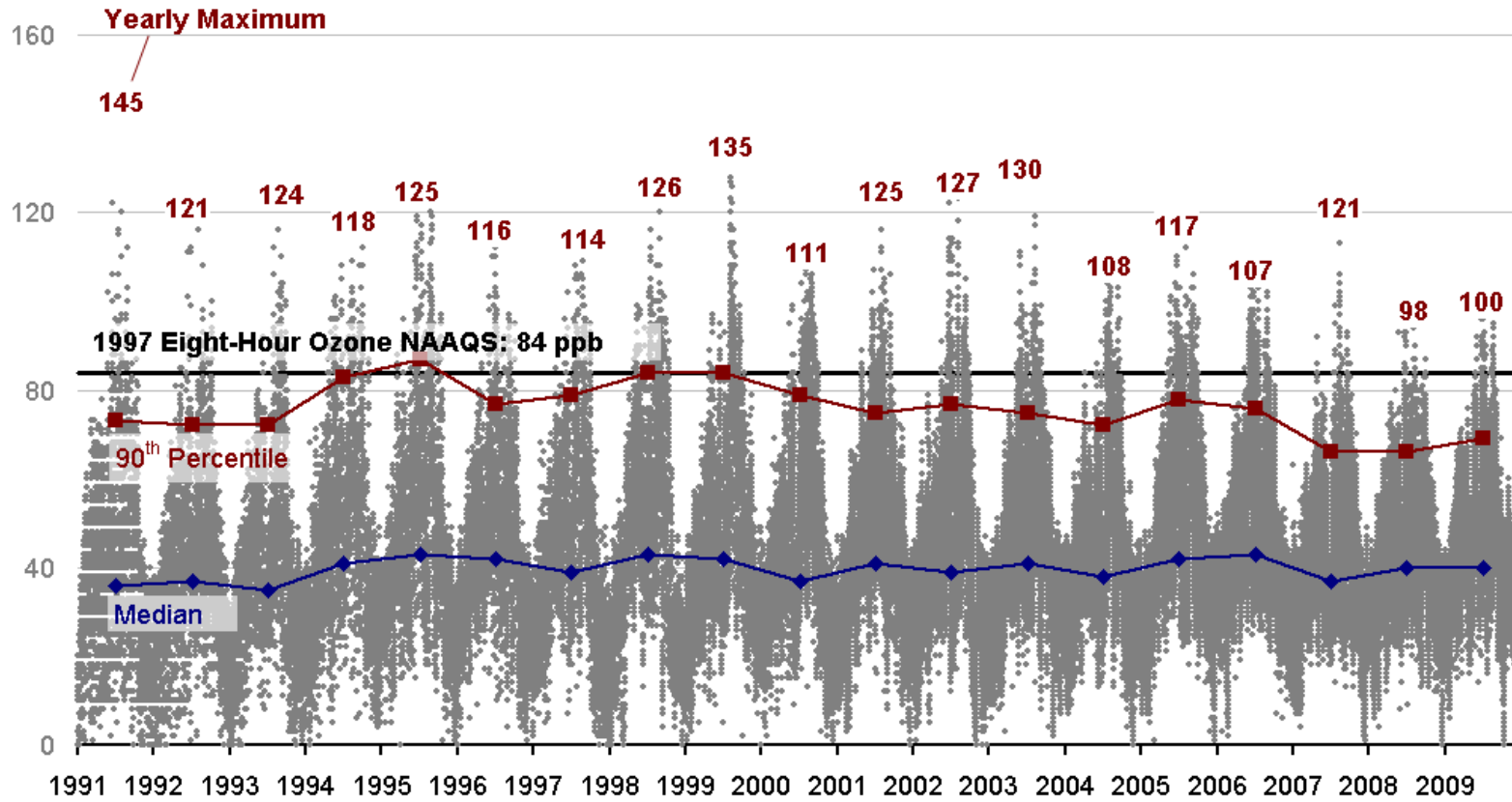


Figure D-1: Daily Peak Eight-Hour Ozone Values in the DFW Area

The annual cycle of ozone is apparent in the figure, as daily peak ozone tends to increase throughout the spring, into the summer, and then falls as winter approaches, when it reaches a nadir. This cycle follows the annual pattern of temperature, which also rises as summer approaches, peaks, then falls in winter. Temperature is likely acting as a proxy for solar radiation or other meteorological factors known to strongly influence ozone formation. Temperature and solar radiation patterns will be discussed in detail in Chapter 3.

The trend in design values is seen more clearly in Figure D-8: *Ozone Design Values for the DFW Area*. While the DFW area continues to exceed eight-hour ozone standards, eight-hour ozone design values have decreased over the past nine years. The eight-hour ozone design value in 2009 was 86 ppb, an 18 percent decrease from the 1991 design value of 105 ppb. The 2009 value is approaching the ozone NAAQS of 84 ppb. Work presented in Chapter 3 investigates whether ozone reductions observed from 2007 to 2009 are due to anomalous meteorology or may be expected to continue as further emission reductions are achieved. Regression of design value on year estimates that eight-hour ozone design values decreased at the rate of 0.6 ppb (0.0006 ppm) per year, which is statistically significant at the 5 percent level ($\alpha = 0.05$). If this trend were to continue at that rate, attainment of the eight-hour standard could be reached in two years.

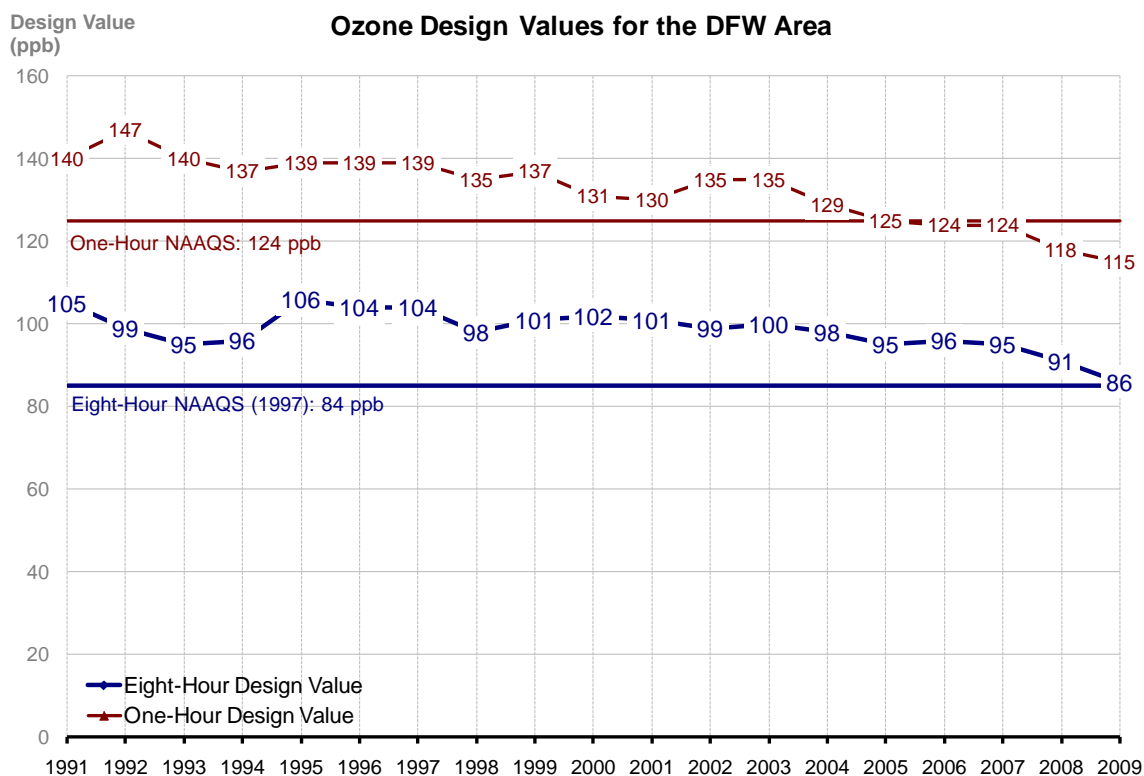


Figure D-2: Ozone Design Values for the DFW Area

The DFW area one-hour ozone design value in 2009 was 115 ppb, an 18 percent decrease from the 1991 design value of 140 ppb. The one-hour design value in the DFW area has met the previous one-hour ozone NAAQS of 124 ppb since 2006. Regression of one-hour design values on year shows they decreased at the rate of 0.85 ppb per year, which is faster than the rate of

decline of the eight-hour ozone design values; the slope is also statistically significant at the 5 percent level ($\alpha = 0.05$).

The design value of record in a metropolitan area is the highest design value of all individual design values at monitors in an area. Because ozone varies spatially, it is prudent to investigate trends at all monitors in an area, not just those recording the highest design values. Table D-1: *Eight-Hour Ozone Design Values by Monitor in the DFW Area* and Table D-2: *One-Hour Ozone Design Values by Monitor in the DFW Area* contain the eight-hour and one-hour ozone design values at all regulatory monitors in the DFW area from 1991 to 2009.

Table D-1: Eight-Hour Ozone Design Values by Monitor in the DFW Area

Monitor/CAMS #	1991	1992	1993	1994	1995	1996	1997	1998	1999	2000	2001	2002	2003	2004	2005	2006	2007	2008	2009
Eagle Mountain Lake C75											95	96	94	95	96	95	89	86	
Keller C17	105	99	95	96	106	104	97	92	95	97	97	98	100	98	95	94	92	87	86
Denton Airport South C56										102	101	99	97	96	93	95	94	91	85
Grapevine Fairway C70											95	100	98	93	93	92	87	84	
Cleburne Airport C77											89	90	90	89	87	85	83	83	
Parker County C76											86	89	86	87	88	91	84	81	
Dallas North No.2 C63											93	89	86	87	90	89	86	80	81
Ft. Worth Northwest C13	97	94	94	88	92	94	96	97	99	99	97	96	96	94	95	94	91	83	79
Frisco C31				92	99	99	101	98	101	101	99	93	88	89	91	92	88	83	79
Dallas Redbird Airport C402							91	91	92	88	84	84	85	87	88	88	85	82	78
Granbury C73											84	84	81	81	84	84	81	77	
Pilot Point C1032																		81	77
Arlington Municipal Airport C61													87	87	87	84	79	77	
Rockwall Heath C69											83	81	82	81	80	78	75	75	
Midlothian OFW C52/C137																		75	73
Midlothian Tower C94/C158								87	92	97	88	86	82	87	84	83	78		
Kaufman C71											70	73	73	73	75	76	73	70	
Dallas Hinton St. C401/C60							90	88	91	93	92	91	90	89	90	87	84	74	67
Greenville C1006														79	79	76	70	66	
Sunnyvale Long Creek C74												83	83	84	73				
Anna C68											83	80	80						
Arlington Reg. Office C57										95	86								
Denton Co. Airport C33					100	103	104												
Denton Colony	83	78	79	93	101	99	99	94	100										
Dallas North C5	92	90	88	90	97	97	95	89											
Bonnieview	71	66	67	68															

*Values are sorted in descending order of design values in 2009, then 2008, 2007, *et cetera*.

Table D-2: One-Hour Ozone Design Values by Monitor in the DFW Area

Monitor/CAMS #	1991	1992	1993	1994	1995	1996	1997	1998	1999	2000	2001	2002	2003	2004	2005	2006	2007	2008	2009
Denton Airport South C56								122	126	126	126	128	122	118	117	118	118	118	115
Eagle Mountain Lake C75										112	117	135	135	129	125	124	124	115	111

Monitor/CAMS #	1991	1992	1993	1994	1995	1996	1997	1998	1999	2000	2001	2002	2003	2004	2005	2006	2007	2008	2009
Keller C17	140	147	140	137	139	139	131	128	128	128	128	128	128	126	117	115	117	111	108
Grapevine Fairway C70										98	118	128	128	125	113	112	111	107	108
Dallas Redbird Airport C402					116	118	134	135	125	118	111	103	112	121	121	111	110	109	105
Dallas North No.2 C63								129	128		128	118	113	118	120	117	116	101	105
Cleburne Airport C77									108		109	110	110	118	108	106	105	105	104
Parker County C76									94		99	111	113	112	116	116	116	106	103
Frisco C31		140	140	126	129	126	132	128	133	130	130	119	113	113	113	113	111	110	102
Ft. Worth Northwest C13	130	140	140	121	121	126	133	127	133	131	130	126	126	123	123	117	118	109	102
Arlington Municipal Airport C61												122	120	120	117	113	113	101	100
Granbury C73/C681									99		109	108	107	101	104	104	104	98	98
Midlothian OFW C52/C137																98	103	98	95
Pilot Point C1032																107	104	101	94
Midlothian Tower C94/C158							130	128	128		117	116	106	116	114	114	99	98	92
Rockwall Heath C69									117		102	102	98	108	101	96	93	92	92
Dallas Hinton St. C401/C60	120	120	121	113	121	121	121	120	128	127	125	118	125	118	115	114	114	97	87
Kaufman C71									81		88	89	90	91	93	87	89	87	87
Italy C1044/A323																		86	86
Corsicana Airport C1051																			86
Greenville C1006												93	93	92		92	90	88	79
Sunnyvale Long Creek C74											89	104	107	107	111	107			
Anna C68									105		105	108	105	103					
Arlington Reg. Office C57							125	137	126		125								
Denton C80		141																	
Denton Co. Airport C33			117	137	138	139	139												
Denton Colony		130	120	120	120	127	129	118	128										
Dallas North C5		130	130	122	122	134	134	134	116										
Terrell C83		110																	
Bonnieview		100	100	93	89														
Ennis C82		100																	
Number of Monitors	8	8	8	8	8	8	8	10	10	17	18	18	19	19	18	20	19	20	21

*Values are sorted in descending order of design values in 2009, then 2008, 2007, *et cetera*.

Figure D-9: *Eight-Hour Ozone Design Value Statistics in the DFW Area* and Figure D-10: *One-Hour Ozone Design Value Statistics in the DFW Area* display three summary statistics for the eight-hour and one-hour ozone design values, respectively: the maximum, median, and minimum values computed across all monitors in the DFW area. These figures facilitate assessment of the range of design values observed within a year, as well as how these distributions change over time. It appears from the figures that neither eight-hour nor one-hour ozone design values exhibited a noticeable trend until about 2000, when both began falling steadily. By 2002, over half the monitors in the area attained the one-hour standard and by 2007, over half of the monitors attained the eight-hour standard, as indicated by the median value falling below the NAAQS in those years. (The median statistic as used here indicates that half the observed design values are above the median, and half below it.) Since 2006, all monitors in the DFW area met the one-hour ozone NAAQS.

Both the Eagle Mountain Lake (CAMS 13) monitor and the Keller (CAMS 17) monitor currently set the eight-hour design value of record for the DFW area. Their 2009 design value, 86 ppb, is

calculated (as with all monitors) by averaging the 2007 through 2009 fourth highest concentrations, and truncating any decimal. At Eagle Mountain Lake (CAMS 13), these values were 84, 85, and 91 ppb (Table D-3: *Annual Fourth Highest Eight-Hour Ozone Values and Design Values*), and at Keller (CAMS 17) these values were 84, 85, and 90 ppb. Because 2007 will be excluded from the 2010 calculation, Eagle Mountain Lake (CAMS 13) would need to record a fourth-highest eight-hour ozone concentration of 79 ppb or higher in 2010 to violate the NAAQS, and Keller (CAMS 17) would need to record a fourth-highest eight-hour ozone concentration of 80 ppb or higher in 2010 to violate the NAAQS. The only other monitor above the eight-hour ozone NAAQS is Denton Airport South (CAMS 56), and that monitor would need a fourth-highest eight-hour ozone concentration of 89 ppb or greater in 2010 to violate the NAAQS.

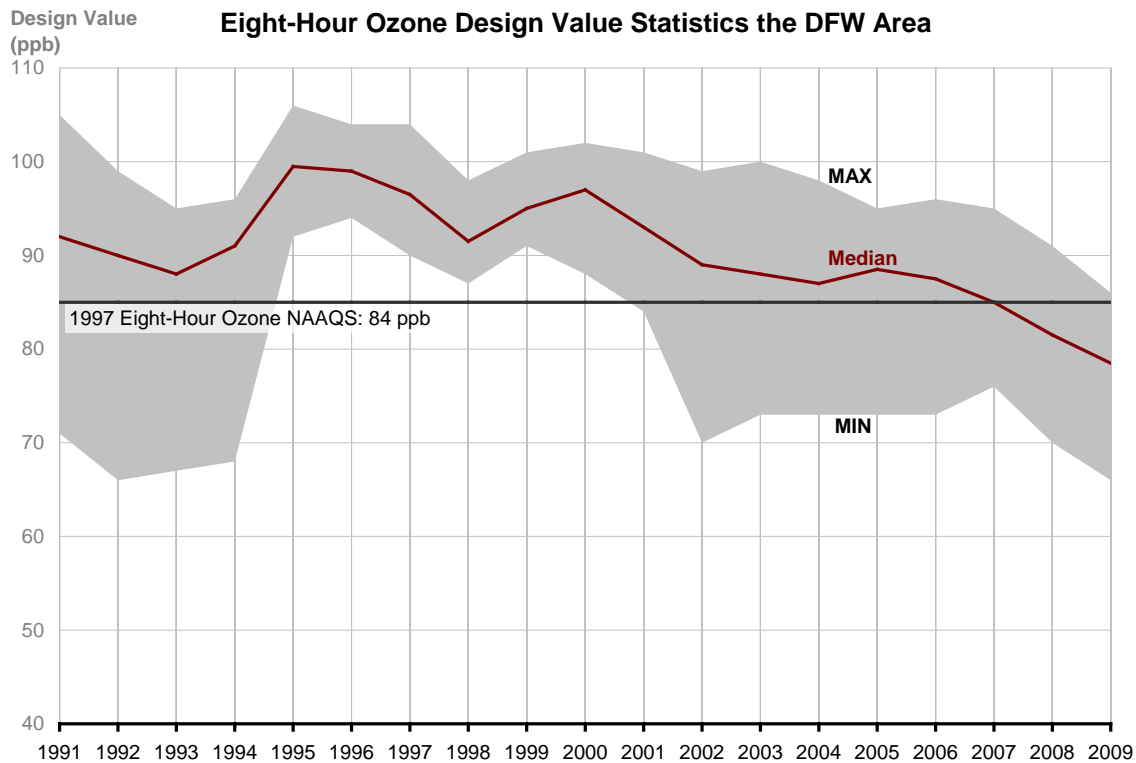


Figure D-3: Eight-Hour Ozone Design Value Statistics in the DFW Area

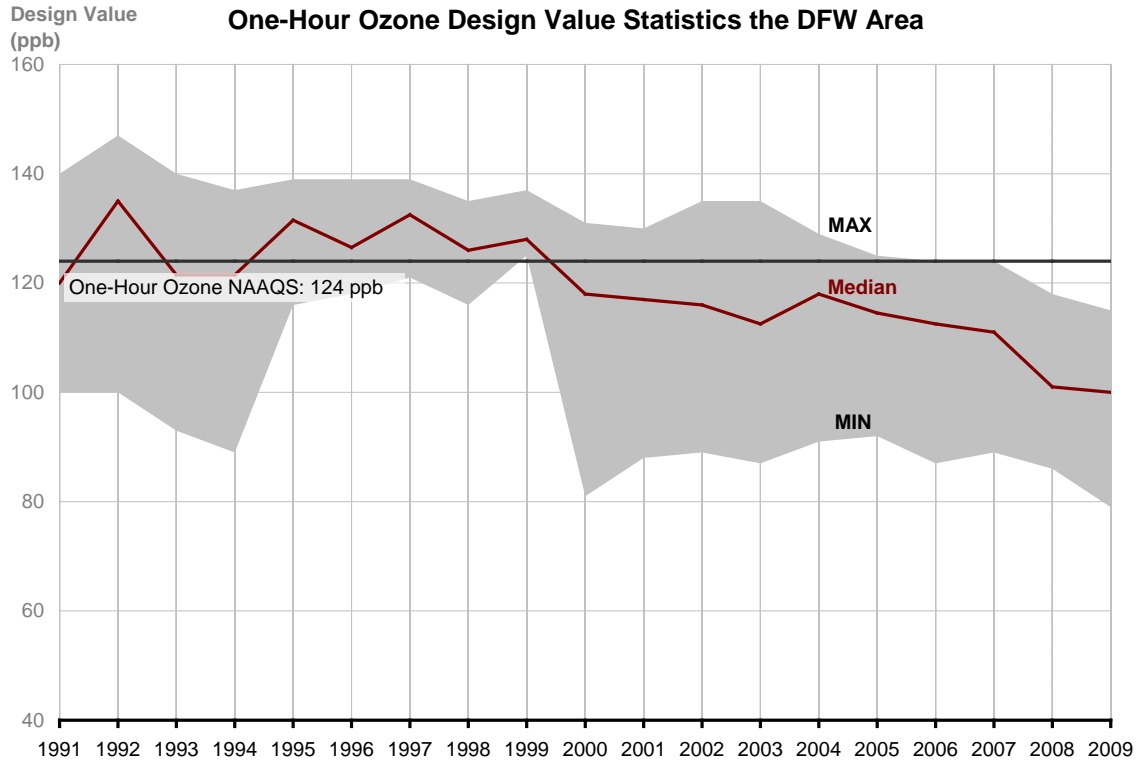


Figure D-4: One-Hour Ozone Design Value Statistics in the DFW Area

Table D-3: Annual Fourth Highest Eight-Hour Ozone Values and Design Values

Monitor	2007 4 th High	2008 4 th High	2009 4 th High	2009 Eight- Hour Ozone Design Value	2010 Fourth- Highest Needed to Violate the NAAQS
	<i>ppb</i>	<i>ppb</i>	<i>ppb</i>	<i>ppb</i>	<i>ppb</i>
Eagle Mountain Lake C75	84	85	91	86	79
Keller C17	84	85	90	86	80
Denton Airport South C56	89	84	82	85	89

*Monitors are sorted in descending order by 2009 design value. The 2009 design value is the average of the 2007 through 2009 fourth high values.

Ozone trends can also be investigated by looking at the number of days an exceedance of the ozone NAAQS was recorded, termed an “exceedance” day. An exceedance day for the eight-hour NAAQS is any day that any monitor in the area measures an eight-hour average ozone concentration greater than or equal to 85 ppb over any eight-hour period. An exceedance day for one-hour ozone is any day that any monitor in the area measures a one-hour average ozone concentration greater than or equal to 125 ppb for at least one hour. Previous research (Savanich, 2006) by the TCEQ has shown that, until 2006, the number of exceedance days was positively correlated with the number of monitors in a particular area. That is, as the number of monitors increases, so does the number of exceedance days recorded, at least until either the area has been saturated with monitors, so that no previously unobserved exceedances are detected, or until ozone concentrations truly decrease. Because of this correlation, when examining exceedance-day trends, the number of monitors must always be considered. Thus, it is especially noteworthy that Figure D-11: *Number of Monitors and Ozone Exceedance Days in*

the DFW Area shows that, despite an increase in the number of monitors, the number of exceedance days for both one-hour and eight-hour ozone has generally decreased. The decrease is especially pronounced for eight-hour ozone over the past four years. Since 1991, the number of eight-hour ozone exceedance days occurring in the DFW area has fallen 54 percent, and in just the last four years, the number of eight-hour exceedance days has fallen 73 percent. No one-hour ozone exceedance days occurred in the DFW area in 2008 and 2009; this represents a 100 percent decrease in the number of one-hour ozone exceedance days from 1991 to the present.

Results for individual monitors, displayed in Figure D-12: *Number of Eight-Hour Ozone Exceedance Days by Monitor* and Figure D-13: *Number of One-Hour Ozone Exceedance Days by Monitor*, support this conclusion: the number of exceedance days at individual monitors also appears to be decreasing. These figures highlight two monitors, Eagle Mountain Lake (CAMS 75) (blue line) and Keller (CAMS 17) (red line), that recorded the highest eight-hour ozone design values. Figure D-13: *Number of One-Hour Ozone Exceedance Days by Monitor* also highlights the two monitors, Denton Airport South (CAMS 56) (blue line) and Keller (CAMS 17) (red line), that recorded the highest one-hour ozone design value. There have not been more than seven one-hour ozone exceedance days per year at any monitor in the DFW area from 1991 through 2009. There has been no one-hour ozone exceedance at any monitor in the DFW area since 2008. Because of the large number of monitors in the DFW area, data from these two figures are presented in Table D-4: *Number of Days with an Eight-Hour Ozone Exceedance* and Table D-5: *Number of Days with a One-Hour Ozone Exceedance*.

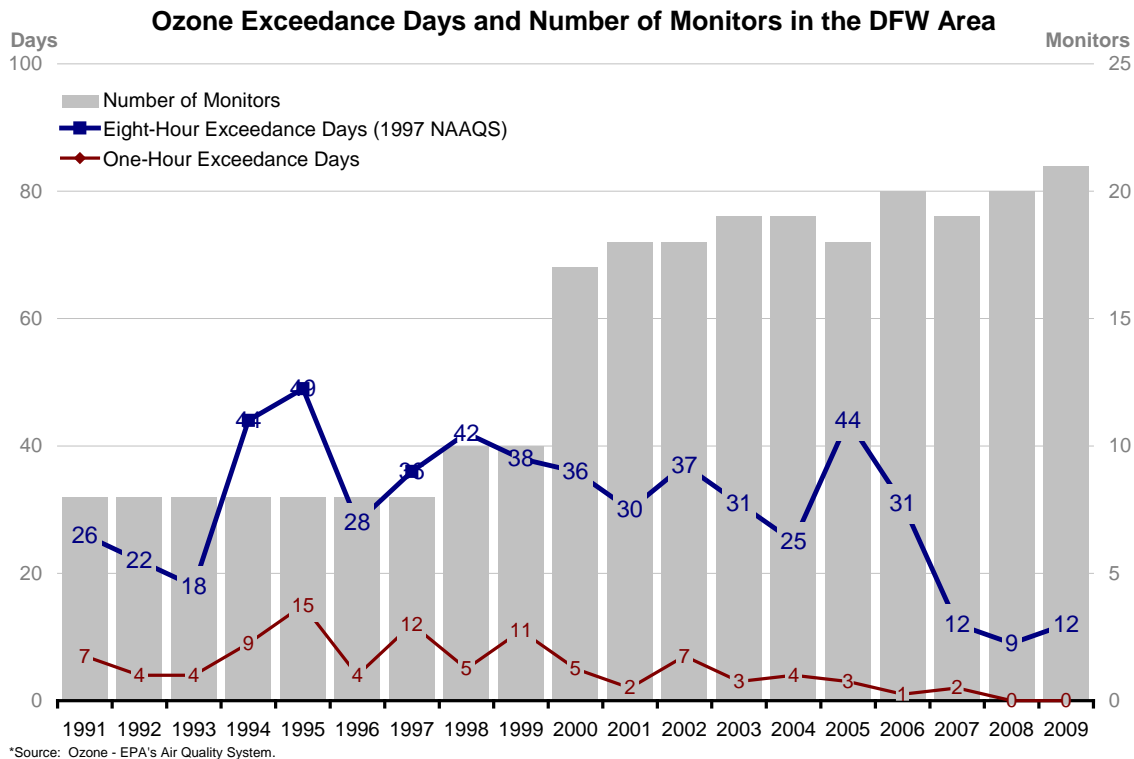


Figure D-5: Number of Monitors and Ozone Exceedance Days in the DFW Area

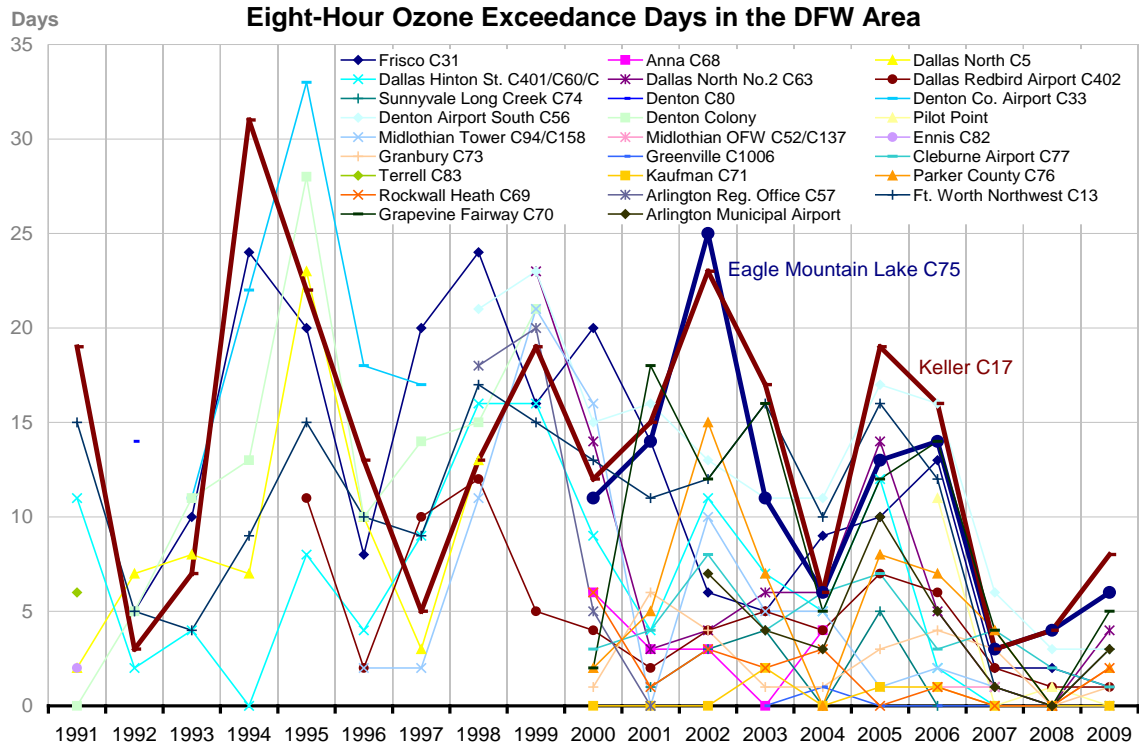


Figure D-6: Number of Eight-Hour Ozone Exceedance Days by Monitor

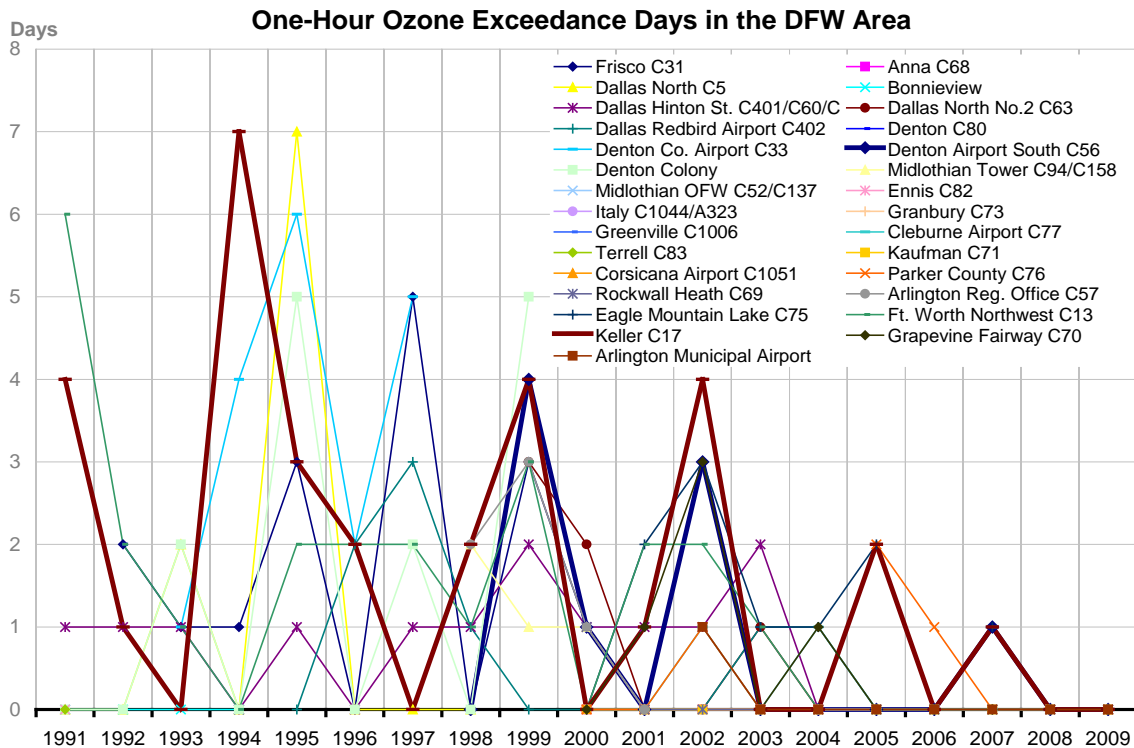


Figure D-7: Number of One-Hour Ozone Exceedance Days by Monitor

Table D-4: Number of Days with an Eight-Hour Ozone Exceedance

Monitor	1991	1992	1993	1994	1995	1996	1997	1998	1999	2000	2001	2002	2003	2004	2005	2006	2007	2008	2009
Keller C17	19	3	7	31	22	13	5	13	19	12	15	23	17	6	19	16	3	4	8
Eagle Mountain Lake C75										11	14	25	11	6	13	14	3	4	6
Grapevine Fairway C70										2	18	12	16	5	12	14	4	0	5
Dallas North No.2 C63									23	14	3	4	6	6	14	5	1	0	4
Denton Airport South C56								21	23	15	16	13	11	11	17	16	6	3	3
Ft. Worth Northwest C13	15	5	4	9	15	10	9	17	15	13	11	12	16	10	16	12	1	0	3
Arlington Municipal Airport												7	4	3	10	5	1	0	3
Parker County C76										2	5	15	7	0	8	7	4	0	2
Rockwall Heath C69										6	1	3	2	3	0	1	0	0	2
Cleburne Airport C77										3	4	8	4	6	7	3	4	2	1
Frisco C31		5	10	24	20	8	20	24	16	20	14	6	5	9	10	13	2	2	1
Dallas Redbird Airport C402					11	2	10	12	5	4	2	4	5	4	7	6	2	1	1
Granbury C73										1	6	4	1	1	3	4	3	0	1
Pilot Point																11	0	1	0
Midlothian OFW C52/C137																1	1	0	0
Dallas Hinton St. C401/C60/C	11	2	4	0	8	4	9	16	16	9	4	11	7	5	12	2	0	0	0
Greenville C1006													0	1	0	0	0	0	0
Kaufman C71										0	0	0	2	0	1	1	0	0	0
Midlothian Tower C94/C158						2	2	11	21	16	0	10	5	5	1	2	1		
Sunnyvale Long Creek C74											1	3	4	0	5	0			
Anna C68										6	3	3	0	4					
Arlington Reg. Office C57								18	20	5	0								
Denton Co. Airport C33			11	22	33	18	17												
Denton Colony	0	5	11	13	28	10	14	15	21										
Dallas North C5	2	7	8	7	23	10	3	13											
Denton C80		14																	
Ennis C82	2																		
Terrell C83	6																		

***Monitors are sorted in descending order by the number of eight-hour ozone exceedance days recorded in 2009, then 2008, 2007, et cetera.**

Table D-5: Number of Days with a One-Hour Ozone Exceedance

Monitor	1991	1992	1993	1994	1995	1996	1997	1998	1999	2000	2001	2002	2003	2004	2005	2006	2007	2008	2009
Eagle Mountain Lake C75										0	2	3	1	1	2	0	1	0	0
Ft. Worth Northwest C13	6	2	1	0	2	2	2	1	3	0	2	2	1	0	2	0	1	0	0
Keller C17	4	1	0	7	3	2	0	2	4	0	1	4	0	0	2	0	1	0	0
Denton Airport South C56								0	4	1	0	3	0	0	0	0	1	0	0
Parker County C76										0	0	1	0	0	2	1	0	0	0
Dallas Redbird Airport C402					0	2	3	1	0	0	0	0	1	1	0	0	0	0	0
Cleburne Airport C77										0	0	1	0	1	0	0	0	0	0
Grapevine Fairway C70										0	1	3	0	1	0	0	0	0	0
Dallas Hinton St. C401/C60/C	1	1	1	0	1	0	1	1	2	1	1	1	2	0	0	0	0	0	0

Monitor	1991	1992	1993	1994	1995	1996	1997	1998	1999	2000	2001	2002	2003	2004	2005	2006	2007	2008	2009
Dallas North No.2 C63								3	2		0	0	1	0	0	0	0	0	0
Arlington Municipal Airport												1	0	0	0	0	0	0	0
Frisco C31		2	1	1	3	0	5	0	3	1	0	0	0	0	0	0	0	0	0
Midlothian Tower C94/C158								2	1	1	0	0	0	0	0	0	0	0	0
Rockwall Heath C69										1	0	0	0	0	0	0	0	0	0
Arlington Reg. Office C57								2	3	1	0								
Denton Colony	0	0	2	0	5	0	2	0	5										
Granbury C73										0	0	0	0	0	0	0	0	0	0
Greenville C1006													0	0	0	0	0	0	0
Kaufman C71										0	0	0	0	0	0	0	0	0	0
Midlothian OFW C52/C137																0	0	0	0
Anna C68										0	0	0	0	0					
Denton Co. Airport C33			1	4	6	2	5												
Dallas North C5	0	0	2	0	7	0	0	0											
Bonnieview	0	0	0	0															
Denton C80		2																	
Italy C1044/A323																		0	0
Corsicana Airport C1051																			0
Ennis C82	0																		
Terrell C83	0																		

***Monitors are sorted in descending order by the number of one-hour ozone exceedance days recorded in 2009, then 2008, 2007, et cetera.**

The ozone season spans March through October in the DFW area (U.S. EPA, 2008a); however, the period when elevated ozone concentrations are observed varies from year to year. Figure D-14: *Eight-Hour Ozone Exceedance Days by Month and Year in the DFW Area* shows the frequency of, and variation in, the number of eight-hour ozone exceedance days in the DFW area by month and year. While the ozone season does vary from year to year, in the past few years the DFW area has experienced fewer ozone exceedance days over fewer months. The darker areas in the figure show that peak ozone season in the DFW area typically occurs in August, with a smaller, secondary peak occurring earlier in some years, roughly in June.

Eight-Hour Ozone Exceedance Days in the DFW Area

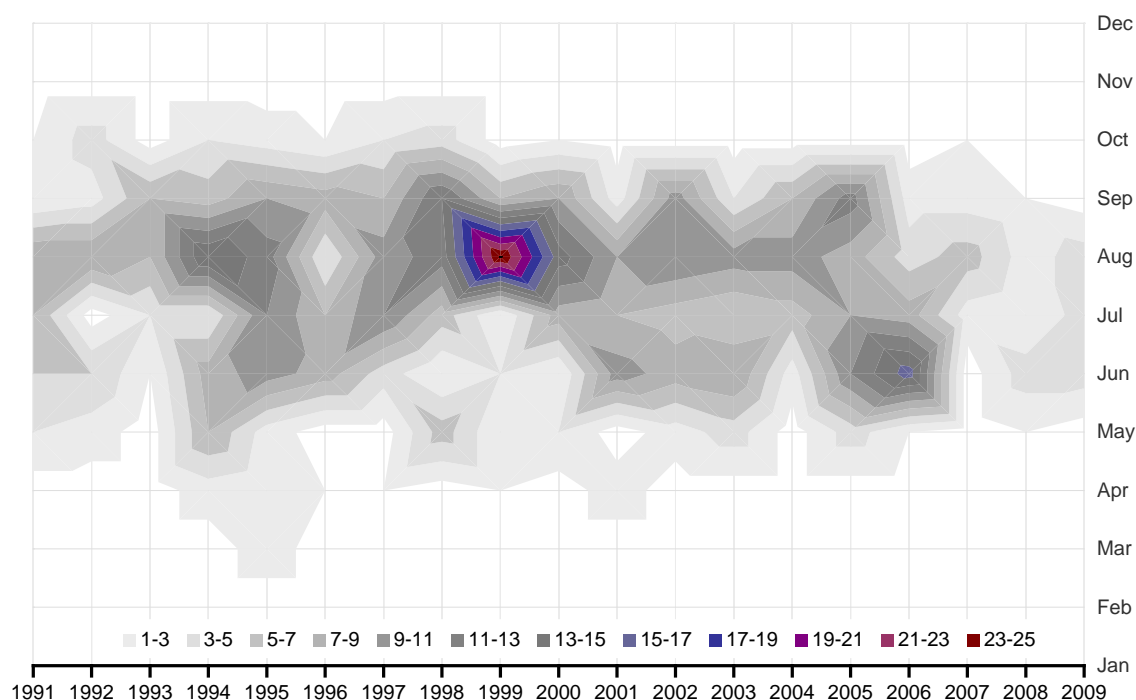


Figure D-8: Eight-Hour Ozone Exceedance Days by Month and Year in the DFW Area

Varieties of analyses have been presented for understanding ozone trends in the DFW area. The results of these analyses generally agree that ozone concentrations have been decreasing; however, the area still faces challenges in achieving attainment of the 1997 ozone NAAQS. Because ozone formation depends on a multitude of factors, these factors must be investigated in detail before conclusions as to causes of the observed decreases can be reached.

2.2 Nitrogen Oxide Trends

Nitrogen oxide (NO_x), a precursor to ozone formation, is a variable mixture of nitric oxide (NO) and nitrogen dioxide (NO₂). NO_x is primarily emitted by fossil fuel combustion, lightning, biomass burning, and soil (Martin, *et.al*, 2006). Examples of common NO_x emission sources, which occur in all urban areas, are automobiles, diesel engines, and other small engines; residential water heaters; industrial heaters and flares; and industrial and commercial boilers. Mobile, residential, and commercial NO_x sources are usually numerous, smaller sources distributed over a large geographic area, while industrial sources are usually large point sources, or numerous small sources, clustered in a small geographic area. Because of the large number of NO_x sources, high ambient NO_x concentrations can occur throughout the DFW area.

Other sources of NO_x that are important to air quality in the DFW area are large electric generating units (EGU) in and around the metropolitan area, as well as other areas upwind of the DFW area. These facilities can produce large concentrated plumes of emissions that can enhance ozone generation. Analyses done by the Rapid Science Synthesis Team of the 2005-2006 Texas Air Quality Study (TexAQS II) indicate that NO_x emissions at several EGUs have decreased by factors ranging from two to four between 2000 and 2006. These reductions were

seen at EGUs that implemented NO_x control features, such as Selective Catalytic Reduction (SCR), between 2000 and 2006, suggesting these control strategies are working (RSST, 2006).

Trends for peak daily NO_x are presented in Figure D-15: *Daily Peak Hourly NOX in the DFW Area*. Daily peak NO_x concentrations in the DFW area appear to be decreasing over time. NO_x concentrations have shown larger decreases in recent years, especially 2009, a year that also recorded some of the lowest ozone concentrations. The graphic also shows that maximum NO_x concentrations typically occur in winter. Although erratic, maximum NO_x levels have decreased by 43 percent, to 398 ppb, from 1991 to 2009, an average of roughly 18 ppb, or nearly 3 percent, per year. The years 1998, 1999, and 2000 saw peak values greater than 900 ppb; the reason for the high values is still under investigation, however, those values appear to be anomalously high. Average daily peak hourly NO_x has dropped even more precipitously, falling 65 percent, or 4 percent per year, from 78 ppb to 27 ppb, since 1991.

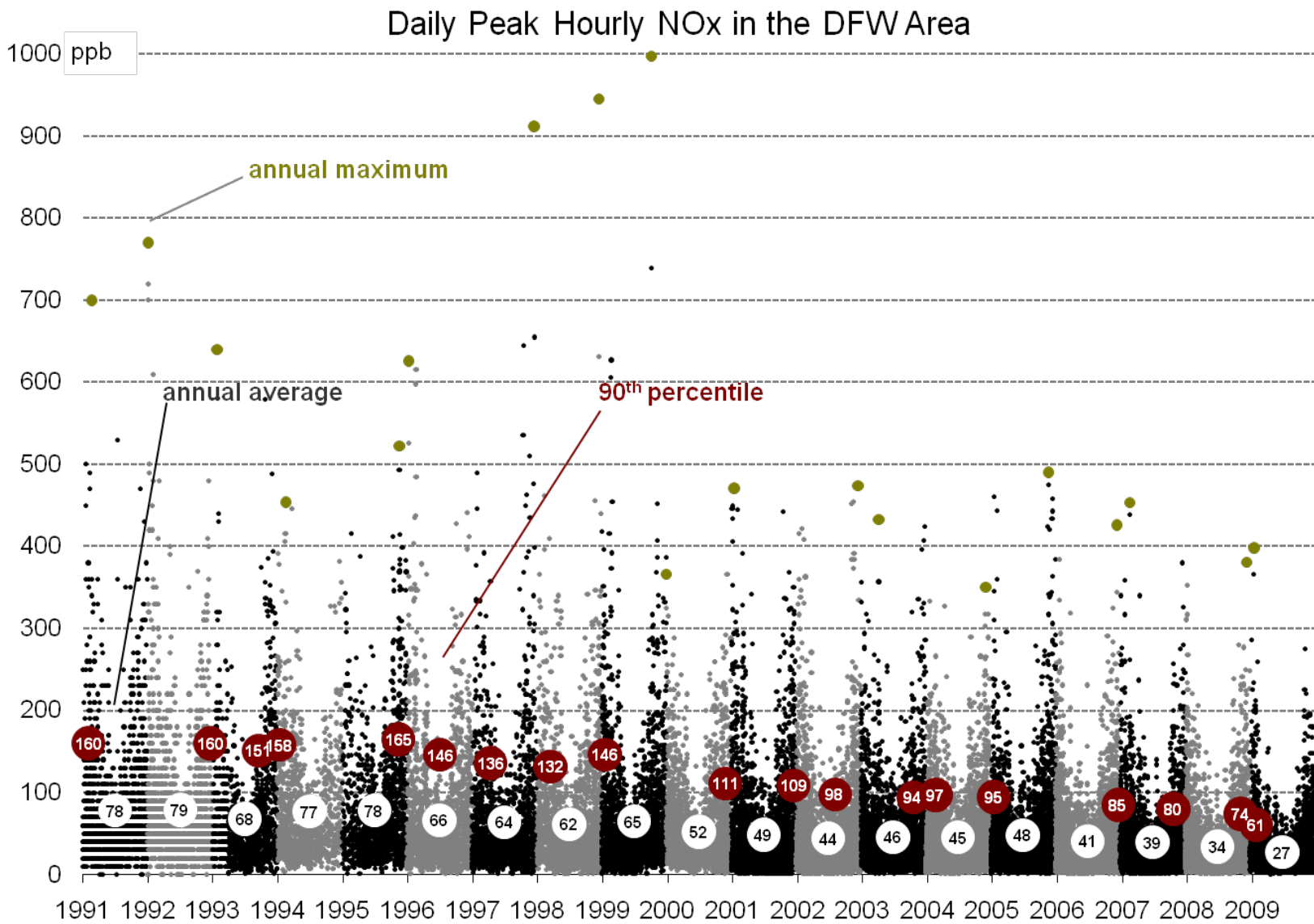


Figure D-9: Daily Peak Hourly NO_x in the DFW Area

Figure D-16: *Annual Mean Daily Peak NO_x* shows annual mean of all one-hour NO_x concentrations in the DFW area from 1991 through 2009. Only years with at least 75 percent data completeness were included in the figure. Most monitors in the area demonstrate decreasing NO_x concentrations since the late 1990s, with the sharpest decreases occurring since 2007. Monitors that show the smallest decreases, or show no change, are at sites that have traditionally had lower NO_x concentrations.

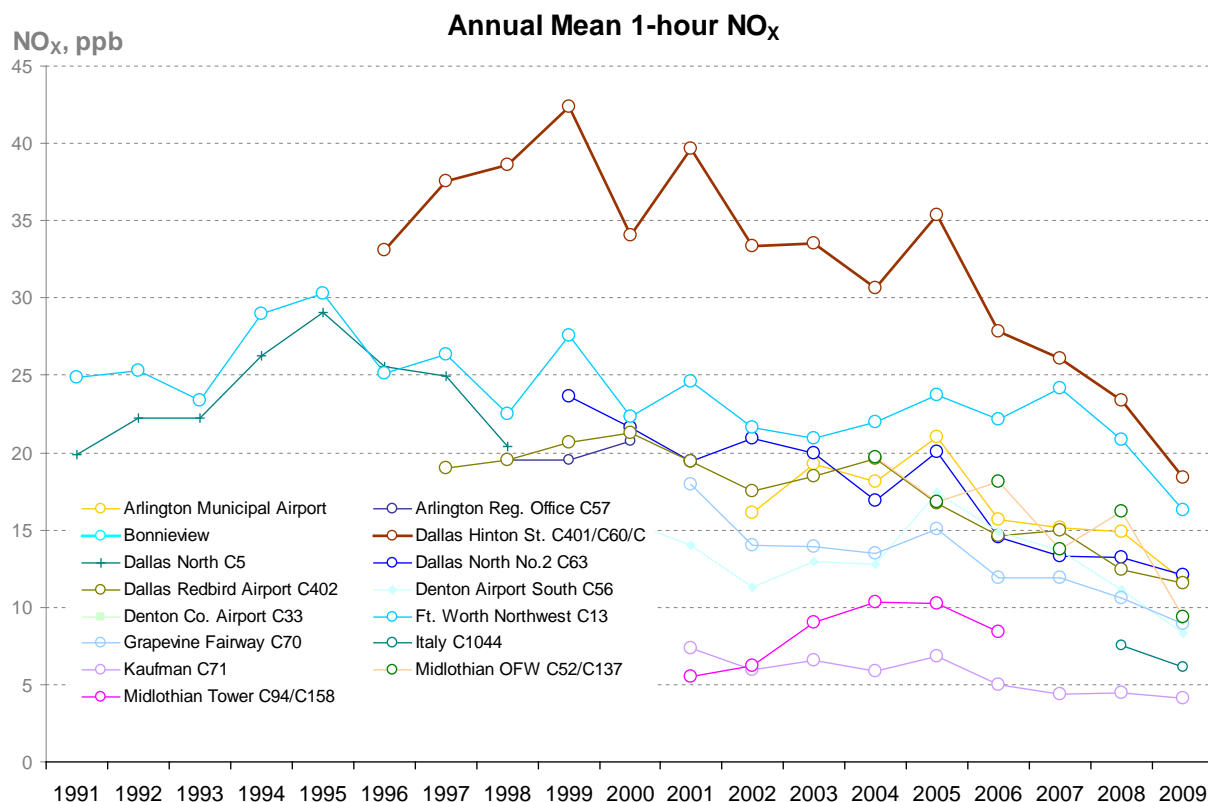


Figure D-10: Annual Mean Daily Peak NO_x

The largest median NO_x concentrations were measured at the Dallas Hinton St. (C401/C60/AH161) monitor, which is in close proximity to Interstate 35E, and at the Ft. Worth Northwest (C13/AH32) monitor which is near Fort Worth Meacham International Airport. The location of both monitors, in combination with their similar trends, suggests that they may be measuring decreases in NO_x emissions from mobile sources. Monitors located further from the center of the Dallas-Fort Worth area, where there are fewer NO_x sources, measured the lowest median NO_x concentrations. Sites recording among the highest NO_x concentrations, for example, Dallas Hinton St. (C401/C60/AH161), are not necessarily the sites with the highest ozone design values. As discussed in Chapter 1, NO_x scavenging of ozone may be taking place near these monitors.

For a more robust examination of the distribution of hourly NO_x concentrations, the 90th percentile was also analyzed. All sites in the Dallas-Fort Worth area appear to exhibit gradual decreases in 90th percentile one-hour NO_x concentrations, with the Dallas Hinton St

(C401/C60/AH161) monitor showing the largest decrease. The Dallas Hinton St. (C401/C60/AH161) monitor showed large variability in 90th percentile NO_x concentrations from the start of monitoring in 1996 through 2001. Since 2001, 90th percentile NO_x concentrations at Dallas Hinton St. (C401/C60/AH161) have steadily decreased and are now within the range of other monitors in the area. This large decrease may be due to decreasing automobile emissions and improved controls, though this has not been rigorously tested. Increases in NO_x concentrations near the Midlothian OFW (C52/C137) monitor may be caused by increased quarry operations near this monitor.

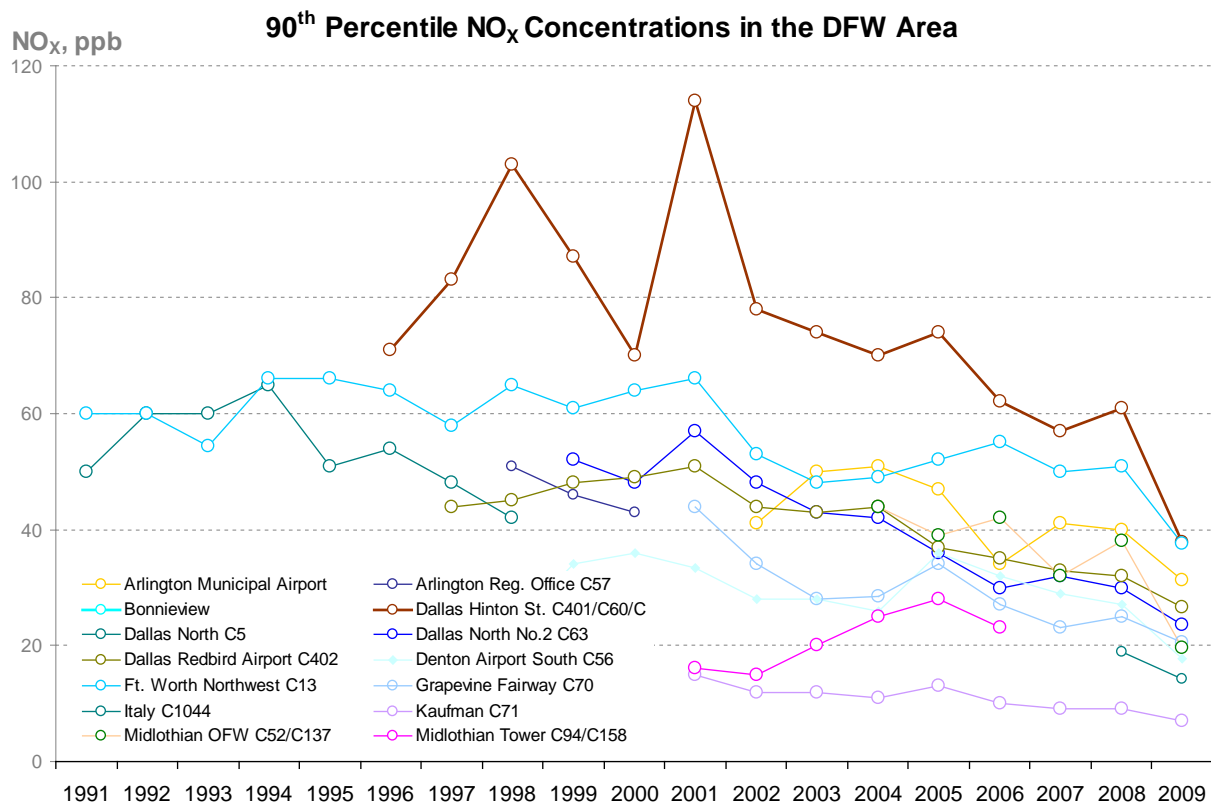


Figure D-11: 90th Percentile Daily Peak NO_x Concentrations in the DFW Area

Table D-6: Decreases in 90th Percentile NO_x Concentrations

Monitor Site	Start Year	Percentage Change from Start Year	Average Annual Percentage Change
Midlothian OFW C52	2004	-55	-10.9
Grapevine Fairway C70	2001	-55	-6.8
Dallas North No.2 C63	1999	-54	-5.4
Kaufman C71	2001	-53	-6.7
Dallas Hinton St. C401	1996	-46	-3.6
Dallas Redbird Airport C402	1997	-39	-3.2
Ft. Worth Northwest C13	1991	-37	-2.0

Monitor Site	Start Year	Percentage Change from Start Year	Average Annual Percentage Change
Arlington Municipal Airport	2002	-24	-3.5
Denton Airport South C56	1998	-22	-2.0

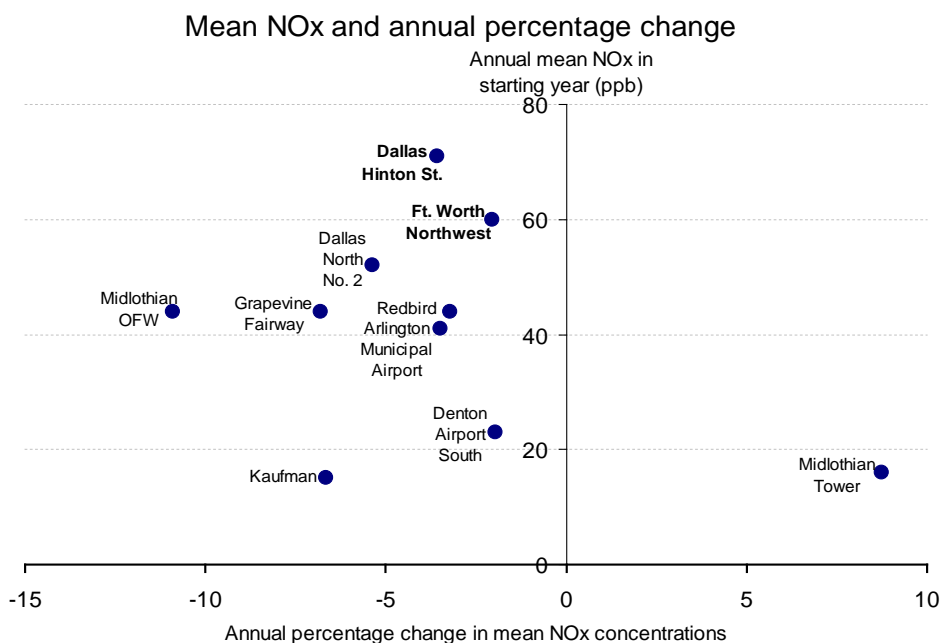


Figure D-12: Mean NO_x and Annual Percentage Change

Table D-6: *Decreases in 90th Percentile NO_x Concentrations* shows changes in 90th percentile measurements since the beginning of data collection at each monitor. While several monitors recorded large decreases in 90th percentile NO_x from 2008 to 2009, most others observed only minimal changes over that same period. These large disparities in patterns of ambient NO_x concentrations across the region are appropriate for further investigation, suggesting that larger decreases are not due solely to variations in meteorological conditions, which would be expected to influence all monitors similarly, though not identically. The differences appear to be related to the relative magnitudes of the overall concentrations: sites with the highest concentrations, which tend to be urban sites, showed the most decrease. More rural sites like Kaufman (C71/A304/X071) and Italy (C1044/A323) may reflect slight changes in background values, while more urban sites may reflect local emission changes (Figure D-18: *Mean NO_x and Annual Percentage Change*).

Similar to ozone, NO_x concentrations in the DFW area appear to be decreasing over time, in large measure, the result of the comprehensive suite of NO_x-targeted controls implemented since 2000. Stringent point source NO_x standards have been adopted along with numerous state and Federal controls affecting mobile source NO_x emissions. Besides normal fleet turnover, as older vehicles are replaced by newer, less polluting ones in the on-road fleet, mobile source NO_x reductions since 2000 could also be due to improvements in the Air Check Texas motor vehicle inspection and maintenance program, expansion of the Low Income Vehicle

Repair and Replacement Assistance Program, and expansion of the Texas Emission Reduction Program for diesel trucks and heavy equipment.

2.3 Volatile Organic Compounds Trends

Volatile organic compounds (VOC) play a central role in ozone production. Since the mid-1990s, the TCEQ has collected 40-minute measurements, on an hourly basis, of some 58 VOC compounds using automated gas chromatograph (auto-GC) instruments. These instruments automatically measure and report chemical compounds resident in ambient air. Initially, there was an only one auto-GC collecting measurement in the DFW area, Dallas Hinton St. (C401/C60/AH161), but in 2003 a second auto-GC monitor was added at Ft. Worth Northwest (C13/AH32).

The TCEQ has also employed two types of canisters in the DFW area, one that samples ambient air over a 24-hour period (Community Air Toxics Monitoring Network or CATMN) and another that samples ambient air for a single hour at a time, usually at four different times of day (Multican or MCAN). The locations of the two auto-GC monitors, as well as the canisters collecting VOC data, in the DFW area are shown in Figure D-19: *Locations of Auto-GC Monitors and Canisters in the DFW Area*. Some monitors shown have been deactivated (see Table D-7: *Description of Auto-GC and Canister Monitors in the DFW Area*), but still have data after 1999.

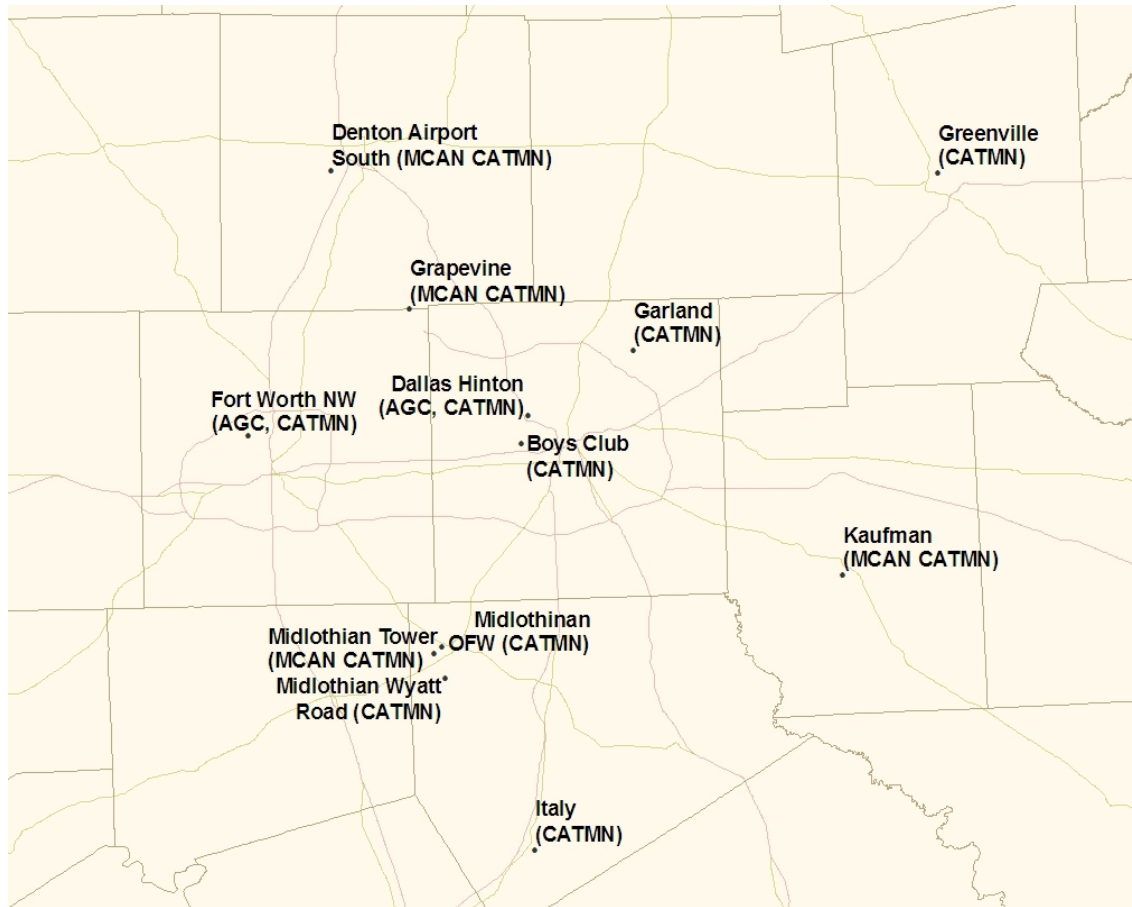


Figure D-13: Locations of Auto-GC Monitors and Canisters in the DFW Area

Table D-7: Description of Auto-GC and Canister Monitors in the DFW Area

Site Name (CAMS Number)	Airs Code	County	Latitude	Longitude	Monitor Type	Currently Active?
Boys Club A134	481130057	Dallas	32.77917	-96.8733	CATMN	N
Dallas Hinton St. C401/C60/AH161	481130069	Dallas	32.81972	-96.86	AGC, CATMN	Y
Denton Airport South C56/A163/X157	481210034	Denton	33.19444	-97.1933	MCAN, CATMN	Y
Ft. Worth Northwest C13/AH302	484391002	Tarrant	32.80583	-97.3564	AGC, CATMN	Y
Garland Hwy Dept C197	481131006	Dallas	32.91056	-96.6692	CATMN	N
Grapevine Fairway C70/A301/X182	484393009	Tarrant	32.98417	-97.0636	MCAN, CATMN	Y
Greenville C1006/A198	482311006	Hunt	33.15306	-96.1153	CATMN	Y
Italy C1044/A323	481391044	Ellis	32.17556	-96.8703	CATMN	Y
Kaufman C71/A304/X071	482570005	Kaufman	32.565	-96.3175	MCAN, CATMN	Y
Midlothian Tower C94/A305/X158	481390015	Ellis	32.43667	-97.0244	MCAN, CATMN	N

Site Name (CAMS Number)	Airs Code	County	Latitude	Longitude	Monitor Type	Currently Active?
Midlothian Wyatt Road C302/A306	481390017	Ellis	32.47361	-97.0425	CATMN	N
Midlothian OFW C52/A137	481390016	Ellis	32.48222	-97.0269	CATMN	Y

2.3.1 VOC Trends at Auto-GC Monitors

Trends in total non-methane hydrocarbons (TNMHC) concentrations, as a proxy for VOC, provide insight into variation in VOC levels in the DFW area over time. Though this analysis includes data from 2009, this data has not been verified by the EPA and is subject to change.

Figure D-20: *Daily Peak TNMHC Concentrations in the DFW Area* displays daily peak hourly VOC values at auto-GC monitors in the DFW area. These daily peaks exhibit large variability and range from less than 100 parts per billion, carbon (ppbC) to more than 1,000 ppbC. Because TNMHC measurements are characterized by a small number of extremely high values, combined with a large number of low and moderate values, plotting TNMHC on a logarithmic scale is necessary to display the range of data and show trends. The increasing density and introduction of the new color of points (gray) plotted beginning in 2003 reflects the deployment of the Ft. Worth Northwest (C13/AH32) auto-GC monitor. To better assess trends at individual monitors, 90th percentile and median TNMHC concentrations by year at each auto-GC monitor are also shown. Note that due to the scales of the data involved, 90th percentile and median concentrations are plotted on a linear scale, while daily peak TNMHC concentrations, which are skewed by a few very high values, are plotted on a logarithmic scale. Only months with 75 percent data completeness were used in this analysis.

The 90th percentile TNMHC at Ft. Worth Northwest (C13/AH32) is much higher than the 90th percentile TNMHC at Dallas Hinton St. (C401/C60/AH161); however, Ft. Worth Northwest (C13/AH32) shows a much greater decrease, 30 ppbC, over the most recent year compared to a decrease of only 2 ppbC at Dallas Hinton St. (C401/C60/AH161). The higher values at the Fort Worth Northwest (C13/AH32) monitor could be due to oil and gas activities at the Barnett Shale, which is further explained in Chapter 3. Because TNMHC is a precursor to ozone formation, it is promising to see reductions in the 90th percentile at both locations. Although the Ft. Worth Northwest (C13/AH32) monitor shows a much higher 90th percentile than Dallas Hinton St. (C401/C60/AH161), its median is only slightly higher. Both medians show downward trends through 2004 and have remained roughly constant since. Daily peak TNMHC concentrations at Dallas Hinton St. (C401/C60/AH161) show a seasonal trend: higher concentrations of TNMHC in the winter and lower concentrations in the summer. Ft. Worth Northwest (C13/AH32) also exhibits a seasonal trend; however, higher VOC concentrations are observed in the summer months compared to Dallas Hinton St. (C401/C60/AH161). The higher summer VOC concentrations at Ft. Worth Northwest (C13/AH32) could be the reason that the 90th percentile is so much higher at that monitor.

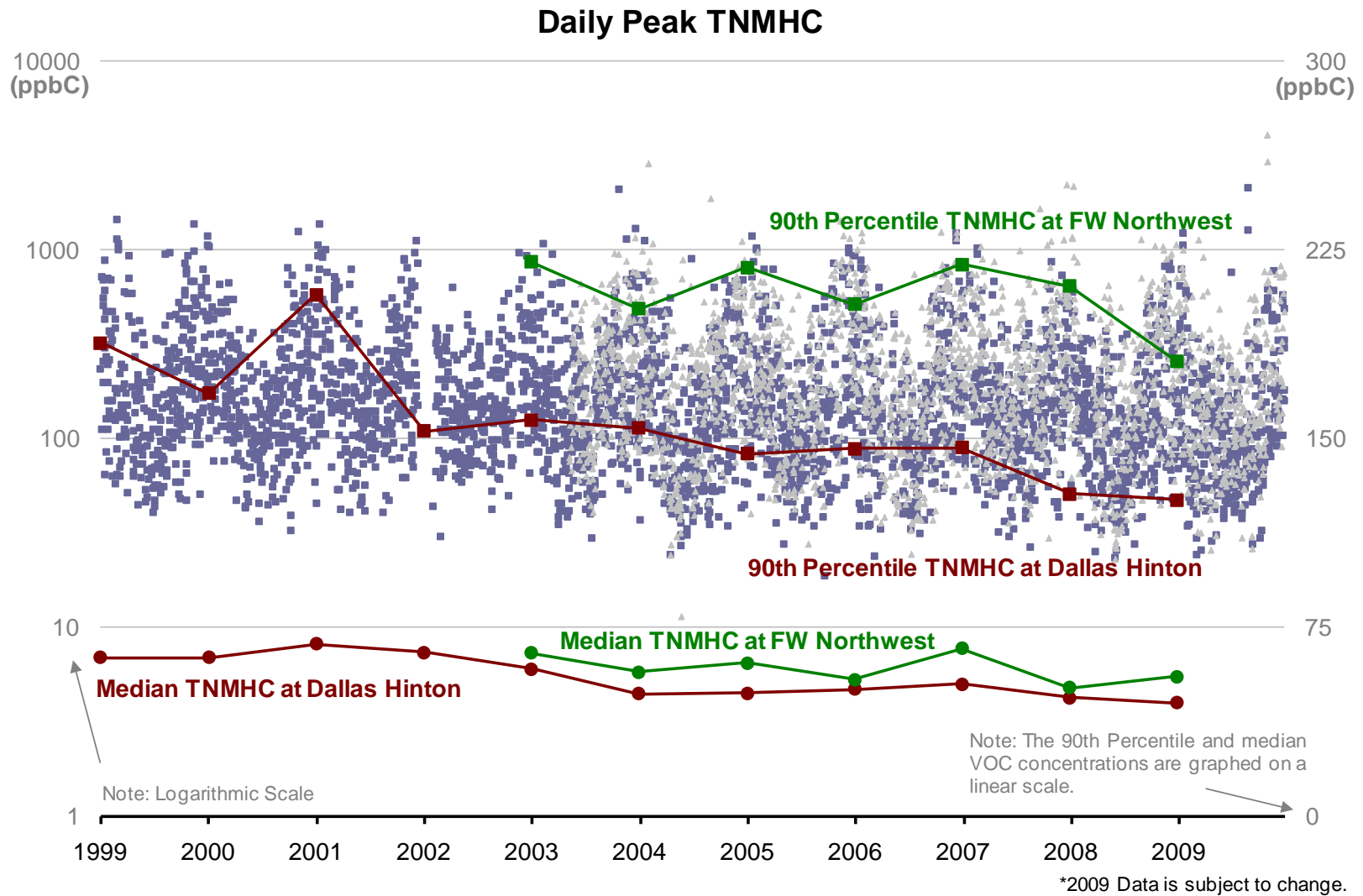


Figure D-14: Daily Peak TNMHC Concentrations in the DFW Area

Approximately 66 percent of anthropogenic emissions of TNMHC at Dallas Hinton St. (C401/C60/AH161) come from motor vehicle emissions (Qin *et al.*, 2007). This seasonal variation may be partly due to the increase in vehicle miles travelled during summer months, and partly due to photochemical removal and dilution of VOC due to fluctuations in depth of the atmospheric mixing layer. Because the mixing layer in summer is much deeper than in winter, ground-level emissions tend to become more diluted in the summer (Qin *et al.*, 2007).

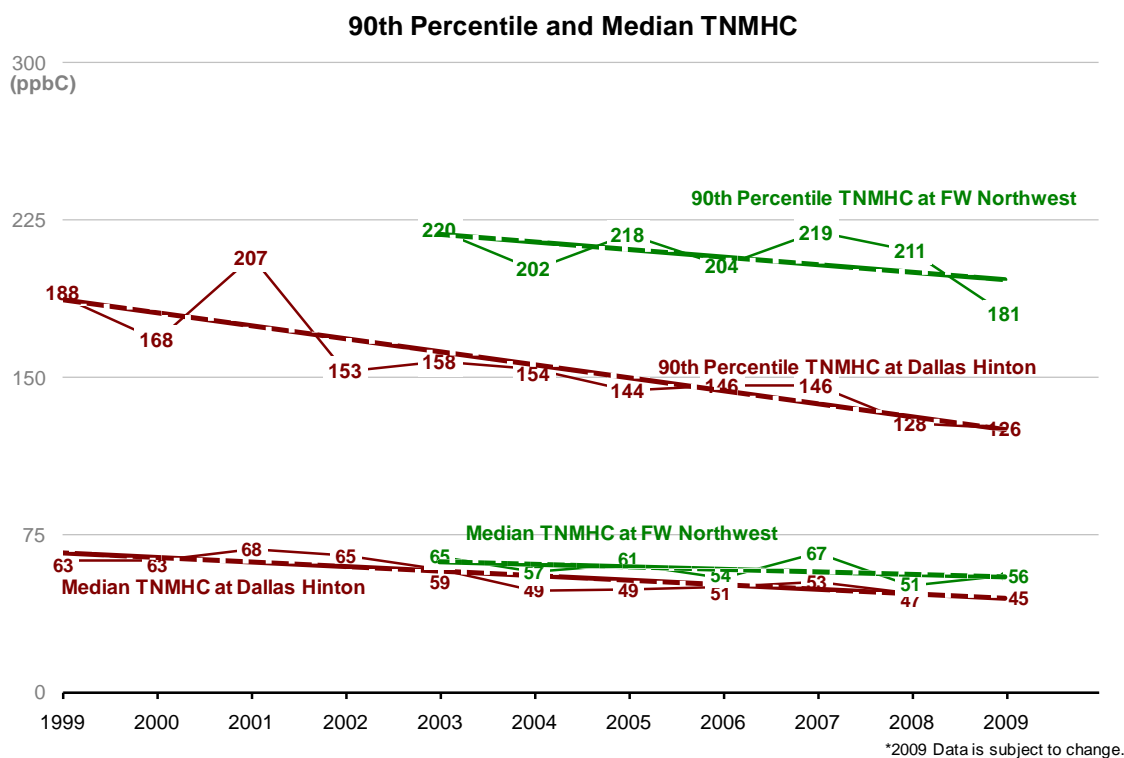


Figure D-15: 90th Percentile and Median TNMHC in the DFW Area

Figure D-21: *90th Percentile and Median TNMHC in the DFW Area* displays 90th percentile and median TNMHC for Dallas Hinton St. (C401/C60/AH161) and Ft. Worth Northwest (C13/AH32) again, but the values are now shown along with estimated regression lines. Table D-8: *TNMHC Yearly Median Linear Regression* reports the results of ordinary least squares regressions of annual 90th percentile and median TNMHC measures against an index of year at the two subject monitors. While all four estimated models exhibit negative slopes, corresponding to downward trends, only the models for Dallas Hinton St. (C401/C60/AH161) are statistically significant at the ten percent ($\alpha=0.10$) level. The adjusted R^2 statistics and F statistics indicate acceptable models for Dallas Hinton St. (C401/C60/AH161) but not Ft. Worth Northwest (C13/AH32), indicating that the negative trends detected at Ft. Worth Northwest (C401/C60/AH161) are not distinguishable from zero, or flat lines, with statistical confidence ($\alpha = 0.05$).

Table D-8: TNMHC Yearly Median Linear Regression

Statistic	Dallas Hinton			
	St. 90th Percentile	Dallas Hinton St. Median	Fort Worth NW 90th Percentile	Fort Worth NW Median
Adjusted R ²	0.693	0.740	0.161	0.069
F	23.621	29.476	2.150	1.445
Significance F	0.001	0.000	0.202	0.283
Slope	-6.209	-2.178	-3.590	-1.260
t-stat	-4.860	-5.429	-1.466	-1.202
p-value	0.001	0.000	0.202	0.283

While these results apply to all VOC species, it is the highly reactive species of VOC that are most important to ozone formation. The next section will explore HRVOC concentrations and trends in the DFW area in more detail.

2.3.2 VOC trends from Canisters

In addition to continuously operating auto-GC instruments in the DFW area, the TCEQ also collects ambient air samples using evacuated canisters at seven locations throughout the DFW area. Data from these canisters are useful for confirming findings from auto-GCs.

This analysis of TNMHC collected with canisters investigates 24-hour measurements of TNMHC and HRVOC. Twelve CATMN canisters that collect 24-hour measurements every sixth day have been active in the DFW area over the past 10 years (see Figure D-19: *Locations of Auto-GC Monitors and Canisters in the DFW Area* for map of site locations). Two canister locations coincide with auto-GC instruments: Dallas Hinton St. (C401/C60/AH161) and Ft. Worth Northwest (C13/AH32). While comparisons with auto-GC measurements will be instructive for observing trends and other patterns, it is important to remember that these instruments have different measurement durations and frequencies, potentially yielding incomparable results.

Similar to the auto-GC measurements, quarterly geometric mean concentrations were calculated by computing the natural logarithm of each 24-hour concentration, averaging these by monitor and quarter, then exponentiating the resulting average. Samples that were invalidated, and those with warning codes regarding sample accuracy or precision, were discarded. Quarters with less than 75 percent valid measurements (less than 12 samples) were also discarded. Note that 2009 includes data only through the second quarter. Resulting quarterly geometric mean concentrations for each HRVOC species were plotted against time. Quarters that did not meet completeness criteria appear as gaps in the time series.

Values measured at each CATMN canister in the DFW area are shown in Figure D-22: *Quarterly Geometric Mean TNMHC at CATMN Monitors*. As with auto-GC measurements, there is a distinct seasonal variation at all monitoring sites, possibly due partly to differences in seasonal driving patterns and partly to photochemical removal and dilution due to atmospheric mixing. The mixing layer in the summer extends to a much higher altitude than in the winter, allowing more dilution of the species.

Because daily and seasonal variability in these series hamper identification of trends, annual geometric mean TNMHC are shown for each site in Figure D-23: *Annual Geometric Mean TNMHC at CATMN Monitors*. Visual inspection suggests that annual geometric mean TNMHC concentrations in DFW are declining. Linear regressions, presented in Table D-9: *Regression*

Results for Annual Geometric Mean TNMHC at CATMN Monitors, provide statistical confirmation of any trends present. Incomplete data from 2009 was excluded.

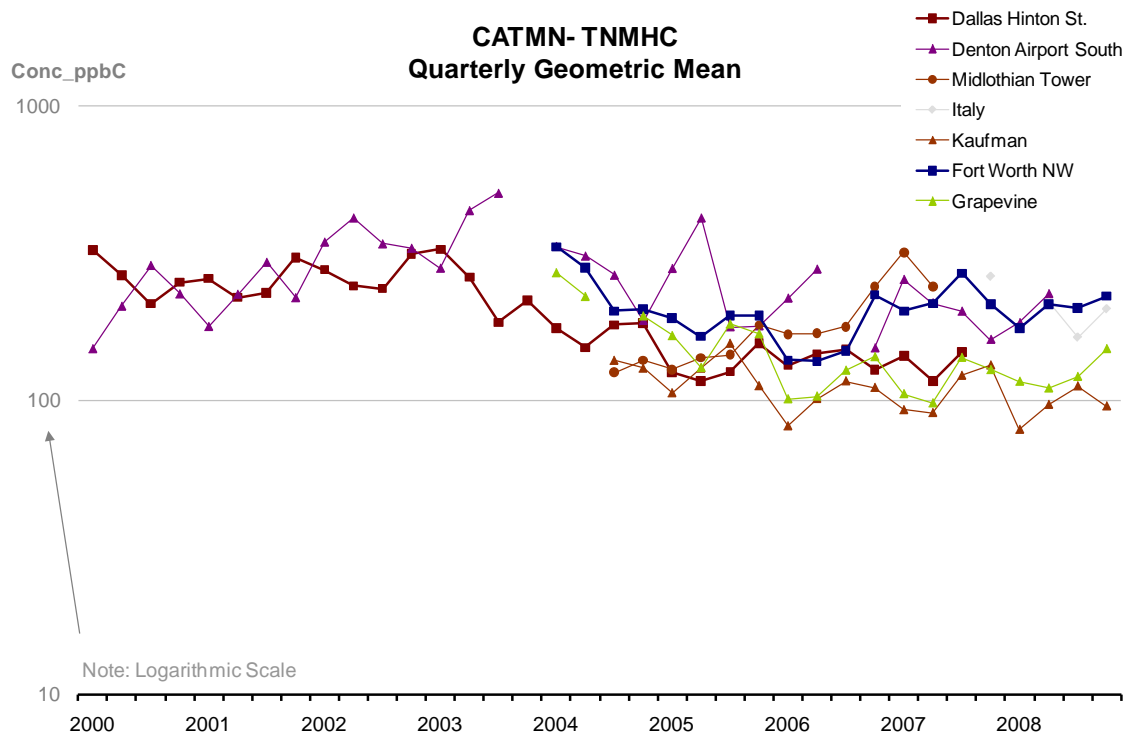


Figure D-16: Quarterly Geometric Mean TNMHC at CATMN Monitors

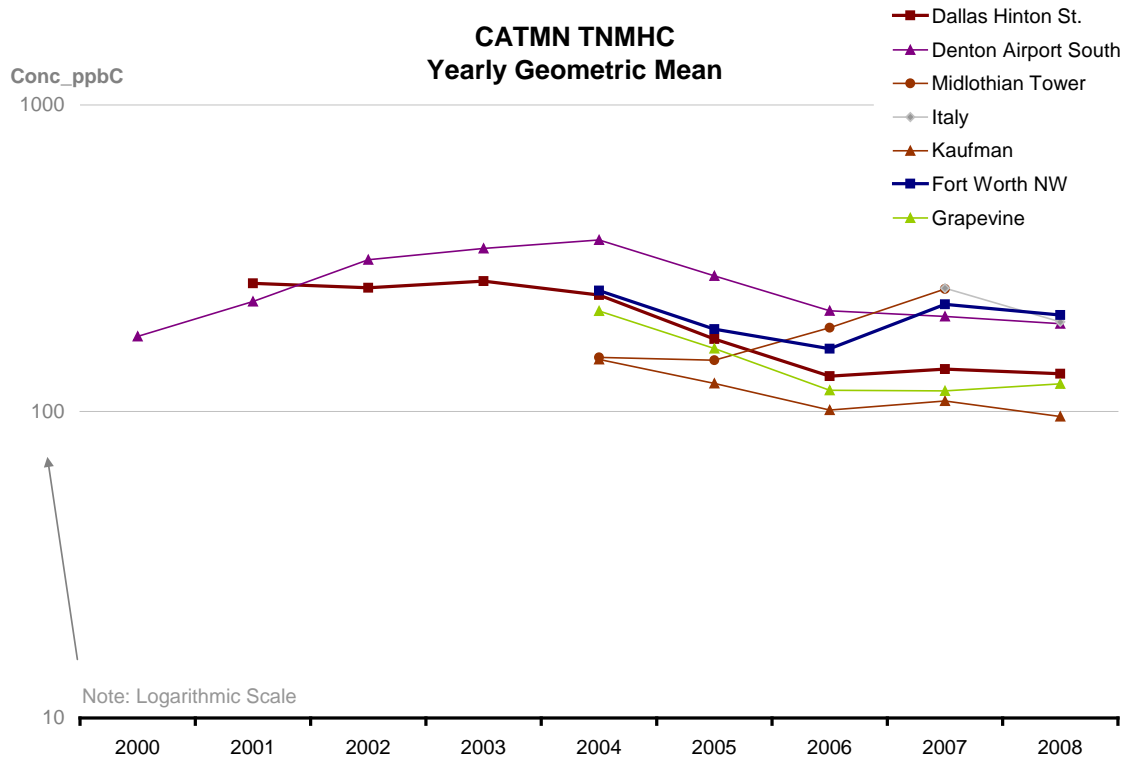


Figure D-17: Annual Geometric Mean TNMHC at CATMN Monitors

Of the seven sites, statistically significant trends, at the 5 percent level ($\alpha=0.05$), were identified for only two: Kaufman ((C71/A304/X071)) and Dallas Hinton St. (C401/C60/AH161). These two sites exhibit negative slopes of -11.86 and -23.31, respectively, which represent quite large decreases. Two other sites exhibited trends significant at the 10 percent level ($\alpha=0.10$): Midlothian Tower (C94/A305/X158) and Grapevine (C70/A301/X182). Midlothian Tower (C94/A305/X158) was the only site that exhibited an increasing trend, which is possibly due to increased quarry operations near that site. Re-estimation for Denton Airport South (C56/A163/X157) for 2004 through 2008 confirmed the observed downward trend since 2004, when this monitor began measuring a downward trend similar to the other sites; these values are displayed in italics in the table. Italy (C1044/A323) had too few years of data to estimate regression trends. Results for Ft. Worth Northwest (C13/AH302) show no significant trend, which may be due to recent increased oil and gas extraction activities in the Barnett Shale formation in Tarrant and Wise counties. These activities are further discussed in Section 4.

Table D-9: Regression Results for Annual Geometric Mean TNMHC at CATMN Monitors

Statistic	Dallas Hinton St	Denton Airport South original	Denton Airport South re-estimated	Midlothian Tower	Italy***	Kaufman	Fort Worth Northwest	Grapevine

Statistic	Dallas Hinton St	Denton Airport South original	Denton Airport South re- estimated	Midlothia Tower	Italy ***	Kaufman	Fort Worth North- west	Grapevine
Adjusted R ²	0.83	-0.11	0.69	0.76	NA	0.74	-0.27	0.63
F	35.48*	0.22	7.75	10.46**	NA	12.34*	0.14	7.84**
p-value	0.00	0.65	0.11	0.08	NA	0.04	0.73	0.07
Slope	-23.31*	-4.41	-25.87	34.34**	NA	-11.86*	-4.56	-22.29**
t-stat	-5.96	-0.47	-2.78	3.23	NA	-3.51	-0.38	-2.80
p-value	0.00	0.65	0.11	0.08	NA	0.04	0.73	0.07

*Significant at the $\alpha=0.05$ level.

**Significant at the $\alpha=0.10$ level.

***Insufficient data.

Analysis of VOC data collected with auto-GCs and canisters revealed statistically significant decreases in total VOC at Dallas Hinton St. (C401/C60/AH161). Although many VOC trends appeared to decrease at Ft. Worth Northwest (C13/AH32), no trends at that location were found to be statistically significant.

2.4 Summary of Trends in Ozone and Ozone Precursors

Identifying and assessing trends in ozone and its precursors provide an initial appraisal of the current ozone situation in the DFW area, the magnitude of progress made to date, and the scale of future challenges. Examination of ozone trends has shown that ozone design values, the statistics used to compare observed ambient ozone levels to the NAAQS, have decreased in the DFW area over the past seventeen years. The eight-hour ozone design value of record in 2009 was 86 ppb, a 18 percent decrease from the 1991 design value of 105 ppb. The 2009 value is only two ppb above the level required to attain the 1997 ozone NAAQS, 84 ppb. A regression analysis of design value on year estimates that eight-hour ozone design values decreased at the rate of 0.6 ppb per year, which is statistically significant at the 5 percent level ($\alpha = 0.05$). The one-hour ozone design value in 2009 was 115 ppb, well below the vacated one-hour ozone NAAQS of 124 ppb, and an 18 percent decrease from the 1991 design value of 140 ppb. Regression of one-hour design values on year show they decreased at the rate of 0.085 ppb per year, which is even faster than the decline in the eight-hour ozone design values.

Examination of design values at individual monitors corroborates these decreases, with over half of those monitors at levels below the eight-hour standard by 2008 and below the vacated one-hour standard by 2000. Since 1991, the number of eight-hour and one-hour ozone exceedance days occurring in the DFW area has fallen 54 percent and 100 percent, respectively. In just the last three years, the number of eight-hour ozone exceedance days has fallen by 73 days. Decreases in exceedance days are apparent despite an increase in the number of monitors located throughout the DFW area. The ozone season was also determined to be less severe in recent years.

A variety of methods has been presented for understanding ozone trends in the DFW area. These methods generally agree that ozone concentrations have been decreasing; however, the area still faces challenges in achieving attainment of the 1997 ozone NAAQS. Because ozone

formation depends on a multitude of factors, these factors must be investigated and understood in detail before conclusions as to the causes of the observed decreases can be reached.

Similar to ozone, NO_x concentrations in the DFW area are decreasing over time. NO_x concentrations have shown larger decreases in recent years, especially 2009, a year that also recorded some of the lowest ozone concentrations. Maximum NO_x concentrations typically occur in winter, and, while variable, have decreased overall by 43 percent, to 398 ppb, since 1991, though 1998, 1999, and 2000 saw peak values greater than 900 ppb. This is an average of roughly 18 ppb per year, or nearly 3 percent. Average daily peak hourly NO_x has dropped even more precipitously, falling 65 percent, or 4 percent per year, from 78 ppb to 27 ppb, since 1991. These trends were corroborated with results from individual monitors, which showed decreases ranging from 24 percent to 55 percent from the time the monitor started operation to 2009.

VOC data collected with auto-GCs and canisters revealed statistically significant decreases in total VOC concentrations at Dallas Hinton St. (C401/C60/AH161). Although many VOC trends appeared to decrease at Ft. Worth Northwest (C13/AH32), no trends at that location were found to be statistically significant.

NO_x trends from 1991 to 2009, and VOC trends from 1999 to 2009, show that most monitors in the DFW area experienced decreases in both median and 90th percentile concentrations of these pollutants. Most strikingly, 2009 experienced not only some of the lowest ozone design values in seventeen years, but also some of the lowest NO_x and VOC values. Note that while NO_x and VOC are precursors to ozone formation, meteorology can play an important, if not more significant, role in ozone concentration and precursor trends. The next chapter will take a closer look at local variables that contribute to ozone formation in the DFW area, including meteorology.

3 RECENT FINDINGS IN LOCAL OZONE DYNAMICS IN THE DALLAS-FORT WORTH AREA

Analyses of ozone trends demonstrate that ozone and its precursors in the DFW area have steadily decreased over the past several years. The complexity of ozone formation, however, requires a comprehensive examination of contributing factors. Observed ozone is the aggregate of background ozone and locally produced ozone. Background ozone is either formed by naturally occurring processes, or generated elsewhere and transported into a region. This type of ozone is largely outside the purview of state and local air control authorities. Even much ozone produced locally is difficult, if not impossible, for state and local authorities to control.

This chapter examines patterns of local precursor emissions, local ozone formation and transport, and local meteorology, beginning with a detailed look at spatial and temporal patterns of ozone variability across the region. This is followed by a presentation of recent findings in local patterns of NO_x and VOC emissions, including discussion of emission variability by day of the week and detailed consideration of emissions from oil and gas activity in the Barnett Shale region. Finally, we explore local meteorological factors and their contributions to local ozone formation. The findings presented here support the conclusion that reductions in ozone observed in the DFW area over the previous decade are due in large part to real, quantifiable reductions in precursors, rather than anomalous meteorological conditions that are unlikely to recur.

3.1 Local Variation in Ozone

The previous chapter showed that ozone concentrations can vary by monitor and location. Taking this finding one step further, this section employs a spatial interpolation method borrowed from the field of geostatistics, “kriging”, to identify which specific parts of the DFW area experience higher or lower ozone concentrations (Krige, 1951). These patterns guide a more detailed examination of variability in the factors contributing to ozone formation, both across time and space.

Annual eight-hour ozone design values at each monitor in the DFW area were interpolated onto a two dimensional grid using the kriging procedure, a spatial estimation technique. The eight-hour ozone design value is the three-year average of the fourth highest values recorded at a monitor. The kriging procedure uses an inverse distance-weighting algorithm to interpolate values for grid cells from nearby monitors, taking into account distances and directions of the monitors. It is most robust where a monitoring network is most dense. Kriging produces estimates of design values at locations that lack monitors. Performing this procedure for multiple years provides additional corroboration of the decreasing temporal trends identified previously. Three years, 2002, 2005 and 2009, were selected for analysis; data was restricted to monitors providing the highest quality measurements, those used for regulatory purposes.

The eight-hour ozone design values for each monitor in the DFW area for the selected years are displayed in Figure D-24: *Eight-Hour Ozone Design Values for 2002, 2005, and 2009*. Note that, on the map, pink represents higher ozone design values while green represents lower ozone design values. The outermost monitors in each direction bound the area of interpolation. As monitors are shut down and others are opened, the interpolation domain changes.

The highest eight-hour ozone design values in 2002 exceeded 96 ppb and occurred to the north northwest of the DFW core area at Denton Airport South (C56/A163/X157), and Keller (C17). The lowest eight-hour ozone design values in 2002 occurred southeast of downtown Dallas at Kaufman (C71/A304/X071).

By 2005, peak eight-hour ozone design values had dropped slightly across the region. The highest concentrations shifted more to the northwest of the DFW core area, occurring at Eagle Mountain Lake (C75), Keller (C17), and Ft. Worth Northwest (C13/AH302). The minimum eight-hour ozone concentration is still observed at Kaufman (C71/A304/X071); however, the minimum eight-hour ozone concentrations appear to have increased slightly.

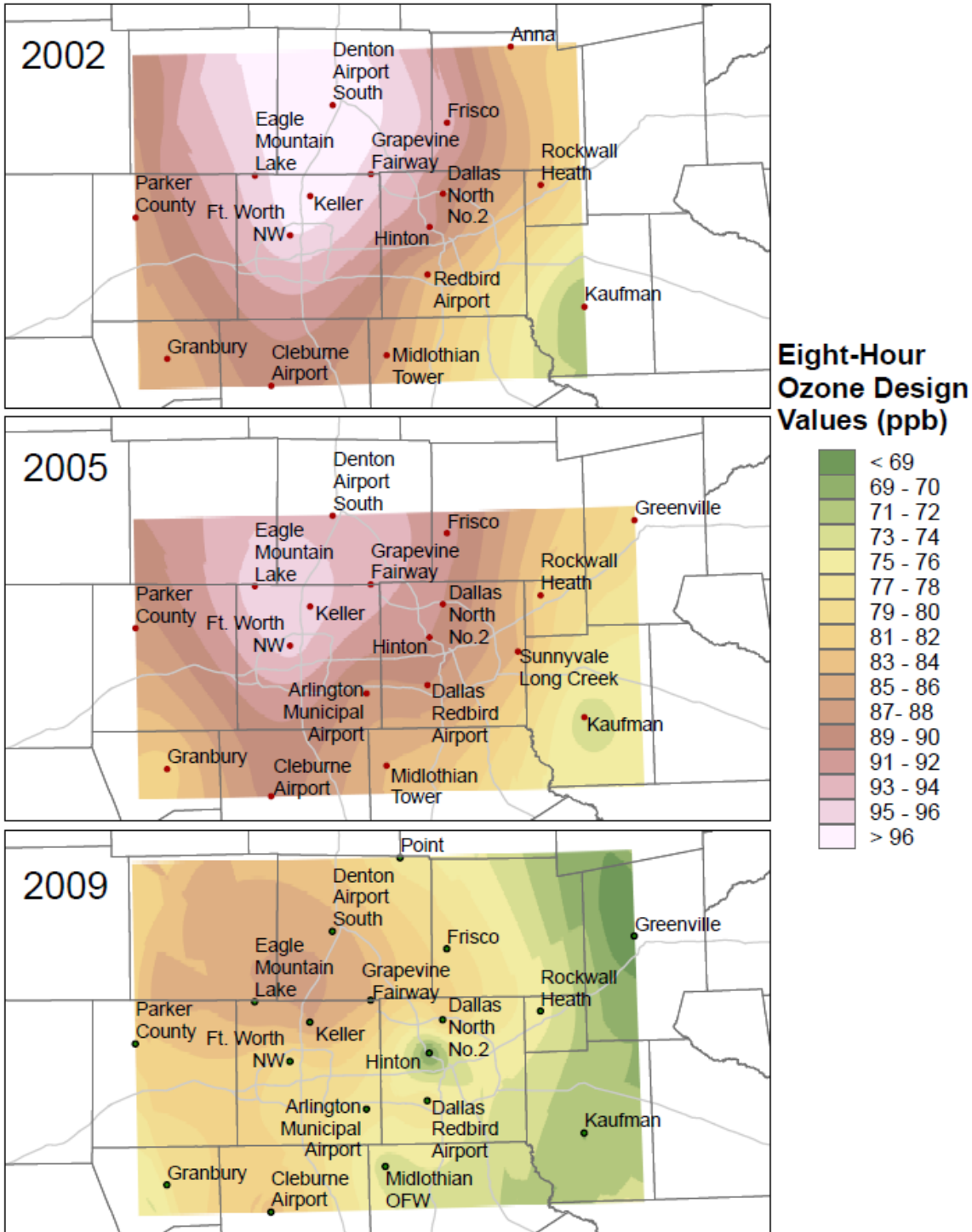


Figure D-1: Eight-Hour Ozone Design Values for 2002, 2005, and 2009

In 2009, eight-hour ozone design values dropped even further. Ozone concentrations are substantially lower across a large part of the DFW area, with the kriging model predicting design values below the eight-hour ozone NAAQS at almost every location. Maximum eight-hour ozone is now considerably lower, between 85 and 86 ppb, and still occurs at Eagle Mountain Lake (C75), Keller (C7), and Denton Airport South (C56). The minimum eight-hour ozone in 2009 is lower, and while there is still a minimum at Kaufman (C71/A304/X071), it is now much lower in the area surrounding Greenville (C1006/A198), and Dallas Hinton St. (C401/C60/AH161).

Notice that while the concentrations of eight-hour ozone are less severe, the areas that experience the highest and lowest ozone remain the same. Spatial interpolation shows that high ozone concentrations continue to occur northwest of the DFW area. The lowest ozone values are found to the southeast and east of the DFW area.

The kriging method can also be employed to investigate the geographic origins of high ozone concentrations. Comparison of temporal patterns of ozone formation on days with high ozone concentrations to days with low ozone concentrations can identify unique features of high ozone days that may corroborate conclusions about sources of high ozone. Daily maximum ozone concentrations were divided into two groups: days with values exceeding the eight-hour ozone NAAQS, and days not exceeding the NAAQS. The time of day when peak ozone was recorded at each monitor was determined for each day, and then averaged across the two groupings of days. Only monitors that report data to the EPA were included. Data from 2000 through 2009 was used and days were restricted to March through October to exclude months when few or no exceedance days occur in the DFW area.

Spatial interpolation with kriging was performed on the average time of day of peak ozone at each monitor, for both low and high ozone days, to identify when and where ozone peaks, on average, throughout the DFW area. Maps of the time of peak ozone in the DFW area are found in Figure D-25: *Time of Day of Peak Hourly Ozone*. Note pinks represent times later in the day, while greens represent times earlier in the day. The top map shows time of day of peak ozone on days when ozone was below 85 ppb, and the bottom map shows time of day of peak ozone on days when ozone was 85 ppb or greater. The top map shows that on days with low eight-hour ozone values, daily maximum values are recorded in northern Dallas County, in the center of the DFW area, between 13:30 Local Standard Time (LST) and 14:00 LST. Peak ozone occurs in the rest of the DFW area within two hours of the initial peak, with areas at the edge of the DFW area observing the peaks last.

By contrast, the bottom map of the daily pattern on high eight-hour ozone days looks quite different. Daily maximum ozone concentrations are observed earlier in the day, around 13:00 LST, at Midlothian OFW (C52/A137), to the south of the DFW urban core. The next peak is not observed until an hour later at Rockwall Heath (C69), to the east of Dallas County. Peak ozone then occurs successively later throughout the DFW area, with the latest peak at Parker County (C76) around 17:00 LST. This pattern appears to suggest more stagnant wind conditions on high ozone days, leading to high ozone later in the day occurring at monitors farther away from the urban core of the DFW area.

The time of day of maximum ozone on high eight-hour ozone days represents a composite pattern: high ozone formed in the urban core of the DFW area is slowly carried to the surrounding areas. Combined with the earlier spatial design value analysis, it appears that ozone concentrations are first formed in the urban areas of the DFW area, and then those concentrations accumulate as they are slowly transported to the northwest and west, where the highest ozone concentrations are routinely observed. To corroborate these findings, a careful analysis of ozone precursors, NO_x and VOC, along with meteorological patterns, follows.

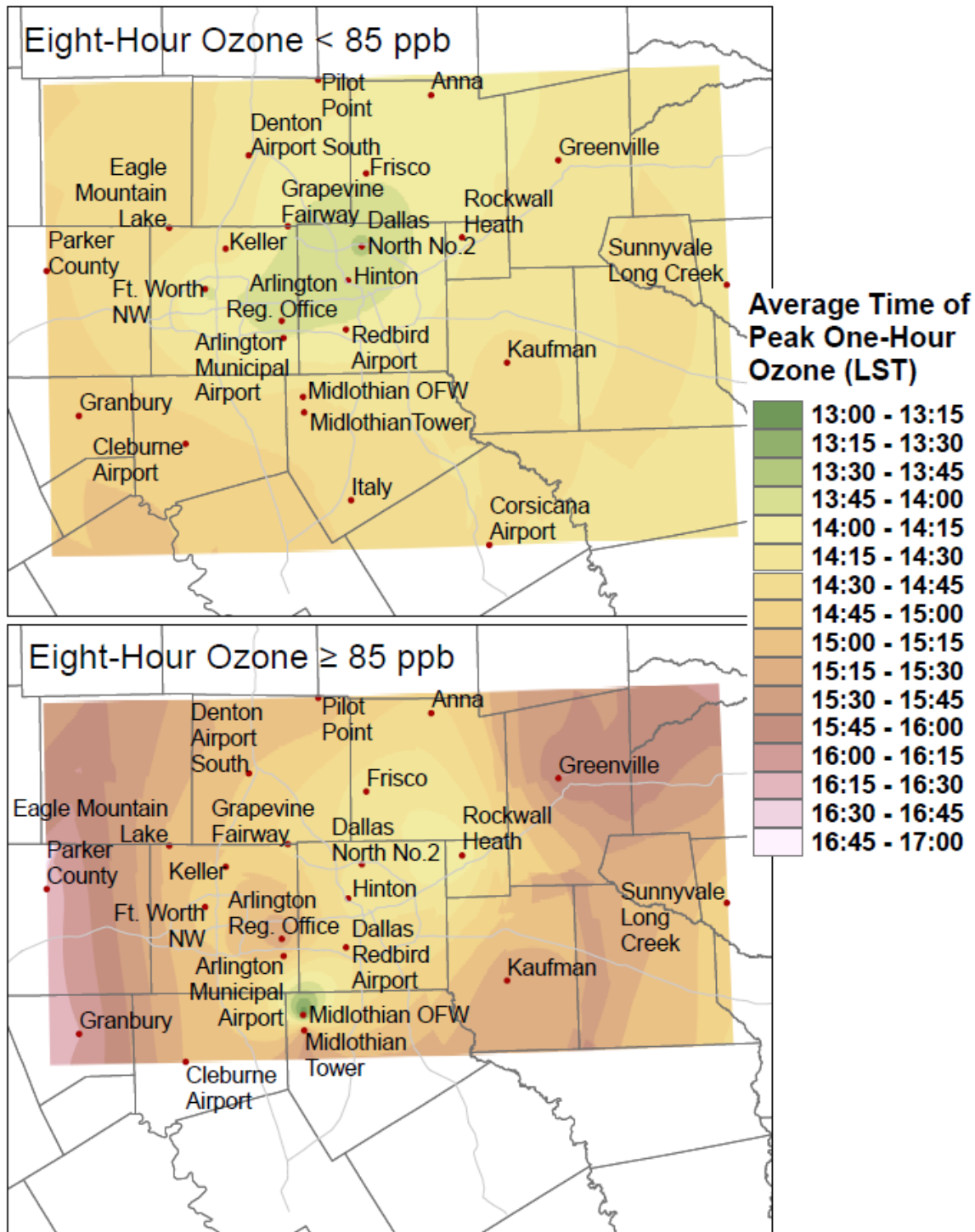


Figure D-2: Time of Day of Peak Hourly Ozone

3.2 Spatial Variation in Nitrogen Oxides

Like ozone, NO_x was shown in Chapter 2 to vary both temporally and spatially. Table D-10: *2009 Mean NO_x Concentrations in the DFW Area* shows a clear spatial trend in NO_x in the

DFW area. Mean 2009 NO_x concentrations in the DFW area range from 4 parts per billion (ppb) at the Kaufman (C71/A304/X071) monitor to 18 ppb at the Dallas Hinton St. (C401/C60/AH161) monitor. Only active regulatory monitors with at least 75 percent data completeness for the period were included. Monitors with the lowest concentrations tend to be located in the south and the southeast side of the DFW area, while monitors with higher concentrations tend to be located in the central DFW area.

Table D-1: 2009 Mean NO_x Concentrations in the DFW Area

Site	2009 Mean NO _x Concentration
	ppb
Dallas Hinton St. C401/C60	18
Ft. Worth Northwest C13	16
Dallas North No.2 C63	12
Arlington Municipal Airport	12
Dallas Redbird Airport C402	12
Midlothian OFW C52/C137	9
Grapevine Fairway C70	9
Denton Airport South C56	8
Italy C1044	6
Kaufman C71	4

The trend in spatial NO_x patterns is clearer when displayed on a map. All monitors with available data in each year were used in this analysis, despite the fact that some monitors were shut down and others were opened during that time. Similar to the ozone plots, ordinary kriging interpolation was used to determine the spatial variation of mean NO_x in 2002, 2005, and 2009 in the DFW area.

Figure D-26: *Mean NO_x Concentrations in the DFW Area for 2002, 2005, and 2009* illustrates the spatial variation of mean NO_x in the DFW area. NO_x concentrations appear to be decreasing over space and time in areas with the highest mean NO_x concentrations including Dallas Hinton St. (C401/C60/AH161) and Ft. Worth Northwest (C13/AH302). Urban parts of the DFW area, which are dominated by mobile source emissions, have the highest NO_x levels, but those levels have decreased from 2002 through 2009. Note that the highest concentrations of mean NO_x occur at Dallas Hinton St. (C401/C60/AH161), the same monitor that first observes peak one-hour ozone concentration on eight-hour ozone exceedance days. It appears that ozone may be formed in the area near Dallas Hinton St. (C401/C60/AH161) and then transported throughout the DFW area.

Monitors that observed the lowest NO_x levels are located to the south and southeast of Dallas County, in areas that are more rural. While areas on the periphery of the DFW area appear to show some decreases from 2002 through 2009, monitors in Dallas County appear to show the largest decreases.

NO_x concentrations at the Dallas Hinton St. (C401/C60/AH161) monitor, which is adjacent to Interstate 35E, have dropped from 33 to 18 ppb over the 2002 through 2009 period. Because mobile source emissions are such a large source of NO_x, sites near major roadways might not always be representative of NO_x in a larger area, which might be the case for Dallas Hinton St. (C401/C60/AH161), near Interstate 35E, and Dallas North No. 2 (C63/C679), near the LBJ Freeway and the Dallas North Tollway. These sites, however, may be useful in examining trends

of mobile source emissions, since close proximity to highways may allow NO_x to arrive at a monitor before substantial reaction has occurred.

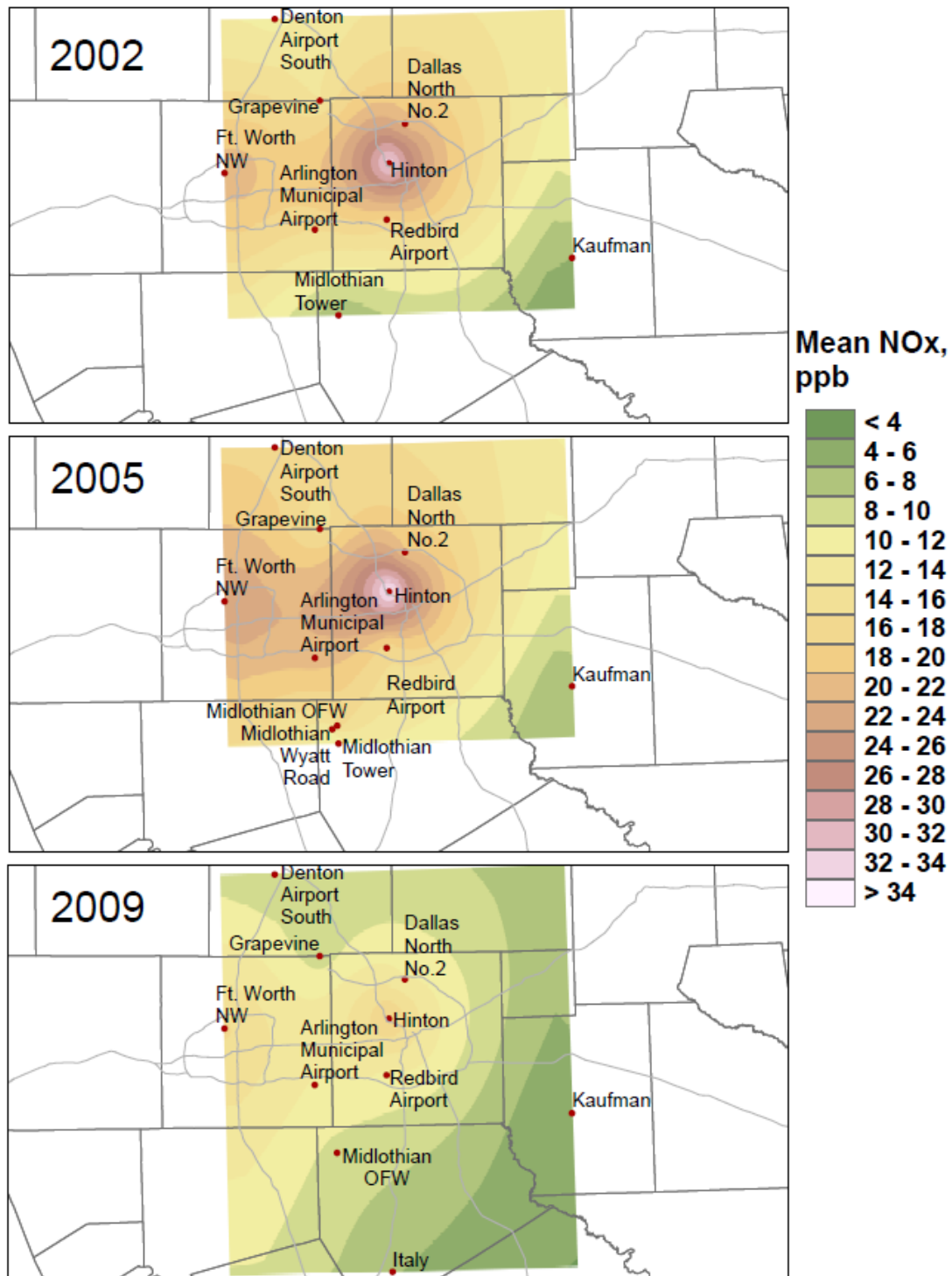


Figure D-3: Mean NO_x Concentrations in the DFW Area for 2002, 2005, and 2009

Because of the variety of NO_x sources, there can be a variety of reasons why NO_x concentrations in DFW have been decreasing. One potential cause for the decrease in NO_x over the entire DFW area is on-road vehicle fleet turnover, though this hypothesis has not yet been rigorously tested. Note that transport of industrial NO_x can obscure the patterns of mobile source emissions. Notice that, while the magnitude of mean NO_x has decreased, the areas that experience the

highest NO_x concentrations remain the same. An investigation of other variables in ozone formation, such as VOC and meteorology, might help to explain not only patterns in ozone, but also observed patterns in NO_x concentrations.

3.3 Recent Findings on VOC and NO_x Limitations

This section examines NO_x and VOC limitation in the DFW area using several methods. Determining if an area is VOC or NO_x limited may inform photochemical modeling and provide a basis for developing control strategies for an area; however, there are many other components of ozone formation potential that must be considered in development of effective control strategies for the DFW area.

A NO_x-limited region occurs where radicals from VOC oxidation are abundant, and therefore ozone formation is more sensitive to the amount of NO_x present in the atmosphere. In these regions, controlling NO_x would reduce ozone concentrations. In VOC limited regions, NO_x is abundant, and therefore ozone formation is more sensitive to the amount of radicals from VOC oxidation present in the atmosphere. In VOC limited regions, controlling VOC would reduce ozone concentrations. Areas where ozone formation is not strongly limited by either VOC or NO_x are considered transitional, and controlling either VOC or NO_x emissions in these regions would reduce ozone concentrations.

Different methods can be used to determine if an area is VOC or NO_x limited, but it is often difficult to compare these different methods because they use different ratios, VOC species, and data sources to determine limitations. This chapter will investigate various methods used to determine VOC and NO_x limitations including: VOC:NO_x ratio analysis, an extent of reaction analysis, an HRVOC analysis, and a weekday/weekend analysis using ozone exceedance days.

3.3.1 VOC:NO_x Ratios

The VOC:NO_x ratio expresses the efficiency of ozone formation in air mixtures containing both VOC and NO_x. The VOC:NO_x ratio, q , is computed as:

$$q = \frac{VOC(ppbC)}{NO_x(ppbV)}$$

If q is less than 5, the area is considered VOC limited, if q is greater than 15, the area is considered NO_x limited, and if q is greater than or equal to 5, but less than or equal to 15, the area is considered transitional (Chinkin, Main, and Roberts, 2005).

Ratios were calculated for two different types of VOC data: auto-GC data, and 24-hour canister data. Although TCEQ also collects VOC data in one-hour canisters in the multi-can (MCAN) network, sampling does not occur each day. MCAN canisters are triggered manually depending on the ozone forecast and the monitor site; therefore, there is not enough data available to do a complete study using MCAN data. Auto-GC data contains 40-minute samples taken every hour at two sites in the DFW area: Dallas Hinton St. (C401) and Ft. Worth Northwest (C13). Data is available at Dallas Hinton St. (C401) from 1999 through 2009 and at Ft. Worth Northwest from 2003 to 2009. The 24-hour canisters, part of the Community Air Toxics Monitoring Network (CATMN), collect samples every sixth day. CATMN data from 1999 to 2009 were used in this study. Although there are several VOC data sources available, varying sample times limit comparisons between the data.

Total non-methane organic carbon (TNMOC) was used as a proxy for VOC concentrations in the VOC:NO_x ratios for both CATMN and auto-GC data. Both types of data directly measure

TNMOC concentrations. VOC:NO_x ratios were calculated for every available day for each type of data, then daily ratios were averaged together to determine limitations in the area.

Figure D-27: *Annual Geometric Mean of Auto-GC VOC:NO_x Ratio* shows the annual geometric mean of daily VOC:NO_x ratios for auto-GC data at Dallas Hinton St. (C401/C60/AH161) from 1999 through 2009, and Ft. Worth Northwest (C13/AH302) from 2003 through 2009. Although VOC:NO_x ratios at both monitors are slowly increasing from VOC limited to transitional, ratios at Dallas Hinton St. (C401/C60/AH161) show that monitor to be more VOC limited compared to Ft. Worth Northwest (C13/AH302), which is more transitional. The difference in VOC:NO_x ratios at the two monitors may be due to the location of the monitors. Dallas Hinton St. (C401/C60/AH161) is located near Interstate 35E, a large source of mobile source NO_x emissions. The spatial NO_x analysis above showed that Dallas Hinton St. (C401/C60/AH161) exhibits higher NO_x concentrations than Ft. Worth Northwest (C13/AH302), which is located farther west, near the Fort Worth Meacham International Airport. Automobile emissions are a large source of ozone precursors in Dallas, with mobile emissions contributing about 86 percent of total NO_x emissions and 66 percent of total anthropogenic VOC emissions (Qin et al., 2007). In addition, Ft. Worth Northwest (C13/AH302) is much closer to oil and gas activity in the Barnett Shale, and exhibits much larger VOC concentrations compared to Dallas Hinton St. (C401/C60/AH161). A detailed analysis of the affect of Barnett Shale emissions on ozone in the DFW area will be discussed later.

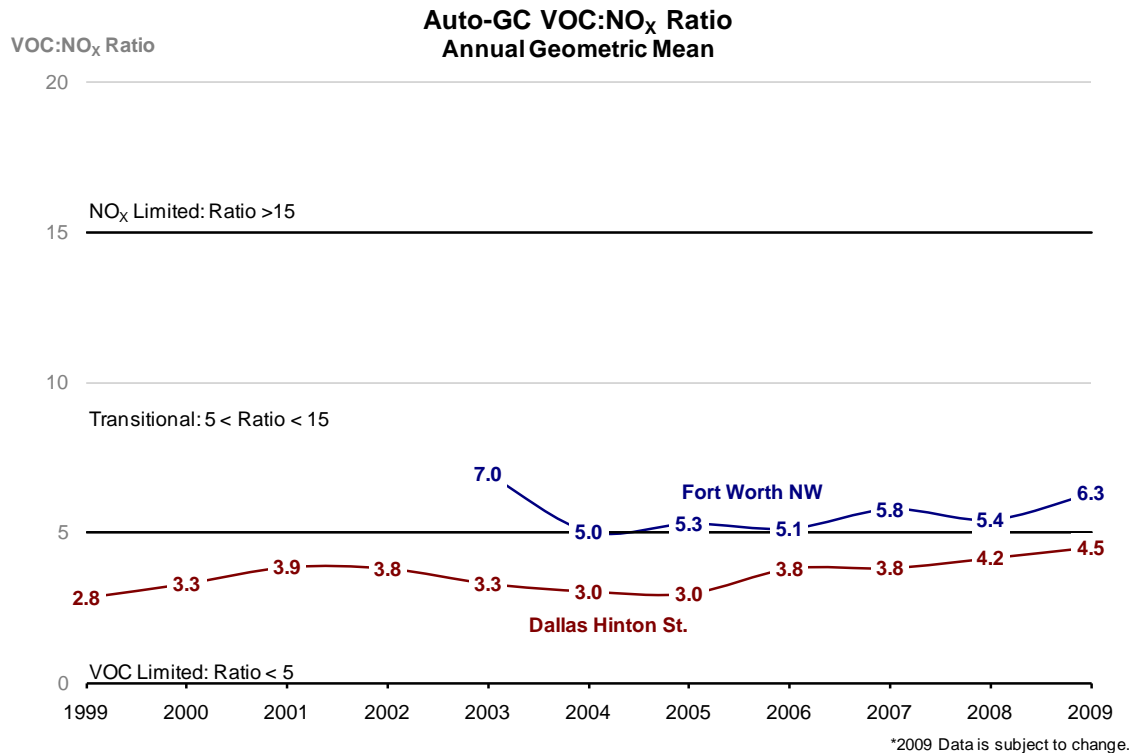


Figure D-4: Annual Geometric Mean of Auto-GC VOC:NO_x Ratio

Because VOC and NO_x emissions vary throughout the day, the VOC:NO_x ratio will also vary during different times of the day. Figure D-28: *Hourly Geometric Mean of Auto-GC VOC:NO_x*

Ratios shows how VOC:NO_x ratios change from hour to hour. For both monitors, the ratio increases during the early morning, from about 0:00 LST (midnight) to 3:00 LST, decreases until about 7:00 LST, begins to increase again until about 12:00 LST (noon), and then decreases throughout the afternoon. In addition to the diurnal variation of the mixing layer height, the morning and afternoon decrease in VOC:NO_x ratios may be related to changes in work commuters' driving patterns, which is a source of NO_x emissions (Qin, *et al.*, 2007). Dallas Hinton St. (C401/C60/AH161) may show less change from hour to hour because it is situated in the midst of many roadways, which may be filled with drivers during all hours of the day. Similar to annual mean ratios, the Ft. Worth Northwest (C13/AH302) monitor mostly exhibits a transitional regime and the Dallas Hinton St. (C401/C60/AH161) monitor exhibits a VOC limited regime. These diurnal patterns illustrate problems that may occur when calculating VOC:NO_x ratios from 24-hour canister data. While 24-hour canister data might not reflect the true VOC:NO_x sensitivity of the DFW area, it can be useful for corroborating findings from auto-GC data, and it is more widely available throughout the DFW area.

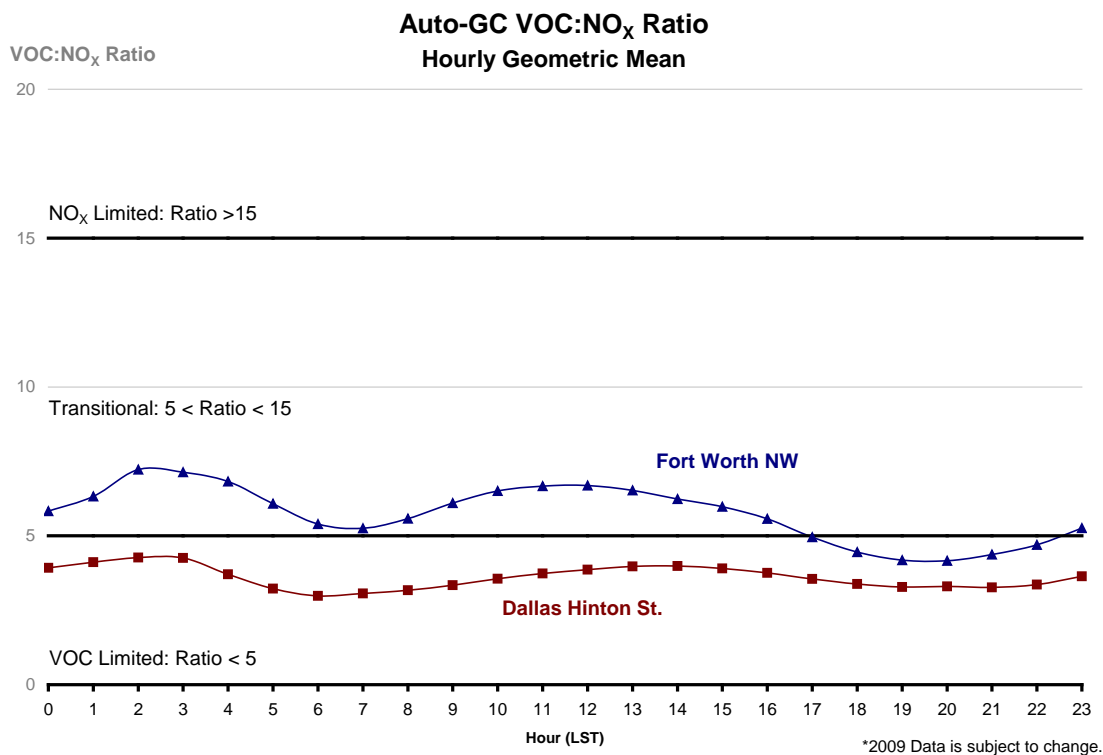


Figure D-5: Hourly Geometric Mean of Auto-GC VOC:NO_x Ratios

VOC:NO_x ratios calculated using seven CATMN monitors are displayed in Figure D-29: *Geometric Mean VOC:NO_x Ratios from Canister Data*. Most monitors exhibit ratios in the transitional to VOC limited range, with Ft. Worth Northwest (C13/AH302), Dallas Hinton St. (C401/C60/AH161), and Grapevine (C70/A301/X182) in the transitional regime, and with Denton Airport South (C56/A163/X157), Midlothian Tower (C94/A305/X158), Kaufman (C71/A304/X071), and Italy (C650) in the VOC limited regime. The Ft. Worth Northwest (C13/AH302) CATMN data shows the area has fluctuated between NO_x limited and transitional since 2003, while the auto-GC data has stayed right along the VOC limited/transitional boundary. The Dallas Hinton St. (C401/C60/AH161) ratio is still lower than Ft. Worth

Northwest (C13/AH302), similar to what was shown from auto-GC data, but instead of being VOC limited with a slight increase in recent years, CATMN data shows the area always to be transitional. Denton Airport South (C56/A163/X157) dropped quickly from its peak in 2002 to 2005 and has stayed stable since then, showing another drop in 2009. Kaufman (C71/A304/X071) appears always to be NO_x limited, showing a similar trend to Denton Airport South (C56/A163/X157) from 2005 to 2009. For the Midlothian Tower (C94/A305/X158) monitor, which was the original monitor in Midlothian, the rapid increase in VOC from 2004 to 2007 is likely due to expanding quarrying operations near the monitor. The monitor has since moved to a location slightly farther north in Midlothian, and is now called the Midlothian OFW monitor (C52/A137). However, the new monitor no longer measures TNMHC so it cannot be used in this analysis. The Italy (C650) monitor shows a substantial drop in the past year, but is still very much NO_x limited. Grapevine Fairway (C70/A301/X182) has alternated between being NO_x limited and transitional with a drop to transitional in 2009.

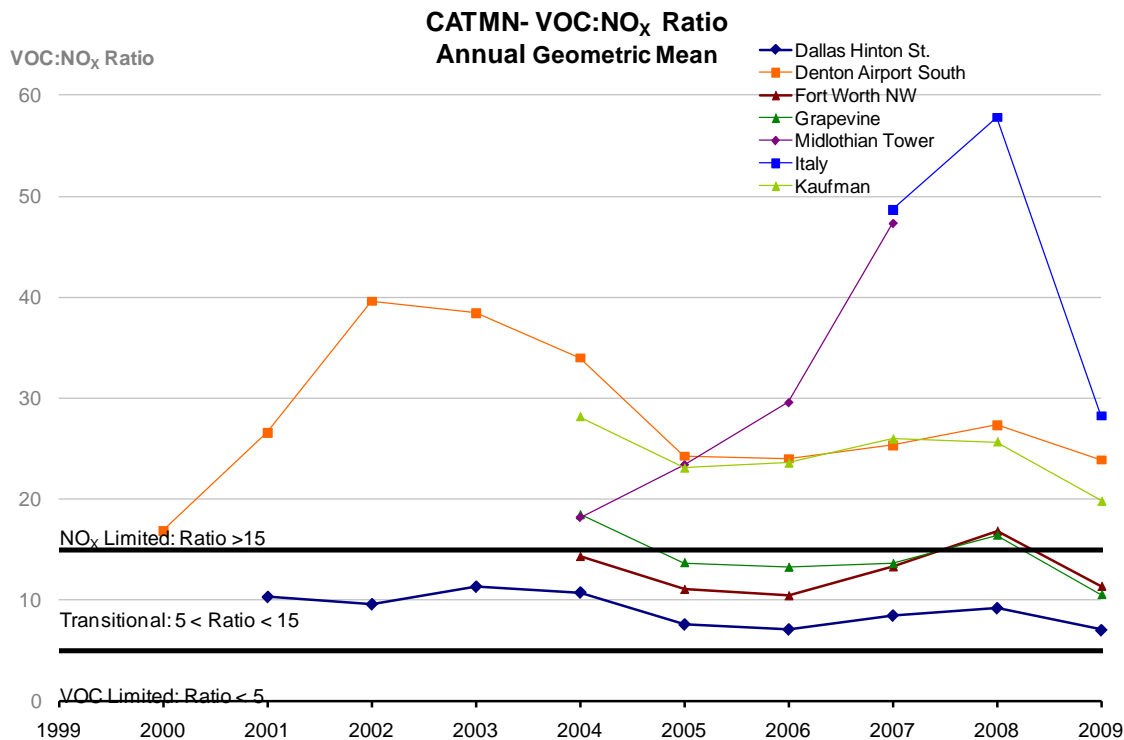


Figure D-6: Geometric Mean VOC:NO_x Ratios from Canister Data

Results from 2009 for each source and monitor are shown in Table D-11: *Summary of 2009 VOC:NO_x Ratios*. Results from different monitor types are similar, but not all of them agree. Auto-GC results show VOC limited and transitional regimes, while canister results appear to be measure transitional and NO_x limited regimes. These results are likely related to the location of each monitoring site and, for sites with two instruments, the difference in source sample times and durations. Site locations, as well as 2009 results for each monitor type, are shown in Figure D-30: *AGC and CATMN VOC:NO_x Ratios, 2009*. Midlothian Tower (C158) has no data because it was deactivated in 2007. Notice that monitors in the urban core, near the center of the circle, record air masses that are transitional to VOC limited (green and blue), whereas monitors on the periphery measure air masses that are transitional to NO_x limited.

Table D-2: Summary of 2009 VOC:NO_x Ratios

Site Name	Auto-GC		CATMN	
	Ratio	Limit	Ratio	Limit
Dallas Hinton St. C401	4.5	VOC	7.1	Transitional
Denton Airport South C56			23.9	NO _x
Ft. Worth Northwest C13	6.3	Transitional	11.4	Transitional
Grapevine Fairway C70			10.54	Transitional
Midlothian Tower C158*				
Kaufman C71			19.8	NO _x
Italy C1044			28.2	NO _x

*Note Midlothian Tower has no data because it was deactivated in 2007

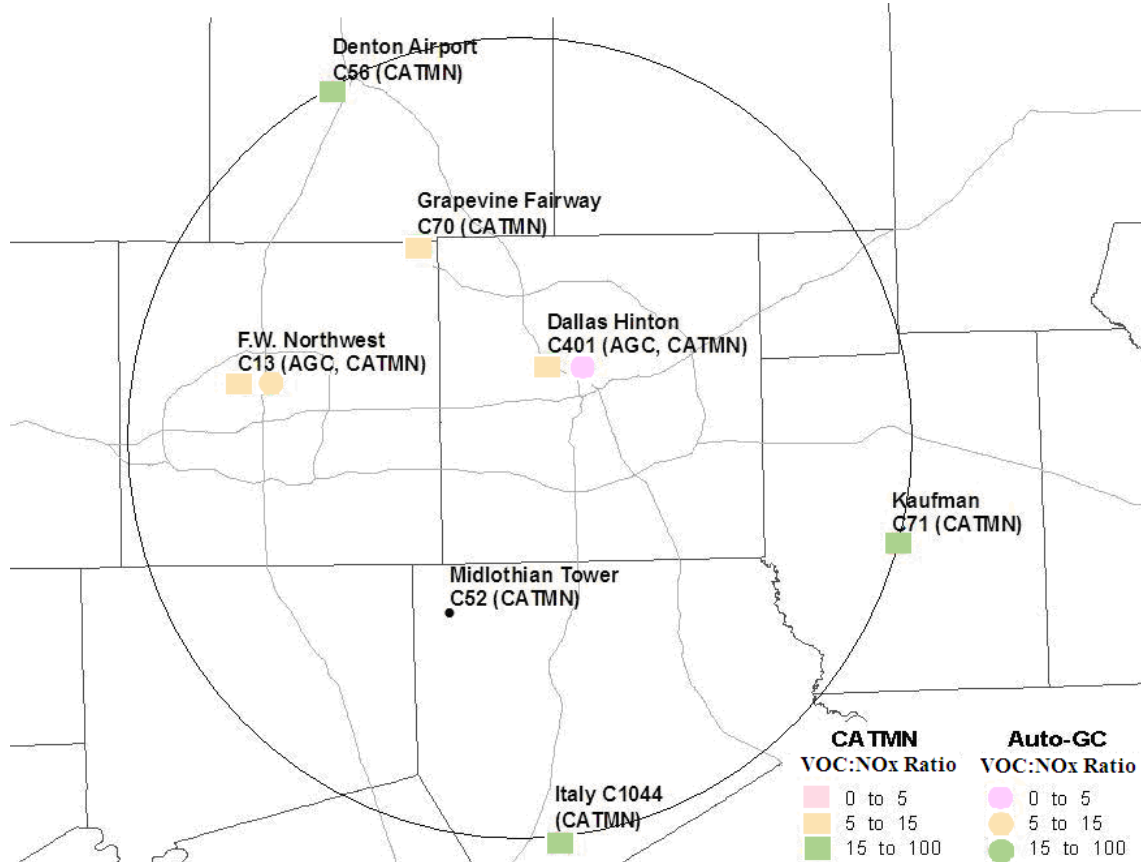


Figure D-7: AGC and CATMN VOC:NO_x Ratios, 2009

3.4 MAPPER

MAPPER, which stands for Measurement-based Analysis of Preferences in Planned Emission Reduction, is an algorithm that estimates where and when ozone formation is VOC or NO_x limited. MAPPER uses a smog production algorithm (SPA) applied to ozone, NO, and NO_x (or NO_y) to determine smog produced (SP) and the extent of reaction (E). Chinkin et al. (2005) report that Johnson developed the following equations using empirical smog chamber results:

$$SP(t) = O_3(t) - O_3(0) + NO(0) - NO(t)$$

$$SP_{MAX} = b(NO_x(i))$$

$$E = \frac{SP(t)}{SP_{MAX}}$$

where t stands for time and O represents initial conditions. The extent of reaction determines if the area is NO_x limited or VOC limited. This algorithm assumes that VOC limited conditions occur with fresh emissions and that NO_x limited conditions occur in aged air masses. Low extents indicate a VOC limited regime while higher extents indicate NO_x limited conditions (Sillman, 2002).

MAPPER was used to estimate ozone formation potential of different regions of the DFW area on high ozone days. Eleven monitors were used in this analysis: Dallas Hinton St. (C401/C60/AH161), Dallas North No.2 (C63/C679), Dallas Executive Airport (C402), Denton Airport South (C56), Ft. Worth Northwest (C13/AH302), Kaufman (C71), Grapevine Fairway (C70/A301/X182), Arlington Airport (C5007), Midlothian Tower (C94/A305/X158), and Midlothian OFC (C52/A137). The top five days with the highest ozone concentrations for each year from 1999 to 2009 were selected. The five hours surrounding peak ozone were chosen for each site and each day. Those five hours were then used to calculate the median extent of reaction for the high ozone days at each site for each year. These results are shown in Table D-12: *Extent of Reaction by Site and Year*. Ozone, NO_x, and NO data for 2009 were taken from the LEADS database, therefore are not official from the EPA and are subject to change.

Table D-3: Extent of Reaction by Site and Year

Monitor/CAMS#	1999	2000	2001	2002	2003	2004	2005	2006	2007	2008	2009	MEAN
Dallas Hinton St. C401	0.66	0.66	0.66	0.67	0.69	0.63	0.7	0.67	0.60	0.52	0.50	0.63
Dallas North No.2 C63	0.77	0.72	0.73	0.71	0.71	0.77	0.72	0.71	0.67	0.68	0.72	0.72
Dallas Executive Airport C402	0.62	0.69	0.65	0.69	0.67	0.71	0.71	0.69	0.65	0.72	0.70	0.68
Denton Airport South C56	0.91	0.81	0.87	0.90	0.79	0.76	0.78	0.84	0.77		0.68	0.81
Ft. Worth Northwest C13	0.66	0.88	0.84	0.87	0.73	0.65	0.71	0.70	0.63	0.60	0.68	0.72
Kaufman C71		0.54	0.74	0.78	0.73	0.70	0.76	0.78	0.74	0.71	0.65	0.71
Grapevine Fairway C70		0.59	0.80	0.84	0.76	0.73	0.77	0.77	0.71	0.69	0.77	0.74
Arlington Municipal Airport C61				0.69	0.65	0.67	0.65	0.65	0.61	0.65	0.65	0.65
Greenville C1006					0.71	0.72	0.73	0.78	0.70	0.63	0.71	0.71
Midlothian OFW C52/C137								0.72	0.64	0.64	0.61	0.65

Monitor/CAMS#	1999	2000	2001	2002	2003	2004	2005	2006	2007	2008	2009	MEAN
Midlothian Tower C94/C15		0.77	1.00	1.00	0.67	0.61	0.66	0.70	0.73			0.77

Green represents larger extents, pink represents lower extents, and orange is midlevel extents.

Figure D-31: *MAPPER Estimated Extent of Reaction by Monitor* shows how the extent of reaction has changed in the DFW area over the past 11 years, 1999-2009. Overall, most extent of reaction values appear to be declining, with areas moving from NO_x limited/transitional to transitional/VOC Limited. The Dallas Hinton St. (C401/C60/AH161) monitor shows a dramatic decrease in recent years to being closer to VOC limited.

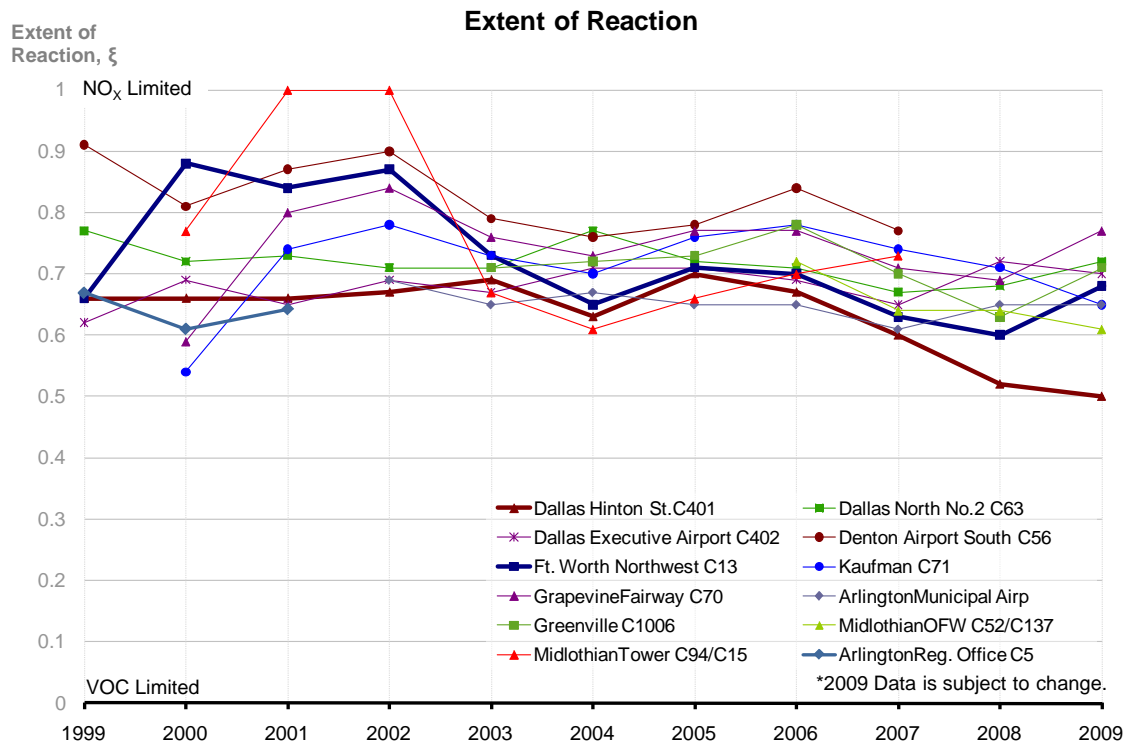


Figure D-8: **MAPPER Estimated Extent of Reaction by Monitor**

Figure D-32: *2009 Extent of Reaction at Each Monitor in the DFW Area* shows the locations of the monitors and extent of reaction at that monitor, denoted by color. Extents closer to one represent NO_x limited conditions while extents closer to zero represent VOC limited conditions. The figure shows that most monitors in the DFW area have extents between 0.6 and 0.8, with Dallas Hinton St. (C401/C60/AH161) being the only monitor with an extent below 0.6.

The SP algorithm used in the MAPPER program has not been rigorously tested with three-dimensional air quality models, and hence has uncertainties associated with it (Sillman, 2002). MAPPER has been shown to have better results predicting VOC limited regimes compared to NO_x limited regimes (Sillman, 2002). Because of these uncertainties, this analysis was not able to distinguish distinct lines between VOC limited and transitional, and transitional and NO_x limited. This analysis shows that most monitors have extents which fall somewhere between NO_x limited and VOC limited, with Dallas Hinton St. (C401/C60/AH161) having the lowest extent, and therefore being the closest to VOC limited.

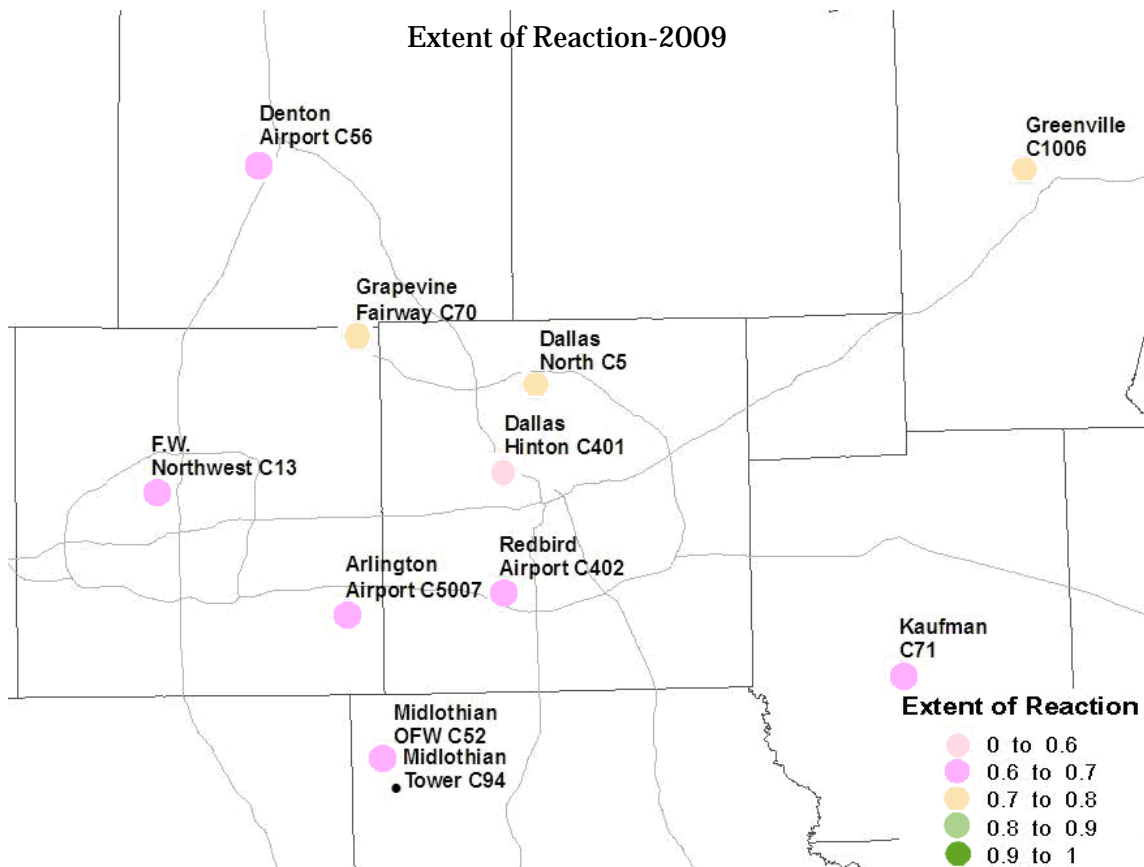


Figure D-9: 2009 Extent of Reaction at Each Monitor in the DFW Area

Results from VOC:NO_x ratios and the MAPPER program suggest that air masses within the city core tend to be VOC limited to transitional, and regions to the northwest of the core are transitional. CATMN (24-hour canister) results showed more transitional conditions in the urban core, but auto-GC results showed the urban core as more VOC limited. This could be due to the different time periods used for each set of data. Results from MAPPER are ambiguous and the extent of reaction tends to fall somewhere in between the extremes, suggesting that the air mass in the DFW area tends to be transitional.

Caution must be taken when analyzing VOC:NO_x limitations. The VOC:NO_x ratio can vary daily as well as hourly. VOC and NO_x limitations show how ozone can be reduced immediately; however, they cannot show what will be needed to attain the eight-hour ozone standard. These limitations provide a starting point to understand how ozone can be controlled effectively in an urban area, but other factors must also be investigated. Reactivity of VOC found in an air mass also plays an important role in ozone formation. Small amounts of highly reactive VOC could lead to production of more ozone, so even if the area is NO_x limited, VOC would still need to be

controlled in order to lower ozone concentrations. The following section investigates VOC reactivity in the DFW area in detail.

3.4.1 Ambient Highly Reactive Volatile Organic Compounds (HRVOC)

Six VOC species monitored by the TCEQ are classified as highly reactive volatile organic compounds (HRVOC): ethene, propene, 1,3-butadiene, 1-butene, cis-2-butene, trans-2-butene (TCEQ, 2006). HRVOC react more rapidly than other VOC species to form ozone; therefore, trends in these species reveal a great deal about changing ozone formation dynamics in the area.

As demonstrated in Chapter 2, VOC measurements exhibit many extremely small values and few extremely high ones. For series with these characteristics, logarithmic transformation often greatly improves analytical capacity. Therefore, for analyses of HRVOC trends, geometric means of each HRVOC were calculated by taking the natural logarithm (log) of all available measurements, averaging these logs, then exponentiating. The geometric mean is preferred to the median or the arithmetic (ordinary) mean for evaluating the central tendency of data when the data are skewed, that is, when the data are not symmetrically, or normally, distributed, but clustered around extreme high or low values. For these series, a geometric mean is more robust than an ordinary average, meaning its value is not greatly influenced by one or a few very high or very low values. The 90th percentile is also examined because it provides information about trends at the upper end of the distributions, but is more robust than the maximum values. Monthly geometric means and 90th percentiles were only computed for months with 75 percent or more valid measurements

Ethene, also known as ethylene, is the HRVOC compound with highest ozone generating potential in DFW because it is among the most reactive, with an Maximum Incremental Reactivity (MIR) of 9.08 grams of ozone per gram of VOC (Carter 2000; Carter 2010; Atkinson 2003). Figure D-33: *Daily Maximum Ethene at Dallas Hinton St. (C401/C60/AH161) Monitor* and Figure D-34: *Daily Maximum Ethene at Ft. Worth Northwest (C13/AH32) Monitor* demonstrate the seasonal fluctuation in daily peak ethene collected with auto-GC instruments. Similar to TNMHC, both monitors detect a clear annual cycle in ambient ethene, evident in the daily maxima (grey points), the monthly geometric means (blue line), and the monthly 90th percentile (red line) measures. Ethene tends to exhibit lower concentrations during summer and higher concentrations during winter. Since 1999, a clear downward trend is apparent in the mean and 90th percentile series. The Ft. Worth Northwest (C13/AH32) monitor also tends to record lower values of ethene than the Dallas Hinton St. (C401/C60/AH161) monitor, and the range, or scatter between high and low values, also appears to be narrower.

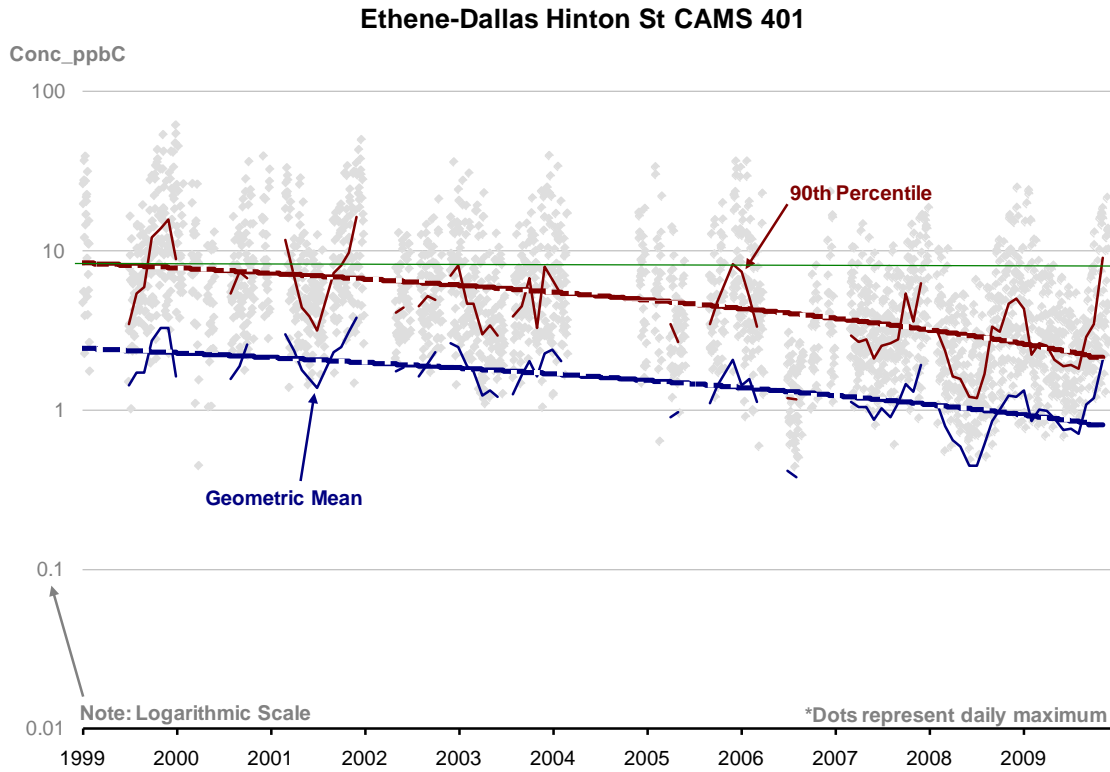


Figure D-10: Daily Maximum Ethene at Dallas Hinton St. (C401/C60/AH161) Monitor

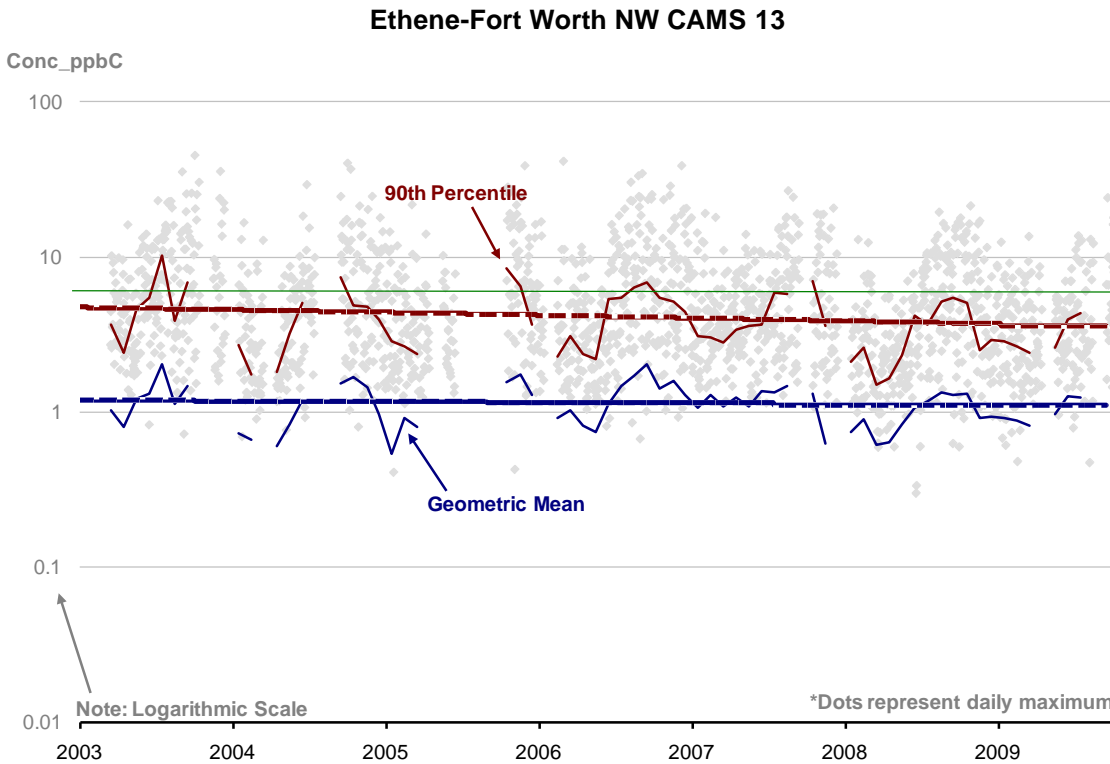


Figure D-11: Daily Maximum Ethene at Ft. Worth Northwest (C13/AH32) Monitor

Figure D-35: Annual Geometric Mean Ethene at Dallas Hinton St. (C401/C60/AH161) and Ft. Worth Northwest (C13/AH32) displays available annual geometric mean values for both monitors. Note that the Ft. Worth Northwest (C13/AH32) auto-GC monitor only began collecting ethene in 2003. Prior to 2006, Dallas Hinton St. (C401/C60/AH161) recorded a higher geometric mean of ethene compared to Ft. Worth Northwest (C13/AH32), but since 2006, geometric mean ethene is larger at Ft. Worth Northwest (C13/AH32). Table D-13: Regression Results for Annual Geometric Mean Ethene reports results of simple linear fits of annual geometric mean ethene and 90th percentile ethene to year. These results confirm a downward trend in ethene at Dallas Hinton St. (C401/C60/AH161), though not at Ft. Worth Northwest (C13/AH32). Although both models estimate negative slopes, only the slope parameter for the Dallas Hinton St. (C401/C60/AH161) annual geometric mean ethene model is statistically significant. Further, the adjusted R² statistic and the F statistic both reveal a poor fit for the Ft. Worth Northwest (C13/AH32) annual geometric mean ethene model, indicating that the slope from this model cannot be differentiated from zero with statistical confidence, suggesting a flat trend. These findings are similar to the results observed for TNMHC above. Similar results for annual 90th percentile ethene models are not reported.

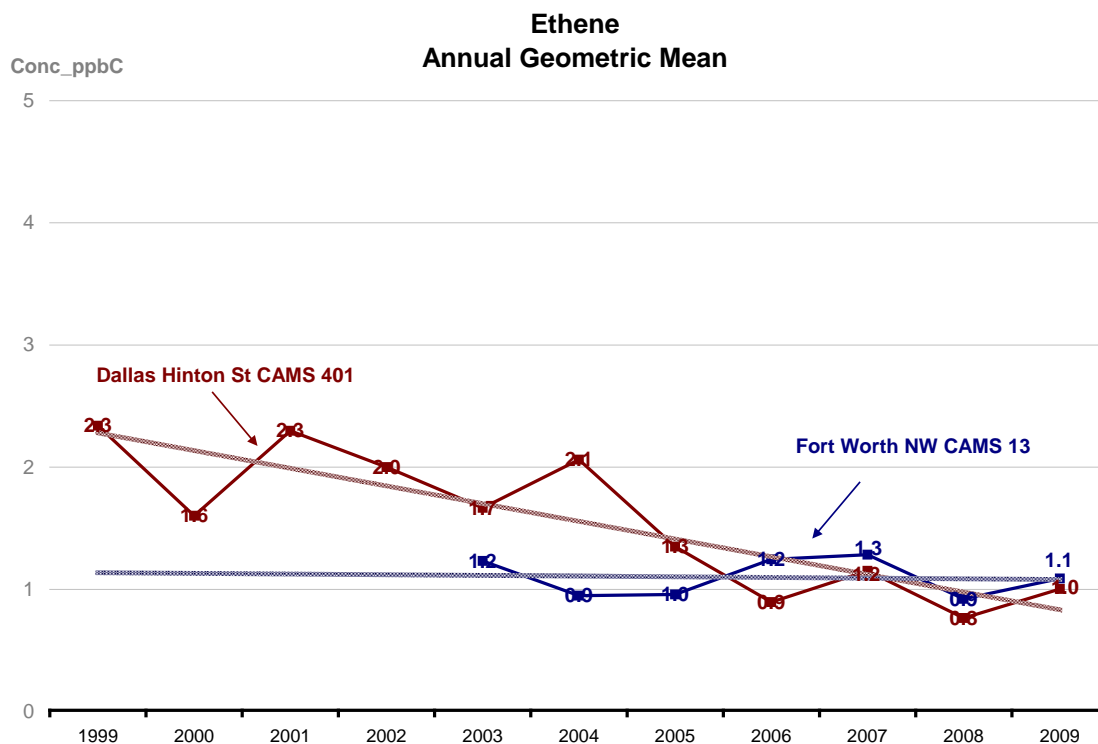


Figure D-12: Annual Geometric Mean Ethene at Dallas Hinton St. (C401/C60/AH161) and Ft. Worth Northwest (C13/AH32)

Table D-4: Regression Results for Annual Geometric Mean Ethene

Statistic	Dallas Hinton St.	Ft. Worth Northwest

Statistic	Dallas Hinton St.	Ft. Worth Northwest
Adjusted R ²	0.696	-0.193
F	23.854	0.030
p-value	0.001	0.869
Slope	-0.145	-0.006
t-stat	-4.884	-0.174
p-value	0.001	0.869

Propene, or propylene, also has a high ozone generating potential, with an MIR of 11.58 grams of ozone per gram of VOC. Patterns observed in propene are similar to those seen in ethene. At the Dallas Hinton St. (C401/C60/AH161) monitor there is again an obvious seasonal variation, with higher propene concentrations measured in the winter and lower concentrations in the summer. Figure D-36: *Propene at Dallas Hinton St (C401/C60/AH161) Monitor* and Figure D-37: *Propene at Ft. Worth Northwest (C13/AH32) Monitor* demonstrate the seasonal fluctuation in daily peak propene collected with auto-GC instruments. Since 1999, a clear downward trend is apparent in the mean and 90th percentile series. The Ft. Worth Northwest (C13/AH32) monitor also tends to record lower values of propene than the Dallas Hinton St. (C401/C60/AH161) monitor, and the range, or scatter between high and low values, also appears to be larger. Again, the Ft. Worth Northwest (C13/AH32) auto-GC monitor only began collecting ethene in 2003. Months with insufficient data (less than 75 percent complete) appear as gaps in the figures.

Figure D-38: *90th Percentile 1,3-Butadiene at Dallas Hinton St. (C401/C60/AH161) Monitor and Ft. Worth Northwest (C13/AH32) Monitor* shows patterns for 1, 3-butadiene similar to those for ethene and propene. The 90th percentile of measured ambient concentrations of 1, 3-butadiene have been declining since 1999. The spike at the Dallas Hinton St. (C401/C60/AH161) monitor at the end of 2009 could be anomalous, though it does not drastically exceed the regular pattern of fluctuation observed for this compound. This figure also shows the similarities in seasonal variation and scale in 1, 3-butadiene concentrations measured at both monitors.

Propene- Dallas Hinton St CAMS 401

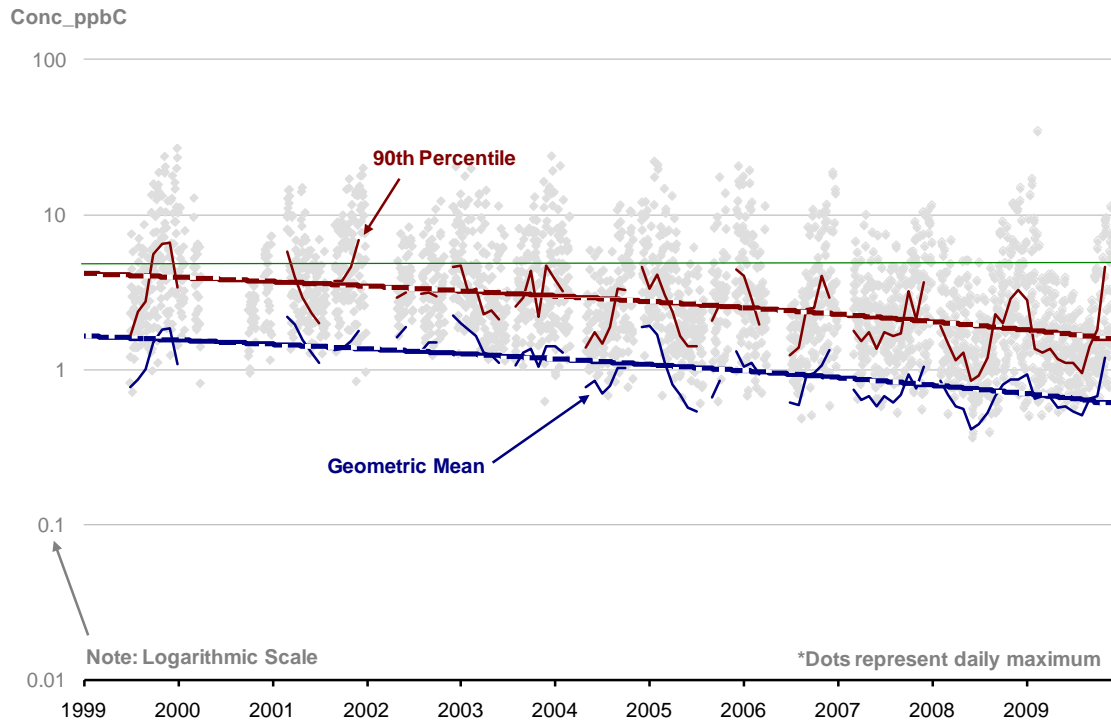


Figure D-13: Propene at Dallas Hinton St (C401/C60/AH161) Monitor

Propene- Fort Worth NW CAMS 13

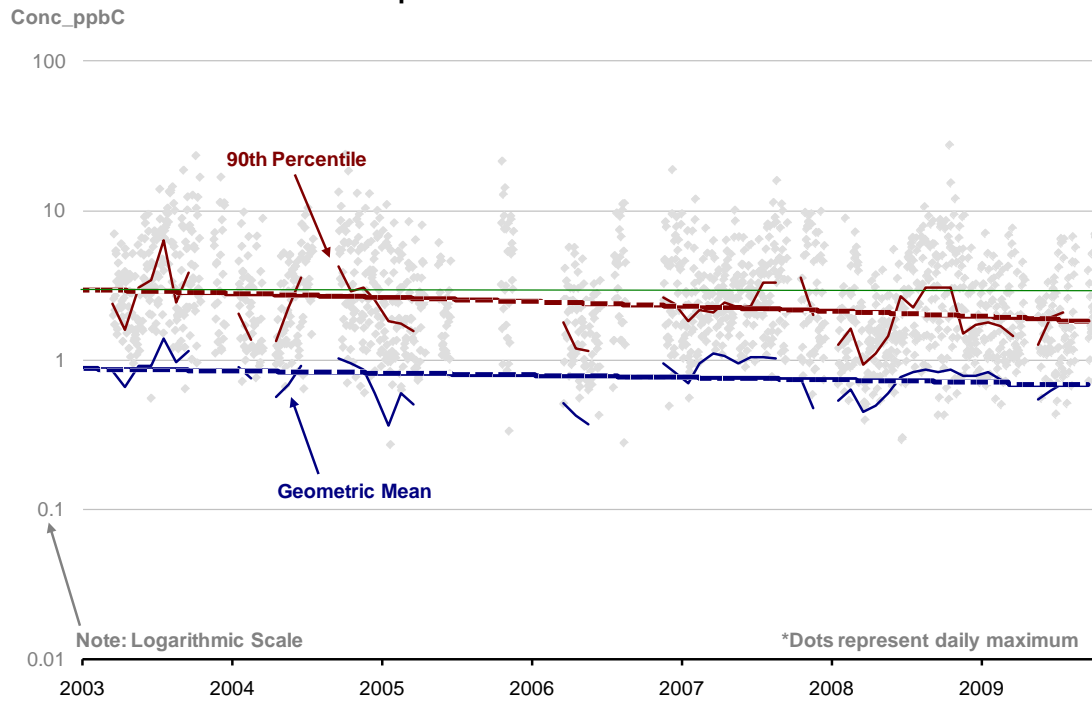


Figure D-14: Propene at Ft. Worth Northwest (C13/AH32) Monitor

1,3 Butadiene- 90th Percentile

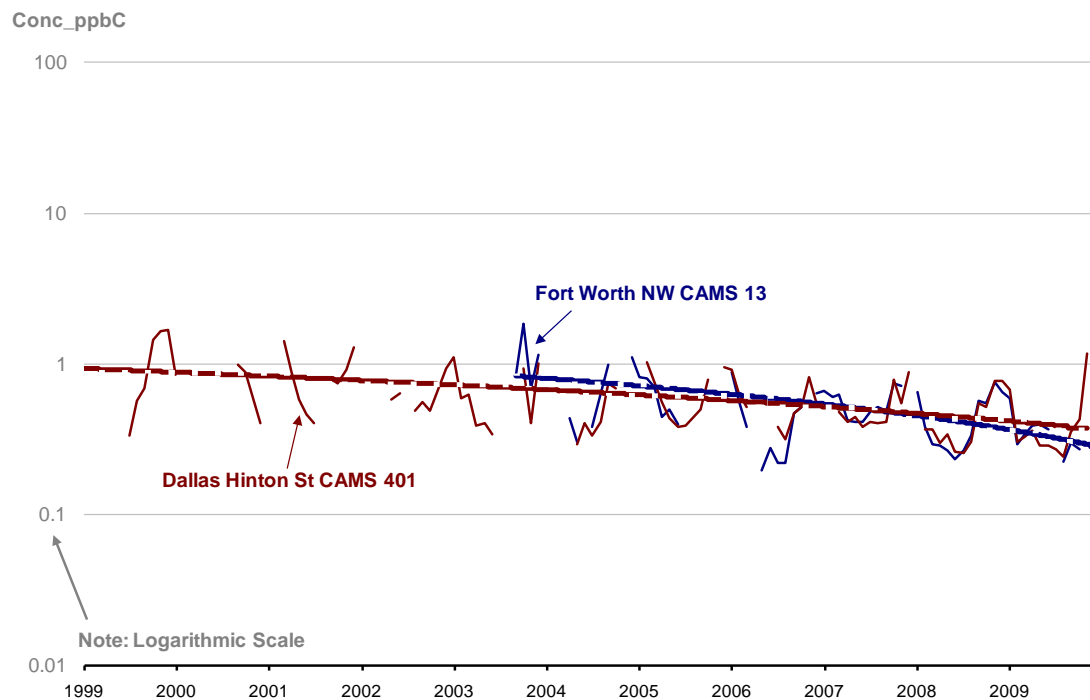


Figure D-15: 90th Percentile 1,3-Butadiene at Dallas Hinton St. (C401/C60/AH161) Monitor and Ft. Worth Northwest (C13/AH32) Monitor

Table D-14: *Summary of HRVOC Linear Regression Fits* reports results from linear regressions of all annual 90th percentiles and geometric means of each HRVOC compound fit to year. Annual 90th percentiles and geometric means, rather than daily peak values or monthly aggregates, were fit to reduce the impact of the observed cyclic effect on parameter estimates and significance levels. While the geometric mean models for all six compounds at Ft. Worth Northwest (C13/AH32) are all fairly poor, indicating that no downward slopes can be statistically confirmed, the 90th percentile models for that monitor confirm downward trends (at the $\alpha=0.05$ level) for all compounds except trans-2-butene (not significant) and ethene (significant at the $\alpha=0.10$ level). Also, the R^2 statistic for the ethene model is fairly low ($R^2 = 0.376$), indicating that there is a fair amount of unexplained scatter in the data. This is not surprising, however, considering the large variability in the original daily peak series.

Model results for the six compounds at Dallas Hinton St. (C401/C60/AH161) are much better: downward slopes in 90th percentiles are statistically confirmed for all six compounds and for four of six geometric mean models, except trans-2-butene and cis-2-butene. Like ethene at Ft. Worth Northwest (C13/AH32), fairly low R^2 values are estimated at Dallas Hinton St. (C401/C60/AH161) for the 90th percentile model ($R^2 = 0.314$) for trans-2-butene and the geometric mean model ($R^2 = 0.299$) for 1,3-butadiene. These results suggest that both monitors are measuring statistically significant downward trends in ambient HRVOC at the upper ends of their respective distributions, and even in the middle (geometric mean) of several of the distributions at Dallas Hinton St. (C401/C60/AH161).

Table D-5: Summary of HRVOC Linear Regression Fits

Annual Geometric Mean and 90th Percentile Linear Regression					
HRVOC	Statistic	Dallas Hinton St.		Ft. Worth Northwest	
		90th Percentile	Geometric Mean	90 th Percentile	Geometric Mean
Ethene	Adjusted R ²	0.820	0.696	0.376	-0.193
	F	46.468*	23.854*	4.618**	0.030
	p-value	0.000	0.001	0.084	0.869
	Slope	-0.607*	-0.145*	-0.205**	-0.006
	t-stat	-6.817	-4.884	-2.149	-0.174
	p-value	0.000	0.001	0.084	0.869
Propene	Adjusted R ²	0.887	0.558	0.557	-0.061
	F	79.847*	13.617*	8.531*	0.654
	p-value	0.000	0.005	0.033	0.455
	Slope	-0.237*	-0.080*	-0.177*	-0.027
	t-stat	-8.936	-3.690	-2.921	-0.809
	p-value	0.000	0.005	0.033	0.455
1,3-Butadiene	Adjusted R ²	0.848	0.299	0.678	-0.049
	F	56.880*	5.265*	13.659*	0.721
	p-value	0.000	0.047	0.014	0.435
	Slope	-0.055*	-0.013*	-0.104*	-0.006
	t-stat	-7.542	-2.295	-3.696	-0.849
	p-value	0.000	0.047	0.014	0.435
Trans-2-Butene	Adjusted R ²	0.314	-0.020	-0.140	-0.200
	F	5.573*	0.804	0.264	0.001
	p-value	0.043	0.393	0.629	0.981
	Slope	-0.053*	-0.019	-0.021	-0.001
	t-stat	-2.361	-0.897	-0.514	-0.025
	p-value	0.043	0.393	0.629	0.981
Cis-2-Butene	Adjusted R ²	0.866	0.096	0.588	-0.196
	F	65.536*	2.062	9.553*	0.017
	p-value	0.000	0.185	0.027	0.902
	Slope	-0.045*	-0.009	-0.038*	-0.001
	t-stat	-8.095	-1.436	-3.091	-0.129
	p-value	0.000	0.185	0.027	0.902
1-Butene	Adjusted R ²	0.704	0.553	0.870	0.024
	F	24.802*	13.372*	41.245*	1.150
	p-value	0.001	0.005	0.001	0.333
	Slope	-0.045*	-0.011*	-0.040*	-0.005
	t-stat	-4.980	-3.657	-6.422	-1.072
	p-value	0.001	0.005	0.001	0.333

*Significant at the $\alpha=0.05$ level.

**Significant at the $\alpha=0.10$ level.

Box plots better display the spike seen in 2009 data at the Dallas Hinton St. (C401/C60/AH161) monitor. Figure D-39: *Box Plots of Ethene and Propene at Two Auto-GC Monitors*, Figure

D-40: *Box Plots of 1,3-Butadiene and Trans-2-Butene at Two Auto-GC Monitors*, and Figure D-41: *Box Plots of Cis-2-Butene and 1-Butene at Two Auto-GC Monitors* display box plots for all HRVOC species at Dallas Hinton St. (C401/C60/AH161) and Ft. Worth Northwest (C13/AH32). Before analyzing the plots, it is important to note that the top of the box is the 75th percentile, the mean is represented by the 'plus' symbol, the median (50th percentile) is the middle line in the box and the bottom of the box is the 25th percentile. Outlying maximum observations are represented by red points. A summary of all statistics used in the box plots is available in Table D-15: *Summary Statistics for HRVOC at Two Auto-GC Monitors*.

For all HRVOC at Dallas Hinton St. (C401/C60/AH161) the extent of the box plot is shrinking, indicating there is less sample variation. Box size is decreasing even though increases were observed in the monthly 90th percentiles. Since box size has decreased, it appears that all statistics of each HRVOC are decreased. HRVOC at Ft. Worth Northwest (C13/AH32) exhibit only a slight decline, which agrees with the observed trends in the monthly 90th percentiles.

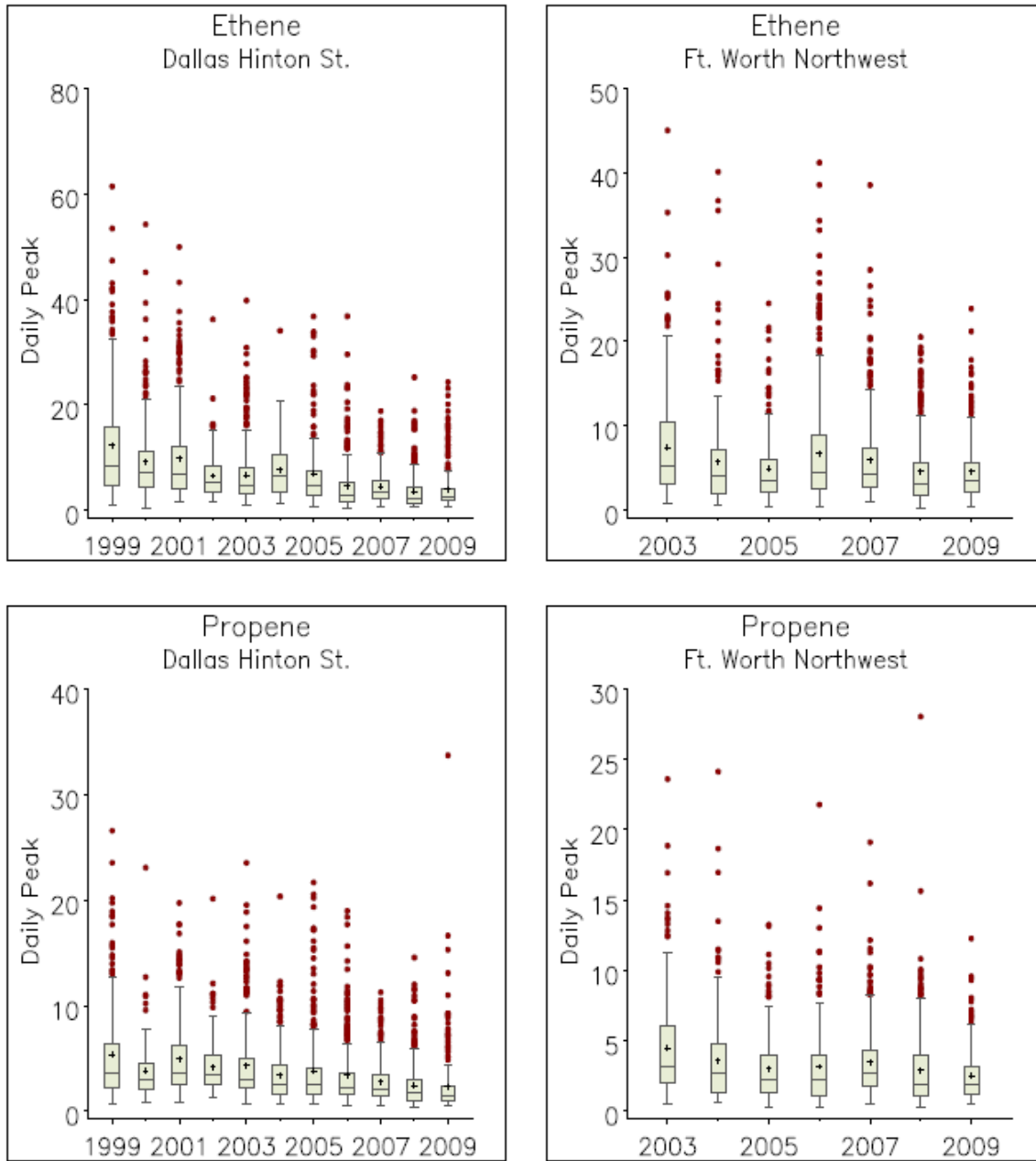


Figure D-16: Box Plots of Ethene and Propene at Two Auto-GC Monitors

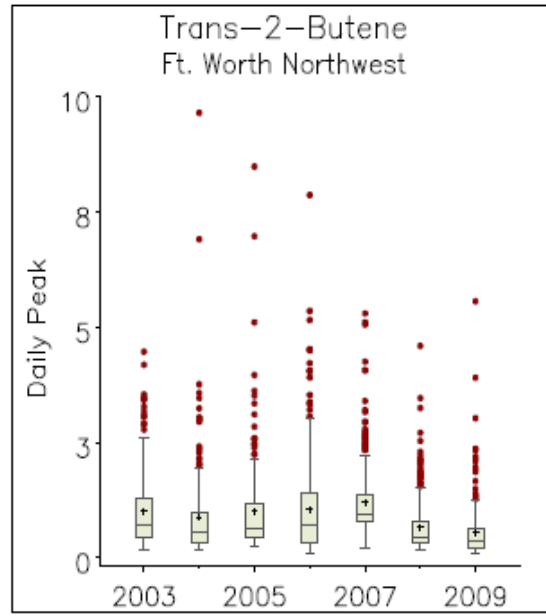
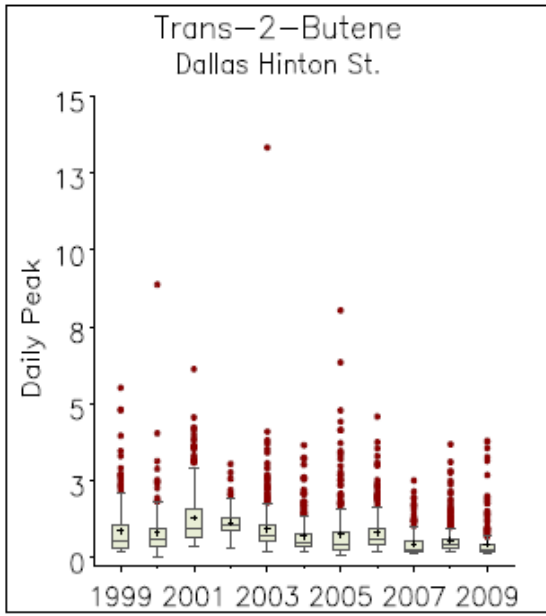
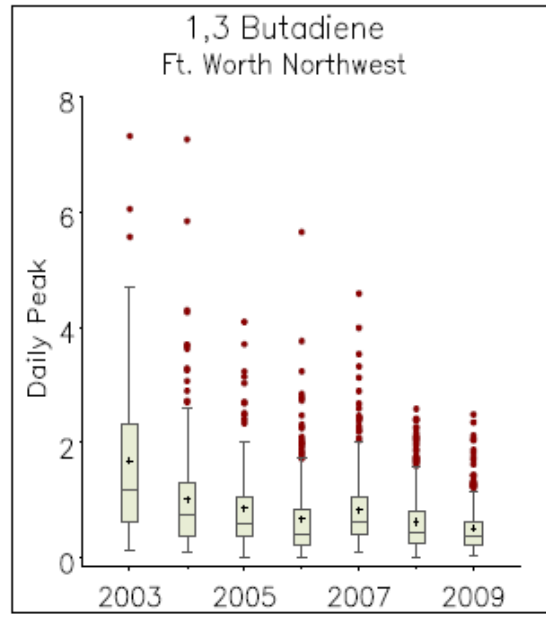
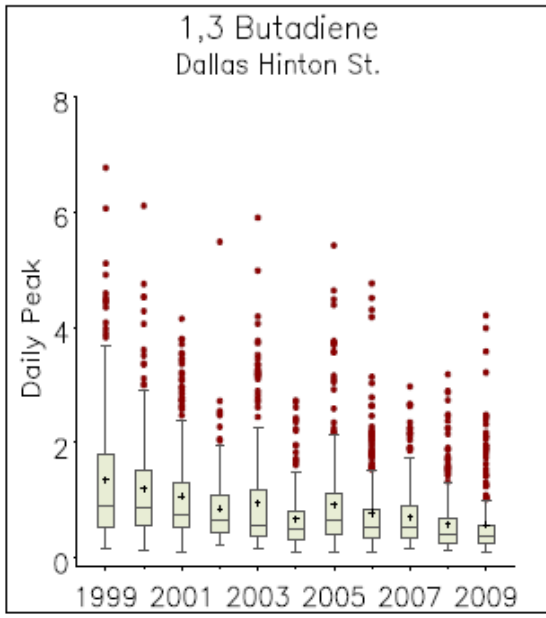


Figure D-17: Box Plots of 1,3-Butadiene and Trans-2-Butene at Two Auto-GC Monitors

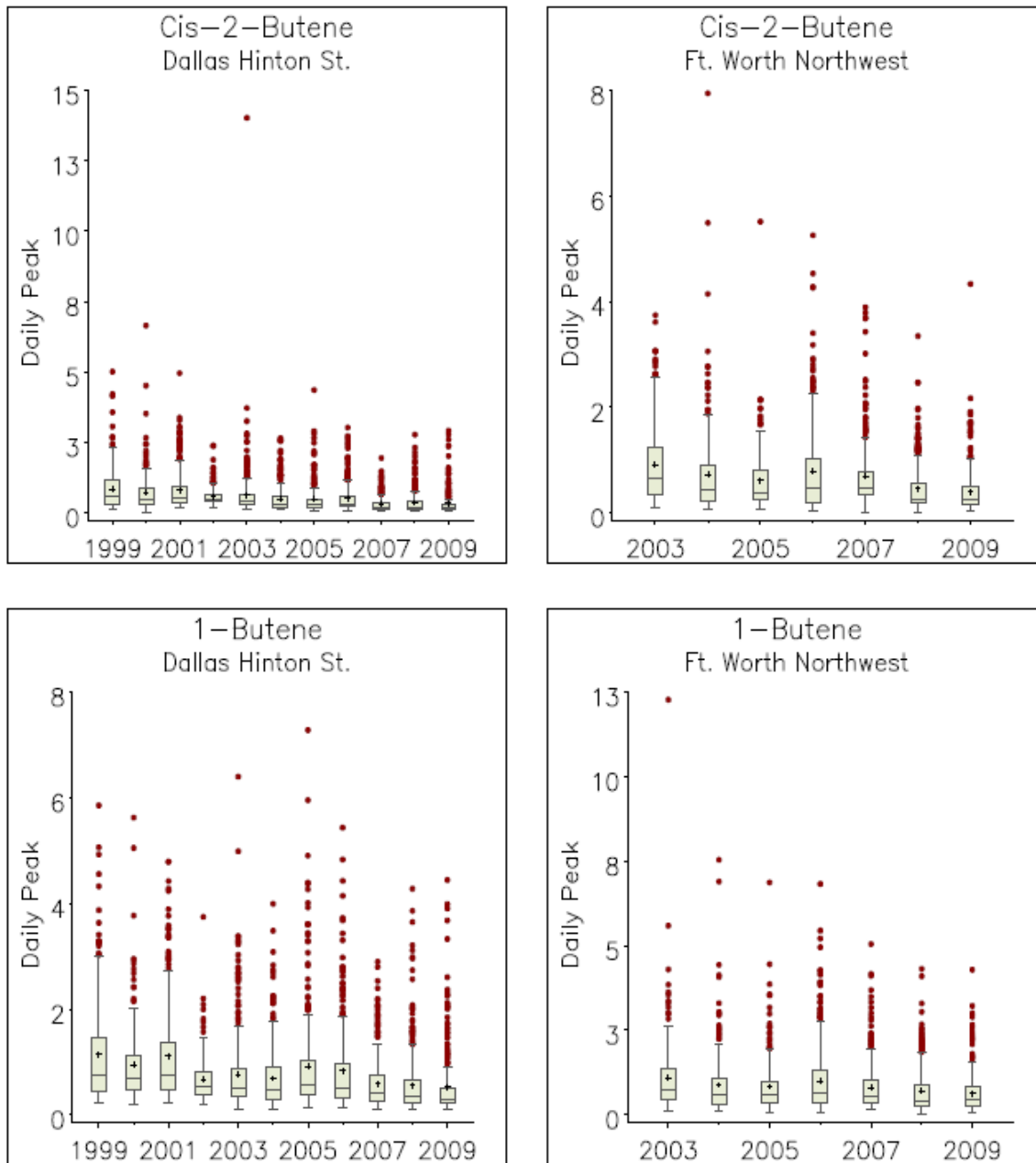


Figure D-18: Box Plots of Cis-2-Butene and 1-Butene at Two Auto-GC Monitors

Table D-6: Summary Statistics for HRVOC at Two Auto-GC Monitors

	1999	2000	2001	2002	2003	2004	2005	2006	2007	2008	2009
Ethene											
	Dallas Hinton St. (C401/C60/AH161)										
Num. obs.	211	210	269	180	331	91	177	207	305	332	330
Maximum	61.41	54.20	49.93	36.21	39.80	34.04	36.74	36.78	18.81	25.23	24.29
Mean	12.34	9.27	9.79	6.52	6.60	7.38	6.88	4.66	4.44	3.48	3.98
Minimum	1.02	0.45	1.39	1.45	1.05	1.25	0.64	0.45	0.61	0.49	0.70
	Fort Worth Northwest (C13/AH32)										

	1999	2000	2001	2002	2003	2004	2005	2006	2007	2008	2009
Num. obs.					211	211	209	335	326	332	302
Maximum					45.03	40.10	24.51	41.20	38.54	20.53	23.89
Mean					7.45	5.75	4.92	6.74	5.97	4.64	4.62
Minimum					0.72	0.70	0.41	0.43	0.93	0.30	0.47

Propene

Dallas Hinton St. (C401/C60/AH161)

Num. obs.	182	121	269	180	331	275	289	265	305	332	330
Maximum	26.58	23.08	19.73	20.14	23.54	20.35	21.67	18.96	11.26	14.55	33.74
Mean	5.35	3.83	4.93	4.17	4.31	3.42	3.76	3.40	2.75	2.38	2.30
Minimum	0.71	0.81	0.83	1.22	0.62	0.67	0.60	0.48	0.52	0.36	0.49

Fort Worth Northwest (C13/AH32)

Num. obs.					211	211	209	153	298	332	302
Maximum					23.60	24.14	13.26	21.79	19.12	28.05	12.27
Mean					4.49	3.58	3.04	3.16	3.46	2.88	2.49
Minimum					0.56	0.65	0.27	0.28	0.50	0.30	0.44

1,3-Butadiene

Dallas Hinton St. (C401/C60/AH161)

Num. obs.	211	181	269	180	270	213	268	268	305	332	330
Maximum	6.77	6.11	4.15	5.48	5.90	2.73	5.42	4.76	2.97	3.18	4.21
Mean	1.35	1.20	1.06	0.84	0.96	0.67	0.93	0.78	0.71	0.58	0.56
Minimum	0.17	0.134	0.108	0.207	0.152	0.089	0.112	0.099	0.16	0.133	0.112

Fort Worth Northwest (C13/AH32)

Num. obs.					120	210	177	301	326	363	301
Maximum					7.32	7.26	4.09	5.65	4.58	2.58	2.49
Mean					1.68	1.01	0.86	0.67	0.83	0.62	0.50
Minimum					0.13	0.11	0.01	0.01	0.10	0.01	0.04

Trans-2-Butene

Dallas Hinton St. (C401/C60/AH161)

Num. obs.	182	151	269	180	331	275	294	268	305	332	330
Maximum	5.53	8.88	6.13	3.04	13.34	3.66	8.04	4.59	2.50	3.69	3.79
Mean	0.88	0.82	1.29	1.13	0.94	0.69	0.74	0.81	0.43	0.55	0.44
Minimum	0.17	0.01	0.36	0.30	0.20	0.19	0.09	0.21	0.10	0.18	0.12

Fort Worth Northwest (C13/AH32)

Num. obs.					211	211	209	335	326	363	302
Maximum					4.46	9.65	8.48	7.86	5.30	4.59	5.56
Mean					0.99	0.87	0.99	1.03	1.20	0.65	0.54
Minimum					0.16	0.16	0.25	0.08	0.21	0.18	0.10

Cis-2-Butene

Dallas Hinton St. (C401/C60/AH161)

Num. obs.	211	210	269	180	331	275	208	268	305	270	330
Maximum	5.01	6.65	4.96	2.39	14.02	2.65	4.36	3.02	1.94	2.78	2.92
Mean	0.83	0.71	0.81	0.58	0.62	0.48	0.48	0.53	0.31	0.35	0.32
Minimum	0.11	0.01	0.16	0.17	0.11	0.10	0.08	0.08	0.07	0.09	0.08

Fort Worth Northwest (C13/AH32)

	1999	2000	2001	2002	2003	2004	2005	2006	2007	2008	2009
Num. obs.					181	210	146	306	295	363	301
Maximum					3.74	7.94	5.51	5.25	3.90	3.35	4.33
Mean					0.90	0.73	0.60	0.79	0.70	0.45	0.40
Minimum					0.09	0.08	0.08	0.03	0.01	0.01	0.03

1-Butene

Dallas Hinton St. (C401/C60/AH161)

Num. obs.	211	181	269	180	331	275	294	268	305	332	330
Maximum	5.86	5.63	4.79	3.75	6.40	3.99	7.28	5.43	2.90	4.28	4.44
Mean	1.14	0.94	1.11	0.66	0.77	0.69	0.92	0.83	0.59	0.56	0.52
Minimum	0.22	0.20	0.21	0.19	0.11	0.10	0.14	0.13	0.10	0.10	0.12

Fort Worth Northwest (C13/AH32)

Num. obs.					211	211	209	335	326	363	302
Maximum					12.28	7.54	6.87	6.83	5.05	4.31	4.29
Mean					1.08	0.89	0.84	0.99	0.81	0.70	0.63
Minimum					0.09	0.11	0.08	0.07	0.14	0.01	0.06

HRVOC data collected with canisters is also useful in corroborating finding from the analysis of data from auto-GCs. Figure D-42: *Quarterly Geometric Mean Ethene at CATMN Monitors* shows trends in ethene at all regional CATMN monitors since 1999. 2009 includes measurements through the second quarter only. Because the figure is using a logarithmic transformation, the trends appear nearly flat or only gradually declining, when they are actually decreasing substantially, especially since 2006 or 2007. The seasonal nature of ambient ethene concentrations is clearly visible in the cyclical rise and fall of these quarterly means. It is interesting, and perhaps worth investigating, why the expected seasonal peaking pattern is missing at all monitors in 2008.

Propene exhibits trends similar to ethene. Figure D-43: *Quarterly Geometric Mean Propene at CATMN Monitors* shows trends in propene at all regional CATMN monitors since 1999. Note that 2009 includes measurements through the second quarter only. Propene shows the same seasonal pattern and the missing 2008 peaking pattern. In general, propene concentrations at all monitors appears to be declining since 1999.

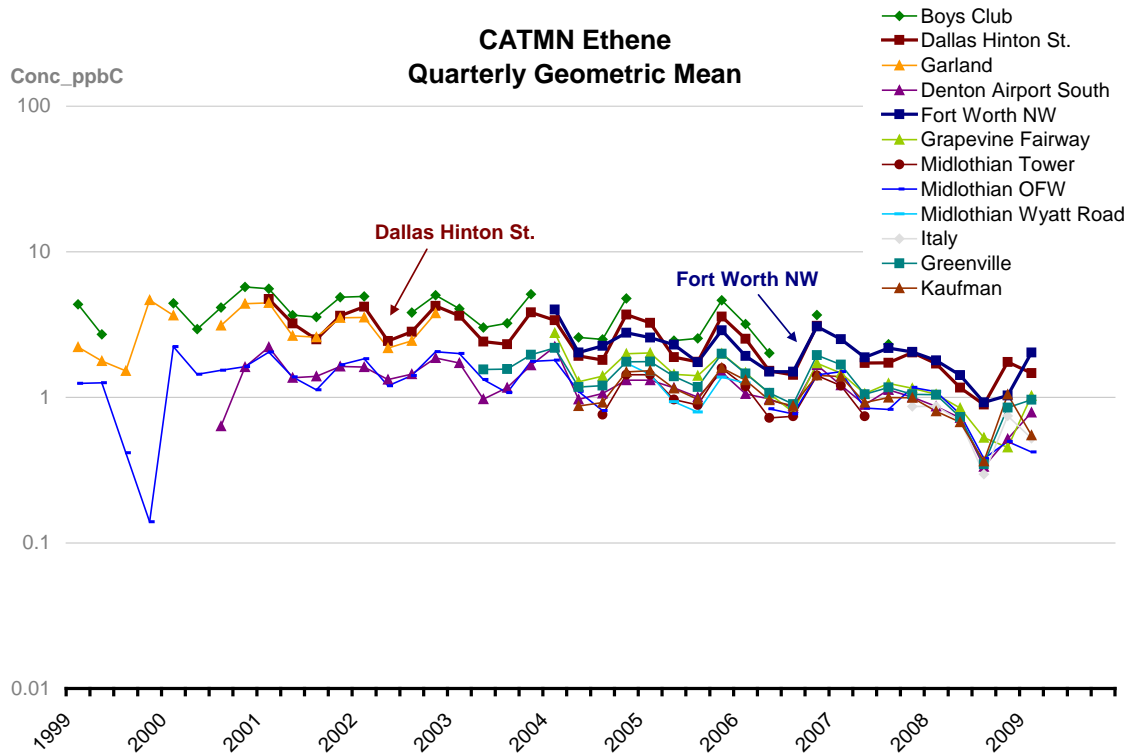


Figure D-19: Quarterly Geometric Mean Ethene at CATMN Monitors

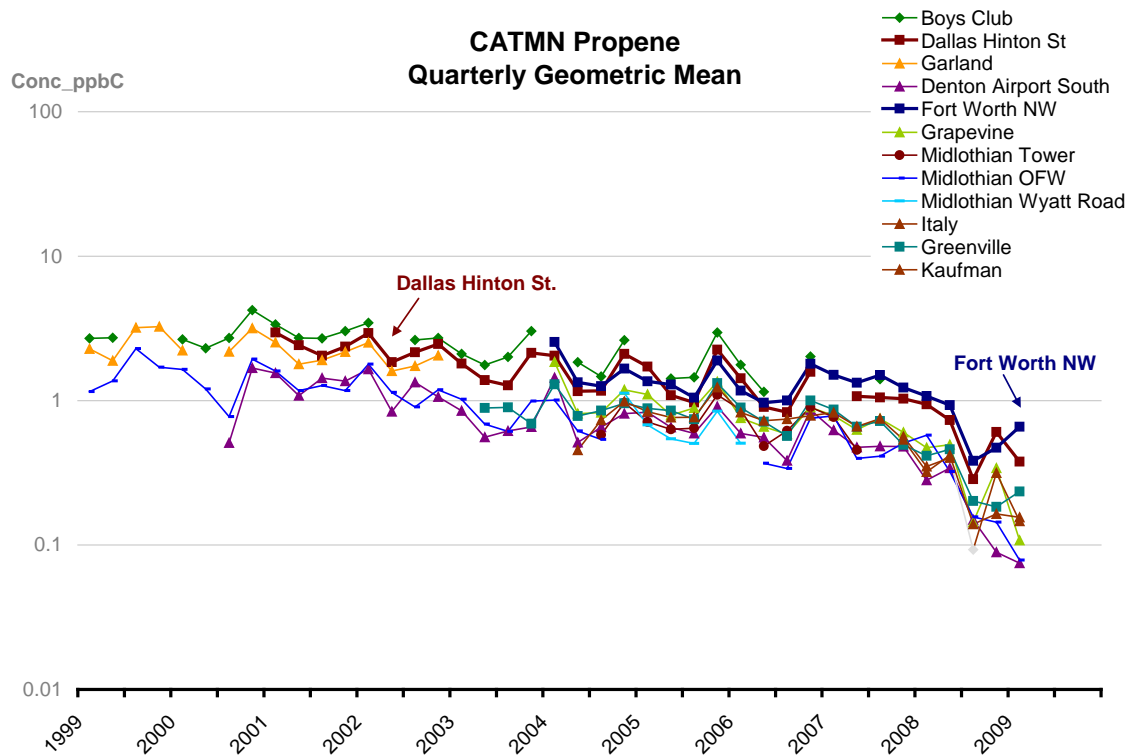


Figure D-20: Quarterly Geometric Mean Propene at CATMN Monitors

Ordinary least squares linear regressions were computed to test these observed trends. The cyclical pattern in the data must be removed before estimation, or the pattern will be replicated in the residual, violating the ordinary least squares requirement for randomly distributed residuals. Because of the cyclical nature of the quarterly means, annual geometric means, which remove the cyclical pattern, were computed for each compound at two sites, and fit to an index of year. Dallas Hinton St. (C401/C60/AH161) and Ft. Worth Northwest (C13/AH32) were chosen as the two monitors in order to compare the results using canister data to the results using auto-GC data. Annual geometric mean ethene and propene at Dallas Hinton St. (C401/C60/AH161) and Ft. Worth Northwest (C13/AH32), along with fitted regression trends, are displayed in Figure D-44: *Annual Geometric Mean Ethene at Two CATMN Monitors* and Figure D-45: *Annual Geometric Mean Propene at Two CATMN Monitors*.

Results of linear regressions for propene and ethene are displayed in Table D-16: *Regression Results for Annual Geometric Mean Ethene and Propene at Two CATMN Monitors*. The annual geometric mean for both compounds at both locations exhibits a negative estimated slope; in fact, ethene has the same slope at both locations so only one fitted line is plotted. These results support the conclusion from the auto-GC measurements that both ethene and propene are exhibiting statistically significant decreases at both locations since 1999. The R^2 statistics for the Dallas Hinton St. (C401/C60/AH161) models are high, over 0.9 in both cases, indicating there is very little variation over time that is not accounted for in these models. While the R^2 statistics for the Ft. Worth Northwest (C13/AH32) models are not as high, they are still very good and are supported by the estimated F statistics and significances of the estimated slope parameters. Propene at Ft. Worth Northwest (C13/AH302) is not a good fit; however, from looking at Figure D-45: *Annual Geometric Mean Propene at Two CATMN Monitors* it can be inferred this is due to the reading in 2007, because excepting that year, propene behaves similarly at both locations.

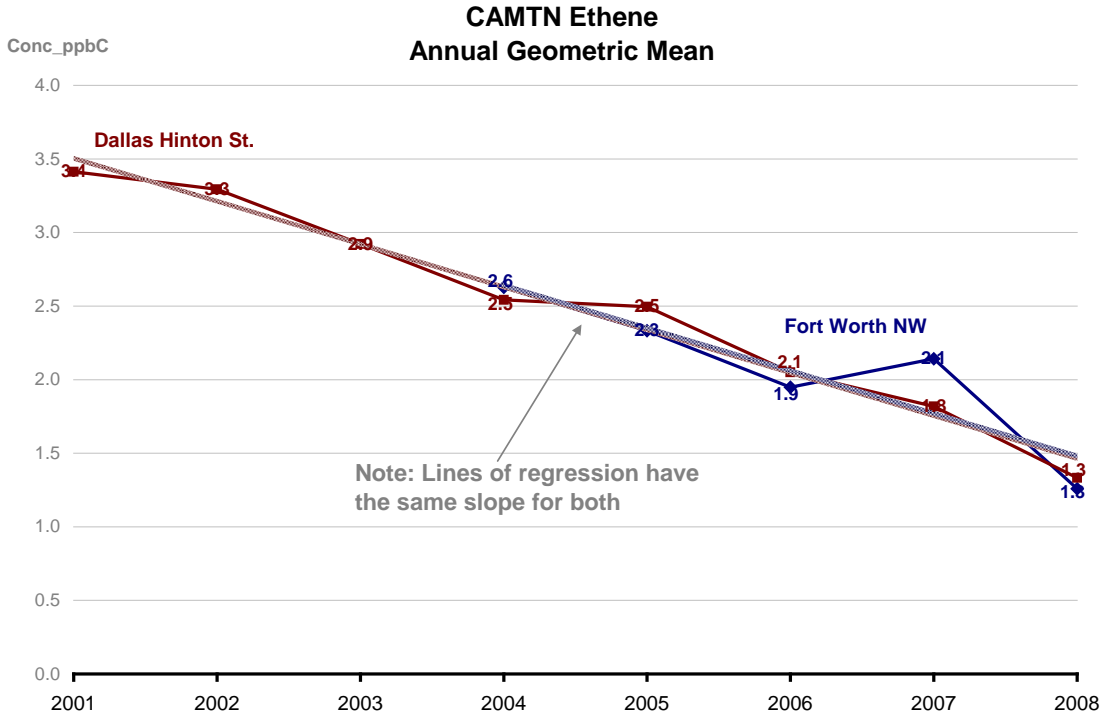


Figure D-21: Annual Geometric Mean Ethene at Two CATMN Monitors

Note: the figure is using a linear scale

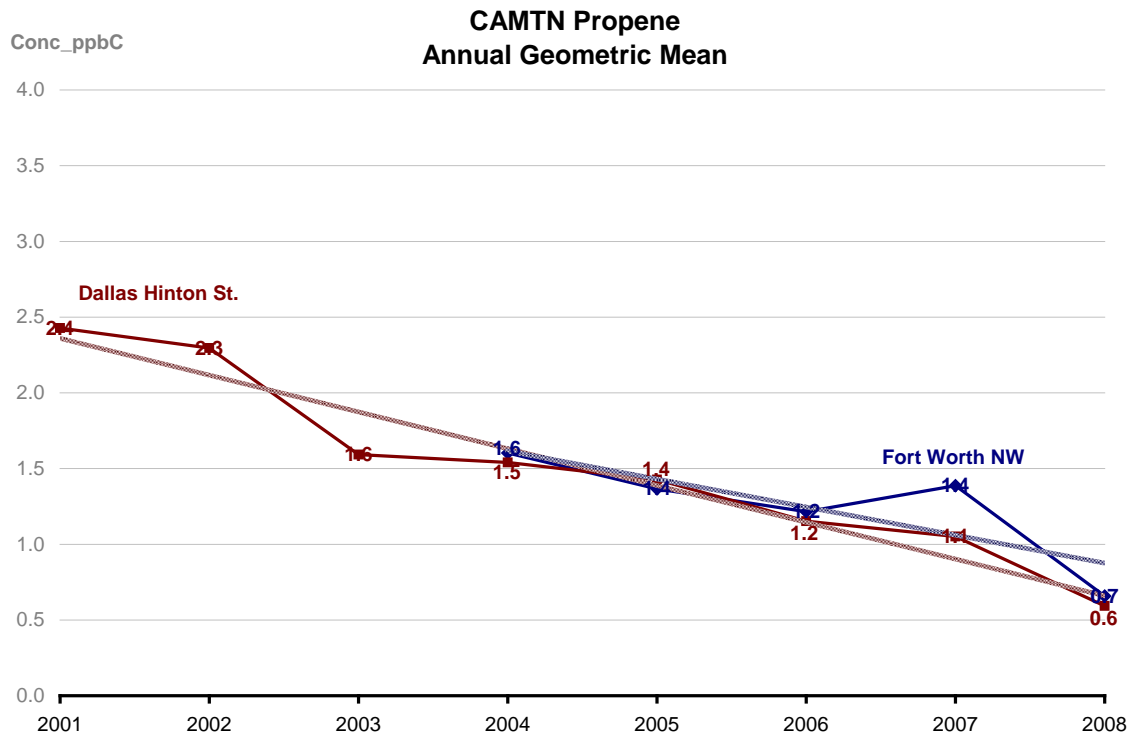


Figure D-22: Annual Geometric Mean Propene at Two CATMN Monitors

Note: the figure is using a linear scale

Table D-7: Regression Results for Annual Geometric Mean Ethene and Propene at Two CATMN Monitors

HRVOC	Statistic	Dallas Hinton St. (C401/C60/AH161)	Ft. Worth Northwest (C13/AH302)
Ethene	Adjusted R ²	0.978	0.748
	F	316.426*	12.847*
	Significance F	0.000	0.037
	Slope	-0.293*	-0.293*
	t-stat	-17.784	-3.584
	p-value	0.000	0.037
Propene	Adjusted R ²	0.933	0.582
	F	98.142*	6.576**
	Significance F	0.000	0.083
	Slope	-0.244*	-0.187**
	t-stat	-9.907	-2.564
	p-value	0.000	0.083

*Significant at the $\alpha=0.05$ level.

**Significant at the $\alpha=0.10$ level.

Quarterly geometric means for 1,3-butadiene, presented in Figure D-46: *Quarterly Geometric Mean 1,3-Butadiene at CATMN Monitors* display the seasonal cycle seen earlier, but appear to lack a trend over time. Two other HRVOC compounds, trans-2-butene and cis-2-butene, exhibit similar patterns and are, therefore, not displayed. The poor significance of the estimated slope parameters from linear regressions of annual geometric means of these compounds on an index

of year, presented in Table D-17: *Regression Results for Annual Geometric Mean 1,3-Butadiene, Trans-2-Butene, and Cis-2-Butene*, statistically confirm the lack of trend. While the estimated slope for 1,3-butadiene at Dallas Hinton St. (C401/C60/AH161) is statistically significant at the 5 percent level ($\alpha=0.05$), the slope parameter itself is so small ($\beta=0.003$) that it can scarcely be considered a trend. The same is true for cis-2-butene at Dallas Hinton St. (C401/C60/AH161), which is only significant at the 10 percent level ($\alpha=0.10$), and has a slope parameter one-third that of 1,3-butadiene ($\beta=0.001$).

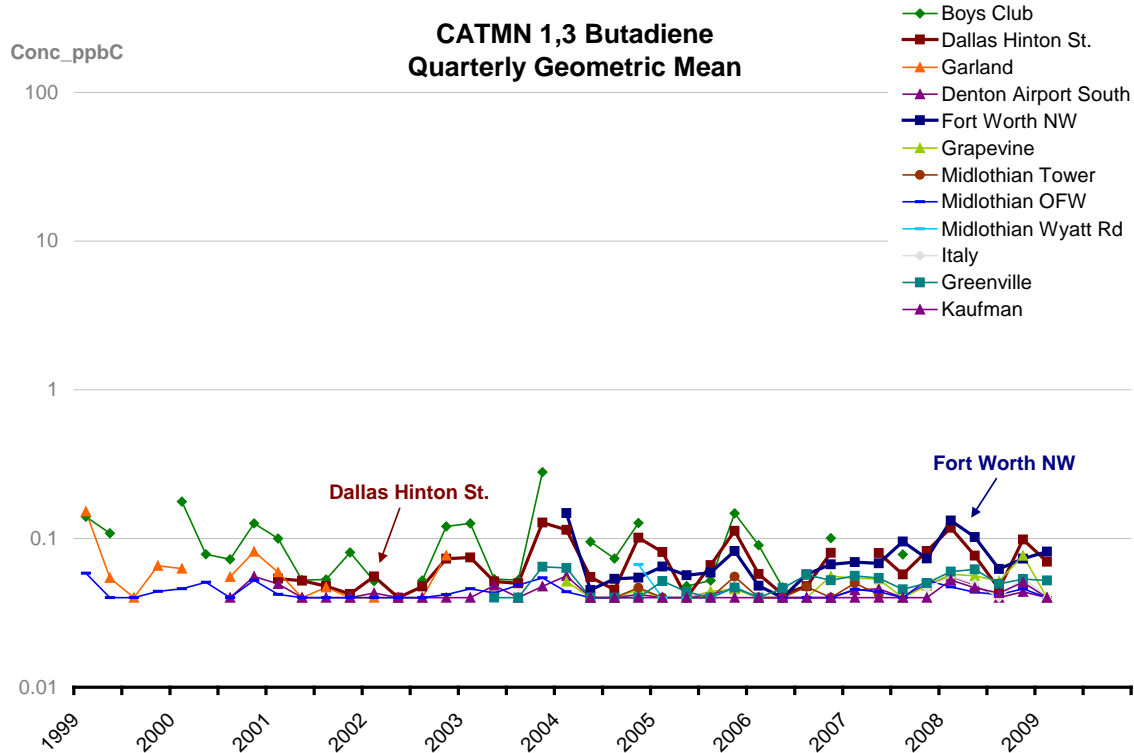


Figure D-23: Quarterly Geometric Mean 1,3-Butadiene at CATMN Monitors

Table D-8: Regression Results for Annual Geometric Mean 1,3-Butadiene, Trans-2-Butene, and Cis-2-Butene

HRVOC	Statistic	Dallas Hinton St. (C401/C60/AH161)	Ft. Worth Northwest (C13/AH302)
1,3-Butadiene	Adjusted R ²	0.443	0.305
	F	6.569*	2.757
	p-value	0.043	0.195
	Slope	0.003*	0.006
	t-stat	2.563	1.660
	p-value	0.043	0.196
Trans-2-Butene	Adjusted R ²	-0.148	-0.042
	F	0.099	0.840
	p-value	0.764	0.427
	Slope	0.000	0.002
	t-stat	0.314	0.917
	p-value	0.764	0.427

HRVOC	Statistic	Dallas Hinton St. (C401/C60/AH161)	Ft. Worth Northwest (C13/AH302)
Cis-2-Butene	Adjusted R ²	0.320	0.383
	F	4.294**	3.483
	p-value	0.084	0.159
	Slope	0.001**	0.003
	t-stat	2.072	1.866
	p-value	0.084	0.159

*Significant at the $\alpha=0.05$ level.

**Significant at the $\alpha=0.10$ level.

The HRVOC compound, 1-butene, exhibits a trend dissimilar to the other HRVOC compounds, which is displayed in Figure D-47: *Quarterly Geometric Mean 1-Butene at CATMN Monitors*. Although seasonal variation is still evident, these monitors appear to measure a wider range of concentrations. A peculiar dip at the end of 2007 is replicated at all monitors. While visual inspection suggests possible downward trends at several of the monitors, statistical results using the annual geometric means are reported in Table D-18: *Regression Results for Annual Geometric Mean 1-Butene at CATMN Monitors* and shown in Figure D-48: *Annual Geometric Mean 1-Butene at CATMN Monitors*.

The linear regression only gives a good fit for the Dallas Hinton St. (C401/C60/AH161) monitor, with a slope of -0.146, significant at the 5 percent level ($\alpha=0.05$). Results for the Ft. Worth Northwest (C13/AH32) monitor, however, are unsatisfactory, and likely due to the large increase that occurred in 2007. All of these regression results should be interpreted with caution, due to the small number of observations available.

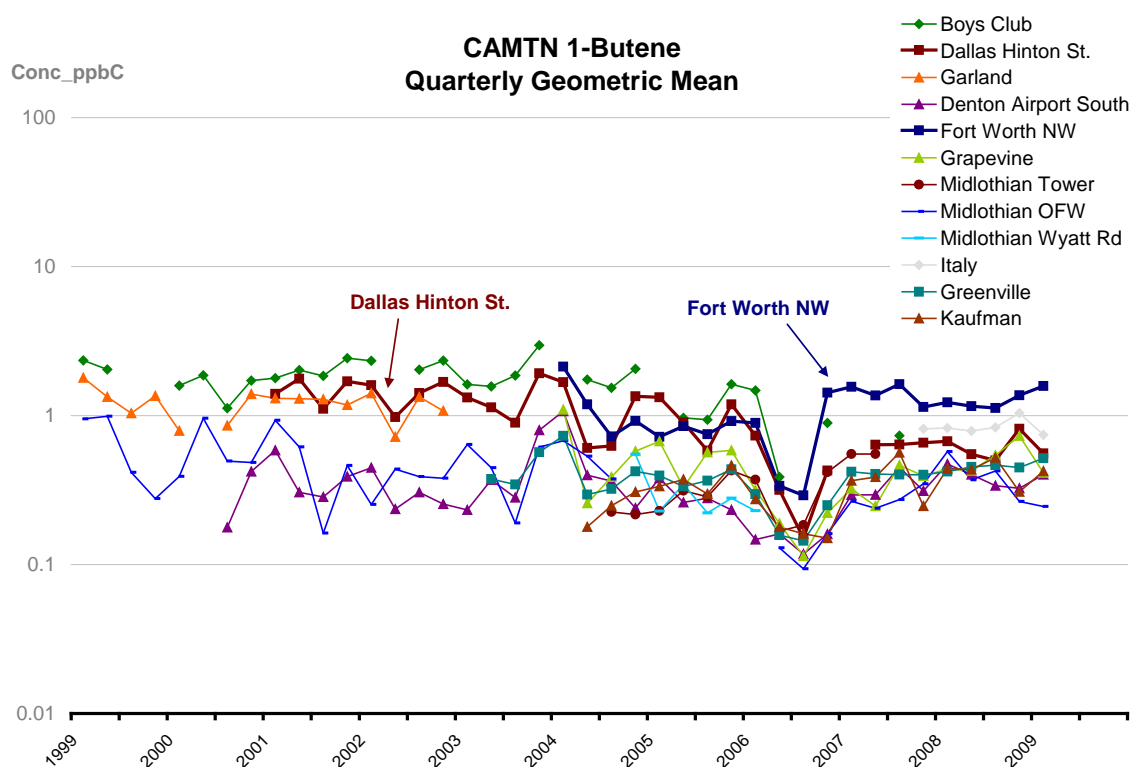


Figure D-24: Quarterly Geometric Mean 1-Butene at CATMN Monitors

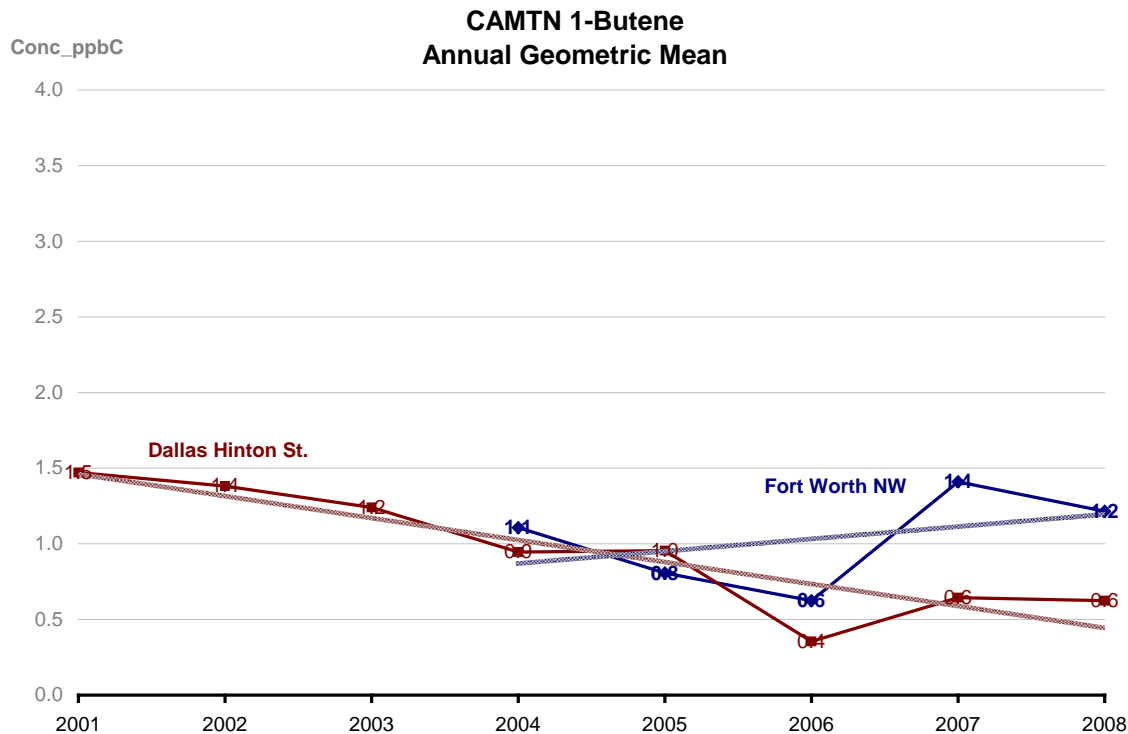


Figure D-25: Annual Geometric Mean 1-Butene at CATMN Monitors

Note: the figure is using a linear scale

Table D-9: Regression Results for Annual Geometric Mean 1-Butene at CATMN Monitors

HRVOC	Statistic	Dallas Hinton St.	Ft. Worth Northwest
1-Butene	Adjusted R ²	0.786	-0.109
	F	26.773*	0.606
	p-value	0.002	0.493
	Slope	-0.146*	0.082
	t-stat	-5.174	0.778
	p-value	0.002	0.493

*Significant at the $\alpha=0.05$ level.
 **Significant at the $\alpha=0.10$ level.

Analysis of HRVOC data collected with auto-GCs and canisters revealed statistically significant decreases in the majority of HRVOC concentrations at Dallas Hinton St. (C401/C60/AH161). Although many HRVOC trends appeared to decrease at Ft. Worth Northwest (C13/AH32), no trends at that location were found to be statistically significant. More analysis must be completed to determine the role that HRVOC play in ozone production in the DFW area; however, it is encouraging that trends in HRVOC are decreasing. The next section will investigate the weekend effect in the DFW area, which can be used as another tool in determining the VOC or NO_x limitations of an air mass.

3.4.2 Comparison of Exceedances on Weekdays and Weekends

Studies (Croes et al., 2003; Fujita et al., 2003a; Fujita et al., 2003b; Heuss et al., 2003) have shown that ozone concentrations can exhibit not only annual and diurnal, but weekly patterns of variation. These studies have found that some cities exhibit substantially greater ozone concentrations on weekends, while others do not. Identification of a weekend effect can be valuable for guiding ozone photochemical modeling and control strategy development. Because a weekend effect is hypothesized to result from emissions from specific types of emitters, that is, mobile rather than point sources, its presence, if confirmed, could be used to tailor policies to target specific sources. Even more importantly, a weekend effect can provide inferences as to whether an area is VOC-limited or NO_x-limited, hence providing clues to the efficacy of various candidate control strategies. A decrease in monitored ozone on weekends (compared to weekday levels) indicates NO_x-limitation, since weekend NO_x concentrations are generally lower compared to their weekday counterparts. Conversely, a weekend increase in ozone concentrations can indicate VOC-limitation. Finally, a weekend effect provides a natural laboratory for evaluating photochemical model response. If the model can reproduce observed weekend effects, then we will have greater confidence in its ability to correctly predict the effects of future emission changes.

Causes of weekly patterns in ozone concentrations have generally been related to changes in emissions during weekends compared to weekdays, and the sensitivity of ozone formation to those changes. Several hypotheses have been proposed to explain increased ozone concentrations on weekends (Croes *et al.*, 2003; Lawson, 2003; Heuss *et al.*, 2003). Generally, these tend to focus on variation in motor vehicle driving patterns and use of recreational and lawn and garden equipment: lower mobile source NO_x emissions are hypothesized to result in less ozone titration by NO, or fewer radical termination reactions, resulting in an increase in radical concentrations; weekend postponement of mobile source NO_x emissions until later in the day enhances ozone formation in aged, NO_x-depleted air; and increased weekend emissions from recreational and lawn and garden equipment enhance weekend ozone formation.

Following extensive investigation by the California Air Resources Board (CARB) and a host of researchers, several of the above hypotheses were discarded (Croes *et al.*, 2003; Fujita *et al.*, 2003a, 2003b; Blanchard *et al.* 2008, Blanchard and Tanenbaum, 2005; Heuss *et al.*, 2003; Pun *et al.*, 2003; Yarwood *et al.*, 2003). Instead, the most likely explanations were attributed to lower mobile source NO_x emissions on weekends. Specifically, studies suggest the primary cause of increased ozone on weekends is a decrease in NO + O₃ titration reactions occurring on weekends due to lower NO_x emissions from heavy duty diesel vehicles. Furthermore, there is some indication that areas that see a pronounced weekend effect, with increasing ozone and decreasing NO_x, exhibit ozone formation in a VOC-limited regime. Areas for which a decrease in NO_x results in a decrease in ozone, however, are more likely to have NO_x-limited ozone formation (Murphy *et al.*, 2007; Gao *et al.*, 2005; Marr and Harley, 2002; Fujita *et al.*, 2003b; Yarwood *et al.*, 2003; Yarwood *et al.*, 2008).

VOC and NO_x limitations in the DFW area may impact temporal and spatial patterns of the frequency of ozone exceedance days. A recent study found that the average ozone concentration significantly increased on weekends compared to weekdays in the DFW area (Blanchard and Tanenbaum, 2005). This increase is likely due to the VOC:NO_x ratios found in the DFW area. To determine the effects these limitations might have on the frequency of ozone events in the area, we investigated eight-hour ozone exceedance day counts and the VOC:NO_x ratio for each day of the week from 1999 to 2009. Spatial patterns of the ozone exceedance day counts on the weekdays and weekends from 2005 to 2009 were also examined.

The number of eight-hour ozone exceedance days (days with peak eight-hour ozone > 85 ppb) were found for each day of the week at all available monitoring sites in the DFW area from 1999 to 2009. If there were two monitors in exceedance on the same day, the day was recorded as one exceedance. Figure D-49: *Frequency of Eight-Hour Exceedances by Day of Week (1999-2009)* shows the total number of eight-hour ozone exceedances for each day of the week from 1999-2009. The eight-hour exceedance count on Saturdays (46) is only three fewer than on Fridays (49), suggesting at most a weak weekday/weekend pattern. While there are fewer exceedances on Sundays, the number is still relatively large at 31 exceedances in the past 11 years.

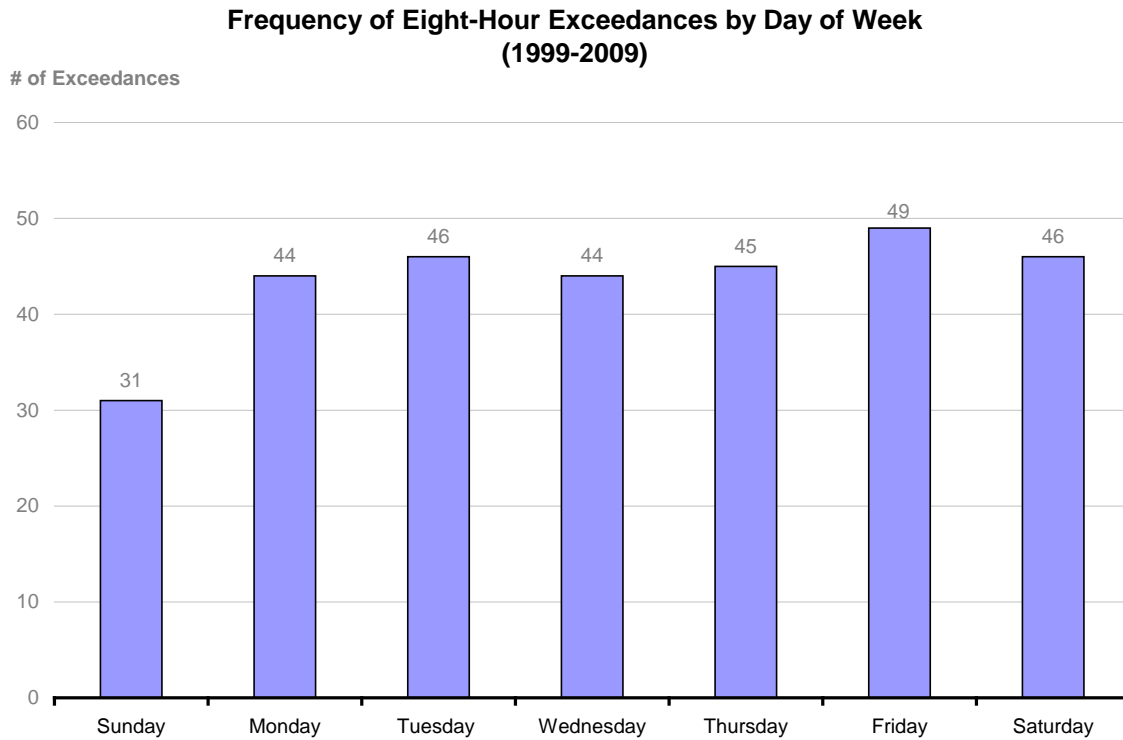


Figure D-26: Frequency of Eight-Hour Exceedances by Day of Week (1999-2009)

Over the past 11 years, as the ozone design value has continued to decline, the number of exceedance days has as well. Figure D-50: *Frequency of Eight-Hour Ozone Exceedance Days by Year and Day of Week* shows the number of exceedance days by year and day of week since 1999. In 1999, ozone exceedances occurred every day of the week. Starting in about 2004, exceedances appear to fall less frequently on Sundays. By 2009, the frequency of exceedances had dropped substantially for all days, disappearing altogether on Sundays and Mondays.

Day	1999	2000	2001	2002	2003	2004	2005	2006	2007	2008	2009
Sunday	5	4	5	5	6	2	1	2	1		
Monday	5	7	5	4	5	4	7	3	2	2	
Tuesday	4	5	7	6	2	4	7	5	2	2	2

Day	1999	2000	2001	2002	2003	2004	2005	2006	2007	2008	2009
Wednesday	5	5	5	4	5	4	7	4	1	2	2
Thursday	5	4	2	7	5	5	6	5	2	1	3
Friday	7	7	2	6	3	3	9	7	1	2	2
Saturday	7	4	4	5	5	3	7	5		3	3

Figure D-27: Frequency of Eight-Hour Ozone Exceedance Days by Year and Day of Week

In the absence of a day-of-week or weekend effect, each day would be expected to have an equal likelihood of observing an ozone exceedance. To isolate a possible day of week effect, the more recent period, 2005-2009, was selected to minimize effects of a possible change in exceedance day patterns over the entire decade. Over the five year period, of 1,516 ozone season days with valid data, there were 96 ozone exceedance days observed, for a frequency of about six percent. Thus, there is about a six percent chance that any particular day will observe an ozone exceedance over the period. However, as shown in Table D-19: *Ozone Exceedance Days by Day of Week, 2005-2009*, Sundays observed exceedance days at much less than half the expected rate. Fridays, on the other hand, observed exceedance days 38 percent more frequently than expected.

A chi-squared goodness of fit test was performed to test whether exceedance days were independent of day of the week. The test compares the observed distribution to a hypothetical pattern of equal likelihood of exceedance on any particular day. The test does not determine whether a particular group, in this case a particular day, is out of the ordinary, but it assesses whether the overall distribution is what would be expected based on random assignment of observations to days (groups). Despite the observed disparity between the probabilities for individual days, the chi-square test ($X^2 = 10.0934$, p-value = 0.1208) determined that the observed distribution was not statistically different from what would be expected if ozone exceedance days were observed randomly, suggesting there is no day of week effect. The contribution to the total chi square value of exceedance on each day is also presented in the table. Although the chi-square value for Sunday exceedance days was much larger than any of the other days, the confidence intervals on the means were too large to differentiate among the means with statistical confidence. Note that chi-square values for non-exceedance days are not presented.

Table D-10: Ozone Exceedance Days by Day of Week, 2005-2009

	Sun day	Mon day	Tues day	Wednes day	Thurs day	Friday	Satur day	All Days
Non-Exceedance Days	227	216	214	216	216	211	216	1,516
Exceedance Days	4	14	16	14	14	19	15	96
Percent (%)	1.73	6.09	6.96	6.09	6.09	8.26	6.49	5.96
Exceedance Day X^2	6.92	0.01	0.39	0.01	0.01	2.05	0.11	

Figure D-51: *Frequency of Eight-Hour Ozone Exceedance Days on Weekdays (2005-2009)* shows a contour plot of the frequency of eight-hour ozone exceedance days on weekdays in the DFW area. The plot shows that on weekdays, eight-hour exceedances occur more frequently outside of the urban core. The maximum percentage on weekdays occurred at Keller (C17), followed by Denton Airport South (C56/A163/X157) at 13.4 percent and 12.1 percent, respectively.

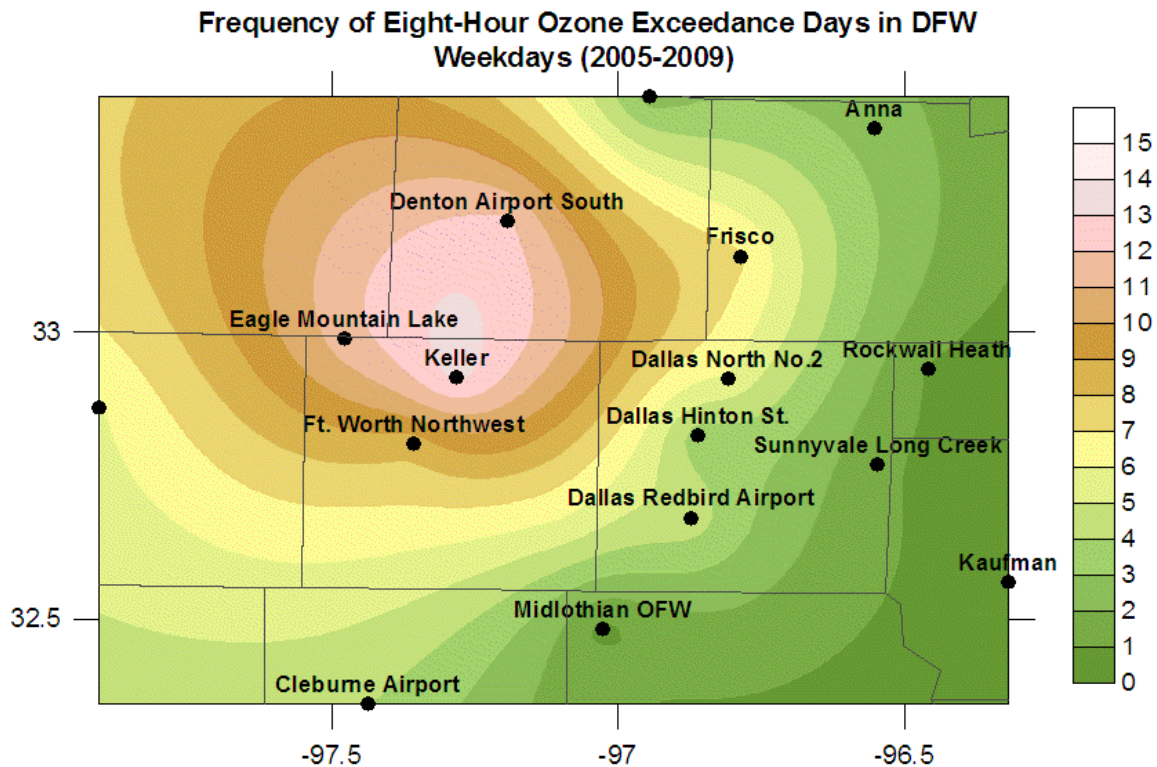


Figure D-28: Frequency of Eight-Hour Ozone Exceedance Days on Weekdays (2005-2009)

On weekends, similar to weekdays, the highest frequency of eight-hour ozone exceedances occurs at Keller (C17) and Denton Airport South (C56/A163/X157); however, the frequencies closer to the urban core are higher. The maximum percent of eight-hour ozone exceedance days is the same at Keller (C17) and Denton Airport South (C56/A163/X157) with 12.8 percent followed by Frisco (C31/C680), Dallas North No. 2 (C63/C679), and Ft. Worth Northwest (C13/AH302) at 10.6 percent. Figure D-52: *Frequency of Eight-Hour Ozone Exceedance Days on Weekends (2005-2009)* shows the frequency of eight-hour ozone exceedance days in DFW on weekends. The map clearly shows that there is a broader area producing exceedance days on weekends, compared to weekdays.

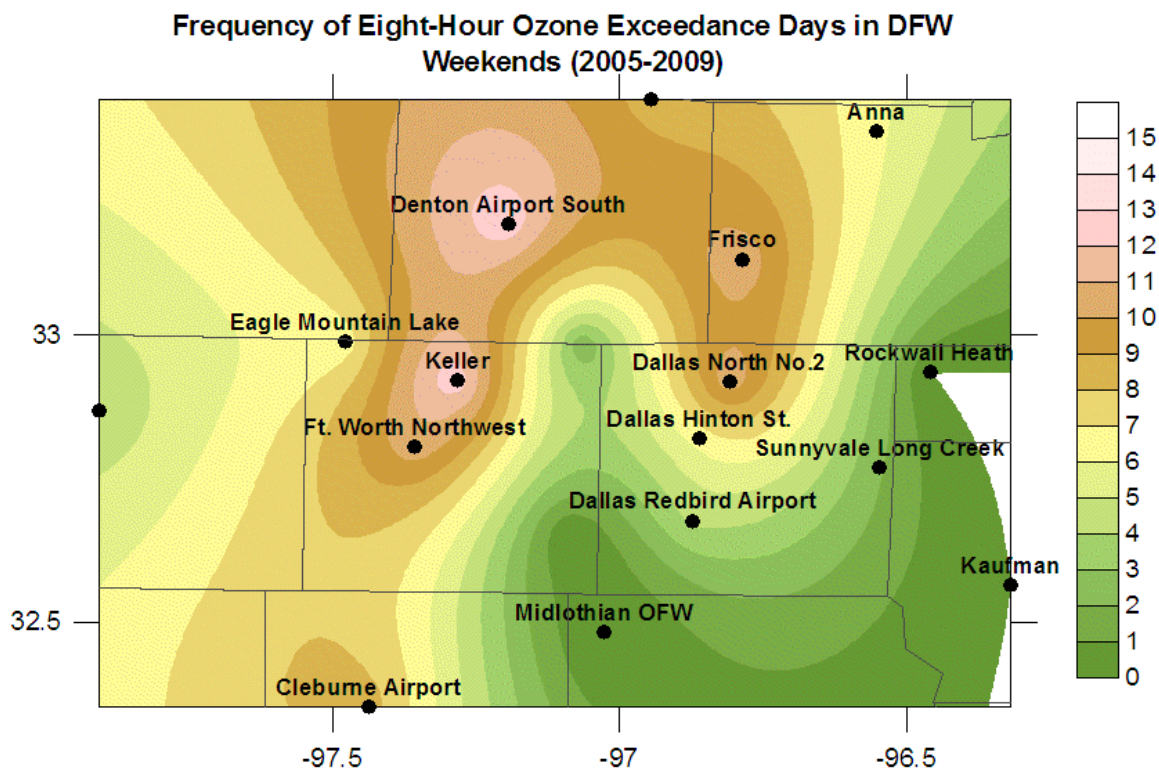


Figure D-29: Frequency of Eight-Hour Ozone Exceedance Days on Weekends (2005-2009)

Auto-GC data from Dallas Hinton St (C401/C60/AH161) and Ft. Worth Northwest (C13/AH302) were then used to find the average VOC:NO_x ratio for each day of the week for each year from 1999 to 2009. Figure D-53: *VOC:NO_x Ratio Annual Geometric Mean (5:00-10:00 LST) Dallas Hinton St. (C401/C60/AH161)* shows the yearly geometric mean VOC:NO_x ratio for Wednesday, Saturday and Sunday for each year from 1999 to 2009 at the Dallas Hinton St. (C401/C60/AH161) monitor. In this study the ratio on Wednesday is assumed to represent the weekday ratio because it is furthest from a weekend day and is thus the day least likely to capture any “long weekend” effects. The figure shows that the VOC:NO_x ratio at Dallas Hinton St. (C401/C60/AH161), which is located in the urban core of DFW, is higher on weekends than on weekdays. The VOC:NO_x ratio is in the VOC limited regime for every day of the week except Sundays, in recent years. During the week, people are commuting to and from work, and in Dallas vehicle emissions are responsible for 86 percent of NO_x emissions (Qin, *et al.*, 2007). More drivers on the road during the week suggests a lower ratio, and, therefore, abundant NO_x.

Ft. Worth Northwest (C13/AH302), shows similar trends when compared to that for Dallas Hinton St. (C401/C60/AH161); however, the Ft. Worth Northwest (C13/AH302) graph shows that the area is more transitional. This trend is shown in Figure D-54: *Annual Geometric Mean VOC:NO_x Ratio at Ft. Worth Northwest (C13/AH302)*. The VOC:NO_x ratio at Ft. Worth Northwest (C13/AH302) is highest on Sundays followed by Saturdays, and is lowest on Wednesdays. Again, Wednesday is assumed to represent non-weekend behavior, and the lower VOC:NO_x ratio is due to more commuters on the road.

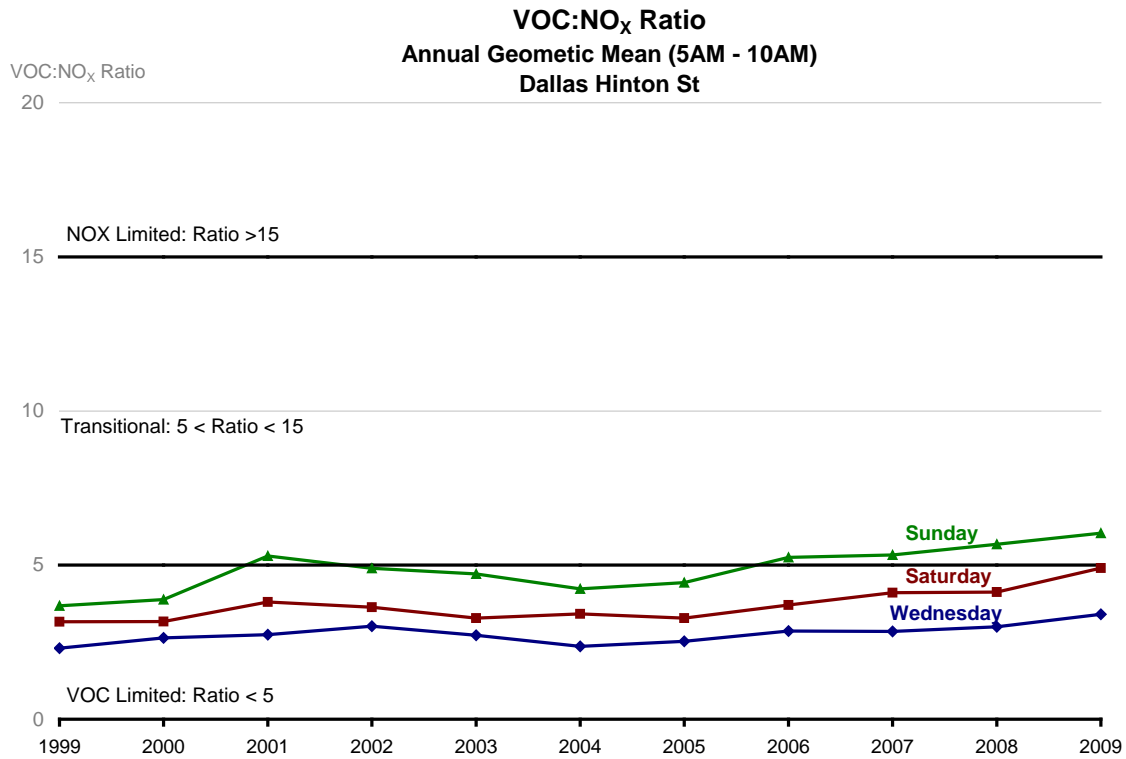


Figure D-30: VOC:NO_x Ratio Annual Geometric Mean (5:00-10:00 LST) Dallas Hinton St. (C401/C60/AH161)

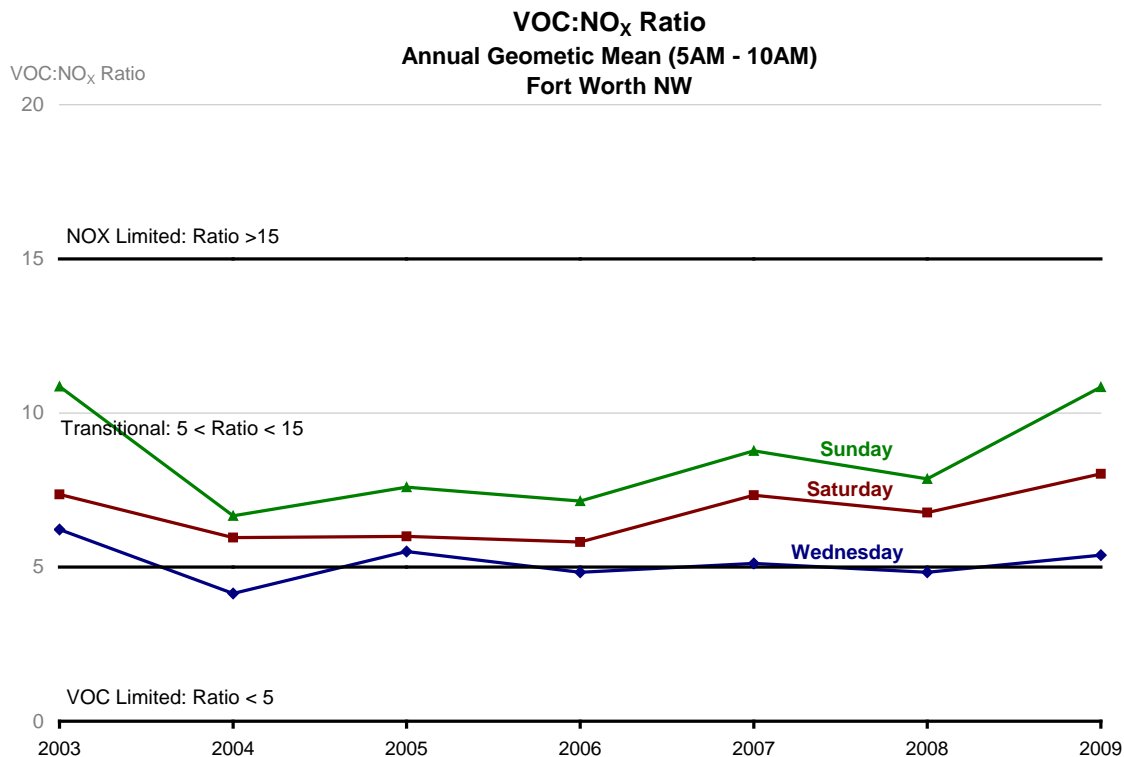


Figure D-31: Annual Geometric Mean VOC:NO_x Ratio at Ft. Worth Northwest (C13/AH302)

The weekday/weekend analysis showed that the number of eight-hour ozone exceedances did not show any significant changes from weekdays to weekends. Spatial analysis showed that weekday exceedances occur most frequently to the northwest outside the urban core of the DFW area. On weekends, however, exceedances occur more frequently within the urban core, in addition to the northwest. These weekday and weekend trends are most likely explained by the VOC and NO_x limitations in the DFW area. On weekdays, the urban core of DFW, represented by the Dallas Hinton St. (C401/C60/AH161) monitor, is VOC limited. The low VOC:NO_x ratio means there is likely a large amount of NO_x in the urban core. Excess NO_x scavenges ozone, making ozone exceedances less frequent. On Saturdays, the urban core is still VOC limited, but on Sundays in recent years it is moving into the transitional regime. The outer periphery of the DFW area, represented by the Ft. Worth Northwest monitor (C13/AH302), shows that on weekdays the area is VOC limited to transitional and on Saturdays and Sundays the area is more transitional to NO_x limited.

The weekend effect helps to demonstrate the relationship between ozone and its precursors; however, all of these precursors can vary depending on meteorological conditions. Evaluating meteorological parameters which are correlated with ozone distinguishes trends resulting from a change in emissions from trends resulting from favorable meteorological conditions.

3.5 Relationship of Barnett Shale to Ozone in the DFW Area

Barnett Shale is a geological formation of sedimentary rock in north-central Texas that contains oil and gas. In the past several years, the quantity of gas produced from wells operating in the play has grown from 79 billion cubic feet (bcf) in 2000 to 1,764 bcf in 2009 (Railroad Commission of Texas, 2010). The geological area containing oil and gas is estimated to extend

from the city of Dallas in the east, west to Shackelford County, south to Coryell County, and north to the Red River, encompassing roughly 5,000 square miles and 18 counties in Texas.

Because of the proximity of the Barnett Shale formation to the DFW area, it has been hypothesized that emissions from oil and gas drilling, extraction, and transport activity in this region could be influencing air quality in the DFW area. The following sections explore this concept and discuss what is currently known about types of emissions from the region, their magnitudes and patterns across time and space, and meteorological factors in the region.

3.5.1 Factor Analysis of Ambient Volatile Organic Compounds in the Fort Worth Area

The species, proportions and magnitudes of volatile organic compounds (VOC) in air parcels can be used to detect their likely sources. Automated gas chromatograph (autoGC) instruments enable speciation of ambient measurements of VOC and, because they operate continuously, provide a detailed picture of temporal patterns in VOC. When combined with meteorological information, such as wind speeds and directions, which indicate likely routes of travel, this data become a valuable source attribution tool.

An autoGC instrument began operation in the town of Dish in 2010, but this type of analysis requires more data than is currently available. However, the data should become available shortly. Instead, 2007 to 2009 data from the autoGC instrument closest to the Barnett Shale region, located at the Ft. Worth Northwest (C13/AH302) monitor, has been examined. While this CAMS station is literally next to the runway at Fort Worth Meacham International Airport, there are only a small number of flights, so aircraft emissions are deemed not to be a significant interference. A similar autoGC located at Dallas Hinton St. (C401/C60/AH151) is excluded from analysis because, currently, it is too far away to be affected by Barnett Shale emissions. However, as future drilling activity in the Barnett Shale formation moves eastward toward Dallas, it may provide valuable insight.

Most VOC sources emit a mixture of VOC species that is characteristic of the source type. For example, natural gas emissions contain a simple mixture of ethane, propane, butane and other light hydrocarbon species. On the other hand, gasoline is a complex mixture containing heavier hydrocarbons such as pentane, hexane, heptane, octane, and many others. Simultaneous measurement of many VOC species permits identification of source types, particularly if this method is used with corroborating information such as wind direction, known source locations, and diurnal patterns. However, the method does not indicate the frequency or severity of impact on a particular area of interest. In some cases, prevailing winds may transport emissions away from the area of interest, so they have very little or no impact. In other cases, emitted species may have low reactivity, and thus little impact on ozone formation. At the other extreme, modest emissions nearby may have a significant effect.

AutoGC data is difficult to analyze, so many methods have been developed. One of the simplest is to examine multiple scatter plots. In this case, we have selected 14 species, to that would be 196 plots, such as the one shown in Figure D-55: *Scatter Chart of Benzene Concentration as a Function of Ethane Concentration*. This plot shows benzene as a function of ethane. Since benzene is a component of natural gas, and ethane is an indicator of natural gas, we expect a simple linear relationship. While there is some indication of this relationship, it is almost lost in the extreme scatter. Subsequent analysis shows that benzene is indeed a component of natural gas related emissions, but it also shows the extreme scatter is the result of a second benzene source.

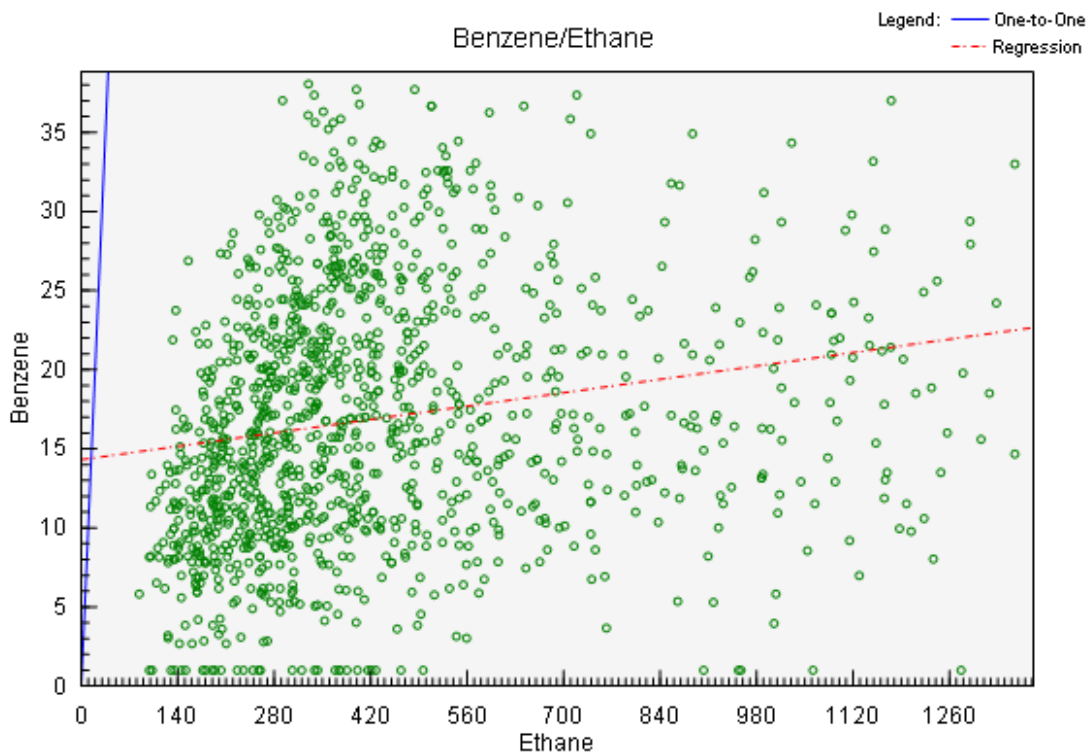


Figure D-32: Scatter Chart of Benzene Concentration as a Function of Ethane Concentration

While several methods are available for identifying groups of species that always occur together, the most useful is Positive Matrix Factorization (PMF), a member of the family of factor analysis techniques. The greatest strength of this method is it does not require prior knowledge of an unknown source or its speciation profile. Observed profiles are first determined by PMF, then compared to reference profiles of known emission sources, candidate source types identified, and finally verified by comparison with wind and temporal data.

Because this method works best with moderate winds, speeds of 2 meters per second (m/s) to 10 m/s (4 mph – 22 mph) were used throughout this analysis. Since increasing wind speed dilutes emissions, observed concentrations were normalized by wind speed, so light wind and heavy wind observations are treated equally.

Closely related VOC species (e.g., n-butane and isobutane) were grouped to simplify both analysis and comparison to reference speciation profiles. Simple descriptive statistical analysis was used to assure the quality of the data, and to identify the most useful VOC species groups. In addition, some species groups were selected primarily because they are indicators of a particular source type, such as acetylene, ethylene, and propylene for engines. Outliers greater than one standard deviation (roughly 68 percent) were removed because they allow nearby sources to unduly influence the results.

Following isolation of the various source types using PMF, observed speciation profiles were plotted and compared with reported speciation profiles of various known sources. A factor rose was plotted over a map of known sources to show the source distribution by wind direction. Finally, factor contributions were plotted by hour of the day to show the diurnal distribution. Table D-20: *Candidate PMF Analysis Scenarios* presents the many scenarios considered for analysis. To obtain accurate results, observations from every possible wind direction are

necessary. Since the wind is predominately from the southeast, many observations are required to obtain an adequate wind direction sample, so scenarios with only a few observations were ruled out.

Table D-11: Candidate PMF Analysis Scenarios

Days	Hours	Daily Maximum Ozone	Typical # Observations
<u>Scenarios selected for analysis</u>			
All year	All Hours	All	3202
All year	Before Dawn	All	661
Ozone Season	All Hours	All	1388
High Ozone	All Hours	1 Hr Pk > 65 ppb	241
Exceedance Day	All Hours	8 Hr Pk > 65 ppb	77
<u>Scenarios considered, but not selected</u>			
Ozone Season	Before Dawn	All	261
High Ozone	Before Dawn	1 Hr Pk > 65 ppb	14
Exceedance Day	Before Dawn	8 Hr Pk > 65 ppb	4

Data collected before dawn provided the most accurate emission profiles, because few VOC species react in the dark. Reaction of VOC during daylight hours substantially complicates identification of source profiles by PMF because many emitted VOC compounds are continually converted to other compounds between the emission source and the receptor monitor in the presence of sun light. However, use of all hourly data provides the best directional and temporal profiles, so both the predawn scenario, and the all data scenario were used. In addition, classification of observations by ozone season, high ozone day, and exceedance day is used to demonstrate that selected days are similar to annual profiles.

Because the PMF method analyzes variation across observations, species that never vary, and sources that always occur together cannot be resolved. For example, gasoline and diesel power vehicles are normally on the same roads at the same time, so their emissions are always mixed, always observed together, and reported as a single source, which we have called gasoline exhaust. Further, we must be satisfied with approximate matches of observed PMF profiles to reference profiles for two reasons. First, some of the more important VOC species are more highly reactive than others, so the observed profile changes over time. Use of predawn data helps correct this problem. Second, reference profiles are only approximate. Profiles used here were compiled from a wide range of data sources (EPA Speciate, industrial publications, TCEQ Emission Inventory), measured by different means, for different purposes, over a period of many years, from processes that may have changed. For example, gasoline sold in Houston in 2000 may not be the same as gasoline sold in the DFW area in 2009, but is close enough to identify an observed profile as gasoline.

Some emission sources can be identified if they occur in isolation, but cannot be identified when mixed with other emissions. For example, crude oil vapor is clearly different from crude natural gas, and separate sources are easily resolved. However, these emissions are frequently mixed, and the resulting mixture is very similar to natural gas condensate. In this case, the source can be clearly identified as petroleum production, but it is not clear if it is oil and gas production or condensate. In some cases, wind direction and diurnal data can be used to attempt resolution of these sources, but such assignments should be regarded with extreme caution.

Finally, like all factor analysis methods, PMF requires the number of factors to be specified, based upon prior knowledge of the system being modeled. For example, a typical urban area should have only a few factors, one of which must be gasoline exhaust, so any solution that does not meet these criteria, should be discarded.

Figure D-56: *Excerpt from a Source Speciation Chart* shows the composition of each VOC profile as a series of vertical bar charts. On the vertical axis is a series of 15 vertical bars indicating the magnitude of the species, one for each VOC species, with acetylene on the bottom and xylenes on the top. The identity of each species is shown by the legend on the right. In this case, ethane is the species found in greatest proportion, followed by propane, butane, and pentane. All other species are zero.

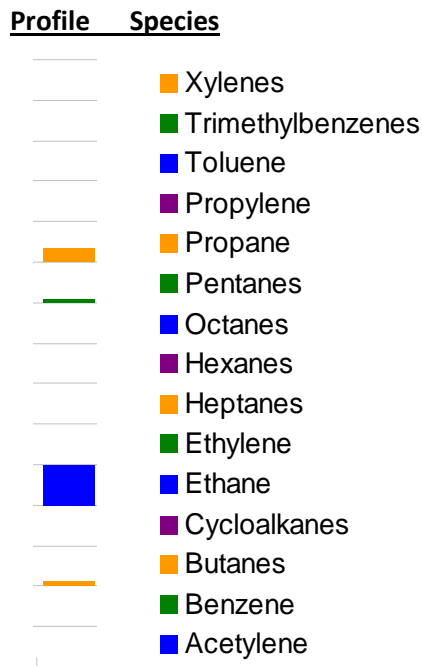


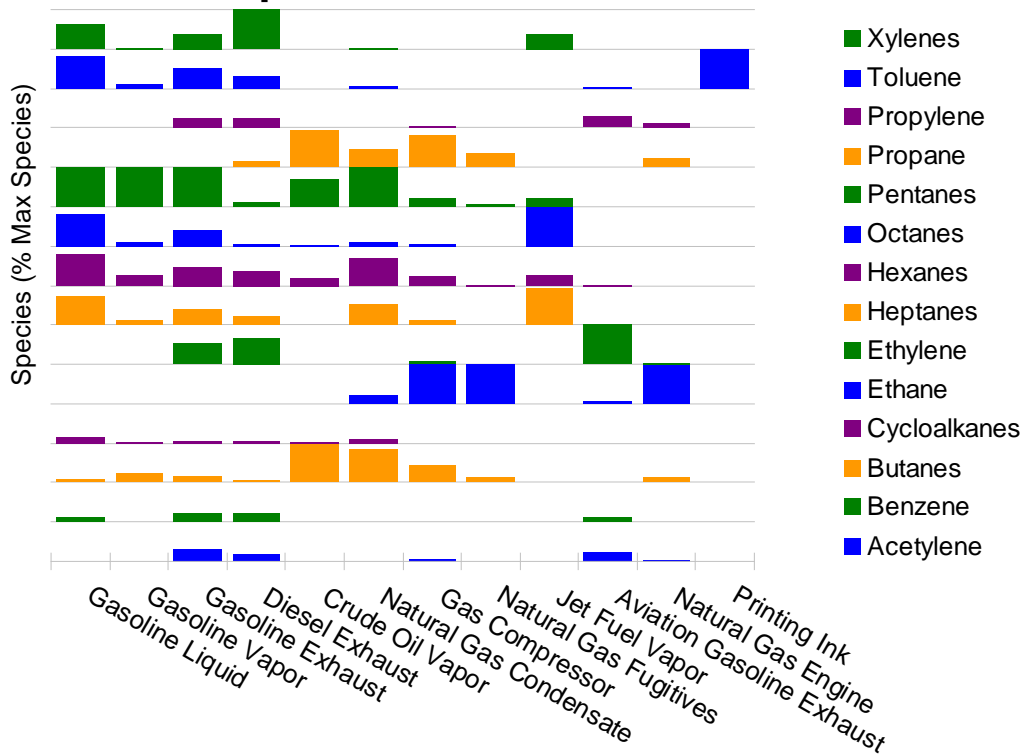
Figure D-33: Excerpt from a Source Speciation Chart

As shown in Figure D-57: *Complete Reference Speciation Profiles Chart*, bar charts for each reference profile are displayed in parallel. Each column shows the complete source speciation for a particular source type. For example, gasoline liquid contains mostly xylenes, toluene, pentane, octane, hexane, and heptane, with traces of cycloalkanes, butane, and benzene. In this case, 12 reference profiles are shown, some of which might possibly match an observed source in the Fort Worth area. Visual inspection is frequently successful in matching an observed profile to one of the reference profiles. As described above, it is not possible to obtain an exact match. In some cases, the match is ambiguous, but may be further resolved by consideration of emission roses, diurnal charts, and knowledge of the typical emission profiles of potential sources.

Figure D-58: *Observed Source Speciation for Ft. Worth Northwest (C13/AH302)* shows VOC speciation of each of the observed profiles as both bar and pie charts. Notice the multitude of species measured and the variation among species profiles that PMF is capable of identifying. Analysis of all predawn measurements during the year shows three readily identifiable sources:

gasoline exhaust, natural gas compressors, and crude natural gas. The distinction between gasoline type sources and natural gas type sources is very clear. While natural gas is mostly ethane, propane, and butane, gasoline is a mixture of many species. However, the distinction between crude natural gas and natural gas compressors is more subtle and may be subject to revision. Regardless, it is clear that gasoline and natural gas are the two major source types.

Reference Speciation Profiles



Only analysis species are shown - Most sources emit additional species

Run: 06/14/10 13:28

Figure D-34: Complete Reference Speciation Profiles Chart

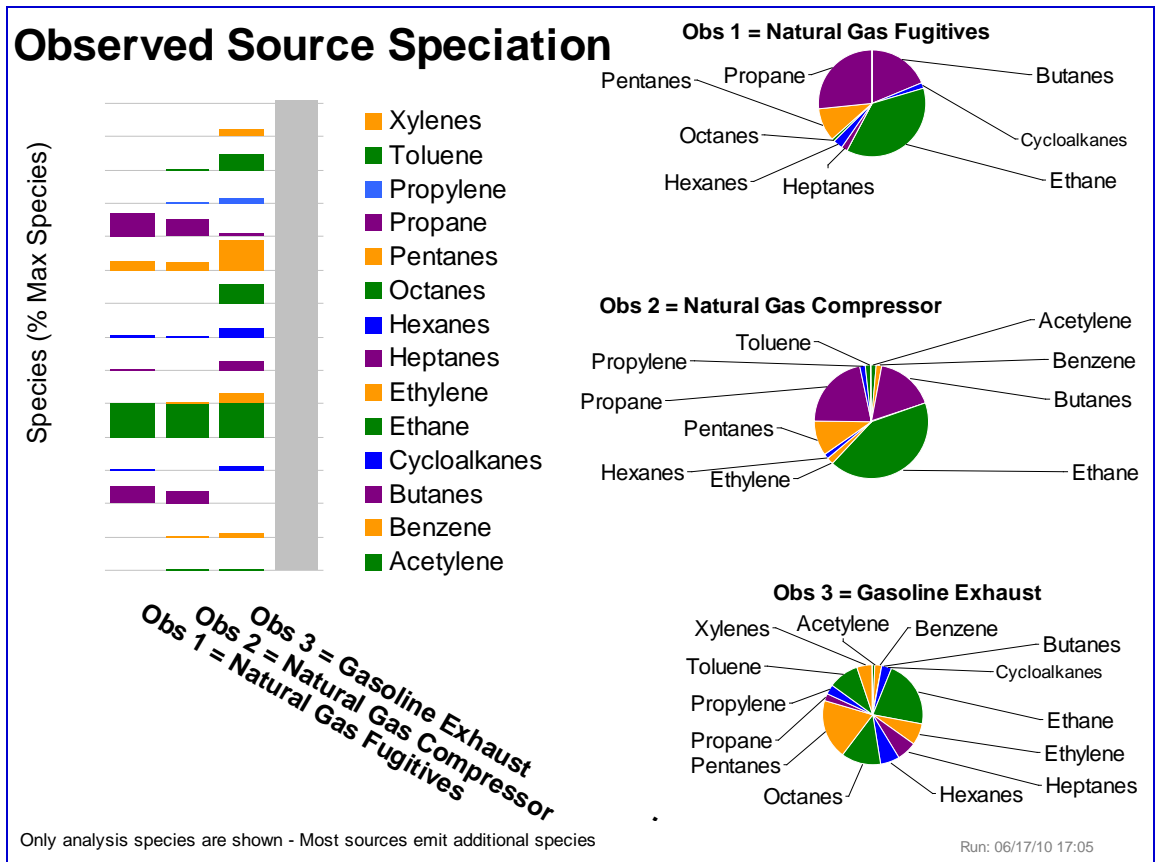


Figure D-35: Observed Source Speciation for Ft. Worth Northwest (C13/AH302)

Figure D-59: *Emission Rose of Observed Source Species for Ft. Worth Northwest (C13/AH302)* shows an emission rose overlaid on a map, and accompanied with a diurnal plot. A larger version of the Barnett Shale map is available at <http://www.tceq.state.tx.us/implementation/barnettshale/bshale-main>. The rose is the annual average source concentration as a function of wind direction when it arrives at the monitor. It is important to note that this chart shows the direction toward the source, but not the distance. For example, the average crude natural gas concentration (shown in blue) is highest when the wind is from the northwest, but the compound may be coming from a nearby source not visible on the map, a distant gas well shown in red, or a more distant oil well shown in blue. However, the wind rose shows that winds from the northwest are very rare, which may limit the impact of those emissions. The diurnal plot shows the concentration of those emissions is slightly higher at night, which is to be expected.

Gasoline exhaust, shown in green, appears to arrive mostly from the southeast, which is the urbanized area. The diurnal plot shows higher concentrations during morning and evening rush hour. Natural gas compressor emissions arrive from both the northwest and the southeast. While the cluster of compressors north of the monitor, near Dish, shown in black, is obvious, there are also numerous compressors spread over a wide area to the south of the monitor.

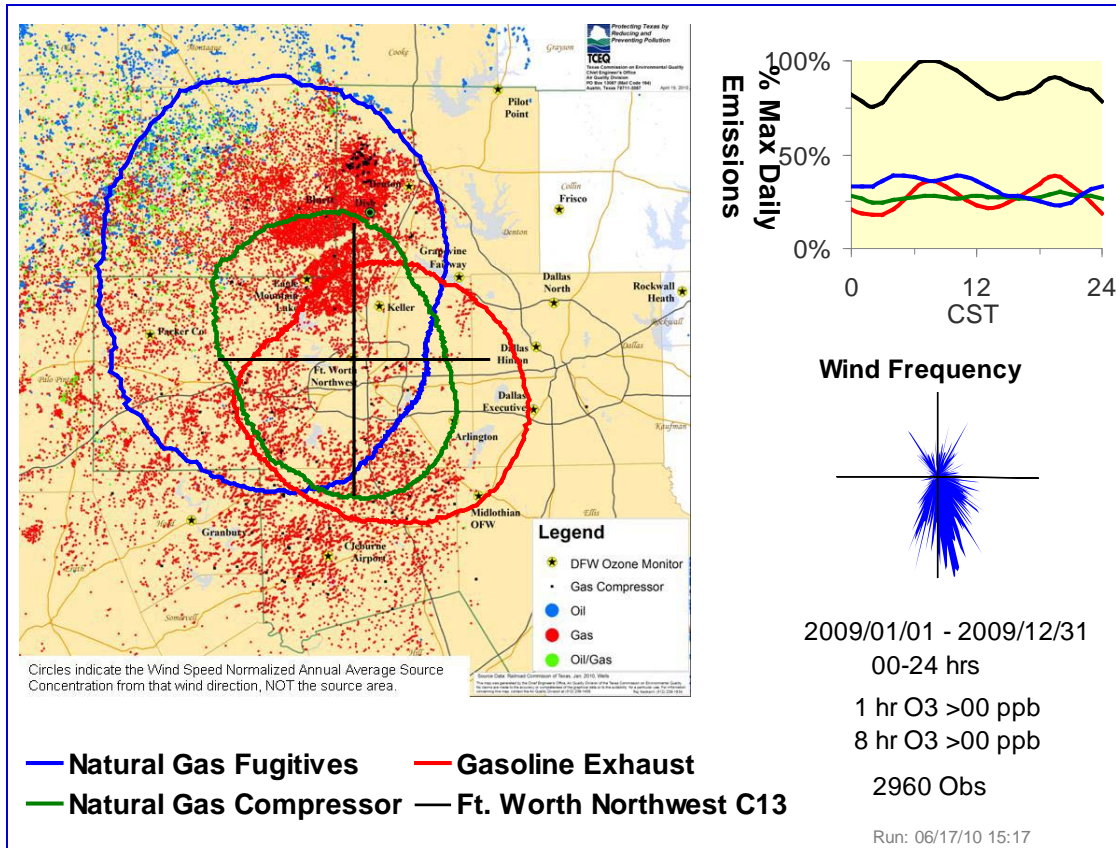


Figure D-36: Emission Rose of Observed Source Species for Ft. Worth Northwest (C13/AH302)

As shown in Figure D-60: *Comparison of Speciation Profiles for Different Scenarios*, the source profiles for each scenario are similar. In all cases: predawn hours of all year, all hours of all year, ozone season, high ozone days, and exceedance days, the same three source types appear: Gasoline Exhaust, Crude Natural Gas, and Natural Gas Compressors. This similarity indicates no major changes of emissions classes between scenarios. While the Ozone Season scenario is poorly resolved, this appears to be caused by additional emissions, probably from natural gas condensate and/or liquid gasoline. Regardless, the general conclusion remains there are only gasoline and natural gas related emissions.

Observed Source Speciation

Ft. Worth Northwest C13

Only analysis species are shown - Most sources emit additional species

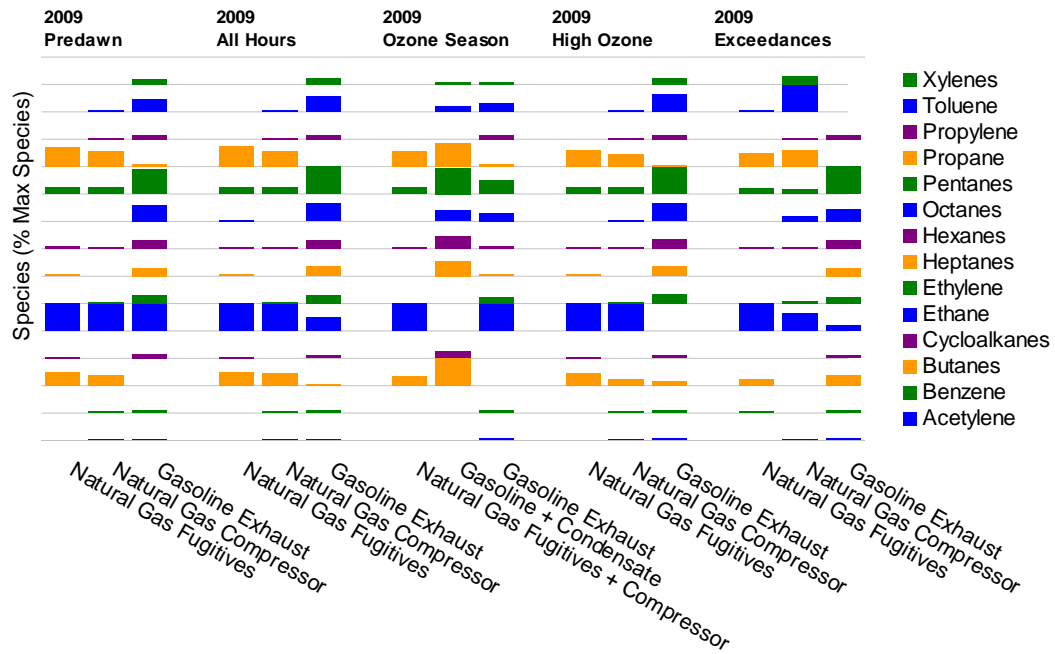


Figure D-37: Comparison of Speciation Profiles for Different Scenarios

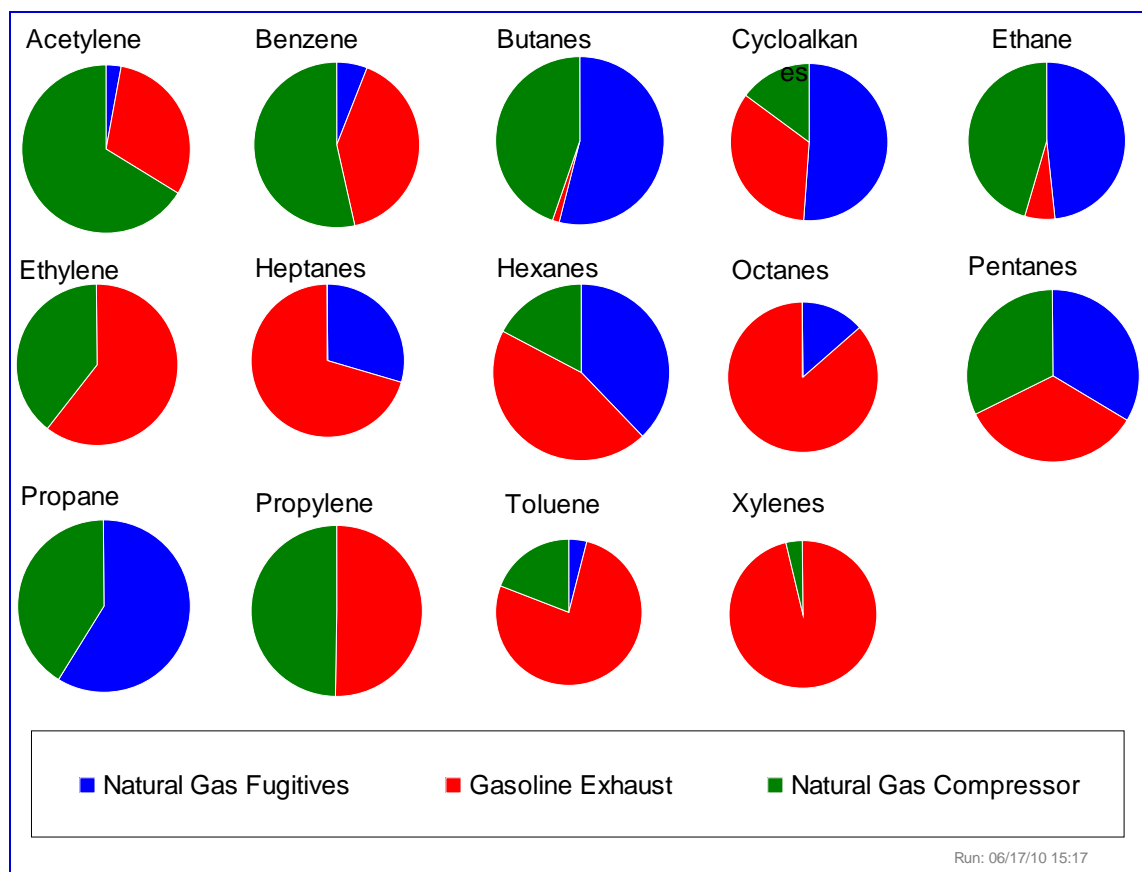


Figure D-38: Species Contributions by Source Type

Figure D-61: *Species Contributions by Source Type* shows the portion of each compound traceable to each of the identified sources. Some species are emitted primarily by one source type, such as xylenes and gasoline exhaust, but others are emitted by all source types, such as pentanes which appear about evenly split among the three source types. Most propane is from crude natural gas or gas compressors, with none from gasoline sources. In the case of benzene, slightly over half is from gas compressors, with most of the remainder from gasoline exhaust.

Positive Matrix Factorization successfully identified two major VOC emission classes in northwest Fort Worth: gasoline exhaust, and natural gas. Natural gas was further factored into crude natural gas fugitives and natural gas pipeline compressors, both associated with drilling operations. There is little evidence of other major VOC emission classes, even during the ozone season, on high ozone days, or on exceedance days. The same classes were observed for all days, ozone season days, high ozone days, and exceedance days, indicating no major variation in emission patterns across these widely varying seasonal and meteorological conditions.

Volatile organic compounds, especially highly reactive species, are known to accelerate ozone formation. However, lack of variation in observed VOC concentrations between high and low ozone days suggests that these emissions, while contributing to ozone formation, are not the factor that determines whether or not an exceedance of the federal ozone standard is recorded.

3.5.2 Analysis of Trajectories at the Eagle Mountain Lake (C75) Monitor

As oil and gas exploration in the Barnett Shale has met with success recently, interest and activity in the region has grown rapidly. Much of the activity and emissions are unknown and must be quantified for inclusion in emission inventories and air quality modeling. Also, the impact of these emissions on the environment and human health are presently unknown.

Figure D-62: *Oil and Gas Wells and Proximity to the Eagle Mountain Lake (C75) Monitor* shows the proximity of the Eagle Mountain Lake (C75) monitor to oil and gas wells. The figure includes only reported and known active wells. Many other locations have been permitted but may or may not have been drilled, and are, therefore, not plotted.

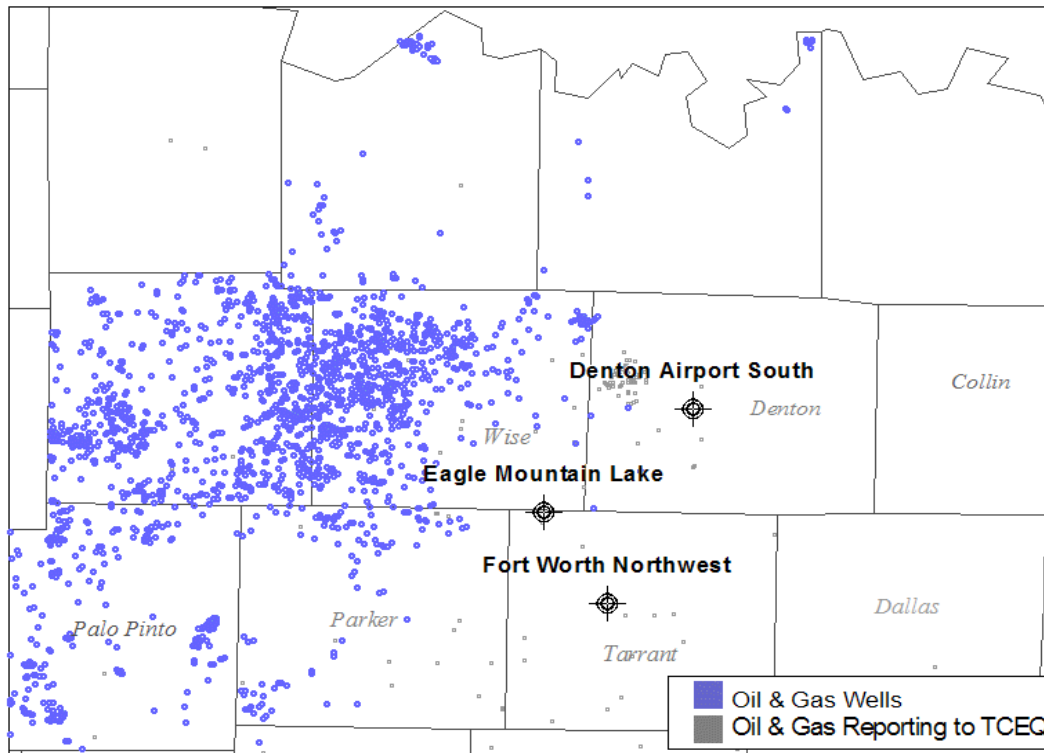


Figure D-39: Oil and Gas Wells and Proximity to the Eagle Mountain Lake (C75) Monitor

To explore the impact of oil and gas drilling in the Barnett Shale on ozone at the Eagle Mountain Lake (C75) monitor, ozone concentrations were linked to both HYSPLIT (upper atmosphere) and surface level backward trajectories. The Eagle Mountain Lake (C75) monitor recently recorded the maximum eight-hour ozone design value in the DFW area. Trajectory analysis will facilitate determination of whether high ozone days (days observing eight-hour ozone ≥ 85 ppb anywhere in the domain) were influenced by oil and gas production activity in the Barnett Shale region, from the DFW metropolitan area, or both.

Ozone and meteorological data were derived from the TCEQ LEADS data system. Native time resolution of this data is one hour. The Hybrid Single Particle Lagrangian Integrated Trajectory (HYSPLIT) model was used to compute 36-hour backward trajectories at 800 meters altitude for the selected days. HYSPLIT performs forward and backward trajectory modeling, and is available on the web site of the National Oceanic and Atmospheric Administration (NOAA)

(ready.arl.noaa.gov/HYSPLIT.php). Each computed trajectory originates at the hour of daily maximum ozone. Surface back trajectories were derived from wind speed and direction data maintained in the TCEQ LEADS data system. Native time resolution of this data is also one hour. Each trajectory consists of the endpoints at one-hour increments over the time period of interest, in this case 36 hours. Thus, each full trajectory is made up of an origin coordinate, a destination coordinate, and 35 intermediate coordinates recording the location of a particle as it moves. VOC canister data were retrieved from the TCEQ TAMIS data system. These are 24-hour duration samples collected every 6th day, reporting a variety of VOC species depending on sampling protocol. Oil and gas drilling information was obtained from the TCEQ and the Texas Railroad Commission.

If emissions from the Barnett Shale regions are impacting ozone concentrations at the monitor that records the DFW area design values, we would expect, at the least, to observe winds originating from the Barnett Shale region arriving at the subject monitor. To accomplish this, back trajectories, both aloft and surface, were examined. Only trajectories meeting rigid straightness, or non-sinuosity, criteria, that is, lacking re-circulation, will be considered. Re-circulation is when the same air mass passes over a monitor more than once, thereby biasing measurements at that monitor.

The Eagle Mountain Lake (C75) monitor sits on the most western edge of the DFW metropolitan area, atop the eastern portion of the Barnett Shale formation. This monitor observes less nearby point source emissions, which can bias measurements, than other monitors such as the Denton Airport South (C56/A163/X157) monitor. HYSPLIT back trajectories for each day with high ozone can be used to identify instances when an air mass arriving at the Eagle Mountain Lake (C75) monitor has entrained emissions. For example, examination of the trajectory can reveal whether an air mass passed over the urban portion of the DFW metropolitan area, or over the oil and gas field of the Barnett Shale, before arriving at the monitor location.

A sinuosity (S), or straightness, factor was calculated for each trajectory to ensure only non-circulated air masses were considered. Only trajectories with $S \geq 0.9$ were considered. Sinuosity estimates the curviness of a trajectory and ranges from zero to one. As S approaches one, the trajectory is more straight; as S approaches zero, the trajectory is more curvy. The sinuosity factor, S, is calculated by dividing the total length of the trajectory (D_{t2}) by the sum of the individual endpoint distances (sum of D_i , for i hours):

$$S = \frac{D_{t2}}{\sum D_i}$$

The least sinuous, or most curvy, trajectories do not have a particular direction, are associated with very light winds or recirculation, and were excluded. A more detailed discussion of sinuosity is available in Chapter 4.

An assessment of the frequency of intermediate HYSPLIT trajectory endpoints that fall within a particular county, for trajectories arriving at the Eagle Mountain Lake (C75) monitor, highlights counties that observe the highest frequencies of winds arriving at that location. Counties observing the highest frequencies are candidate counties for more detailed investigation of emission sources. Of the six counties located proximate to the monitor: Collin, Dallas, Denton, Parker, Tarrant, and Wise Counties, several were found to have high frequencies. All endpoint that did not fall into these six counties were aggregated into an 'other' category. A total of 1,702 HYSPLIT endpoints compose days with ozone greater than or equal to 85 ppb from 2000-2009. Table D-21: *Frequency of Upper Level Trajectory Endpoints by County on High Ozone Days* reports the number of endpoints falling in each county.

Table D-12: Frequency of Upper Level Trajectory Endpoints by County on High Ozone Days

Rank	County	Frequency of	Percentage
		Endpoints	of Total
		#	%
1	Tarrant	135	7.9
2	Denton	68	4.0
3	Wise	49	2.9
4	Collin	38	2.2
5	Dallas	30	1.8
6	Parker	6	0.4
7	Other	1,376	80.8
	Total	1,702	100.0

Wise County has an unexpectedly large number of endpoints, considering the few trajectories that actually traverse the county. This appears to be related to the meteorology seen on high ozone days in the DFW area, which includes light wind speeds. Because the Eagle Mountain Lake (C75) monitor is located in Tarrant County less than a mile from the border with Wise County, many of the trajectories arriving at the monitor cross the border into Wise County momentarily. Further, due to the model resolution, HYSPLIT occasionally puts the endpoint in Wise County. However, overwhelmingly, the majority of the endpoints fall in Tarrant County. Because the monitor is located in the far northwest of Tarrant County, this implies that on days with ozone greater than 85 ppb, most air masses arrive at the monitor from the east, southeast, and south after passing over the DFW source region. This also suggests that, on high ozone days, few trajectories arrive from the west.

3.5.3 Cluster Analysis of Winds on Elevated Ozone Days Using HYSPLIT

A cluster analysis was conducted on HYSPLIT trajectories to identify the most common trajectory paths by grouping similar trajectories into broad clusters. The analysis found consistent solutions for either two or seven factors. Both solutions were used to calculate cluster means, or average trajectories for each identified cluster, but the 7-factor solution is more informative, as it provides more insight on variation in wind directions arriving at the monitor. Cluster average trajectories are presented in Figure D-63: *Seven HYSPLIT Cluster Means Centered at Eagle Mountain Lake (C75)*. These results suggest that Wise County does not influence Eagle Mountain Lake (C75) on days when ozone is at least 85 ppb, since there are no trajectory means crossing into Wise County.

Trajectory means with the highest frequencies arrive from the southwest (two trajectory clusters with 18 percent and 15 percent of overall trajectories) and south (two trajectory clusters with 22 percent and ten percent of overall trajectories) of the Eagle Mountain Lake (C75) monitor. A further 24 percent of trajectories arrive from the northeast (two trajectory clusters with 19 percent and five percent of overall trajectories). No trajectory clusters were found to arrive from the north, the direction of Wise County, the northwest, or the west, the direction of the vast majority of Barnett Shale drilling activity. Nine percent of trajectories arrived from directions that were observed so infrequently they could not be clustered. Table D-22: *Source Directions of Trajectory Clusters Arriving at Eagle Mountain Lake (C75) on High Ozone Days* presents estimated trajectory cluster directions and the share of trajectories in each cluster.

Trajectories in the figure are computed for days with ozone at least 85 ppb in the DFW area. All trajectories are at 800 meters in altitude and end at the hour of peak ozone. Annotations indicate the cluster number and the percentage of trajectories in the cluster.

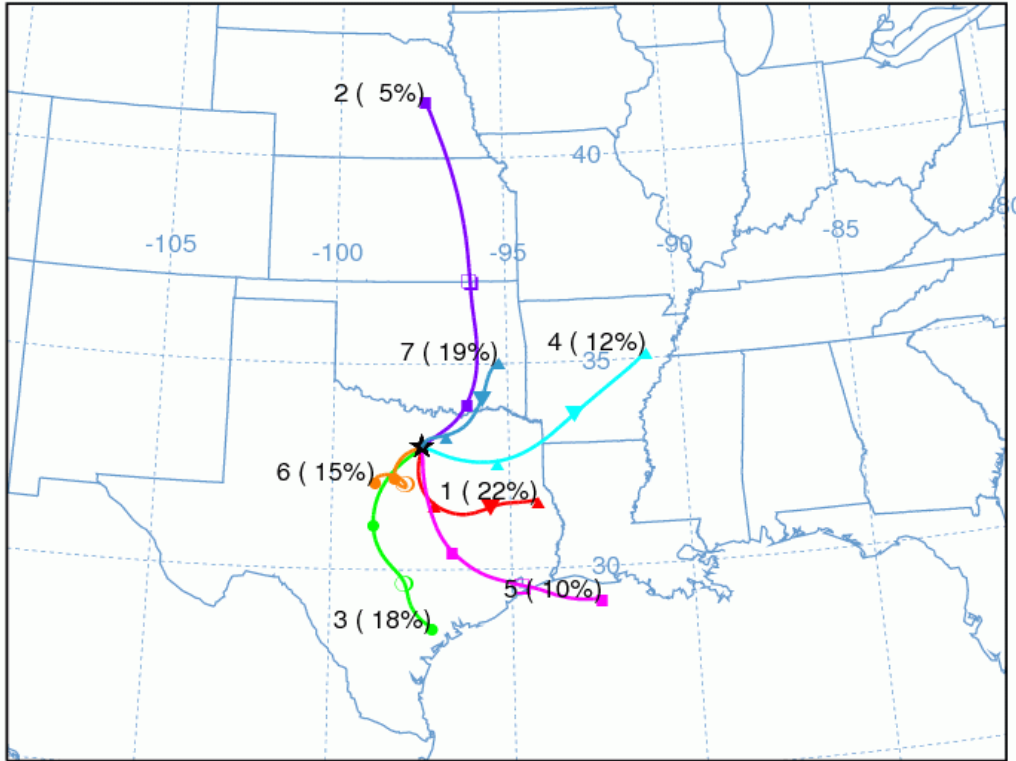


Figure D-40: Seven HYSPLIT Cluster Means Centered at Eagle Mountain Lake (C75)

Table D-13: Source Directions of Trajectory Clusters Arriving at Eagle Mountain Lake (C75) on High Ozone Days

Source Direction	Cluster	Percentage of Trajectories in Cluster	Percentage of Trajectories Arriving From Source Direction
north	-	0	0
northeast	7	19	24
east	4	12	12
southeast	-	0	0
south	1	22	32
southwest	3	18	33

Source Direction	Cluster	Percentage of Trajectories in Cluster	Percentage of Trajectories Arriving From Source Direction
		%	%
	6	15	
west	-	0	0
northeast	-	0	0
no cluster		9	9

Three of the clusters, 1, 6, and 7, exhibit relatively short trajectories, indicating low wind speeds, or indicate that on high ozone days in the DFW region, influence can be from other parts of Texas or elsewhere. The trajectory means labeled 2 and 7 suggest possible interstate transport.

3.5.4 Frequency of Surface Winds on Elevated Ozone Days

Backward trajectories for surface level (up to ten meters above ground level) winds were calculated at the Eagle Mountain Lake (C75) monitor using wind measurements from ground-based weather stations. The trajectories were 10 hours duration for days with 8-hour ozone at least 85 ppb for years 2000 to 2009. The approach uses inverse weighting of wind speed based on distances of meteorological sites contributing wind information from the subject monitor. Ten hour trajectories enable most trajectories to traverse the eight-county area, therefore not biasing results toward counties closest to the receptor site. Figure D-64: *Surface Back Trajectory Endpoints on High Ozone Days* presents hourly trajectory segment endpoints (grey circles) of paths ending at Eagle Mountain Lake (C75), without sinuosity filtering, that is, without excluding sinuous (curvy) trajectories. Sites providing meteorological data for this exercise are displayed as black points.

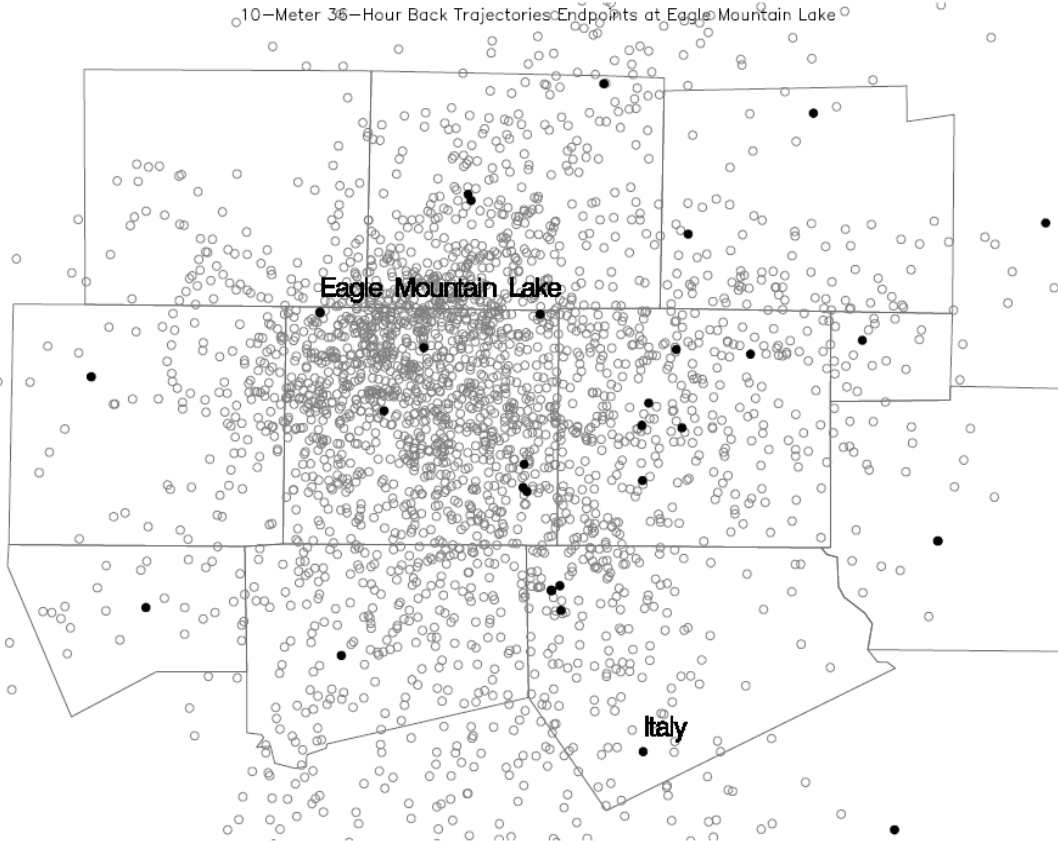


Figure D-41: Surface Back Trajectory Endpoints on High Ozone Days

Only a very small minority of the segment endpoints fall in Wise County, indicating that very few trajectories traverse Wise County, where a large portion of the oil and gas drilling occurs, before arriving at the Eagle Mountain Lake (C75) monitor. Most of the trajectories pass over portions of Tarrant County to the east and south, followed by Dallas County to the east and Denton County to the north and northeast. This implies that a high proportion of the compounds measured at the Eagle Mountain Lake (C75) monitor on high ozone days likely arrive from sources emitting in those areas, namely mobile sources, such as automobiles, and area sources.

This result can be quantified by counting the number of trajectory endpoints that fall in each county, as was done for the 800 meter HYSPLIT trajectories above. Sinuosity measures were used to remove trajectories containing re-circulating air parcels by filtering out trajectories with a sinuosity factor less than 0.9. Results are presented in Table D-23: *Frequencies of Surface Back Trajectory Endpoints by County on High Ozone Days*.

Table D-14: Frequencies of Surface Back Trajectory Endpoints by County on High Ozone Days

Rank	County	Frequency of	Percentage of
		Endpoints	Total Endpoints
		#	%
1	Tarrant	519	32
2	Dallas	243	15

Rank	County	Frequency of Endpoints	Percentage of Total Endpoints
3	Denton	137	8
4	Collin	67	4
5	Parker	50	3
6	Wise	28	2
7	Other	595	36
	Total	1,639	100

Most trajectories pass over Tarrant and Dallas Counties, as expected. But many of the Tarrant County trajectories also pass over Dallas County, where they encounter a large number of emission sources. Eight percent pass over Denton County, twice as many as the next most frequent county, Collin County, which is also located north and east of the monitor. In fact, Parker and Wise Counties, the counties west and northwest of the monitor, combined only contribute five percent of the total endpoints of trajectories arriving at the monitor. This suggests that the regions hosting the vast majority of oil and gas activity, Parker and Wise counties, appear to have very little influence on the Eagle Mountain Lake (C75) monitor on days with ozone greater than 85 ppb. While there is a small cluster of oil and gas activity in far western Denton County, none of the trajectories appear to traverse this area, suggesting the area has little influence on measurements at the monitor on high ozone days.

3.5.5 Examination of VOC Canister Data at Denton Airport South (C56/A163/X157)

Examination of ambient air samples collected using evacuated canisters provides insight on the relationship between VOC and ozone. VOC canister data are available at 13 sites throughout the DFW region. In particular, canister data collected at Denton South Airport (C56/A163/X157) is of interest because of its proximity to the areas of greatest oil and gas activity. Unfortunately, currently, collection of VOC samples at Eagle Mountain Lake (C75), the monitor setting the ozone design value of record for the DFW area, has yet to commence. Therefore, Denton Airport South (C56/A163/X157) was chosen as a surrogate for Eagle Mountain Lake (C75). While ambient VOC concentrations at these monitors are likely to be similar in composition, they may not be similar in magnitude.

All data used in this document are derived from the TCEQ TAMIS data system. Sampling duration was 24 hours. Canisters are stainless steel evacuated tanks with a control valve to precisely meter the rate at which the canister fills with ambient air. Canister samples are taken every 6th day and analyzed at a laboratory. All data used in this document have satisfied TCEQ standards for quality assurance (QA) and quality control (QC).

VOC concentrations at the Denton Airport South (C56/A163/X157) monitor are the highest observed in the DFW area, most likely due to the proximity of oil and gas activity surrounding this monitor. In this respect, the Denton Airport South (C56/A163/X157) monitor is similar to the Eagle Mountain Lake (C75) monitor, and is therefore believed to be an adequate proxy at this time.

Figure D-65: *VOC at Denton Airport South (C56/A163/X157)* displays VOC concentrations on all sampling days from 2000 to 2009 when ozone was at least 85 ppb. VOC is plotted as grey circles; blue points highlight days when ozone was at least 85 ppb.

Higher VOC concentrations tend to coincide with cooler months. VOC concentrations above about 20 ppbV only began occurring at the end of 2001 and are regular, though not particularly common compared to the total number of samples collected, through the end of the period.

High ozone days do not necessarily occur only on days when ambient VOC concentrations are also high. An ordinary least squares regression fit (not reported) of total VOC on daily ozone peak found no statistically significant relationship, as evident in a very low R^2 statistic and other poor parameter estimates.

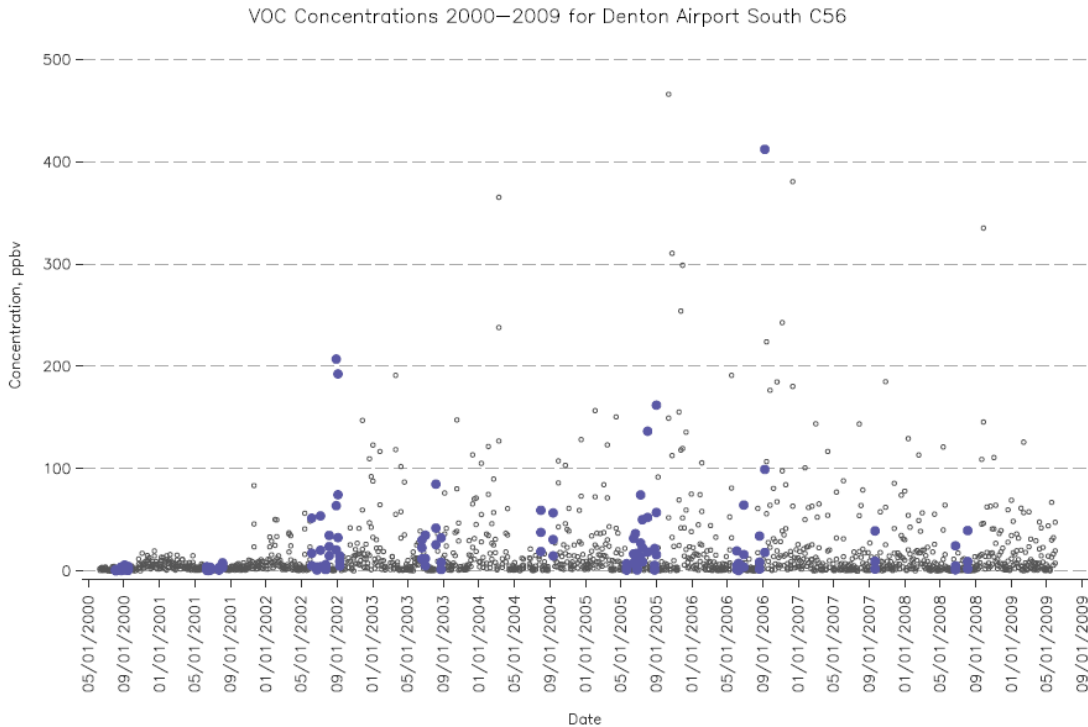


Figure D-42: VOC at Denton Airport South (C56/A163/X157)

Using both aloft (HYSPLIT) and surface trajectories, VOC samples were traced backward to potential source regions. Traditional wind roses were rejected for this exercise because wind roses fail to address re-circulation. Inclusion of the sinuosity criterion ensures that most re-circulation is addressed. Also, aloft and surface trajectory estimation procedures produce slightly varying results. Trajectory models used here vary markedly, using different data at different spatial scales. While it is not possible to say with certainty that one is better than the other, consistency of results from both procedures strengthens the ultimate conclusions.

Results from both aloft and surface trajectories suggest that on days with ozone at least 85 ppb, winds, and their entrained emissions, arriving at monitors located in the northwest part of the DFW area originate mainly from Tarrant County with little influence from Wise County. This implies that the influence of oil and gas drilling on ozone concentrations at Eagle Mountain Lake (C75) is minimal. VOC canister samples corroborate these findings, suggesting there is no relationship between VOC concentrations and ozone concentrations at the Denton Airport South (C56/A163/X157) monitor, a surrogate for the Eagle Mountain Lake (C75) monitor. Though the Denton Airport South (C56/A163/X157) monitor is not the monitor that has recently been registering the DFW area ozone design value of record, it does rank second or third in the area depending on year.

3.5.6 Case Study of Barnett Shale Emission on July 1, 2009

On July 1, 2009, eight-hour ozone reached a peak of 98 ppb in the DFW region. Wind speeds were mostly light and the temperature for the area was about 98°F. What is remarkable is that the winds during this day were mostly from the west for a significant period of time, which is rare. In mid-afternoon, winds reversed and could have contributed to elevated ozone in the DFW region. However, for a few hours that day, air masses sampled at the Eagle Mountain Lake (C75) monitor and elsewhere in the Fort Worth region were being transported from the Barnett Shale area, located to the west. An analysis of wind trajectories on that day will facilitate an understanding of the possible impacts the emissions from the Barnett Shale had on ozone concentrations recorded at Eagle Mountain Lake (C75).

Wind trajectories were created for each day that Eagle Mountain Lake (C75) recorded eight-hour ozone greater than 75 ppb during 2009. The trajectories use 10 meter altitude winds measured at all monitors housing meteorological instruments in the DFW region. The model computes a distance weighted 2-dimensional trajectory starting at the hour that maximum 8-hour ozone was recorded, backward in time seven hours, using all monitors reporting meteorology in the area. Results are presented graphically in Figure D-66: *Back Trajectory at Eagle Mountain Lake (C75) Monitor for One-Hour Ozone on 1 July 2009* and Figure D-67: *Back Trajectory at Eagle Mountain for Lake (C75) Monitor for Eight-Hour Ozone on 1 July 2009*. Trajectory end times coincide with the hours of maximum ozone, 17:00 LST in the case of one-hour ozone and 13:00 LST in the case of eight-hour ozone. All data are derived from the TCEQ LEADS database.

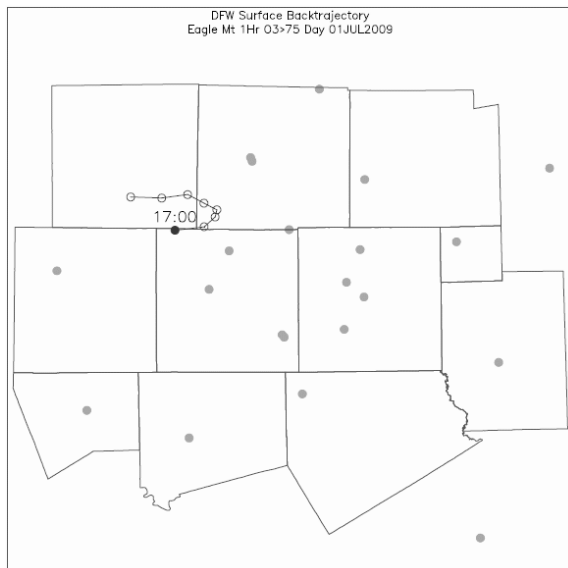


Figure D-43: Back Trajectory at Eagle Mountain Lake (C75) Monitor for One-Hour Ozone on 1 July 2009

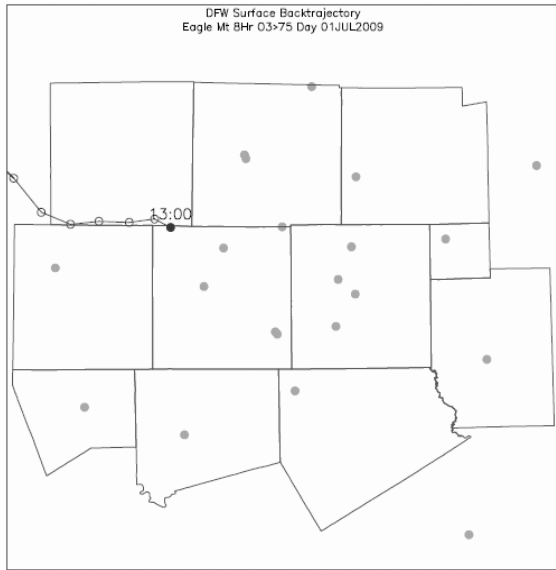


Figure D-44: Back Trajectory at Eagle Mountain for Lake (C75) Monitor for Eight-Hour Ozone on 1 July 2009

Of 19 days with eight-hour ozone greater than 75 ppb at the Eagle Mountain Lake (C75) monitor, only one day, July 1, 2009 observed wind consistently from the west, the direction of the Barnett Shale. Winds prevailed from the west for approximately 12 hours, 0:00-12:00 LST (midnight to noon). The peak eight-hour ozone average was recorded as 75 ppb at 13:00 LST and the peak one-hour ozone average was 82 ppb at 17:00 LST. An eight-hour ozone average is denoted with the first hour of the eight hours used for averaging. Therefore, the peak daily value on July 1, 2009, averaged measurements from 13:00 to 20:00 LST.

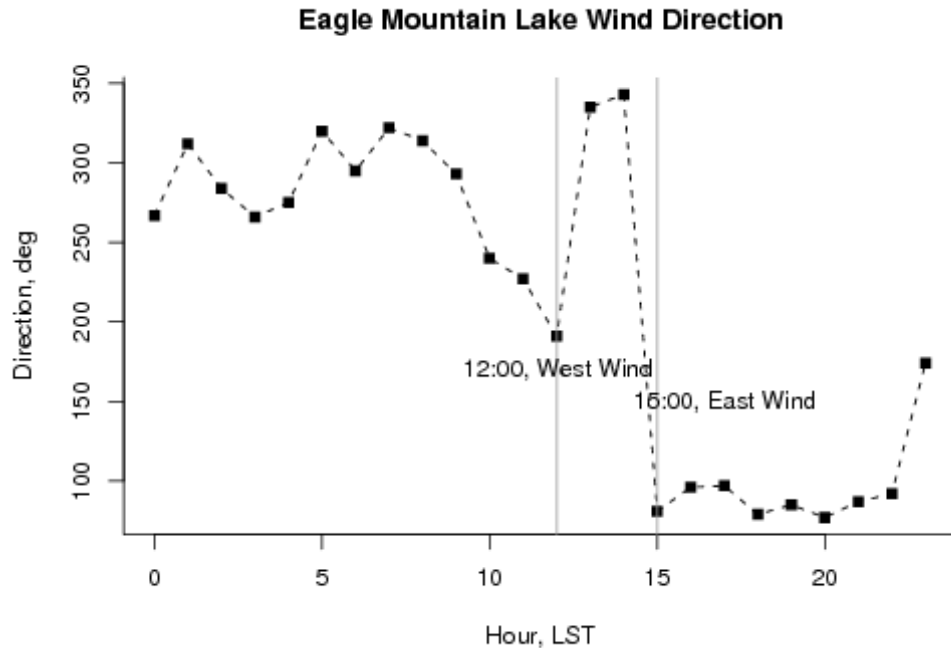


Figure D-45: Wind Directions at Eagle Mountain Lake (C75) Monitor Showing Wind Shift from West to East on July 1, 2009

Between 12:00 and 15:00 LST, winds shifted substantially, from a westerly direction before to an easterly one after (Figure D-68: *Wind Directions at Eagle Mountain Lake (C75) Monitor Showing Wind Shift from West to East on July 1, 2009*). The peak daily eight-hour ozone average was recorded over an eight hour period beginning after noon. Inspection of Table D-24: *One-Hour Ozone Averages Recorded at Eagle Mountain Lake (C75) July 1, 2009* reveals that when winds originated from the west, ozone concentrations were well below 70 ppb, either because there had not been enough hours of sunlight for ozone production to occur, ozone production was cut short because of the wind shift, or there were insufficient precursors to produce high levels of ozone. The reversal in wind direction produced several hours of stagnation before complete reversal. Once the winds began arriving from the east, ozone production began to rise. This rise in ozone concentrations was most likely due to emissions from the DFW area, located east of the monitor. However, the contribution of Barnett Shale emissions that circulated over the DFW area during the stagnation period cannot be ruled out.

Table D-15: One-Hour Ozone Averages Recorded at Eagle Mountain Lake (C75) July 1, 2009

Hour	One-Hour Ozone	Hour	One-Hour Ozone
	<i>ppb</i>		<i>ppb</i>
Mid	36	Noon	69
01:00	28	13:00	69
02:00	27	14:00	71
03:00	23	15:00	74
04:00	26	16:00	78
05:00	28	17:00	82
06:00	22	18:00	81
07:00	28	19:00	*

Hour	One-Hour Ozone	Hour	One-Hour Ozone
	<i>ppb</i>		<i>ppb</i>
08:00	38	20:00	*
09:00	50	21:00	43
10:00	63	22:00	42
11:00	67	23:00	42

* No reading due to calibration in progress.

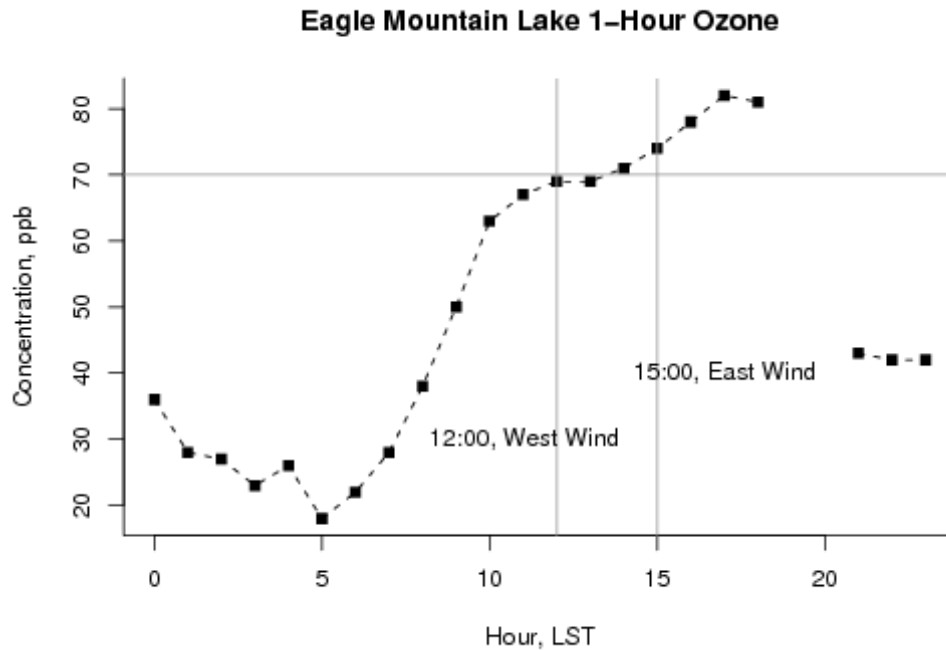


Figure D-46: One-Hour Ozone at Eagle Mountain Lake on July 1, 2009

Figure D-69: *One-Hour Ozone at Eagle Mountain Lake on July 1, 2009* demonstrates how the wind shift over the course of the day, from westerly to easterly, coincided with the increase in ozone concentrations. One-hour ozone concentrations began rising at 05:00 LST and continued until about 12:00 LST. Vertical reference lines indicate the time period when winds shifted from westerly to easterly. During the three or so hours of shifting winds, the increase in ozone concentrations slowed and leveled off, before continuing to increase after the wind had shifted. By 15:00 LST, winds had begun arriving consistently from the east. Elevated ozone concentrations measured after 15:00 LST were likely the result of precursor emissions from the Barnett Shale region being carried east and mixing with other precursors from the metropolitan area, then being transported back to the west during the sunniest, most ozone-conducive time of day. Figure D-70: *One-Hour Ozone and Wind Direction at Eagle Mountain Lake (C75) on July 1, 2009* provides another perspective showing ozone levels by wind direction for each hour of the day. Unfortunately, it is not possible to determine how much of the measured afternoon ozone was attributable to precursor emissions from the Barnett Shale and how much was from urban-sourced precursor emissions.

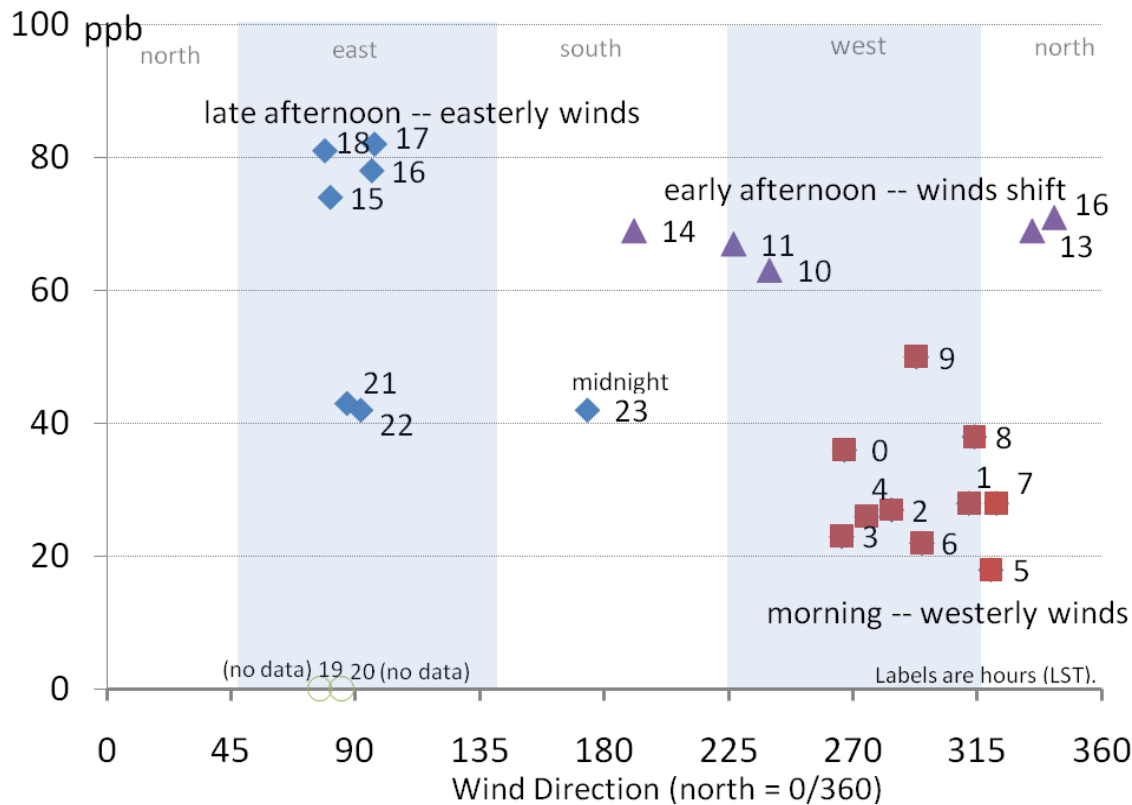


Figure D-47: One-Hour Ozone and Wind Direction at Eagle Mountain Lake (C75) on July 1, 2009

Further investigation of events on July 1, 2009 involved examination of speciated VOC compounds. For this exercise, an auto-GC monitor which is both upwind of the DFW area and downwind of the Barnett Shale region, was selected to help differentiate sources contributing precursors to DFW area ozone formation. The auto-GC monitor farthest upwind in the western direction in the DFW area is the Ft. Worth Northwest (C13/AH302) monitor. This monitor is also downwind of most activity in the Barnett Shale region, even though samples collected there will likely have some contamination from nearby, non-Barnett Shale, sources upwind of the monitor.

Preliminary auto-GC results show that propane, butane, ethane, 2-methylpentane and isobutane are primary emissions found downwind of oil and gas drilling and production (Sullivan 2009). Detection of elevated concentrations of these compounds at this monitor, compared to levels seen in areas not impacted by oil and gas drilling, would suggest this monitor is observing emissions from oil and gas activities in the Barnett Shale region.

Table D-25: *Cross-Correlations (R2) for VOC Compounds Sampled at Ft. Worth Northwest (C13/AH302) Monitor July 1, 2009* reports cross-correlations of speciated VOC compounds observed at the monitor and Figure D-71: *Scatter Plot Matrix for July 1, 2009 at the Ft. Worth Northwest (C13/AH302) Monitor* plots them. Note that some of the scatter plots and correlation coefficients show well defined correlations, signified by the points falling more or less along a straight line, such as seen with the plots of propane with n-butane and benzene with toluene. Other plots suggest influences from two sources, visible in the plots as points falling along two distinct groupings. Examples of these include the plots of propane with isopentane and n-butane with isopentane. Several of these will be examined in more detail later. Other

plots show no correlation. High correlations signify co-occurrence of two compounds. Of the VOC species measured, ethane, propane, and butane are indicative of oil and gas activity.

Table D-16: Cross-Correlations (R^2) for VOC Compounds Sampled at Ft. Worth Northwest (C13/AH302) Monitor July 1, 2009

VOC	n_butane	propane	isopentane	isoprene	benzene	toluene
ethane	0.82	0.88	0.08	0.00	0.04	0.01
n_butane		0.97	0.23	0.00	0.15	0.06
propane			0.11	0.00	0.06	0.01
isopentane				0.00	0.63	0.86
isoprene					0.03	0.00
benzene						0.70

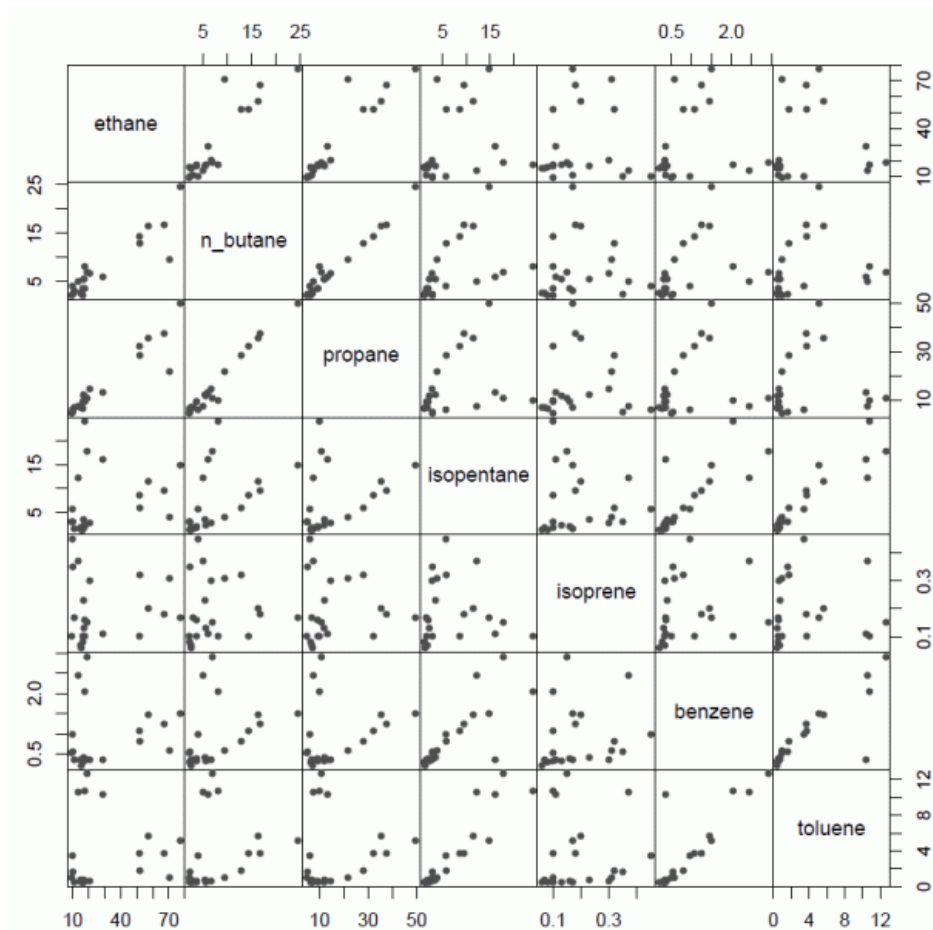


Figure D-48: Scatter Plot Matrix for July 1, 2009 at the Ft. Worth Northwest (C13/AH302) Monitor

High correlations between ethane and n-butane (0.82), ethane and propane (0.88), and n-butane and propane (0.97) indicate co-occurrence of these compounds. Co-occurrence of all three compounds strongly suggests emissions from oil and gas extraction activities.

Benzene measured at the Ft. Worth Northwest (C13/AH302) monitor shows a high correlation ($R^2=0.97$) to toluene, which is typically used to determine the “age” of an air mass (Main, et al., 1996). The age of an air mass is useful for identifying likely emission sources. If an air mass is found to contain compounds that were created recently, it is probable that the source is nearby automobile emissions, rather than more distant Barnett Shale activities. The ratio of two compounds, benzene and toluene, is used as an indicator of age: because toluene reacts fairly quickly compared to benzene, it will be found in lower concentrations in more aged air masses. The ratio of the two will be much lower in air masses containing relatively more recent emissions of these compounds, and become much higher over time, as the level of toluene drops due to reaction in ambient air.

The ratio of benzene to toluene at the Ft. Worth Northwest (C13/AH302) is 0.33, suggesting that the air mass was recently created or “fresh.” Typical ranges for the benzene/toluene ratio are that air masses with ratios less than 0.4 are considered to be recent or “fresh” and those with ratios above 0.4 are aged. Both benzene and toluene exhibit a bimodal diurnal pattern, with both peaking at about 3:00 LST, and are at their lowest at 22:00 LST. Peak measured benzene was 2.92 ppb and peak toluene was 12.63 ppb. Figure D-72: *Correlations Between Toluene and Benzene at Ft. Worth Northwest (C13/AH302) on July 1, 2009, With (Left) and Without (Right) Outlier* plots measured toluene and benzene concentrations on that day, including and excluding one anomalous outlier, and demonstrates the fairly close correlation between the two.

Typically, benzene and toluene are associated with automobile exhaust. However, as demonstrated in Figure D-73: *Diurnal Profile of Benzene and Toluene at Ft. Worth Northwest (C13/AH302) on July 1, 2009*, benzene and toluene concentrations do not resemble a typical automobile source diurnal profile, which exhibits two modes typically centered around 5:00 and 16:00, that is, morning and evening commute times. This pattern seems to match more closely the expansion and contraction of the atmospheric mixing layer, given the times of the maximum and minimum. But given the high correlation between the two compounds, it is very likely that the Ft. Worth Northwest (C13/AH302) monitor is measuring automobile exhaust.

During the hours of 0:00 to 17:00 LST, the wind was primarily from the west; not until after 17:00 LST did wind direction reverse course. A regression fit showed a positive association between toluene and benzene. However, the reversal in wind direction was not detected in the regression fit as a second source. A second source might appear in a scatter plot as two trends with different slopes and intercepts. Detection of a second source could be modeled by subsetting the data by wind direction. A distinct automobile signature would be expected only from the east (Fort Worth and Dallas) and the emissions signature would be considerably different from the west (the Barnett Shale).

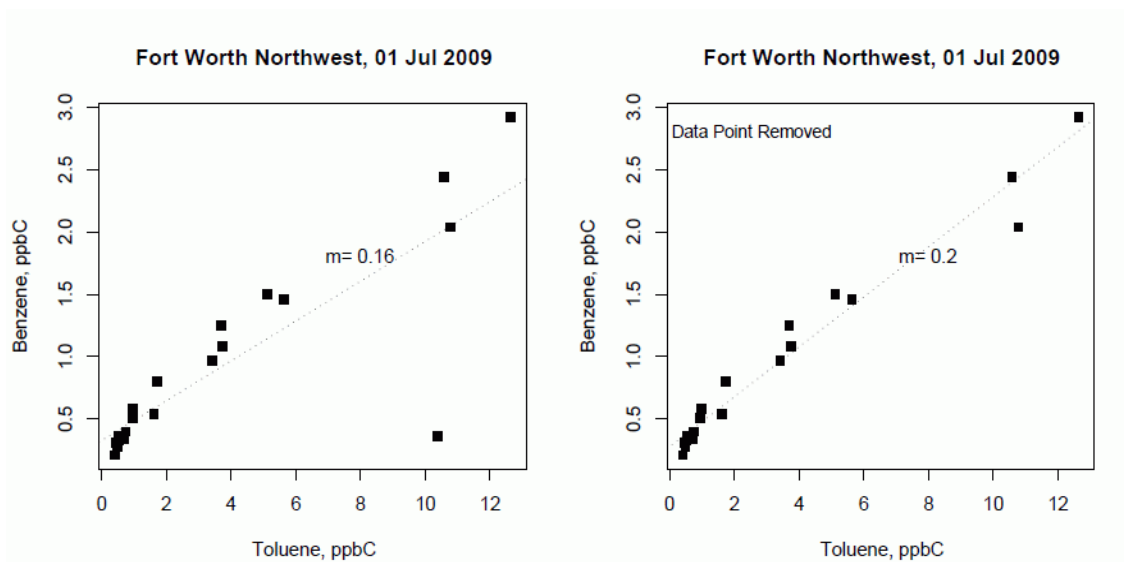


Figure D-49: Correlations Between Toluene and Benzene at Ft. Worth Northwest (C13/AH302) on July 1, 2009, With (Left) and Without (Right) Outlier

In Figure D-72: *Correlations Between Toluene and Benzene at Ft. Worth Northwest (C13/AH302) on July 1, 2009, With (Left) and Without (Right) Outlier*, the panel on the left ($R^2=0.70$) and the panel on the right ($R^2=0.97$) contain the same data but the right panel excludes one outlier, yielding a better fit. Both models are significant at the 0.1 percent level (p -values < 0.001). Notice that the slope does not change appreciably, rising from 0.16 to 0.20, but the R^2 improves considerably. The removed data point corresponds to winds from the south, which occurred briefly at the end of the day (23:00 LST or 11 p.m.), as seen in Figure D-68: *Wind Directions at Eagle Mountain Lake (C75) Monitor Showing Wind Shift from West to East on July 1, 2009*.

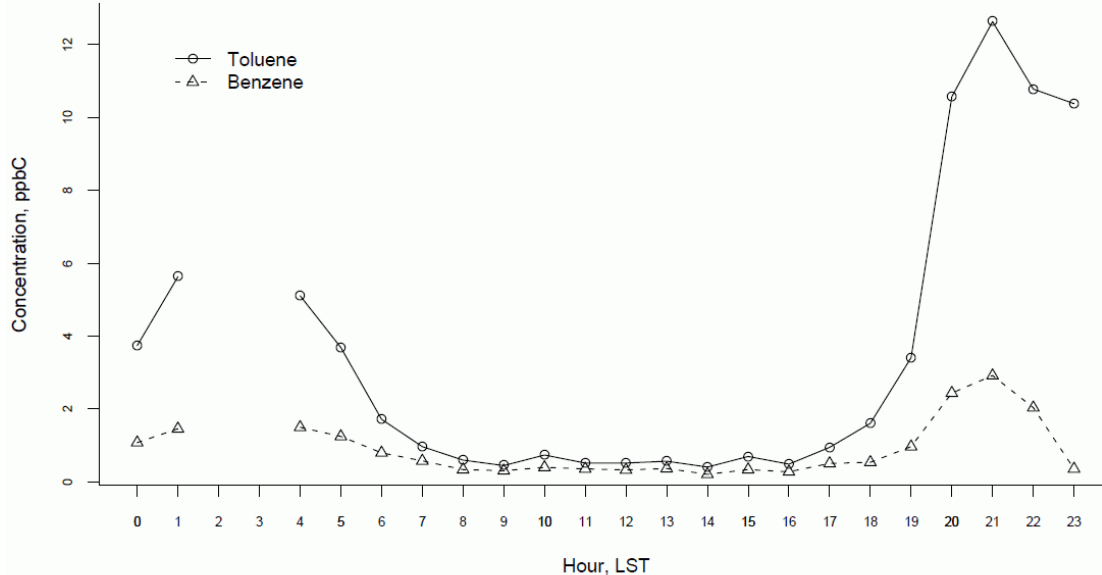


Figure D-50: Diurnal Profile of Benzene and Toluene at Ft. Worth Northwest (C13/AH302) on July 1, 2009

Similarly, the scatter plot of n-butane and isopentane revealed two likely sources. Figure D-74: *Scatter Plot of N-Butane Versus Isopentane at Ft. Worth Northwest (C13/AH302) on July 1, 2009* shows this scatter plot, replicated from the earlier matrix, with the hour of the day of the sample noted and least squares fits to two subsets of the values shown. The plot shows that samples collected from 0:00 LST to 16:00 LST, when winds were from the west, compose one of the correlations, and samples collected from the hours of 17:00 LST to 23:00 LST, when winds were from the east, compose the other.

The regression lines had high R^2 values, 0.95 and 0.97, confirming the presence of two distinct sources, from different directions, affecting the monitor. Also, note the change in the plot from one source to the other coincides with the hour the wind direction reversed. The exact sources being detected on this day will remain unknown until more information is collected and a thorough review of known sources has been performed. Regression results are presented in Table D-26: *Results of Regression of Isopentane on N-Butane at Ft. Worth Northwest (C13/AH302) on July 1, 2009*. These results indicate there is more isopentane when the winds are from the east, and more n-butane when winds are from the west. The implication is that westerly winds carry the Barnett Shale signature.

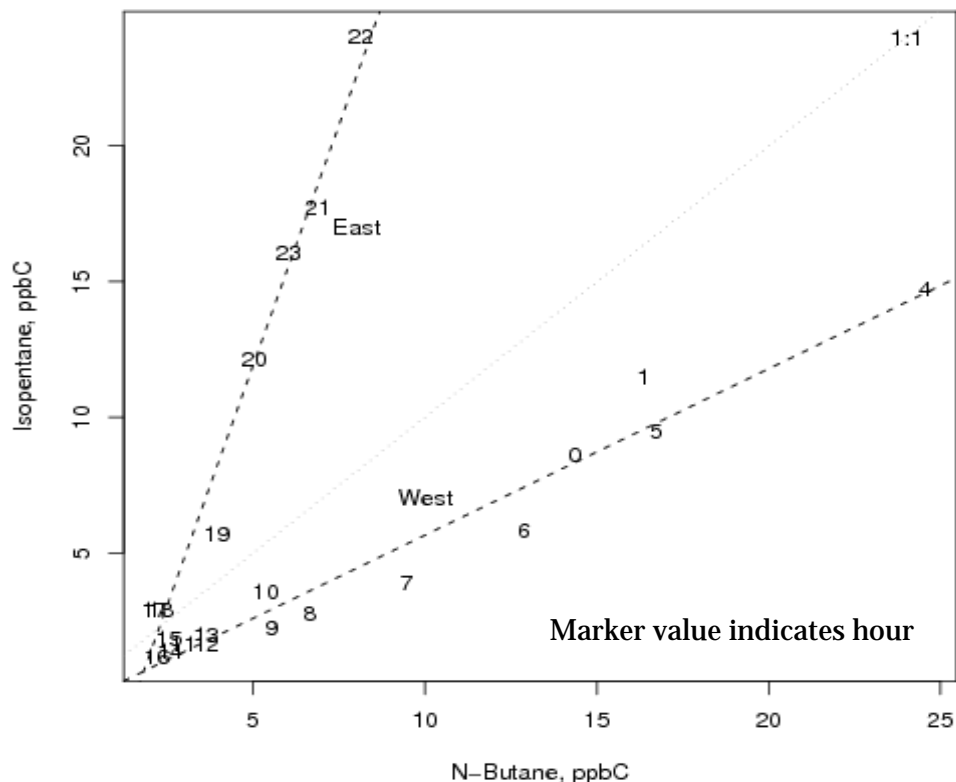


Figure D-51: Scatter Plot of N-Butane Versus Isopentane at Ft. Worth Northwest (C13/AH302) on July 1, 2009

Table D-17: Results of Regression of Isopentane on N-Butane at Ft. Worth Northwest (C13/AH302) on July 1, 2009

Direction	# of Hours	Obs.	R ²	Estimated	
				Slope	Intercept
West	0:00-16:00	17	0.95	0.61	-0.47
East	17:00-23:00	7	0.97	3.54	-5.77

Propane and benzene also exhibited a bi-directional pattern (Figure D-75: *Scatter Plot of Propane Versus Benzene at Ft. Worth Northwest (C13/AH302)*). Linear fits of two subsets of the samples of these compounds also revealed directional influences corresponding to the mid-afternoon shift in wind direction. Regression results confirm that samples collected when winds were from the west follow a pattern that differs from samples collected when winds were from the east. Emissions from the west show an R² greater than 0.93, but emissions from the east show a poor R² at 0.11. Regression results are reported in Table D-27: *Results of Regression of Propane on Benzene at Ft. Worth Northwest (C13/AH302) on July 1, 2009*.

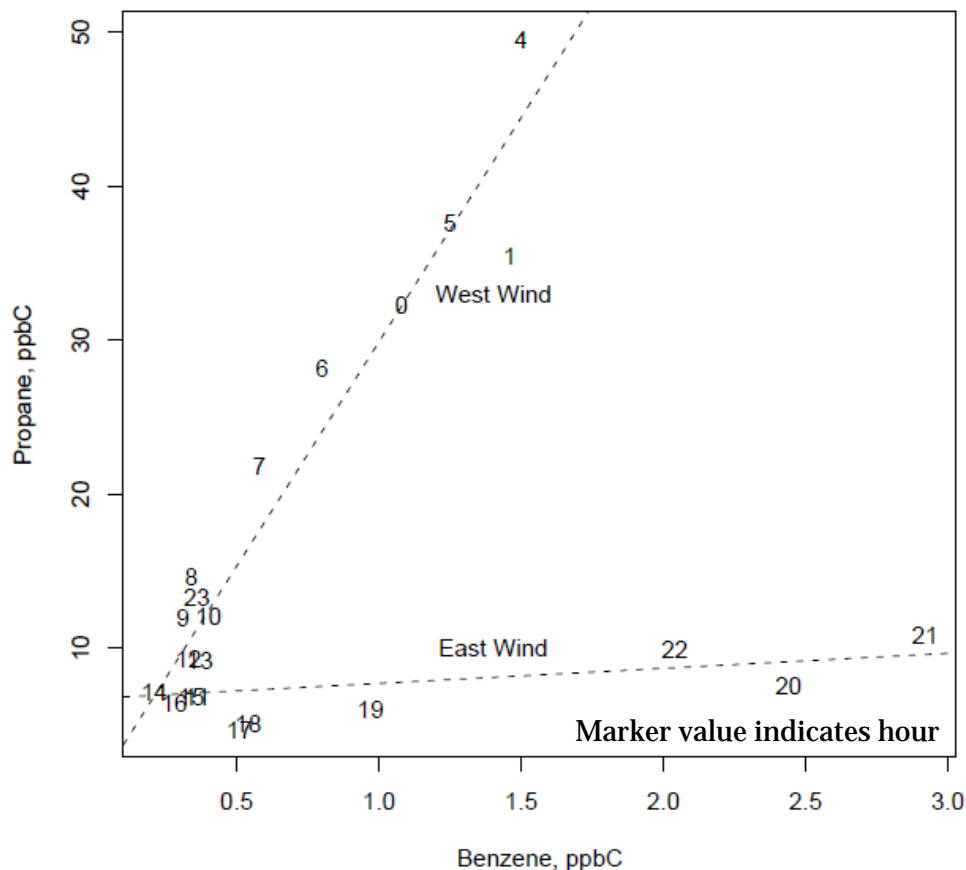


Figure D-52: Scatter Plot of Propane Versus Benzene at Ft. Worth Northwest (C13/AH302)

Table D-18: Results of Regression of Propane on Benzene at Ft. Worth Northwest (C13/AH302) on July 1, 2009

Direction	# of Hours	Obs.	R ²	Estimated	
				Slope	Intercept
West	0:00-16:00	17	0.93	29.1	0.77
East	17:00-23:00	7	0.11	0.9	6.7

While winds on July 1, 2009 were from the west most of the day, implying transport from the direction of the Barnett Shale, a reversal occurred at about 12:00 LST, which began transporting compounds from the urban parts of the DFW area, to the east. When such reversals occur, it is likely that the air mass has further entrained emissions.

The cause of high eight-hour ozone is most likely the combinations of emissions from Fort Worth (and other parts of the DFW area) and the Barnett Shale, due to the wind reversal. However, there is not enough evidence to suggest that the Barnett Shale emissions alone raised ozone concentrations enough to exceed the ozone standard. The peak eight-hour concentration on the day was about 70 ppb when winds were from the west.

Investigation of compounds that act as tracers for emissions sources provided further corroboration. Benzene and toluene were found to co-occur, with strong association with good fit statistics. Despite the wind shift, no noticeable change in regression fit was observed. These compounds were found to arrive from multiple sources, which suggests automobile exhaust.

Examination of n-butane and isopentane suggested two possible sources, one associated with easterly winds, the other with westerly winds. Scatter plots identified two strong sources, and each had good fit statistics. This switch in sources coincides with the shift in wind direction. Findings suggest the west source could be the Barnett Shale signature and the east source could be an urban Fort Worth-Dallas source.

While Eagle Mountain Lake (C75) was the intended focus of this investigation, use of the Ft. Worth Northwest (C13/AH302) auto-GC monitor for part of the analysis does introduce some measure of uncertainty. The Eagle Mountain Lake (C75) and Ft. Worth Northwest (C13/AH302) monitors are approximately 15 miles apart and may or may not be sampling the same air masses. Finally, this analysis only examined one day; more work is needed to support preliminary conclusions presented here.

3.6 Meteorological Characterization and Trends

Ozone formation and transport are greatly influenced by atmospheric conditions, including wind patterns in the lower and upper atmosphere that determine the vertical and horizontal mixing and dispersion of ozone and precursors, altitude of the mixing layer, humidity, temperature, and others.. This section will examine the relationship between ozone and wind fields, including surface winds and upper level winds, and the effect of temperature and low wind speeds on ozone .

Temperatures above 90° Fahrenheit are favorable for increased ozone formation and are common on high ozone days. Figure D-76: *Climatological Temperature Profile at the Ft. Worth Northwest (C13/AH302) Monitor* shows the climatological temperature profile at the Ft. Worth Northwest (C13/AH302) monitor, located in the northwestern part of the DFW area. This site was chosen based on its duration of operation while still being located in the urban portion of the area. The figure plots the record daily maxima and record daily minima for each day, as well as the average of the maxima and minima for each day, over a 30-year period (1980-2009). Average high temperatures typically exceed 90 degrees from mid-June through early September, which includes August when the area typically experiences its highest number of exceedance days (see Chapter 2).

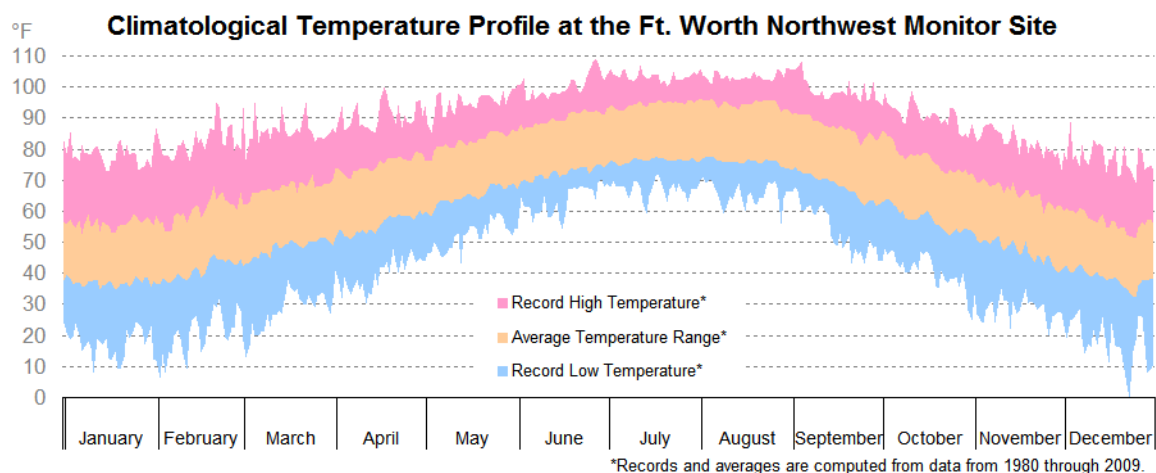


Figure D-53: Climatological Temperature Profile at the Ft. Worth Northwest (C13/AH302) Monitor

While temperature is a familiar measure, and correlates with ozone concentrations, it is not ideal for predicting ozone because it acts as a proxy for ultraviolet radiation, which has a more direct correlation with ozone through photochemistry (see Chapter 1). Figure D-77: *Daily Maximum Temperature and Insolation at the Ft. Worth Northwest (C13/AH302) Monitor* plots temperature and insolation, a measure of incident solar radiation, and reveals the positive correlation between the two.

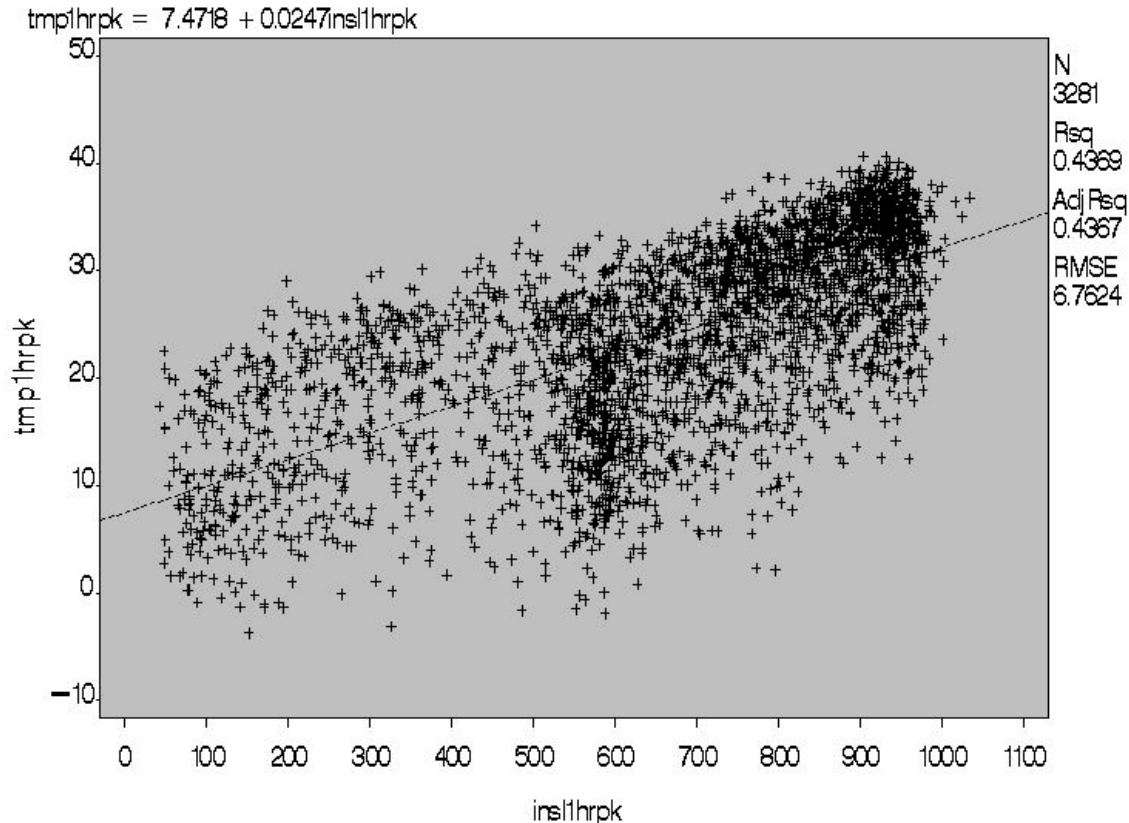


Figure D-54: Daily Maximum Temperature and Insolation at the Ft. Worth Northwest (C13/AH302) Monitor

Figure D-78: *Daily Peak Ozone and Maximum Temperature at the Ft. Worth Northwest (C13/AH302) Monitor* and Figure D-79: *Daily Peak Ozone and Maximum Insolation at the Ft. Worth Northwest (C13/AH302) Monitor* show the similarity between the two measures when plotted against ozone. Both are positively correlated with ozone and both exhibit a non-linear relationship, with higher values of temperature and insolation corresponding to quite elevated ozone concentrations. The R^2 on the ozone-insolation relationship is a bit higher than the ozone-temperature relationship, suggesting just a bit less scatter in the plot.

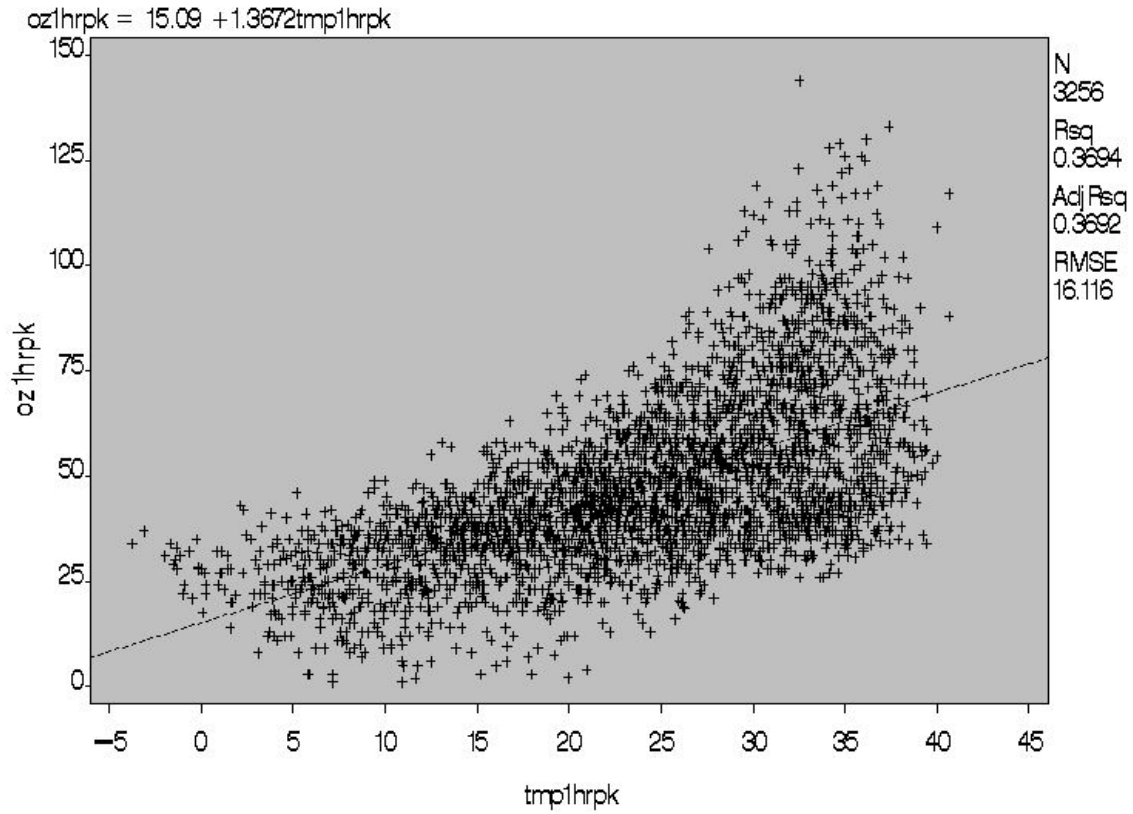


Figure D-55: Daily Peak Ozone and Maximum Temperature at the Ft. Worth Northwest (C13/AH302) Monitor

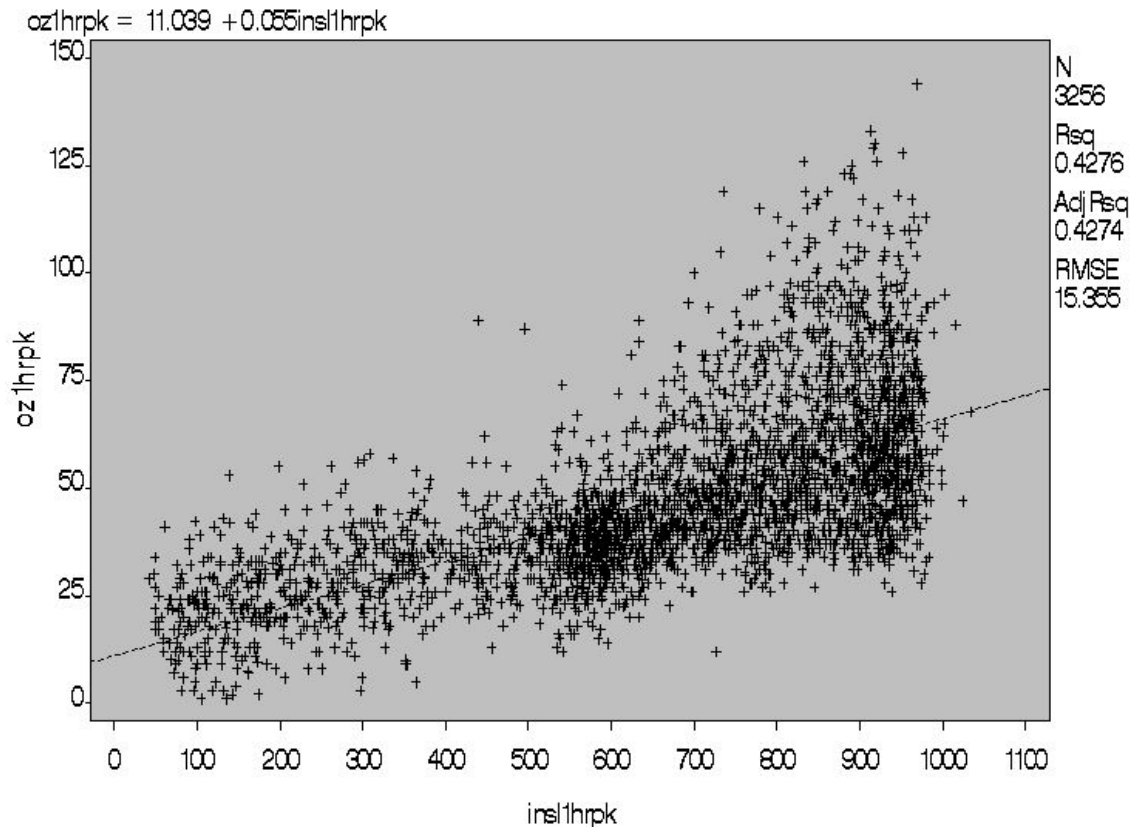


Figure D-56: Daily Peak Ozone and Maximum Insolation at the Ft. Worth Northwest (C13/AH302) Monitor

Wind speed and direction play an important role in ozone formation by affecting mixing and dilution of ozone and ozone precursors. Higher wind speeds tend to dilute precursors and move ozone out of an area. Slower winds can result in stagnation, allowing ozone concentrations to increase in an area as precursors are converted into ozone. Figure D-80: *Wind Climatology in the DFW Area* shows the frequency distribution of daytime winds for March through October, 2000 through 2009. Directions on the x-axis range from 0, which is due north, to 90 (east), 180 (south), 270 (west), and 360, which is back to north again. The colors of the bar segments indicate the frequency with which winds of various speeds were observed from a particular direction.

The figure illustrates that wind speed and direction vary as the season transitions from spring into summer. During May and June, prevailing winds in the DFW area tend to come out of the south and south-southeast with few observations below 5 miles per hour (mph). During July, there is a notable decrease in winds above 15 mph with an increase in winds both in the 5 to 10 mph range and in the calm range (0-5 mph). In August, there is a decrease in wind out of the south with an increase in wind below 10 mph out of the east and southeast. A further decrease in the frequency of wind out of the south is seen in September. The majority of the wind observations in this month is either calm or between 5 and 10 mph, with directions ranging from northerly to southerly. Winds out of the north through east generally indicate continental air masses moving into the area, while winds out of the south and southeast have a larger maritime (i.e., Gulf of Mexico) component to the air mass. In October, wind speed begins to increase again and there are fewer observations of wind out of the northeast.

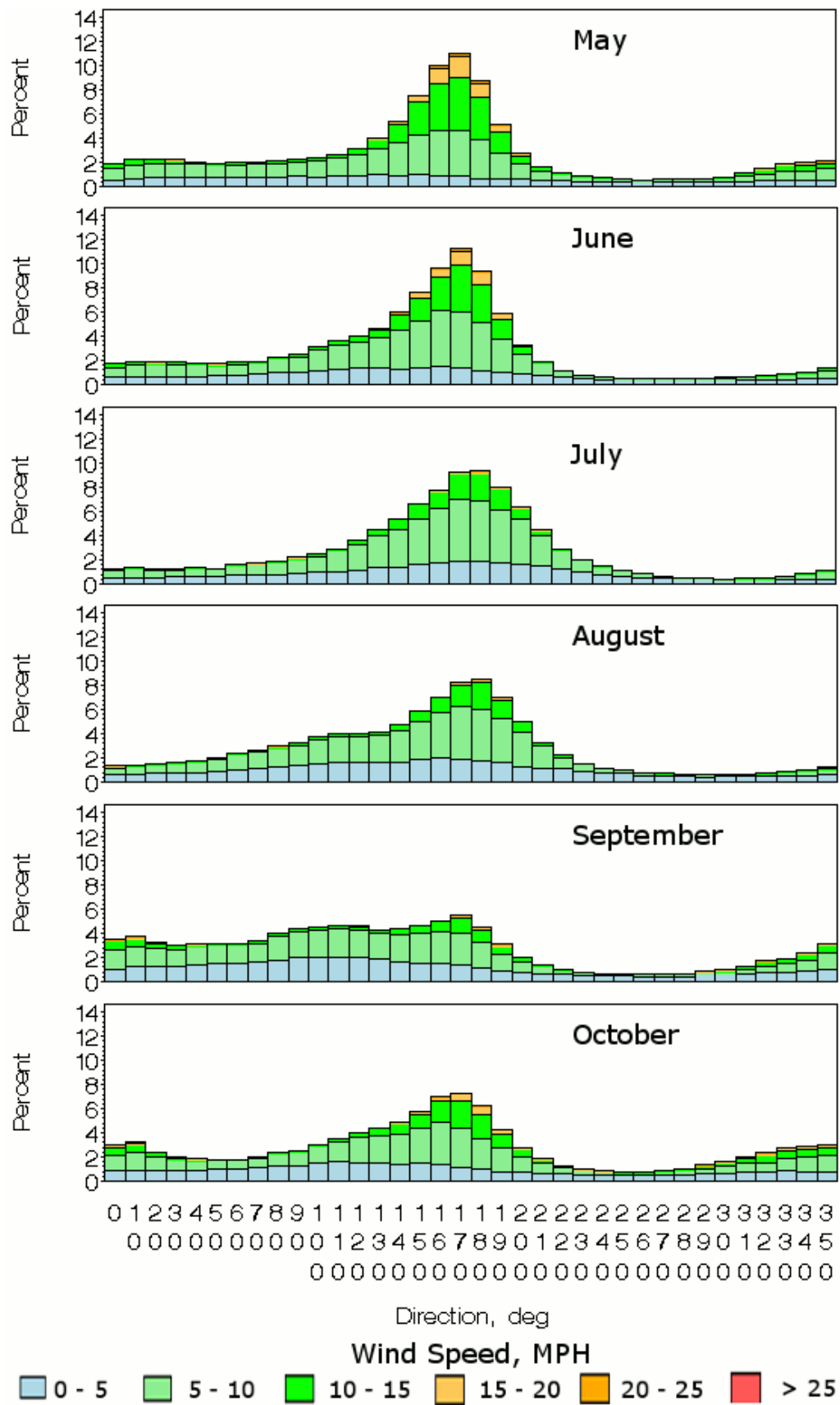


Figure D-57: Wind Climatology in the DFW Area

The topography of the DFW area is mostly flat with no large bodies of water and minimal variation in elevation. This topography contributes to creation of a wind field, or three-dimensional wind system, which is uniform across a large area. This type of wind pattern influences ozone formation and transport in ways that are distinct from areas with hilly topography, mountains, or nearby oceans or gulfs. Meteorological data from surface ETA Data Assimilations System (EDAS) monitors were used to characterize and describe the unique wind field in the DFW area. Data for daytime hours (0700 – 2000 LST), May to October, 2000 to 2009, were used for surface level winds analysis. Only monitors with six or more years of data were included.

Figure D-81: *Wind Speeds by Wind Direction on High Ozone Days* and Figure D-82: *Wind Speeds by Wind Direction on Low Ozone Days* show that surface winds were predominately from the southeast and south-southeast on high ozone days, but mainly from the south on low ozone days. High ozone days are defined as days when any monitor in the DFW area recorded an eight-hour ozone average of 85 ppb or above. Low ozone days are those that did not. Wind speeds were remarkably higher on low ozone days, as expected. On high ozone days, very few winds reach the 10 to 15 mph category while on low ozone days winds can get into the 20 to 25 mph category. Slower wind speeds tend to be more conducive to ozone formation; however, the extent of this relationship is unknown.

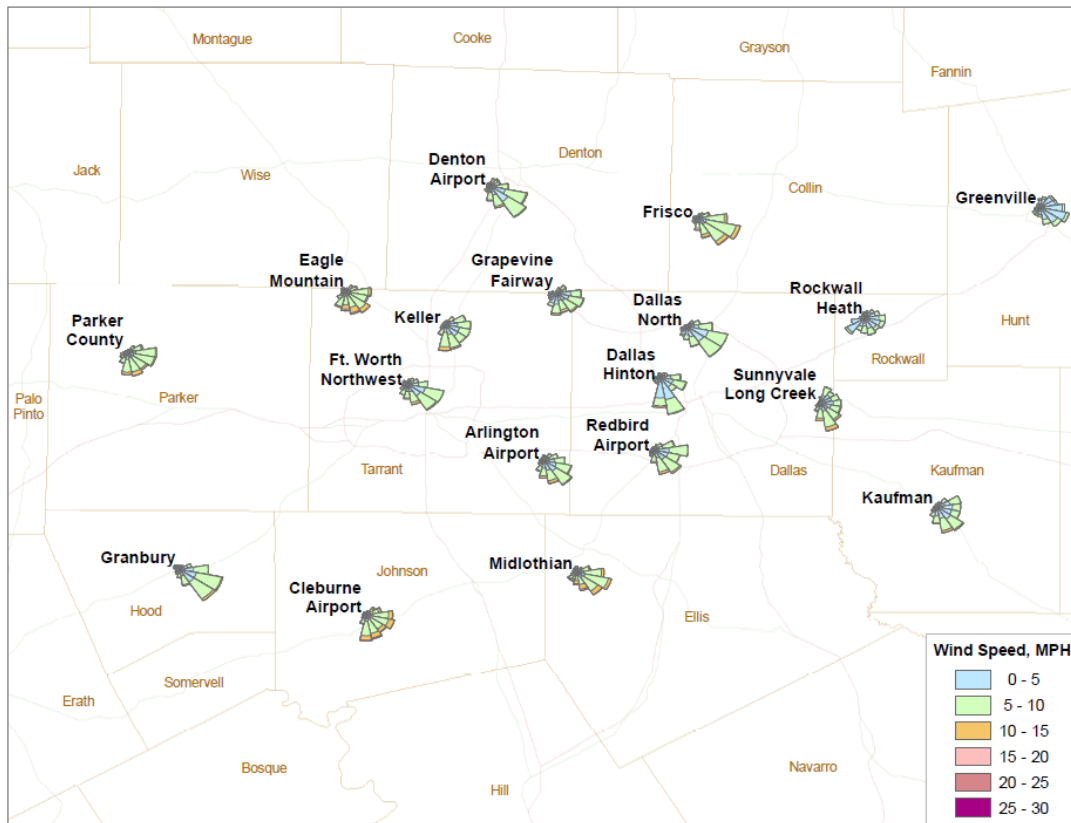


Figure D-58: Wind Speeds by Wind Direction on High Ozone Days

Site Name	Years of Data	Predominate wind direction on high days (O3 ≥ 85 ppb)	Average wind speed on high days (mph) (O3 ≥ 85 ppb)	Predominate wind direction on low days (O3 < 85 ppb)	Average wind speed on low days (mph) (O3 < 85 ppb)
Sunnyvale Long Creek C74	2000 - 2006	SE	5.61	S	8.38
Denton Airport South C56/A163/X157	2000 - 2009	SE	5.58	S	7.11
Granbury C73/C681	2000 - 2009	SE	5.22	SE	6.66
Greenville C1006/A198	2003 - 2009	SE, E	3.54	S	5.00
Cleburne Airport C77/C682	2000 - 2009	S, SE, E	7.18	S	9.68
Kaufman C71/A304/X071	2000 - 2009	SE	4.86	S	6.58
Parker County C76	2000 - 2009	S, SE, E	6.24	S	7.98
Rockwall Heath C69	2000 - 2009	SW, S, SE, E	3.97	SW	5.59
Eagle Mountain Lake C75	2000 - 2009	SE	6.97	S	9.65
Ft. Worth Northwest C13/AH302	2000 - 2009	SE	5.28	S	7.43
Keller C17	2000 - 2009	S	5.37	S	7.46
Grapevine Fairway C70/A301/X182	2000 - 2009	S, SE, E	5.07	S	6.97
Arlington Municipal Airport C61	2002 - 2009	SE	5.51	S	8.35
Midlothian Tower C94/A305/X158*	2000 - 2007	SE	6.90	S	10.04
Midlothian OFW C52/A137*	2006 - 2009				

The above figures also suggest that surface winds on high ozone days tend to arrive from a south to southeast direction. On low ozone days, surface winds have a more southerly component. The wind analysis shows that both upper level and surface level winds are generally uniform over the area. High ozone days tend to have slower winds that come from a southeasterly direction while low ozone days tend to have faster winds that come from a more southern direction.

3.7 Summary of Recent Findings in Local Ozone Dynamics

An investigation of geographic patterns in ozone reveals that, while ozone concentrations in the DFW area have been decreasing, the same geographic areas tend to experience the highest ozone concentrations year after year. The highest levels of ozone typically occur in the northwestern part of the region. This is largely due to the southeasterly direction of prevailing winds on high ozone days, which slowly advect ozone and precursors over populated areas, where they mix and accumulate before reaching the northwest.

Kriging showed that both peak eight-hour ozone concentrations and peak NO_x concentrations have been declining across the region since 2002. Despite the reductions in severity, regions that observe the highest and lowest concentrations remain roughly the same. The time of day and location of ozone peaks were shown to differ on high and low ozone days.

Investigation of the ratio between VOC and NO_x revealed a variable pattern across the DFW area. An urban monitor (Dallas Hinton St. (C401)) was found to be VOC limited, while others to the northwest were transitional between VOC limited and NO_x limited. Monitors on the periphery tended to measure NO_x-limiting conditions. These findings mean that different photochemical processes likely dominate in different regions of the modeling domain. An analysis using MAPPER supported this result, showing both the variability in ozone reaction photochemistry across monitors, but also the trend over time toward VOC-limited conditions.

An analysis of ozone exceedances by day of the week was performed to attempt to identify patterns in emission sources. An anomaly on Sundays from 2005 to 2009, that is, noticeably fewer exceedance days than any other day of the week, was not confirmed statistically. Spatial patterns, however, show similar clustering of exceedances in the northwest part of the DFW area on weekdays and weekends.

Extensive analyses of available data from monitors possibly impacted by emissions from the Barnett Shale region failed to confirm its influence on ozone. Positive Matrix Factorization (PMF) identified source profiles from automobiles and drilling activity (crude natural gas and emissions from pipeline compressors). However, analysis of upper level and surface wind trajectories indicated that emissions from drilling activity are rarely encountered east of the Barnett Shale region. A case study of one day, July 1, 2009, found a possible influence of emissions from that region at the Eagle Mountain Lake (C75) monitor, but this was determined to be a rare occurrence.

The local geography, topography and meteorology of the DFW area all contribute to ozone dynamics. The physical environment is described by a relatively flat topography, lack of nearby marine influences, and lack of mountains that might constrain air masses. Winds are predominately from the south and southeast, with the majority from the southeast on high ozone days. Wind speeds tend to be slower in the summer months, when ozone is observed to increase.

4 RECENT FINDINGS IN BACKGROUND OZONE AND OZONE TRANSPORT INTO THE DALLAS-FORTH WORTH AREA

This chapter discusses background ozone and ozone precursor concentrations that are transported into the DFW area from sources outside the region and the state. A better understanding of background and transport phenomena will guide selection of appropriate approaches to state and local control strategy development. Background ozone, defined as ozone that is not produced locally, has been found to vary considerably by geographic region, by season of the year, across years, and by direction of transport (Nielson-Gammon et al., 2005a). Further, background ozone is a substantial contributor to overall ozone levels in the DFW area. When high concentrations of background ozone are transported into the DFW area, local ozone production exacerbates an already high baseline concentration, resulting in greater likelihood of violating the National Ambient Air Quality Standards (NAAQS).

In this chapter, we examine background ozone concentrations at selected monitoring sites, under specific meteorological restrictions, to determine whether a trend across time is apparent. This approach builds on work by Nielson-Gammon (2005a) and others (Camalier 2007, Draxler 2000) and determines that there is no discernible trend in background ozone. An apparent

trend in background ozone, either increasing or decreasing, would have ramifications for local ozone control strategies adopted in the DFW area. Rising background ozone concentrations could overwhelm improvements made through local emission reductions, while falling background ozone concentrations could moderate the amount of local control needed to attain the NAAQS. Further, temporal changes in background ozone complicate modeling by introducing additional complexity in identifying appropriate model input values.

4.1 Background Ozone

Though definitions vary, background ozone usually refers to regional or transported ozone that has not been influenced, or has been influenced only minimally, by emissions from the area of interest within a day or two of the measurement period. In practice, it is difficult to determine whether the area of interest has influenced regional background, especially when air is stagnant or when recirculation occurs, as is often the case during ozone season in Texas. Techniques that account for locally produced ozone and precursors can reduce or minimize their impacts on estimations of background ozone. Currently, the EPA estimates one-hour background ozone to be approximately 40 ppb.

The following definitions and pointers are useful for understanding background ozone and transport:

- Natural background is defined as the ozone concentration that would be present in a location if there were no influences from *any* anthropogenic emissions. Many researchers use this definition of background ozone, though it is very difficult to sample an air mass anywhere on the globe that truly has no anthropogenic influence.
- Regional background ozone is the amount of ozone entering a locality from outside. Background ozone, as measured in Texas, usually means regional background ozone that has (probably) not been influenced by emissions from the city of interest within a day or two of the measurement period. In practice, it is difficult to determine whether the city of interest has influenced the regional background, especially when air is stagnant or recirculating, as is often the case during ozone season in Texas. Usually, this is the definition used when describing background ozone that can actually be measured.
- EPA defines policy-relevant background as the level of a specific pollutant that would exist in the absence of anthropogenic North American emissions of that pollutant and its precursors. EPA's policy-relevant background cannot be measured with certainty in Texas; it can only be estimated by modeling.
- Rule of thumb: Natural background is lower than EPA policy-relevant background, which is lower than regional background.
- Background ozone must be defined carefully. Lacking standardization, studies often use incomparable definitions. Among the definitional differences are such factors as: length of the averaging period (e.g., 1-hour or 8-hour); months examined (e.g., all year, May-September, April-October); monitoring sites chosen as background sites; and use of surface-, aircraft-, or balloon-based measurements. All of these are important factors affecting calculations for background ozone. Sometimes subtle differences in definition can lead to different conclusions (Estes, 2010).

Several analyses were employed to explore regional background ozone. First, various studies from several researchers are presented. Then two analyses from the TCEQ are used to verify the findings from these studies. First, wind directions and forty-eight hour back trajectories were

used to identify and then calculate regional eight-hour averaged background ozone arriving at the boundary of the DFW area. Second, the AQPlot tool, an in-house wind back-trajectory application, was used to develop animations of wind patterns on days when ozone exceeded 85 ppb. These animations were then used to identify upwind ozone sources and compute one-hour background ozone for high ozone days.

4.1.1 Regional Background Ozone in the Dallas-Fort Worth Area and Other Eastern Texas Cities

Although fewer background ozone studies have been performed for DFW and the rest of eastern Texas compared to other areas of the state, several important studies with findings about regional background ozone can be applied to the DFW area. Hardesty et al. (2007) estimated regional background ozone from August through September 2006 using airborne LIDAR to examine urban ozone plumes from the DFW and the Houston-Galveston-Brazoria (HGB) areas and comparing those urban plumes to the surrounding air masses. Once plumes from the urban areas were identified, regional background ozone was estimated using ozone observed on the edges of the transects. The study estimated regional background ozone entering Texas from the northeast, southeast, and the Gulf of Mexico. The findings, presented in Figure D-83: *Observed Background Ozone Concentrations in Eastern Texas* demonstrate that regional background concentrations in northeast Texas were considerably higher than background for southeast Texas, or for the Gulf. The results also show that, during August through September 2006, the estimated regional background concentrations commonly exceeded 60 ppb, and occasionally exceeded 85 ppb. Average values of regional background ozone for the different regions in eastern Texas during August through September 2006, summarized in Table D-29: *Background Ozone Concentrations During TexAQS II in 2006 (Hardesty et al., 2007)*, also demonstrate that northeast Texas observes some of the highest background ozone concentrations.

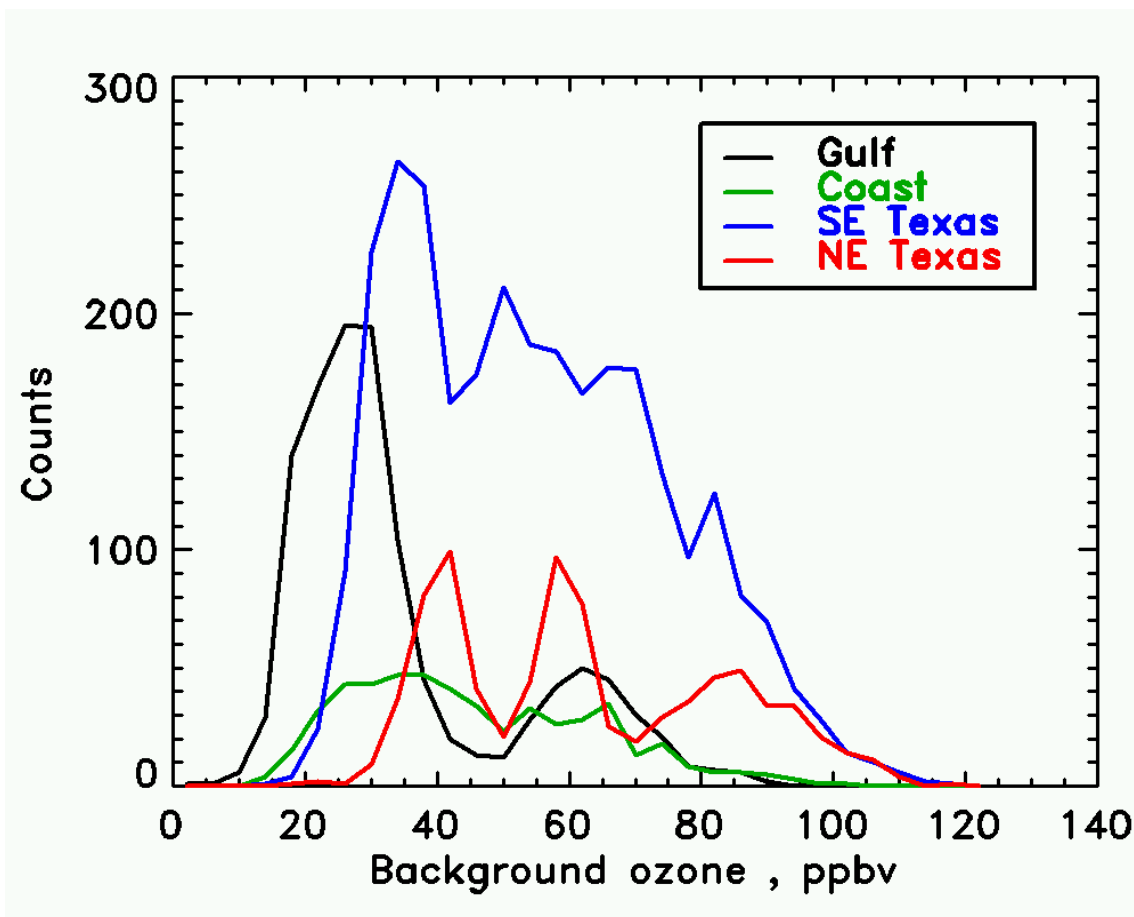


Figure D-1: Observed Background Ozone Concentrations in Eastern Texas

Table D-1: Background Ozone Concentrations During TexAQS II in 2006 (Hardesty et al., 2007)

Region	Background Ozone (ppb)
Gulf of Mexico	39
Gulf Coast	46
SE Texas	51
NE Texas	61

A study by Tobin and Nielsen-Gammon (2010), estimated regional background concentrations with complex multivariate statistical analyses of ozone data from 1998-2007. Figure D-84: *Dallas Ozone from 1998 Through 2007 (black line), Partitioned by Estimated Background Contribution (blue) and Estimated Local Contribution (red)* (Tobin and Nielsen-Gammon, 2010) shows that, for DFW, regional background eight-hour ozone 15-day moving averages were about 40 ppb, with 50 to 55 ppb persisting for most of the summer. Nielsen-Gammon et al. (2005) performed a similar analysis of background ozone for DFW for each year from 1994-2003 (Figure D-85: *Monthly Average Background Ozone (in units of ppm) Estimated for the DFW Area* (Nielsen-Gammon et al. (2005a))), and for other non-attainment and near nonattainment areas in Texas (Figure D-86: *Annual Variation in Regional Background Ozone Estimated for 1998 Through 2003 at Eastern Texas Cities* (Nielsen-Gammon (2005a))), and

found similar results . The results show that background concentrations for cities near the Gulf Coast tend to have lower background concentrations on average than inland cities.

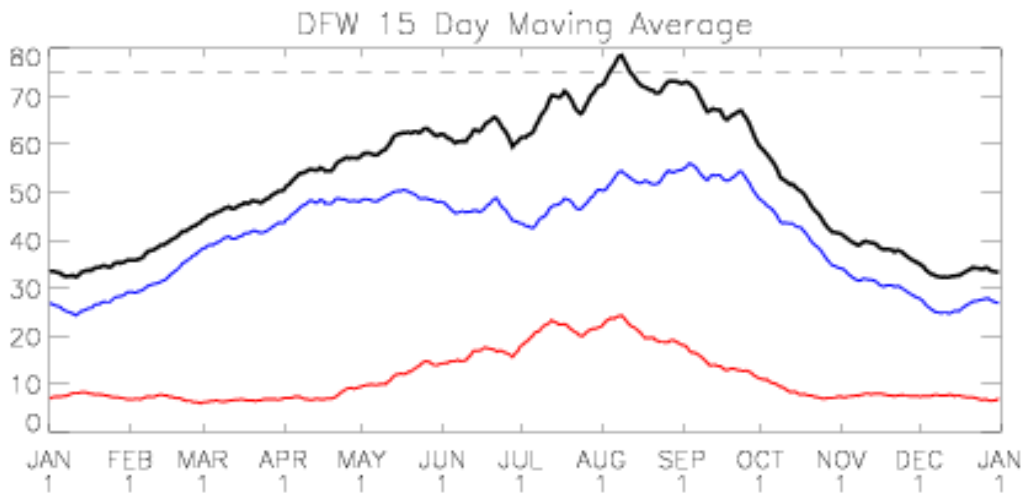


Figure D-2: Dallas Ozone from 1998 Through 2007 (black line), Partitioned by Estimated Background Contribution (blue) and Estimated Local Contribution (red) (Tobin and Nielsen-Gammon, 2010)

DFW Monthly Mean Background Ozone

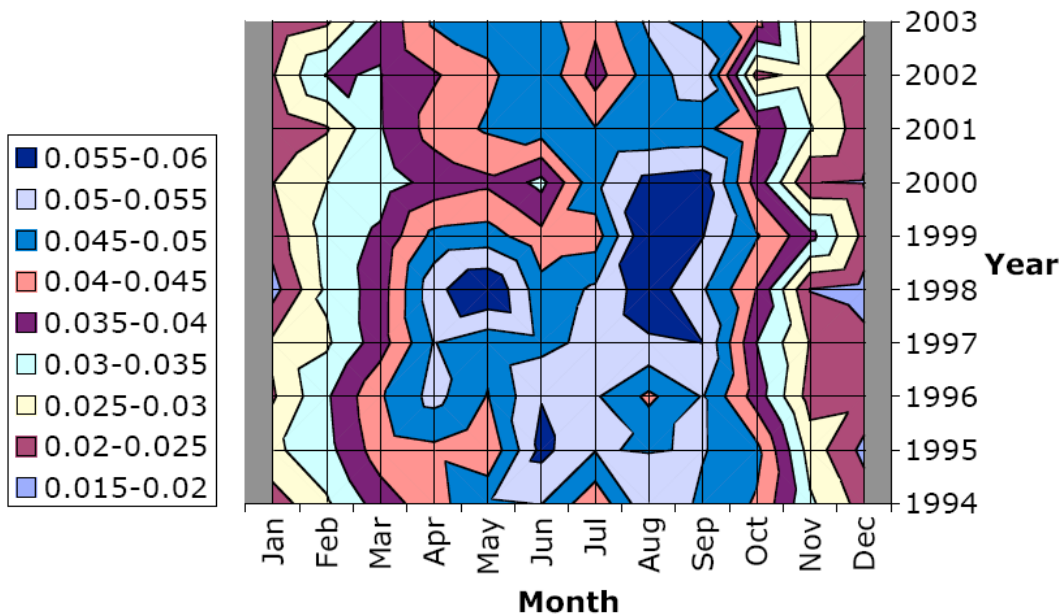


Figure D-3: Monthly Average Background Ozone (in units of ppm) Estimated for the DFW Area (Nielsen-Gammon et al. (2005a))

Background Ozone, 1998-2003

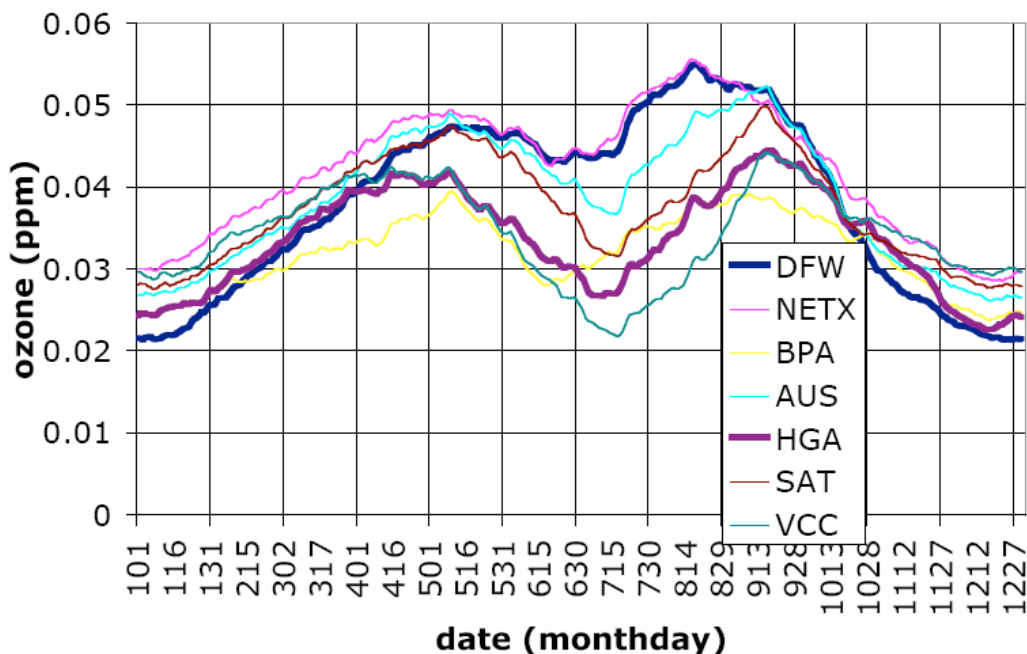


Figure D-4: Annual Variation in Regional Background Ozone Estimated for 1998 Through 2003 at Eastern Texas Cities (Nielsen-Gammon (2005a))

The TCEQ estimates of background one-hour ozone entering Texas from 2000 through 2008 were included in the 2009 SIP submittal for the HGB area (TCEQ, 2010). Table D-30: *Range of Monthly 90th Percentile Daily Peak One-Hour Ozone Concentrations for Subject Wind Directions* displays the estimates of background ozone entering the state of Texas from the east. Variability of monthly medians was relatively large at each site, and percentiles of the distributions showed that variation within each month was also relatively large. Monthly median one-hour ozone concentrations at the southerly sites, SETRPC Mauriceville 42 (C642/C311/C665) and West Orange (C9/A141), varied from about 20 ppbv to 50 ppbv. For the Karnack (C85/AFHP303) site in northeast Texas, background concentrations varied from about 30 ppbv to 70 ppbv. At a fourth site, Hamshire (C64/C654), located between Beaumont and Houston, monthly median one-hour concentrations varied between about 15 ppbv and 40 ppbv. These observations are consistent with the work by Hardesty et al. (2007) and Nielsen-Gammon et al. (2005), in that higher regional background ozone is observed further inland.

Table D-2: Range of Monthly 90th Percentile Daily Peak One-Hour Ozone Concentrations (ppb) for Subject Wind Directions

Year	Hamshire	Hamshire	Karnack	Karnack	SETRPC	SETRPC	West	West
	C64/C654	C64/C654	C85/AF	C85/AF	Mauricevil	Mauricevil	Orange	Orange
	min	max	HP303	HP303	le 42	le 42	C9/A14	C9/A14
			min	max	C642/C31	C642/C31	1 min	1 max
					1/C665	1/C665		
					min	max		
2000	38	74	.	.	56	81	43	83
2001	50	71	.	54	45	69	57	68
2002	51	62	58	84	40	68	53	69

Year	Hamshire	Hamshire	Karnack	Karnack	SETRPC	SETRPC	West	West
	C64/C654 min	C64/C654 max	C85/AF HP303 min	C85/AF HP303 max	Mauricevil le 42 C642/C31 1/C665 min	Mauricevil le 42 C642/C31 1/C665 max	Orange C9/A14 1 min	Orange C9/A14 1 max
2003	30	68	60	64	39	61	38	66
2004	43	71	39	66	30	61	41	66
2005	55	79	62	75	43	76	52	75
2006	45	76	42	78	32	63	43	75
2007	37	62	55	67	40	62	47	69
2008	40	62	.	65	47	70	50	60
9-Yr Period	30	79	39	84	30	81	38	83

Note: Though data has been restricted by wind direction to mitigate influences from nearby pollution sources, there may be unknown influences that are unaccounted for. Maximum values for each year are highlighted in boldface type.

Based upon these few studies, regional background ozone in eastern Texas appears to increase with distance from the Gulf of Mexico. One-hour regional background ozone concentrations higher than 60 ppbv have been observed along the Louisiana-Texas border, including a few excursions above 85 ppb. These studies also showed that the level of background ozone varies greatly during the ozone season. Regional transport studies indicate that easterly and northerly flow is, on average, associated with higher background concentrations than southerly flow. In DFW, regional background ozone appears to comprise a greater percentage of the observed maximum concentrations than in the HGB area.

4.1.2 Estimating Regional Background Ozone

Characterization of regional background ozone for the DFW area was performed using ozone and wind directions from four monitors located on the perimeter of the DFW area. Data were restricted to wind direction windows that ensured that observed ozone was being transported from upwind sources outside the area. These restrictions were necessary to minimize the influence of local ozone and ensure that observed ozone most closely represented regional background ozone. Only data from May through September, the peak ozone season in the DFW area, were considered. The monitor location, name, and wind directions used are presented in Table D-31: *Perimeter Monitors Selected for Background Analysis*; and Figure D-87: *Regional Background Ozone Monitors and Wind Direction Windows* displays these monitors on a map.

The four selected perimeter monitors, Kaufman (C71/A304/X071), Eagle Mountain Lake (C75), Pilot Point (C1032), and Italy (C1044/A323) allow a more accurate analysis of the regional background ozone because they exclude emissions from most of the major NO_x sources in the area. Because NO_x can quickly be transformed into ozone under the right conditions, it is imperative that local NO_x sources be avoided. Other monitors in the DFW area were deemed to be too influenced by local NO_x emissions to provide acceptable estimates of background ozone. Two of the four monitors used observe ozone arriving from the north and northwest; the two others monitor ozone coming from the south and southeast.

Table D-3: Perimeter Monitors Selected for Background Analysis

Site (CAMS number)	AIRS code	County	Operational Since	Directional Window
Eagle Mountain Lake (C75)	484390075	Tarrant	June 6, 2000	300° – 360°
Italy (C1044/A323)	481391044	Ellis	August 31, 2007	90° – 240°
Kaufman (C71/A304/X071)	482570005	Kaufman	September 11, 2000	90° – 180°
Pilot Point (C1032)	481211032	Denton	May 3, 2006	300° - 360°, 0° - 60°

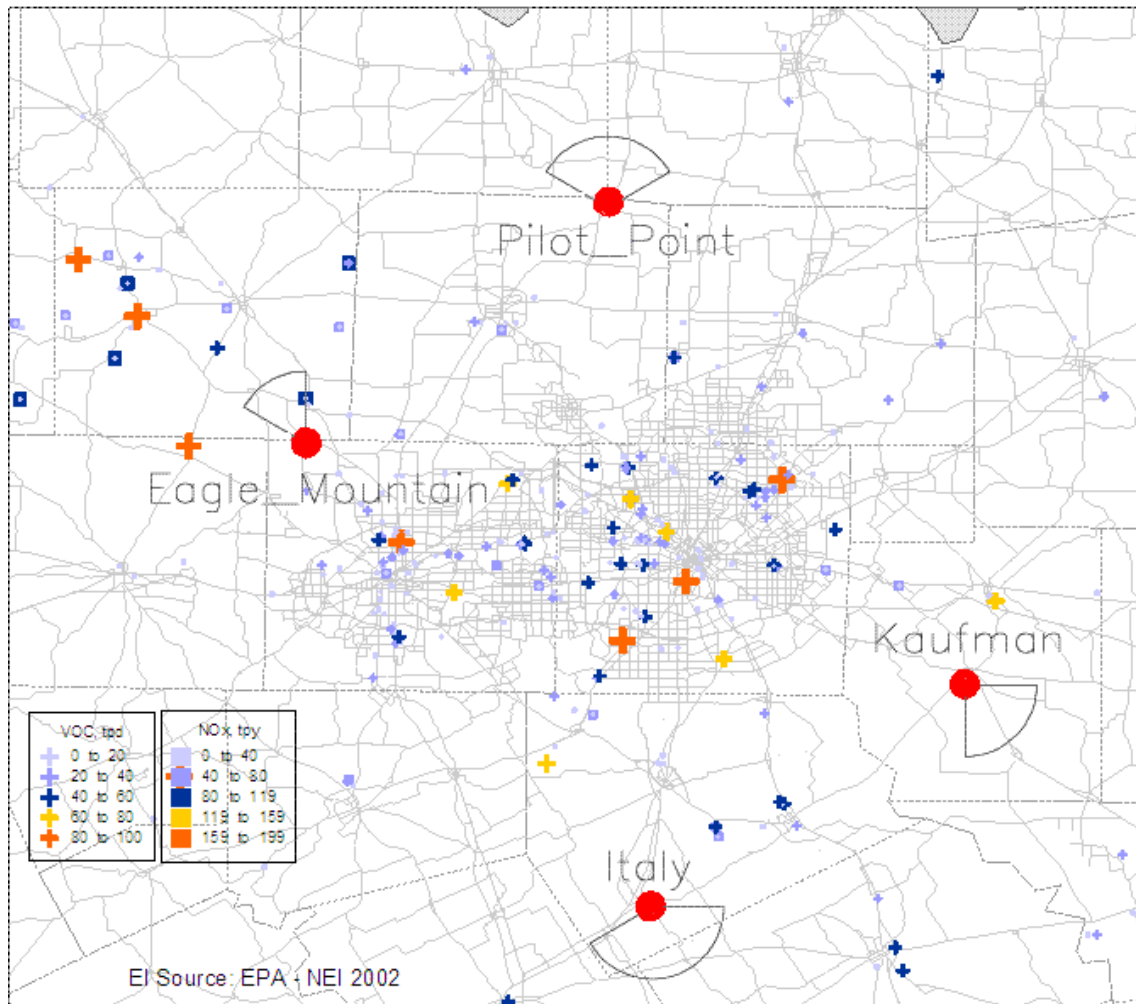


Figure D-5: Regional Background Ozone Monitors and Wind Direction Windows

From these observations, the highest one-hour ozone observation during a 24-hour period was chosen as the peak hour for that monitor. An eight-hour average was then calculated using ozone concentrations from seven hours before the peak hour up through the peak hour. In addition, wind directions during that eight-hour period had to fall within the restricted wind window for all eight hours. Using an eight-hour average for background ozone provides a measure that is comparable to the eight-hour design value. To account for any recirculation and stagnation occurring in the area, eight-hour averages were only included if the 48-hour

backward trajectories from those sites at a height of 80 meters met a 0.8 sinuosity (straightness) criterion and also had a total trajectory length of 150 kilometers over that 48-hour period. See sinuosity discussion in section 4.2 for more information.

A summary of the results for each monitor is displayed in Table D-32: *Summary Statistics for Background Ozone at Kaufman (C71/A304/X071)*, Table D-33: *Summary Statistics for Background Ozone at Eagle Mountain Lake (C75)*, Table D-34: *Summary Statistics for Background Ozone at Pilot Point (C1032)*, and Table D-35: *Summary Statistics for Background Ozone at Italy (C1044/A323)*. The tables show that the maximum eight-hour ozone is much higher at Kaufman (C71/A304/X071), which represents ozone coming from southeast of the DFW area, compared to the other monitors. As shown in Chapter 3, southeasterly winds are the predominant winds on high ozone days in the DFW area.

Table D-4: Summary Statistics for Background Ozone at Kaufman (C71/A304/X071)

Year	Restricted Days	Days in Ozone Season	Max Eight-Hour Ozone Value	Average One-Hour Wind Speed	Max One-Hour Wind Speed
	#	#	<i>ppb</i>	<i>mph</i>	<i>mph</i>
2001	62	153	112	7.02	18.30
2002	61	153	122	6.08	17.40
2003	54	153	89	6.14	16.40
2004	53	153	91	7.05	15.50
2005	48	153	112	5.53	13.90
2006	45	153	107	6.68	15.50
2007	61	153	101	5.43	16.30
2008	60	153	98	6.52	19.60
2009	53	153	92	5.88	16.00

*All ozone and wind values are based on the restricted days

Table D-5: Summary Statistics for Background Ozone at Eagle Mountain Lake (C75)

Year	# of Restricted Days	# of Days in Ozone Season	Max Eight-Hour Ozone Value	Average One-Hour Wind Speed	Max One-Hour Wind Speed
			<i>ppb</i>	<i>mph</i>	<i>mph</i>
2000	5	153	66	10.03	19.9
2001	2	153	58	6.53	18.9
2002	7	153	82	8.10	23.6
2003	5	153	73	6.34	21.3
2004	8	153	62	5.99	13.3
2005	4	153	63	7.25	19.6
2006	13	153	82	7.07	16.7
2007	2	153	52	6.60	13.9
2008	14	153	77	10.28	23.0
2009	13	153	61	7.88	23.5

*All ozone and wind values are based on the restricted days

Table D-6: Summary Statistics for Background Ozone at Pilot Point (C1032)

Year	# of Restricted Days	# of Days in Ozone Season	Max Eight-Hour Ozone Value	Average One-Hour Wind Speed	Max One-Hour Wind Speed
			<i>ppb</i>	<i>mph</i>	<i>mph</i>
2006	24	153	75	6.12	15.9
2007	15	153	75	6.04	16.9
2008	27	153	78	6.76	21.4
2009	22	153	77	6.32	14.6

*All ozone and wind values are based on the restricted days

Table D-7: Summary Statistics for Background Ozone at Italy (C1044/A323)

Year	# of Restricted Days	# of days in a Ozone Season	Max Ozone eight-hour value (ppb)	Average Wind Speed (mph)	Max one-hour Wind Speed (mph)
2008	55	153	77	7.48	20.7
2009	44	153	72	6.95	16.3

*All ozone and wind values are based on the restricted days

The following three figures present ozone season distributions based on several selected statistics of the directionally restricted data for each of the four selected monitors. Italy (C1044/A323) was omitted because it began operation in August 2007 and thus only has data for two ozone seasons. The median, which provides a measure of the “typical” background ozone entering the DFW area, is around or just under 40 ppb in most years at all four monitors (Table D-36: *Selected Summary Statistics for Three Background Monitors in the DFW Area*). The 90th percentile provides an indicator of the upper range of background ozone concentrations entering the area, while the 10th percentile provides a measure of the lower range.

Figure D-88: *Regional Background Ozone at Kaufman (C71/A304/X071)* shows that at Kaufman (C71/A304/X071), from 2001 to 2009, the 90th percentile background concentration was never below 50 ppb, and exceeded 60 ppb in 2005. This means there were about 15 days per ozone season, every year, when background ozone observed at Kaufman (C71/A304/X071) was greater than 50 ppb. These high values of background ozone illustrate the difficulty facing local areas working to attain ozone NAAQS by controlling local contributions to ozone. The 10th percentile background concentration at Kaufman (C71/A304/X071) ranges from about 23 ppb to 33 ppb, which is in rough agreement with EPA estimates of continental, or non-anthropogenic, background ozone; however, ninety percent of the days in each ozone season observe background concentrations above continental background levels.

As demonstrated in Figure D-89: *Regional Background Ozone at Eagle Mountain Lake (C75)*, background ozone appears to be more variable at Eagle Mountain Lake (C75) during ozone season. The median at Eagle Mountain Lake (C75) ranges from 32 to 50 ppb, while the 90th percentile ranges from about 42 ppb to as high as 70 ppb. The data for this site, however, was limited due to lack of winds from the north to northeast.

The four years of data collected at Pilot Point (C1032), shown in Figure D-90: *Regional Background Ozone at Pilot Point (C1032)*, have median background ozone ranging from 39 to

47 ppb. The 90th percentile background ozone, however, never drops below 50 ppb and never exceeds 60 ppb. Pilot Point (C1032) also suffers from low data availability due to the paucity of winds arriving from the northerly direction during ozone season.

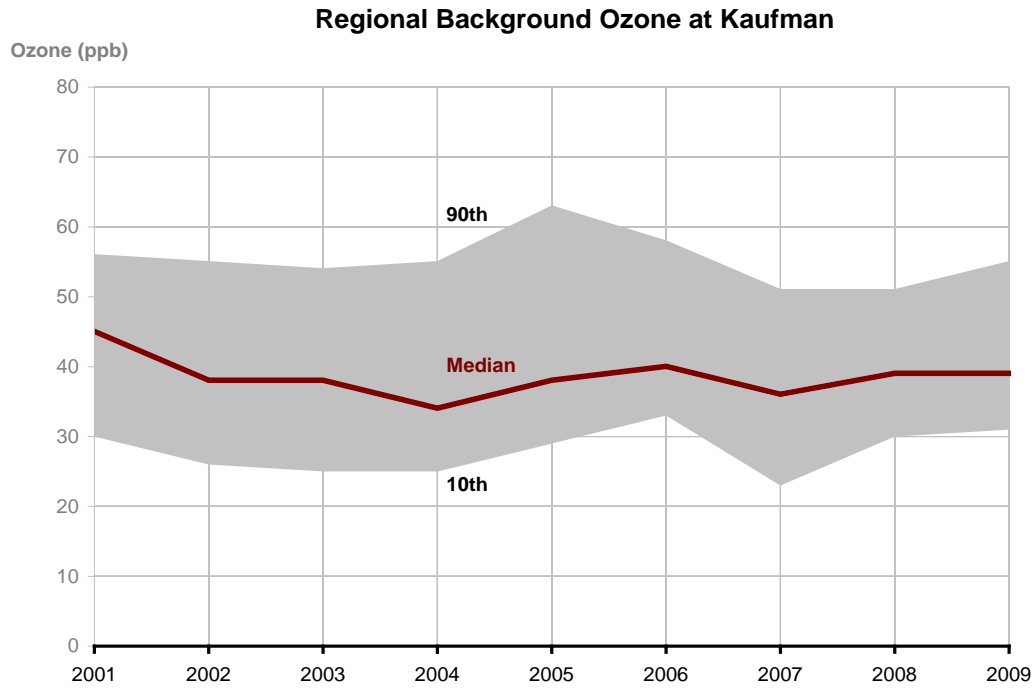


Figure D-6: Regional Background Ozone at Kaufman (C71/A304/X071)

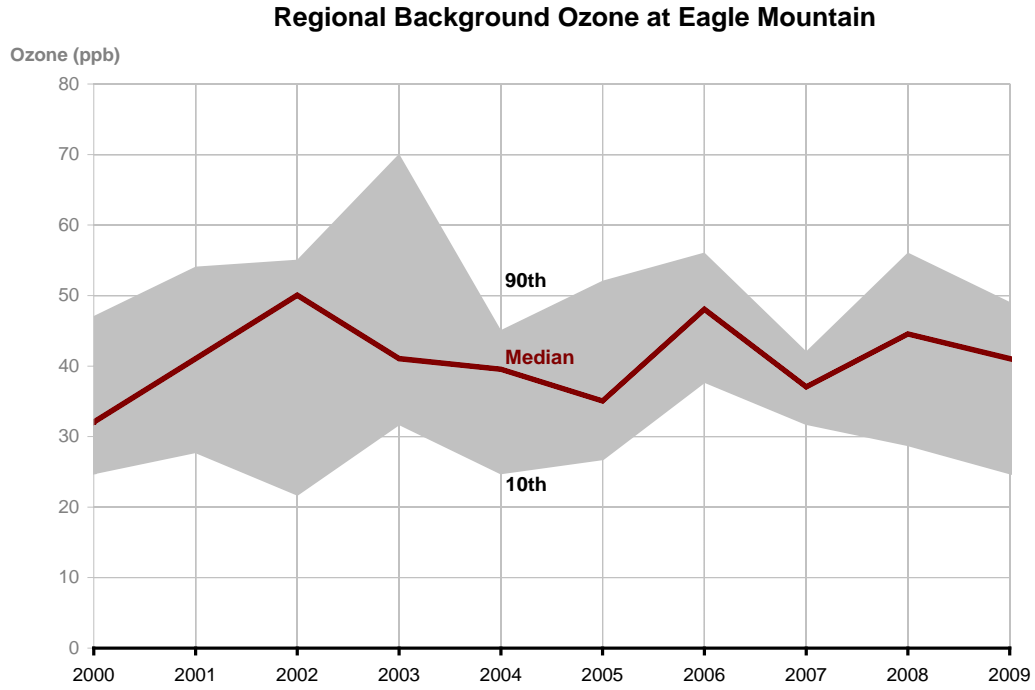


Figure D-7: Regional Background Ozone at Eagle Mountain Lake (C75)

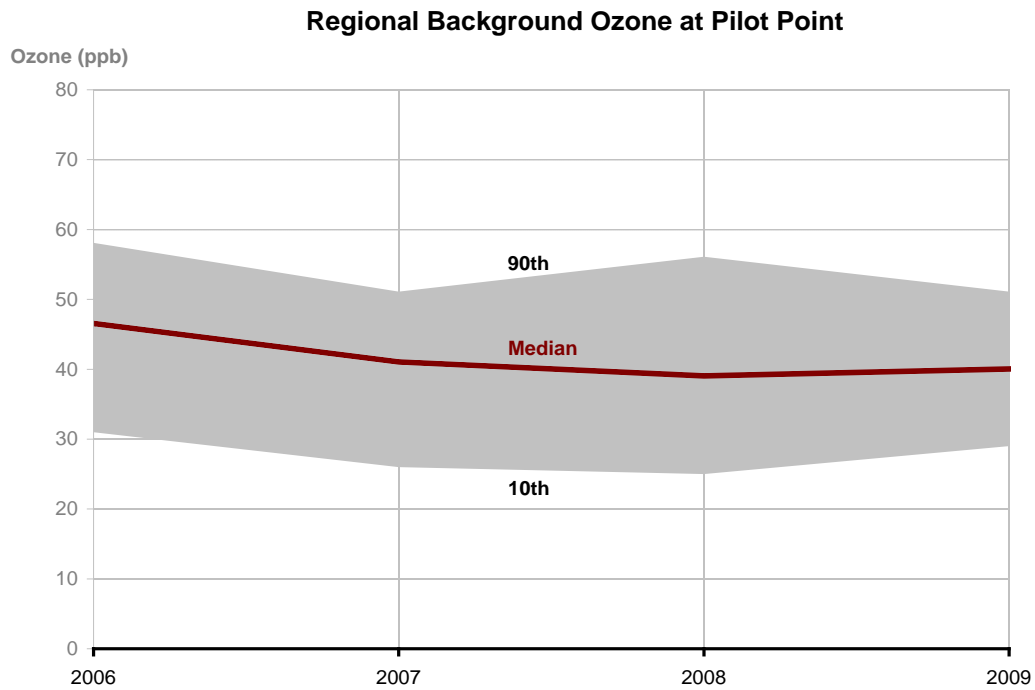


Figure D-8: Regional Background Ozone at Pilot Point (C1032)

Table D-8: Selected Summary Statistics for Three Background Monitors in the DFW Area (ppb)

Year	Kaufman (C71/A304/X071)			Eagle Mountain Lake (C75)			Pilot Point (C1032)		
	10 th	Median	90 th	10 th	Median	90 th	10 th	Median	90 th
2000	-	-	-	25	32	47	-	-	-
2001	30	45	56	28	41	54	-	-	-
2002	26	38	55	22	50	55	-	-	-
2003	25	38	54	32	41	70	-	-	-
2004	25	34	55	25	40	45	-	-	-
2005	29	38	63	27	35	52	-	-	-
2006	33	40	58	38	48	56	31	47	58
2007	23	36	51	32	37	42	26	41	51
2008	30	39	51	29	45	56	25	39	56
2009	31	39	55	25	41	49	29	40	51

Linear regressions performed on the median and 90th percentile background ozone values for Kaufman (C71/A304/X071), Eagle Mountain Lake (C75), and Pilot Point (C1032) monitors failed to identify statistically significant trends in these values. This suggests that, although background ozone entering the DFW area is quite variable and dependent on direction, it is neither increasing nor decreasing over time.

4.1.3 Background Ozone on High Ozone Days Versus Low Ozone Days

Differentiating background ozone concentrations on high ozone days from concentrations on low ozone days yields important insight into the characteristics of ozone arriving from upwind sources. For these comparisons, wind restricted background ozone concentrations for the ozone season at the Kaufman (C71/A304/X071) and Pilot Point (C1032) monitors were split into high ozone days (ozone greater than 75 ppb), and low ozone days (ozone less than 75 ppb). Italy (C1044/A323) and Eagle Mountain Lake (C75) monitors had too few observations to produce reliable results.

Figure D-91: *Regional Background Ozone on High vs. Low Ozone Days at Kaufman (C71/A304/X071)* shows the difference between background ozone on high ozone days and low ozone days at the Kaufman (C71/A304/X071) monitor. From 2001 to 2009, background ozone on high ozone days in the DFW area consistently exceeded 50 ppb; however, on low ozone days, the contribution of background ozone in the DFW area never exceeded 40 ppb. On high ozone days, background ozone, on average, was anywhere from 15 to 22 ppb higher than on low ozone days. It is noteworthy that there were single days in 2002, 2005, and 2008 on which the background ozone concentration exceeded 75 ppb. On those days, any contribution of locally produced ozone greater than 9 ppb would have generated an exceedance of the 1997 standard. Further, because the approach employed here has filtered out all days with stagnation and recirculation, these observations of background ozone use only days with relatively straight winds, which would possibly give a low bias to background estimates for high ozone days.

Comparison Between High and Low Ozone Days at Kaufman

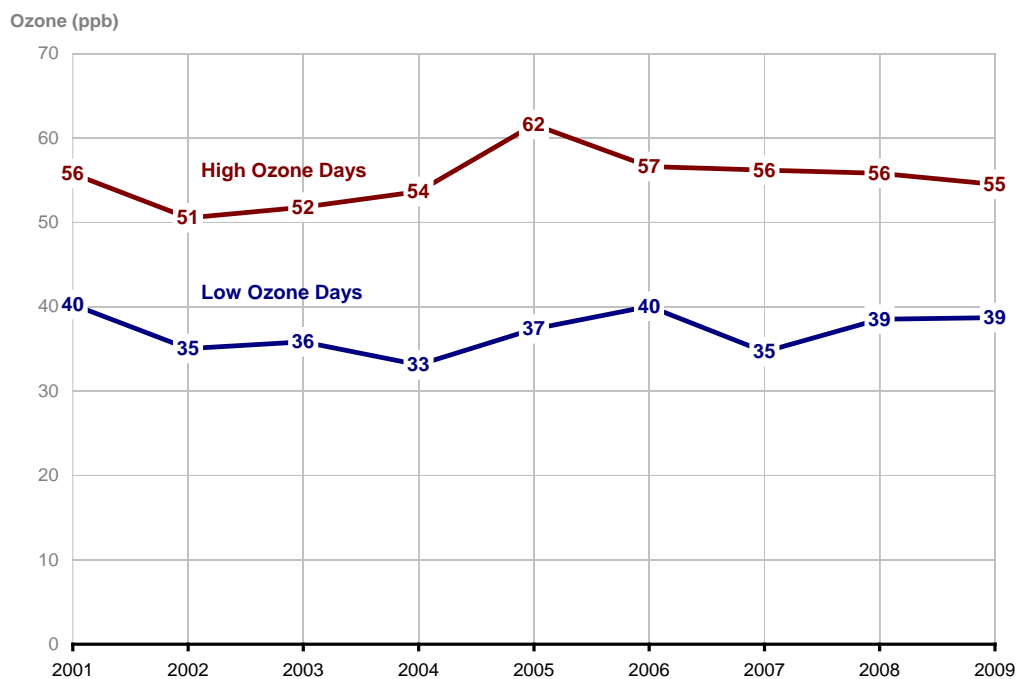


Figure D-9: Regional Background Ozone on High vs. Low Ozone Days at Kaufman (C71/A304/X071)

Results for Pilot Point (C1032), displayed in Figure D-92: *Regional Background Ozone on High vs. Low Ozone Days at Pilot Point (C1032)*, are similar to those at Kaufman (C71/A304/X071), with background ozone concentrations on high ozone days consistently 8 or more ppb higher than those on low ozone days. Pilot Point, however, did not observe any days with background ozone concentrations above 75 ppb. There was only one day in 2008 where Pilot Point (C1032) observed a background ozone concentration higher than 65 ppb; a local contribution in excess of 19 ppb on that day would have generated an exceedance of the 1997 standard.

Comparison Between High and Low Ozone Days at Pilot Point

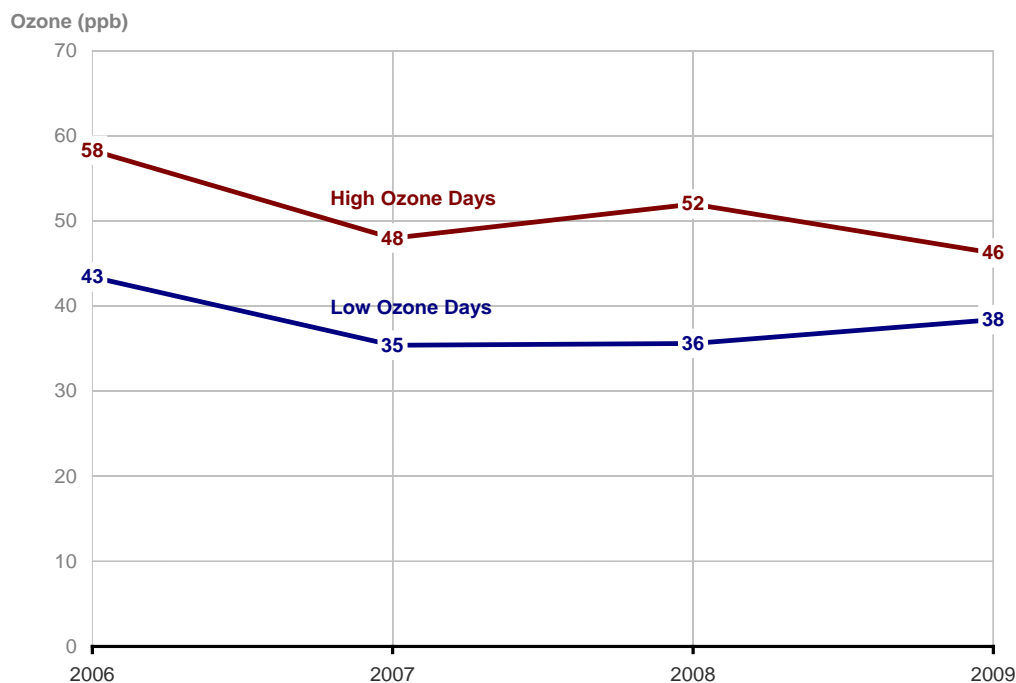


Figure D-10: Regional Background Ozone on High vs. Low Ozone Days at Pilot Point (C1032)

4.1.4 Estimating Background Ozone by Month

An assessment of background ozone over the course of a year enhances understanding of annual cycles. Monthly averages of wind restricted background ozone for 2009 at Kaufman (C71/A304/X071) and Italy (C1044/A323) are presented in Figure D-93: *Monthly Regional Background Ozone at Kaufman (C71/A304/X071) in 2009* and Figure D-94: *Monthly Regional Background Ozone at Italy (C1044/A323) in 2009*. Neither Eagle Mountain Lake (C75) nor Pilot Point (C1032) recorded enough data to use in the analysis, largely due to the lack of winds coming from the north and northwest. Results show that at both Kaufman (C71/A304/X071) and Italy (C1044/A323), background ozone rises from the beginning of the year through March, remains mostly steady until September, then falls. Thus, the greatest contribution from background ozone occurs from March through September, the peak ozone season, in the DFW area.

Results for Kaufman (C71/A304/X071) and Italy (C1044/A323) exhibit background ozone peaks in March, July, and September, which are slightly different from the peak observed in the analysis from Nielsen-Gammon (2005a). Differences between the two approaches, the data used, and the directional restrictions used to mitigate recirculation and stagnation may account for the variation in results.

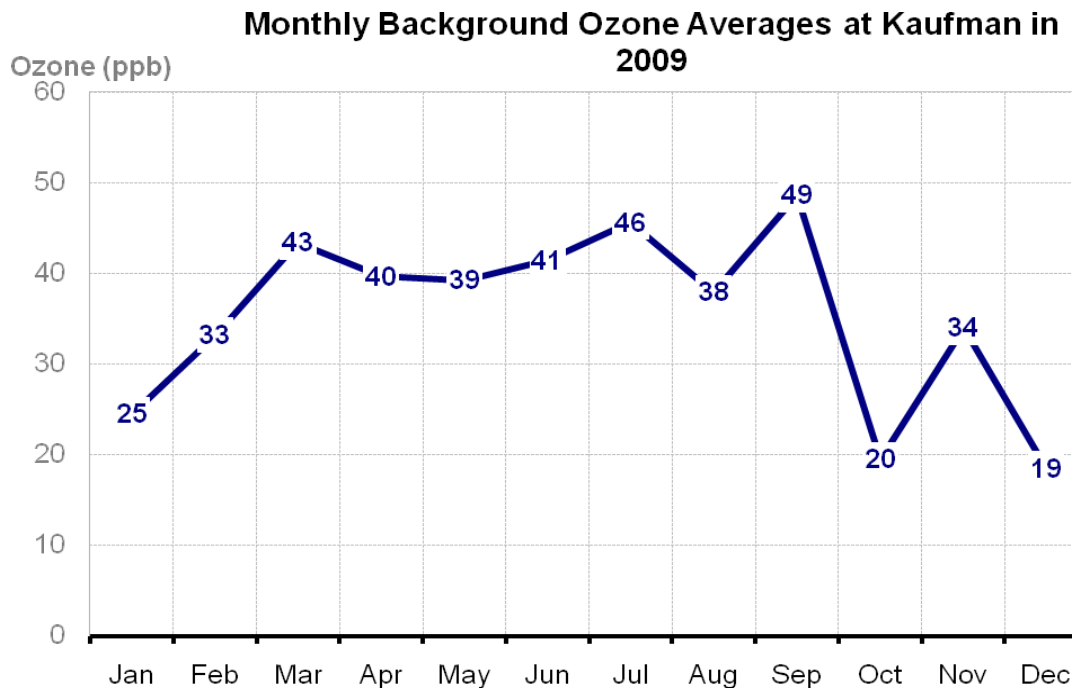


Figure D-11: Monthly Regional Background Ozone at Kaufman (C71/A304/X071) in 2009

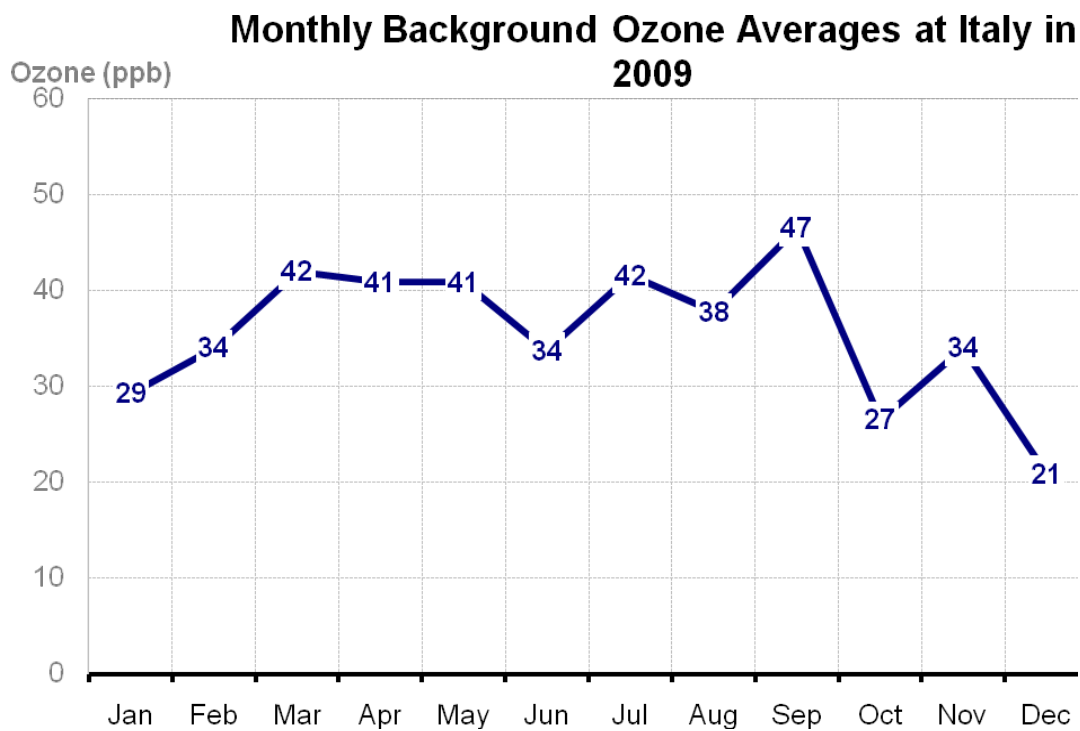


Figure D-12: Monthly Regional Background Ozone at Italy (C1044/A323) in 2009

4.1.5 Estimating Background Ozone Using Trajectories

Another method used to estimate background ozone is an upwind and downwind analysis. This type analysis uses surface trajectories to determine what days had consistent wind directions with no recirculation and then uses those winds to determine the one-hour ozone concentration at a monitor upwind of the region and the one-hour ozone concentration at a monitor downwind of the region. The difference between the upwind and downwind ozone concentrations provides an estimate of the local contribution from the DFW area to total ozone concentrations.

A TCEQ application called AQPlot was used to compute surface wind forward trajectories and plot them, as well as one-hour ozone concentrations, on a map. Figure D-95: *Example AQPlot Image Showing Forward Wind Trajectories (August 10, 2004) in Northeast Texas* shows forward wind trajectories computed using AQPlot. These trajectory plots are combined for each hour to form an animation for each day, then these animations are used to determine which days had straight winds with no recirculation. Figure D-95: *Example AQPlot Image Showing Forward Wind Trajectories (August 10, 2004) in Northeast Texas* presents an example of a day when evidence of recirculation is clearly discernible and Figure D-96: *Example AQplot Image Showing Constant Easterly Flow (August 13, 2004) in Northeast Texas* indicates a day with constant flow out of the east. Because determination of whether or not there was constant flow was done by reviewing the animations, this analysis should not be used alone to determine background ozone concentrations. Data from 2002 through 2006 was used for this analysis because that was the only AQPlot data available at the time of the analysis.

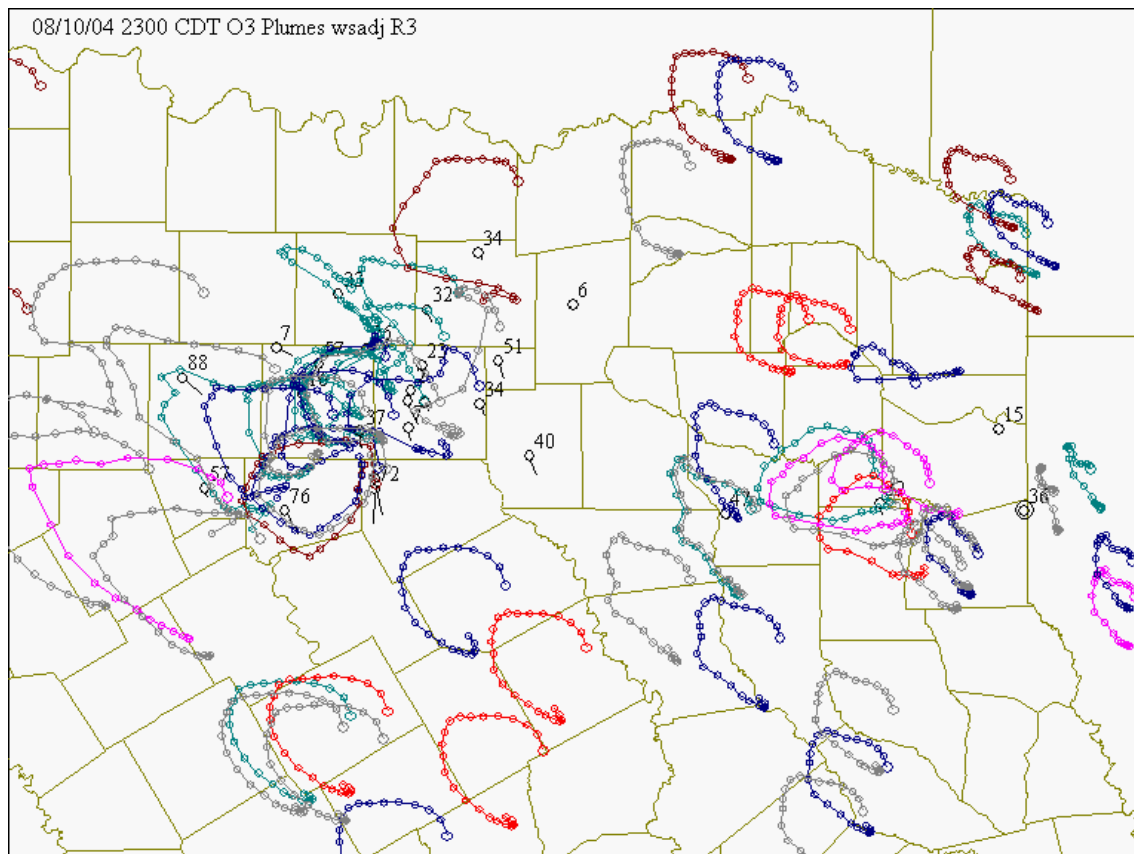


Figure D-13: Example AQPlot Image Showing Forward Wind Trajectories (August 10, 2004) in Northeast Texas

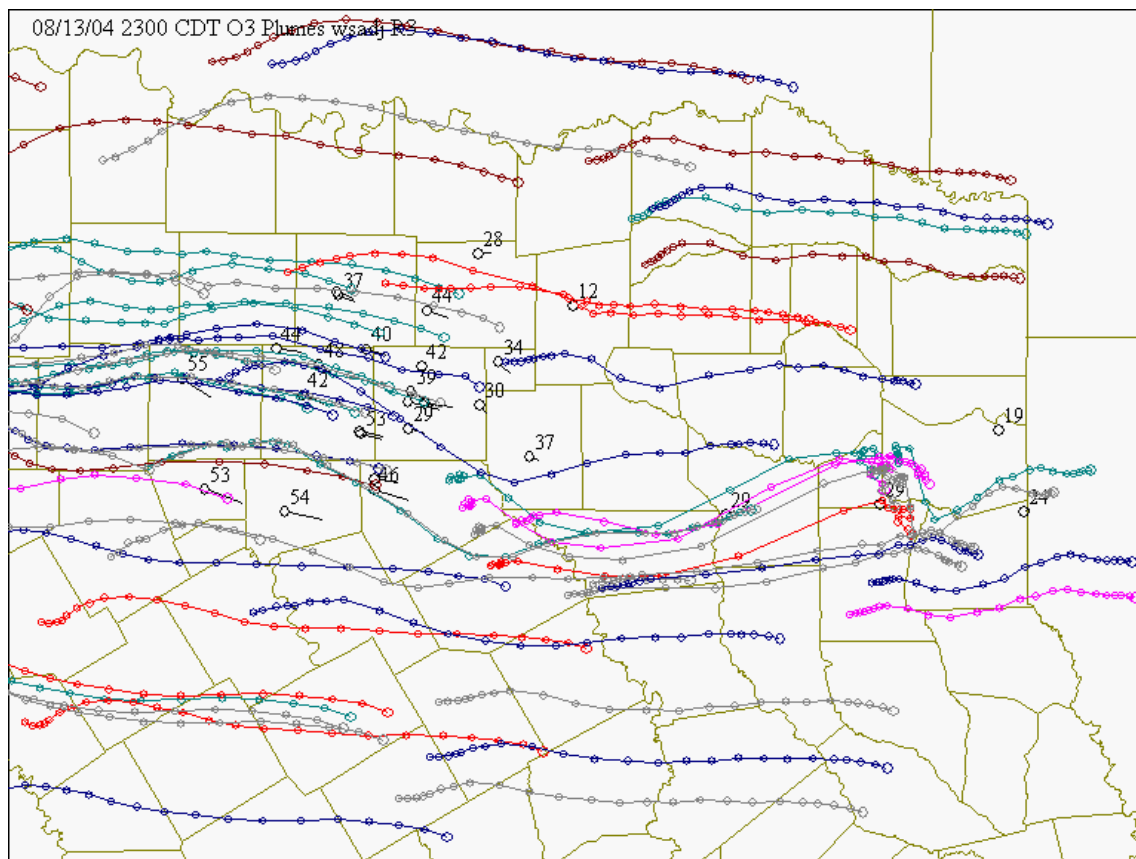


Figure D-14: Example AQplot Image Showing Constant Easterly Flow (August 13, 2004) in Northeast Texas

Table D-37: *Estimated Background and Local Contributions to One-Hour Ozone Concentrations by Wind Direction* shows the upwind, downwind, and local contributions of ozone on days with winds out of the east, southeast, and south. Only these directions are shown because they are the directions with the largest sample sizes. This method produced estimates of background ozone concentrations ranging from 54 to 66 ppb. Of these directions, the lowest background ozone concentrations, 54 ppb on average, tend to occur when the wind is out of the south. Background concentrations on days when wind was coming from the east had the highest average concentration of 66 ppb. Local contribution showed little dependence on wind direction, ranging from a low of 40 ppb on days when the wind was out of the southeast to 43 ppb when winds were out of the south. From this analysis, one-hour ozone concentrations entering the Dallas-Fort Worth area typically range from 40 to 75 ppb with concentrations in the low 60s being most frequent.

Table D-9: Estimated Background and Local Contributions to One-Hour Ozone Concentrations by Wind Direction

	East			Southeast			South		
	Up wind	Down wind	Local Contrib.	Up wind	Down wind	Local Contrib.	Up wind	Down wind	Local Contrib.
	ppb	ppb	ppb	ppb	ppb	ppb	ppb	ppb	ppb
	69	104	35	39	83	44	65	91	26
	68	124	56	56	92	36	47	100	53
	65	99	34	68	112	44	60	97	37
	66	102	36	68	102	34	46	91	45

	<u>East</u>			<u>Southeast</u>			<u>South</u>		
	Up wind	Down wind	Local Contrib.	Up wind	Down wind	Local Contrib.	Up wind	Down wind	Local Contrib.
	<i>ppb</i>	<i>ppb</i>	<i>ppb</i>	<i>ppb</i>	<i>ppb</i>	<i>ppb</i>	<i>ppb</i>	<i>ppb</i>	<i>ppb</i>
	50	91	41	66	95	29	50	105	55
	75	130	55	75	112	37			
	66	105	39	55	103	48			
				66	105	39			
				68	120	52			
				55	98	43			
				57	90	33			
				55	100	45			
Mean	66	108	42	61	101	40	54	97	43

4.2 Transport Wind Trajectories

A thorough assessment of background ozone must include an evaluation of upper altitude winds to supplement our understanding of surface level patterns. Winds at high altitude can transport ozone from sources far upwind of the region. Mixing and subsidence can bring this ozone from the upper atmosphere into the surface layer. Assessing the contribution of these high-level transport winds enhances our understanding of the meteorological factors determining ozone generation, transport, and fate in an area.

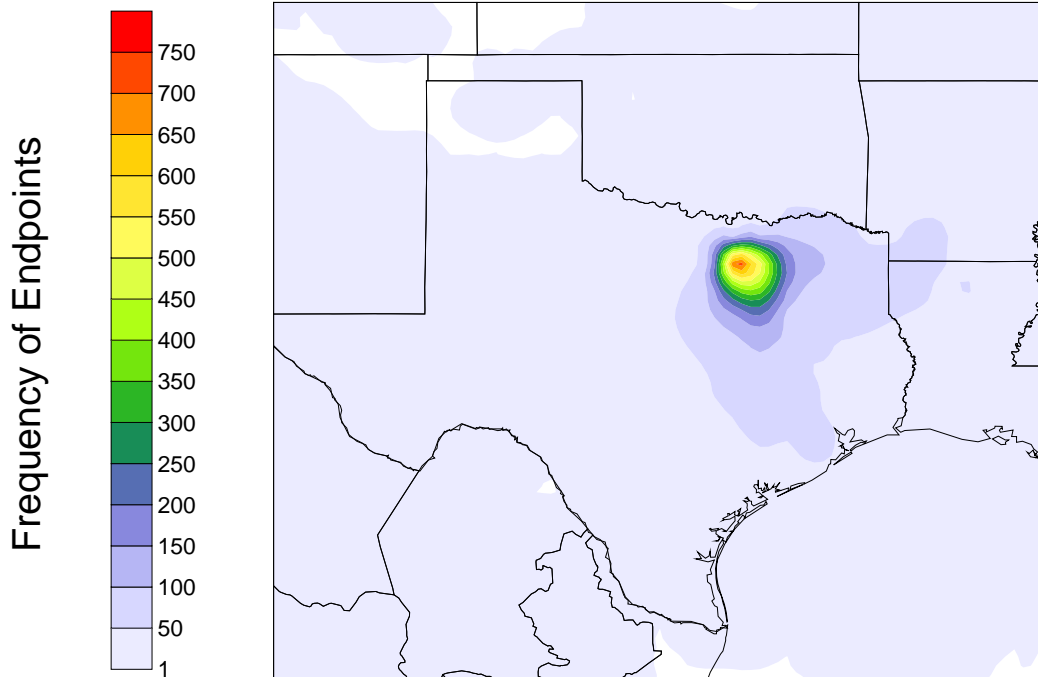
While surface level winds can be analyzed using data from ground level monitors, transport trajectories require techniques that are more advanced. Transport winds are modeled in this analysis with Hybrid Single Particle Lagrangian Integrated Trajectory (HYSPPLIT) model 48-hour back-trajectories at 800 meters altitude, for May through October, 2000 to 2009. HYSPPLIT performs forward and backward trajectory modeling, and is available on the web site of the National Oceanic and Atmospheric Administration (NOAA) (ready.arl.noaa.gov/HYSPPLIT.php). HYSPPLIT reports coordinates of the hourly end points of trajectory segments. Distances between each trajectory hour endpoint were summed to calculate a total length and the deviation of the actual path taken from the shortest possible path (sinuosity) was calculated.

Ozone season months were used in this analysis because they are not often influenced by synoptic cold fronts. Start times were set at 20:00 GMT (03:00 LST) to coincide with the median time of the ozone peak occurrence for high ozone days. Because of its central location in the DFW area, the Dallas Hinton St. (C401/C60/AH161) monitor was chosen as the arrival location for the estimated trajectories.

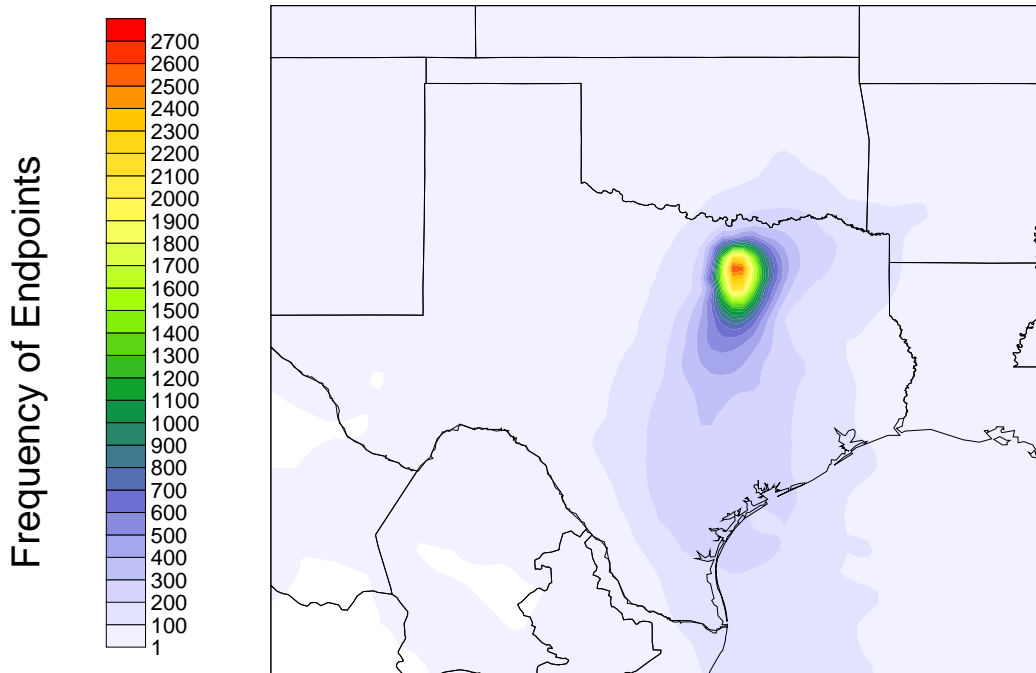
Figure D-97: *High Ozone Versus Low Ozone Back Trajectory Density* shows density plots of the frequencies of end points of the hourly segments of the backward trajectories, separated into high ozone days (days when any monitor in the DFW area recorded eight-hour ozone concentration at or above 85 ppb) and low ozone days (days when no monitors recorded an eight-hour ozone concentration at or above 85 ppb). On high ozone days, trajectory lengths tend to have a more easterly and southeasterly direction. Trajectory lengths on those days also tend to be shorter, signifying that wind speeds are slower. Trajectories for low ozone days tend to be longer, signifying higher wind speeds. Wind directions on low ozone days tend to have a more northeasterly or southerly direction, with only a slight westerly component. These trajectories appear to corroborate results from the analysis of surface winds: on high ozone days, wind speeds in the DFW area are slower and from the southeast.

Trajectory Density for the DFW region

Years of 2000 - 2009 at height of 800 meters
Start time 20:00 GMT (Greenwich Mean Time)
48 Hours Back Trajectories centered at Hinton



Days where Ozone \geq 85 ppb



Days where Ozone $<$ 85 ppb

Figure D-15: High Ozone Versus Low Ozone Back Trajectory Density

Measures of sinuosity, or “curviness,” of the trajectory of an air parcel can be used to determine its original source (Nielson-Gammon, et al, 2005a). When winds are straighter, or less sinuous, source identification is enhanced because there is less variability, and thus less uncertainty, in computations of originating directions. This section investigates the sinuosity of winds, specifically transport winds, traveling into the DFW area to determine whether these winds varied from year to year. Variability in transport winds across years could complicate determination of regions contributing background ozone to the DFW area, and, thus obscure selection of appropriate model input values for background ozone.

For purposes of this analysis, transport winds are defined as high elevation winds capable of moving air masses over long distances. These winds can carry pollutants from one area to another and affect local ozone concentrations (Cooper et al., 2006). A measure of sinuosity used by Xie and Berkowitz (2005) can be computed for a trajectory using wind speeds and directions. Sinuosity of transport winds (S) is calculated as the tip-to-tip (start point and end point) length (D_{t2t}) of a 48-hour trajectory – i.e., the distance from one tip to the other, “as the crow flies” – divided by the sum of intra-distances between adjacent hourly endpoints for the same trajectory (sum of D_i , for i hours):

$$S = \frac{D_{t2t}}{\sum D_i}$$

When D_{t2t} equals D_i , the trajectory is straight and the sinuosity equals one, the highest possible value. As a trajectory becomes less straight, that is, as $\sum D_i$ increases with respect to D_{t2t} , the sinuosity increases and S becomes smaller. This is depicted in Figure D-98: *Comparison of Two Trajectories, One More and One Less Sinuous*, which compares a trajectory with sinuosity equal to 1.0 (the straight trajectory) with one with a sinuosity equal to 0.8 (the curved trajectory). For the straight trajectory, the numerator and denominator of the above equation are the same. For the curved trajectory, the numerator is the total distance of the straight trajectory, while the denominator is the total distance of the curved trajectory, summing the lengths of all intermediate segments. Higher sinuosity values, therefore, correspond to straighter winds.

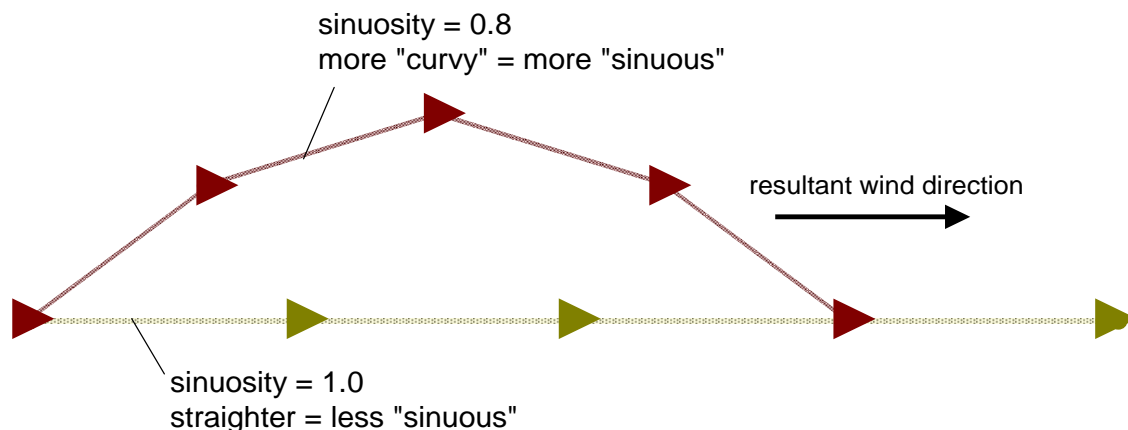


Figure D-16: Comparison of Two Trajectories, One More and One Less Sinuous

The jagged trajectory (red line) is more sinuous, S is smaller ($S = 0.85$), than the straight trajectory (khaki line) where S is larger ($S = 1.0$).

The two groupings of days, high ozone and low ozone days, resulted in distributions that were not statistically normal. Because of this non-normality, a non-parametric test, the Wilcoxon Means Test, was performed to check equality of trajectory length mean and sinuosity mean. Sample lengths and sinuosity were found to be statistically different at the five percent level ($\alpha=0.05$). This suggests that different meteorological patterns prevail for high altitude transport winds on high ozone days, compared to low ozone days, in the DFW area.

On days when eight-hour ozone is at or above 85 ppb, mean trajectory length was 874.60 km and sinuosity is 0.69. On low ozone days, the mean trajectory length was 1,288.12 km and sinuosity was 0.75. Trajectory lengths were shorter on high ozone days with lower sinuosity, implying that winds are slower and more stagnant on those days. On low ozone days, however, trajectory lengths were longer and sinuosity was higher, signifying that winds are faster and have less circulation.

Further work is necessary to link these results to observed ozone concentrations. The complexities of the effects of sinuosity on ozone concentrations are copious. Regarding local ozone production, it is not entirely clear from the available research that straighter winds correspond to higher ozone concentrations, due to the absence of dilution from sources of ozone precursors, or whether the reverse is true, that winds that are more sinuous cause greater mixing of ozone precursors and thus dilution. This analysis focuses on large-scale sinuosities, which would not necessarily apply to ozone production on a local level. This analysis does corroborate results from Chapter 3, which show that on high ozone days, winds appear to be slower and from the southeast, while on high ozone days, winds are faster and from the south.

4.3 Summary of Recent Findings in Background Ozone Transport

The need to quantify background ozone, or ozone transported from outside the DFW area, in addition to quantifying local ozone production, is essential given that a large metropolitan area, such as Dallas-Fort Worth, regularly generates enough local ozone to exceed the standard when starting from a high background. Modifying procedures developed by TCEQ and Nielson-Gammon, et al. (2005a), this chapter has demonstrated that background eight-hour ozone levels traveling into Texas are regularly as high as 60 ppb, and often higher.

Examination of 90th percentile ozone concentrations at selected upwind monitors from 2000 to 2009, with data restricted by wind direction and season of the year, revealed no discernible trend in background ozone over the nine-year period observed. The absence of trend simplifies interpretation of influences from background and local components of ambient ozone, as well as computation of benefits of local control strategies.

Studies of regional background eight-hour ozone in the DFW area show that regional background eight-hour ozone is high on days with high ozone. Typically, on days with no exceedances, background ozone is roughly 40 ppb, as estimated by the EPA. Evaluation of ozone transported from both the north and south showed regional background ozone was higher when the ozone concentration for that day exceeded 75 ppb. While monthly wind-restricted data did not match results from Nielsen-Gammon (2005a), the overall results showing higher background concentrations during ozone season were similar. These analyses show that regional background eight-hour ozone often exceeds 50 ppb and is especially pronounced during ozone season in the DFW area.

The lower range of background ozone estimates using the first method were in the range of the EPA estimate; however, the upper range of background ozone estimates using this method were much larger than the 40 ppb used by the EPA. Estimates of background ozone using the AQPlot method were consistently higher than 40 ppb. Because the two methods use different measures

of ozone, eight-hour averages in one case, one-hour averages in the other, results from the two methods will naturally differ.

Investigation of HYSPLIT back trajectories identified likely transport of ozone into north Texas on days following elevated ozone episodes in eastern U.S. states. Back trajectories also showed that on high ozone days slower winds from the east and southeast are most frequent, while on low ozone days winds were much faster and from the south.

These background and transport analyses show that efforts focused solely on controlling local emissions may be insufficient to bring the DFW area into ozone attainment given that, on many days, background estimates are well over half the eight-hour ozone NAAQS of 85 ppb.

5 REFERENCES

- Atkinson, R.; Arey, J. Atmospheric degradation of volatile organic compounds. *Chem. Rev.* 2003, 103, 4605–4638.
- Banta, R.M., C.J. Senff, J. Nielson-Gammon, L.S. Darby, T.B. Ryerson, R.J. Alvarez, S.P. Sandberg, E.J. Williams, and M. Trainer. 2005. A Bad Air Day in Houston. *Bulletin of the American Meteorological Society*, 86(5): 657-669.
- Bell, M. L., A. McDermott, S. L. Zeger, J. M. Samet, and F. Domenici. 2004: Ozone and short-term mortality in 95 US urban communities. *J. Amer. Med. Assoc.*, **292**, 2372-2378.
- Blanchard, C., S. Tanenbaum, and D. Lawson. 2008. Differences between weekday and weekend air pollutant levels in Atlanta; Baltimore; Chicago; Dallas-Fort Worth; Denver; Houston; New York; Phoenix; Washington, DC; and surrounding areas. *J. Air & Waste Manage. Assoc.*, 58: 1598-1615.
- Blanchard, C. and S. Tanenbaum. 2005. Weekday/weekend differences in ambient concentrations of primary and secondary air pollutants in Atlanta, Baltimore, Chicago, Dallas-Fort Worth, Denver, Houston, New York, Phoenix, Washington, and surrounding areas, Final Report, NREL Project ES04-1, May 16, 2005.
- Camalier, L., W. Cox, and P. Dolwick. 2007. The effects of meteorology on ozone in urban areas and their use in assessing ozone trends. *Atmos. Environ.*, **41**, 7127–7137.
- Carter, W.P.L., 2000. Documentation of the SAPRC-99 chemical mechanism for VOC reactivity assessment, Report to the California Air Resources Board, Contracts 92-329 and 95-308. (<http://www.cert.ucr.edu/~carter/absts.htm#saprc99>)
- Carter, W.P.L., 2010. Development of the SAPRC-07 Chemical Mechanism and Updated Ozone Reactivity Scales; Final Report to the California Air Resources Board, Contract No. 03-318, 06-408, and 07-730, Revised January 27, 2010. (<http://www.cert.ucr.edu/~carter/SAPRC/>)
- Chinkin, L., H. Main, and P. Roberts. 2005. PAMS Data Analysis Workshops, Illustrating the use of PAMS Data to Support Ozone Control Programs. (Accessed November 21, 2005, Last updated on Friday, June 12, 2009). <http://www.epa.gov/oar/oaqps/pams/analysis/index.html#preface>
- Cooper, O. R., et al. 2006. Large upper tropospheric ozone enhancements above midlatitude North America during summer: In situ evidence from the IONS and MOZAIC ozone measurement network, *J. Geophys. Research*, 111: D24S05, doi:10.1029/2006JD007306.
- Croes, B. et al. (2003), The O₃ “weekend effect” and NO_x control strategies: Scientific and public health findings and their regulatory implications. *EM*, pp. 27-35, July 2003.
- Currie, J., E. Hanushek, E.M. Kahn, M. Neidell, S. Rivkin, 2007. Does Pollution Increase School Absences? National Bureau of Economic Research, Working Paper 13252. <http://www.nber.org/papers/w13252>.
- Draxler, R. 2000. Meteorological Factors of Ozone Predictability at Houston, Texas. *J. Air. and Waste Manage. Assoc.*, **50**, 259-271.

- Estes, M. 2010. Background ozone for Texas cities: Findings from recent studies of background ozone. White paper on background ozone, April 2, 2010, Mark Estes.
- Fujita, E., et al. 2003a. Evolution of the magnitude and spatial extent of the weekend ozone effect in California's South Coast Air Basin, 1981-2000. *J. Air & Waste Manage. Assoc.*, **53**, 802-815.
- Fujita, E., et al. 2003b. Diurnal and weekly variations in the source contributions of ozone precursors in California's South Coast Air Basin. *J. Air & Waste Manage. Assoc.*, **53**, 844-863.
- Gao, O. H., B. A. Holmen, D. A. Niemeier. 2005. Nonparametric factorial analysis of daily weigh-in-motion traffic: implications for the ozone 'weekend effect' in Southern California, *Atmos. Environ.*, **39**, 1669-1682.
- Hardesty et al. (2007). Mixing heights and three-dimensional ozone structure observed during TexAQS II, presentation at the American Geophysical Union Fall Meeting, December 14, 2007. Background ozone was estimated from downward looking ozone lidar data.
- Heck, W.W., W.W. Cure, J.O. Rawlings, L.J. Zaragosa, A.S. Heagle, H.E. Heggstad, R.J. Kohut, L.W. Kress, and P.J. Temple. 1984. Assessing impacts of ozone on agricultural crops: crop yield functions and alternative exposure statistics. *J. Air Pollut. Control Ass.*, **34**, 810-817.
- Heuss et al. 2003. Weekday/weekend ozone differences: What can we learn from them? *J. Air & Waste Manage. Assoc.*, **53**, 772-788.
- Krige, Danie G. (1951). "A statistical approach to some basic mine valuation problems on the Witwatersrand". *J. of the Chem., Metal. and Mining Soc. of South Africa* **52** (6): 119-139.
- Lawson, D. R. 2003. The weekend ozone effect—The weekly ambient emissions control experiment, EM, pp. 17-25, July 2003.
- Main, H., et al. 1996. PAMS Data Analysis Workshop: Illustrating the Use of PAMS Data to Support Ozone Control Programs.
- Marr, L., and R. Harley. 2002. Modeling the effect of weekday-weekend differences in motor vehicle emissions on photochemical air pollution in central California, *Environ. Sci. Technol.*, **36**:4099.
- Martin, R.V, C. E. Sioris, K. Chance, T. B. Ryerson, T. H. Bertram, P. J. Woodridge, R. C. Cohen, J. A. Neuman, A. Swanson, F. M. Flocke. 2006. Evaluation of space-based constraints on global nitrogen oxide emissions with regional aircraft measurements over and downwind of eastern North America, *J. Geophys. Res.*, **111**, D15308, doi:10.1029/2005JD006680.
- Murphy, et al. 2007. The weekend effect within and downwind of Sacramento—Part 1: Observations of ozone, nitrogen oxides, and VOC reactivity. *Atmos. Chem. Phys.*, **7**, 5327-5339.
- National Academy of Sciences. 1991. *Rethinking the Ozone Problem in Urban and Regional Air Pollution*. National Academies Press, 524 pp.
- Nielsen-Gammon, J.W., J. Tobin, and A. McNeel. 2005a. A Conceptual Model for Eight-Hour Ozone Exceedances in Houston, Texas, Part I: Background Ozone Levels in Eastern Texas,

January 29, 2005. <http://files.harc.edu/Projects/AirQuality/Projects/H012.2004/8HRA/H12-8HRA-FinalReport2.pdf>

Nobis, T.F., G.R. North, R.C. Harris, N.W. Tindale, D.W. Sullivan, H.J. Newton, August 1998. Texas A&M University Master of Science Thesis: An Ozone Climatology of the Dallas-Fort Worth Area and Its Relationship to Meteorology. <http://www.dtic.mil/cgi-bin/GetTRDoc?AD=ADA356380&Location=U2&doc=GetTRDoc.pdf>

Pun, B. K., et al. 2003. Day-of-week behavior of atmospheric ozone in three U.S. cities, *J. Air & Waste Manage. Assoc.*, **53**, 789-801.

Qin, Y, T. Walk, R. Gary, X. Yao, S. Elles. 2007. C₂-C₁₀ nonmethane hydrocarbons measured in Dallas, *Atmos. Environ.* 41:6018.

Rapid Science Synthesis Team. 2006. Final Rapid Science Synthesis Report: Findings from the Second Texas Air Quality Study (TexAQS II), A Report to the Texas Commission on Environmental Quality, *2006 Texas Air Quality Study*.

Savanich, K. 2006. Ozone Exceedance Days as a Function of the Number of Monitors, TCEQ, February, 2006.

Sillman, S. 2002. Evaluation of Observation-Based Methods for Analyzing Ozone Production and Ozone-NO_x-VOC Sensitivity. Draft Report to the U.S. EPA National Exposure Research Laboratory <http://www-personal.umich.edu/~sillman/web-publications/OBMDraftreport4f.pdf>

Sullivan, D. 2009. Effects of Meteorology on Pollutant Trends. Final Report to TCEQ. Grant Activities No. 582-5-86245-FY08-01. Prepared by Dave Sullivan, University of Texas at Austin Center for Energy and Environmental Resources, Prepared for Kasey Savanich, for the Texas Commission on Environmental Quality, March 16, 2009. http://www.tceq.state.tx.us/assets/public/implementation/air/am/contracts/reports/da/5820586245FY0801-20090316-ut-met_effects_on_pollutant_trends.pdf

Tobin, J., Nielsen-Gammon, J.W., Modeling Ozone as a Function of Meteorological Conditions in the Houston Non-Attainment Region: Identifying Meaningful Meteorological Controls and Estimating Trends in Meteorologically Adjusted Ozone. H-107 Final Report, January 29, 2010.

Texas Commission on Environmental Quality. 2010. Houston-Galveston-Brazoria Attainment Demonstration State Implementation Plan for the 1997 Eight-Hour Ozone Standard. Chapter 5: Weight of Evidence, pp. 5-74-5-81.

Texas Commission on Environmental Quality. 2006. Subchapter A: Definitions, 30 TAC § 115.10, adopted December 7, 2006.

Texas Railroad Commission. 2010. Website on the Barnett Shale as updated March 1, 2010: <http://www.rrc.state.tx.us/barnettshale/index.php>

U.S. Census Bureau, Population Division. 2010. Table 1. Annual Estimates of the Resident Population for Counties of Texas: April 1, 2000 to July 1, 2009 (CO-EST2009-01-48), Release Date: March 2010.

U.S. Environmental Protection Agency. Tuesday, January 19, 2010. Proposed Rules, National Ambient Air Quality Standards for Ozone. Vol. 75, No. 11, Proposed Rules, Title 40, Code of

Federal Regulations, Parts 50, and 58.

<http://www.epa.gov/air/ozonepollution/fr/20100119.pdf>

U.S. Environmental Protection Agency. April 2007. Guidance on the Use of Models and Other Analyses for Demonstrating Attainment of Air Quality Goals for Ozone, PM_{2.5}, and Regional Haze, EPA -454/B-07-002. <http://www.epa.gov/ttn/scram/guidance/guide/final-03-pm-rh-guidance.pdf>.

U.S. Environmental Protection Agency. February 28, 2006. Air Quality Criteria for Ozone and Related Photochemical Oxidants, Volumes I, II, and III, EPA 600/R-05/004aF-cF. <http://cfpub.epa.gov/ncea/cfm/recordisplay.cfm?deid=149923>.

U.S. Environmental Protection Agency. Friday, April 30, 2004. Ozone National Ambient Air Quality Standards for Ozone, Vol. 69, No. 84, Rules and Regulations, Title 40, Code of Federal Regulations, Parts 50, 51 and 81. <http://edocket.access.gpo.gov/2004/pdf/04-9152.pdf>.

Westenbarger, D.A., and G. B. Frisvold. 1994. Agricultural exposure to ozone and acid precipitation. *Atmos. Environ.*, **28**, 2895-2908.

Xie, Y., and C. M. Berkowitz. 2005. Source attribution and emission adjustment study: Task 1. Back trajectory climatology and identification of key source regions. 10 January 2005. http://www.tceq.state.tx.us/assets/public/implementation/air/am/contracts/reports/ei/Source_Attribution_and_Emission_Adjustment_Study_Task1.pdf.

Yarwood, G., J. Grant, B. Koo, A. M. Dunker. 2008. Modeling weekday to weekend changes in emissions and ozone in the Los Angeles basin for 1997 and 2010, *Atmos. Environ.*, **42**, 3765-3779.

Yarwood, G., et al. 2003. Modeling weekday/weekend ozone differences in the Los Angeles region for 1997, *J. Air & Waste Manage. Assoc.*, 53, 864-875.